Extreme environments: tufa formation at high pH from lime kiln waste, South Wales

NATURAL ENVIRONMENT RESEARCH COUNCIL

Louis Emery
School of Earth and Ocean Sciences,
Cardiff University, Cardiff, UK. CF10 3YE.

Abstract

Invasive tufa deposits on Foel Fawr, South Wales are forming from lime kiln waste deposited from the 18th century until the 1950s. The tufa deposits are unusual in their anthropogenic origin and form the largest site of this type in the UK. At emergence pH is extreme (>11) and this consequently generates significant pressure on organisms living in and around the system.

Morphologically, the calcium carbonate tufa deposits are similar to those formed in other extreme environments (e.g. hot springs, caves), forming many of the same features (e.g. terraces, rimpools, pisoids, stalactites). By identifying and mapping tufa facies at Foel Fawr, the spatial distribution of these facies has been directly compared to these potentially analogous environments. Analysis of the fabrics associated with each facies highlights the importance of physico-chemical precipitation in the system; proximal facies are dominated by abiotic fabrics, while distal and marginal facies show an increasing degree of biological influence. This process is comparable to the partitioning of fabrics and facies observed in hot spring systems, however, the role of microbes in precipitation is apparently less important on Foel Fawr.

The present day extreme chemistry of the site selectively excludes organisms and generates a partitioning of biology. Hydrochemical monitoring of the site reveals that the extreme pH of the system is in decline. The recession of the extreme hydrochemistry is confirmed by colonisation of previously excluded organisms and allowed the physical decay of the site. Fabrics preserved within the deposits support the suggestion that the extreme environments were previously much more widespread.

Table of Contents

Chapter 1: Introduction

1.1. Project overview

This thesis focuses on an unusual and poorly described sub-type of tufa forming from hydroxide waters on Foel Fawr, South Wales. Pentecost (2005) uses the term invasive travertine to refer to deposits of this type; however, here the term invasive tufa is preferred owing to the ambient temperature of the deposits.

The site on Foel Fawr is one of only a few identified invasive tufa sites in the world and is the most extensive site in Britain, extending for several kilometers along a series of springs. There is a paucity of information published regarding both these deposits and those from other comparable invasive systems. The broad aim of this study is to consider the processes and morphologies associated with carbonate precipitation on Foel Fawr and compare them to other invasive systems and to other terrestrial carbonate systems. Comparisons to other terrestrial carbonate systems allow these new deposits to be placed within a framework of deposition, which informs both the results of this thesis, as well as providing a valuable analogue environment against which existing research may be referred.

Much of the recent focus within tufa and travertine research has been on the role of microorganisms (and specifically biofilms) in the formation of deposits (e.g. Pedley, 2011, Okumura et al., 2012, Perri et al., 2012). Pedley and Rogerson (2010a) highlight the link between morphology and the interplay between physico-chemically and biologically dominated precipitation (figure 1.1a, overleaf). Environmental pressures (i.e. darkness, temperature, salinity) in tufa, travertine and subterranean environments are principally responsible for this variable dominance of physico-chemical and biological processes. On Foel Fawr (and in other invasive systems) extreme pH likely plays a similar role in defining the relative roles of physico-chemical and biological processes.

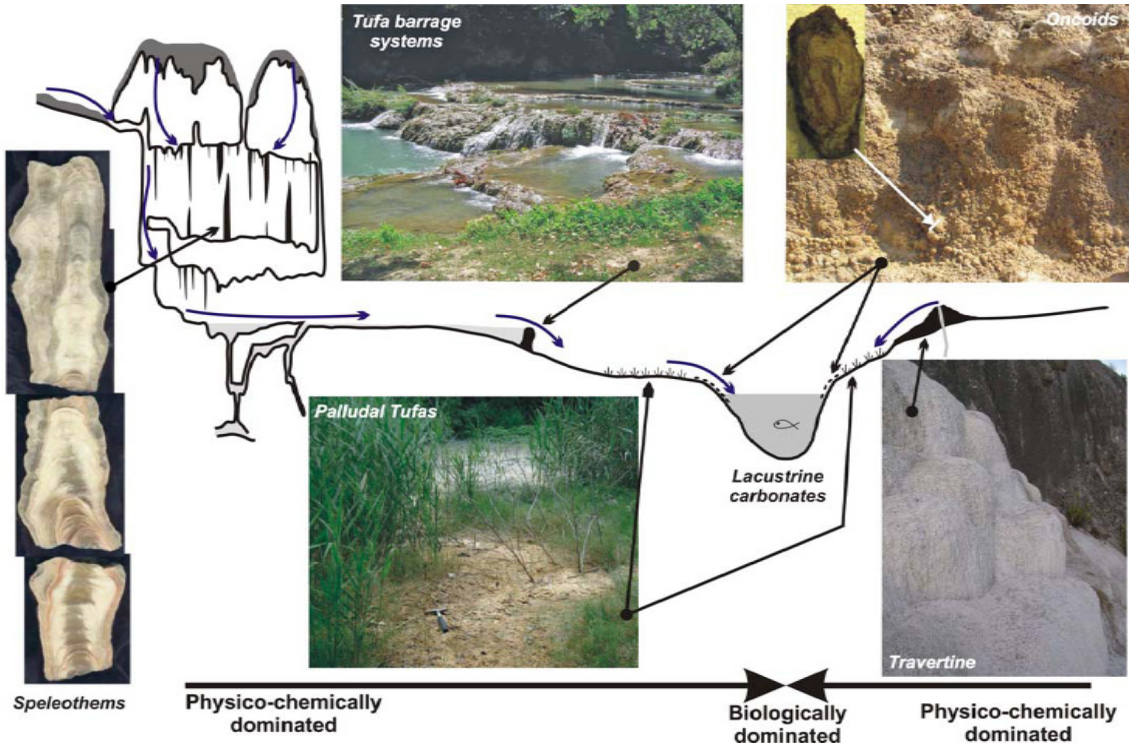

Figure 1.1a. Schematic diagram of terrestrial carbonate deposition showing the relationship between physico-chemically and biologically dominated systems and morphology. From Pedley & Rogerson (2010a).

1.1.1. Nomenclature

There is a great variety of terminology associated with tufa and travertine research, often with little consistency even at the broadest scale. This thesis uses the definitions laid out in Ford and Pedley (1996) and defines tufa as being ambient temperature deposits and travertine as thermally fed deposits. This nomenclature is more satisfactory than the other commonly used alternative, as proposed by Pentecost (2005); whereby all deposits are referred to as travertine, being either meteogene (ambient temperature) or thermogene (thermally sourced) forms. The terms tufa and travertine are more readily definable and less likely to be confused, and therefore make any literature easier for a non-specialist reader to understand. These and other terms contained within this thesis are defined in a glossary at the back of this thesis to aid clarity.

1.2. Foel Fawr, Black Mountain

1.2.1. Study location

Unusual tufa deposits have been precipitated on the northern slopes of Foel Fawr, Black Mountain, South Wales. The deposits are located just below a ridge, at an altitude of between 350m and 500m above mean sea level. The site is encompassed by the co-ordinates 273000 218700, 273850 218700, 273850 219200, 273850 218700 [OSGB], close to the western edge of the Brecon Beacons National Park and the Fforest Fawr Geopark (figure 1.2.1a).

The deposits are located on north-facing scarp slopes below Foel Fawr, Black Mountain and transect the northern edge of the South Wales Coalfield (see figure 1.2.1b). Outcrops on the scarp slope expose several lithologies on the northern limb of the South Wales Coalfield synform: the Grey Grits Formation at the top of the Old Red Sandstone generates a stepped relief on the slope; overlying this are impermeable shales, which generate a springline at the southernmost extent of the step. The combination of this step and the springs results in the formation of a peat-bog system. Above this, Lower Carboniferous (Mississippian) Limestone (Dowlais Limestone Formation & Oxwich Head Limestone Formation) has been extensively quarried and burned for lime. Wide areas of tips of lime kiln waste remain from the lime burning, and these tips cause the tufa precipitation on Foel Fawr.

Many springs and seeps drain the lime-tips, flowing over and around the peat-bog system. The flat areas created by the underlying geology allow the formation of pools and reduce the rate at which material is transported from the site.

The Dowlais Limestone features numerous caves, all of which are likely related to the Llygad Llwchwr master system (Stratford, 1995), which resurges approximately 5km west of Foel Fawr. The most significant system on Foel Fawr is the Ogof Pasg-Ogof Foel Fawr system, which is nearly 1km in length and is found beneath Foel Fawr at the eastern end of the site.

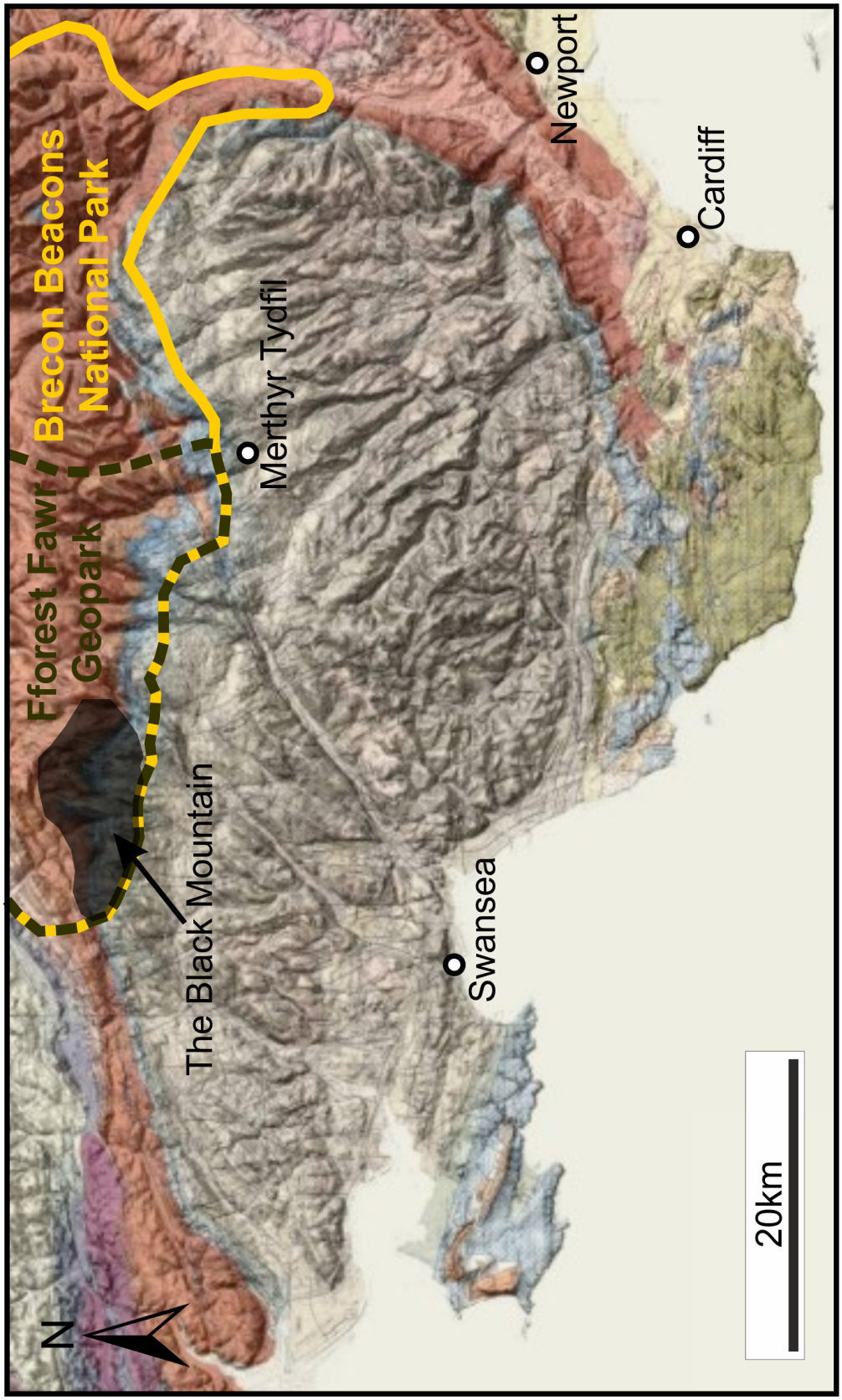

Figure 1.2.1a. Outline of study area. Major urban areas and Brecon Beacons National Park/Fforest Fawr Geopark are both marked, along with geographical extent of Black Mountain. The geology is colour coded representing: the South Wales Coalfield (central grey expanse), encircled by Carboniferous Limestone (thin blue line) and Old Red Sandstone (red areas). Shading represents topography.

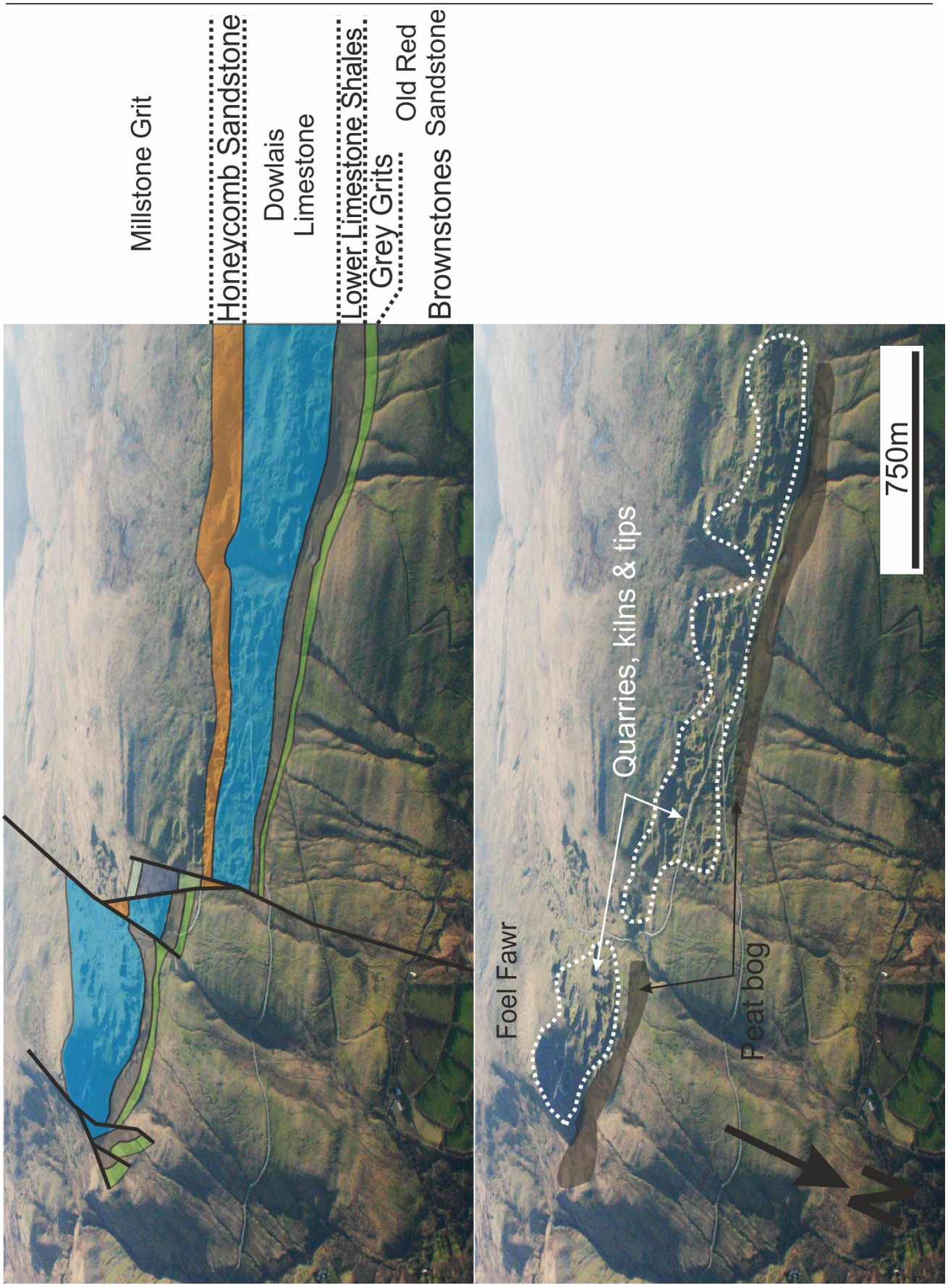

Figure 1.2.1b. Aerial photograph of the site with solid geology (top) and land cover (bottom) overlaid. © Allan Cuthbertson.

1.2.2. Site history

The site has a long history as a lime production site. The Dowlais Limestone outcrops above (and south) of the tufa deposits have been extensively quarried and burnt to produce quicklime (CaO).

There are a large number of kilns on the site, with some kilns marked on the earliest Ordnance Survey of the area (1877). At this time, the size and extent of the quarries were comparable to their present extent (see figures 1.2.2a and 1.2.2b overleaf), indicating that the industrial history of the site precedes this date significantly. An information board at the site states that the site has been used to make lime since 1750; however, it is unclear how quickly the site grew to its 1877 extent. The site has not expanded notably since 1877, however some kilns were still active in the 1950s (Percival, 1986). The history of burning is complex, however, there is a general trend of older kilns to the west and younger kilns to the east (Duncan Schlee, Dyfed Archaeological Trust, personal communication).

Lime slag from the kilns is deposited extensively in tips between the kilns and the study area. The kilns appear to be simple shaft kilns, and it is likely that coal was used to fuel them (Brecon Beacons National Park, 2007). Lime slag is typically composed of a mixture of quicklime (CaO) and portlandite ($Ca(OH)_2$), combined with the remains of the fuel source. Estimating the thickness of the tips is made difficult by the fact that they are lenticular and comprised of several different levels of deposition. The tips directly above the site are typically around 3m in height and extend between 5 and 30m back to the quarry faces directly above. There are similar sized tips on another tier above this.

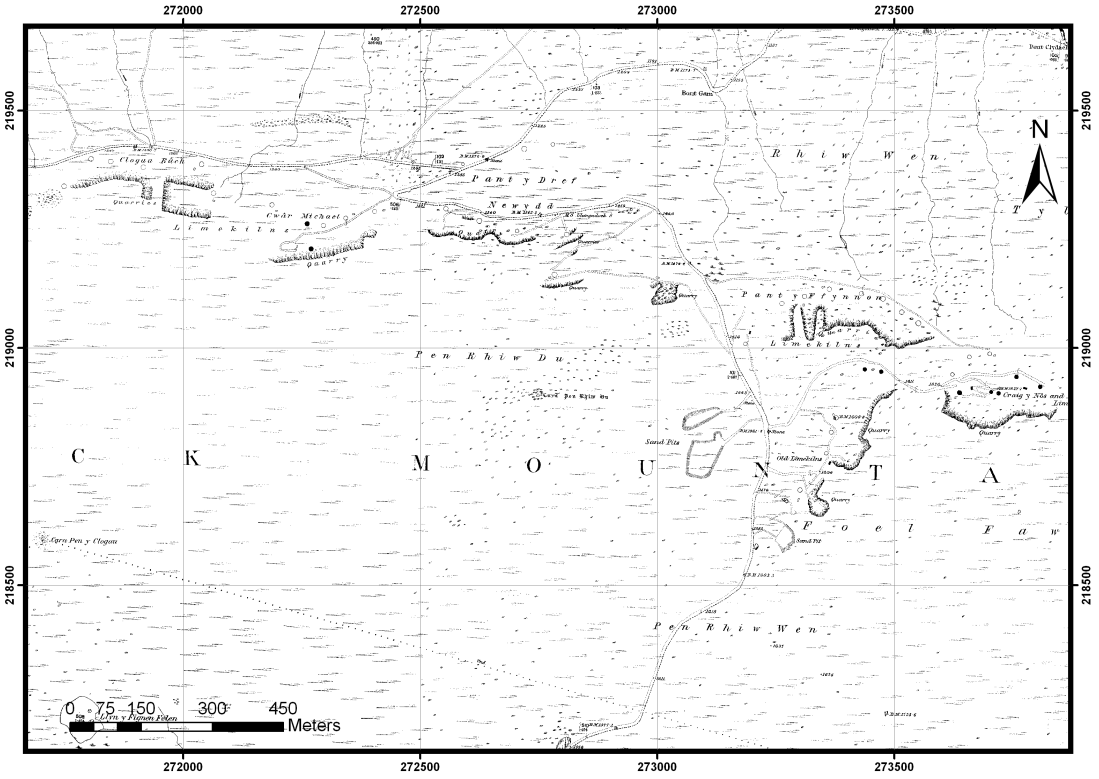

Figure 1.2.2a. The extent of quarrying and lime burning at the site in 1877. ©Ordnance Survey, 2012.

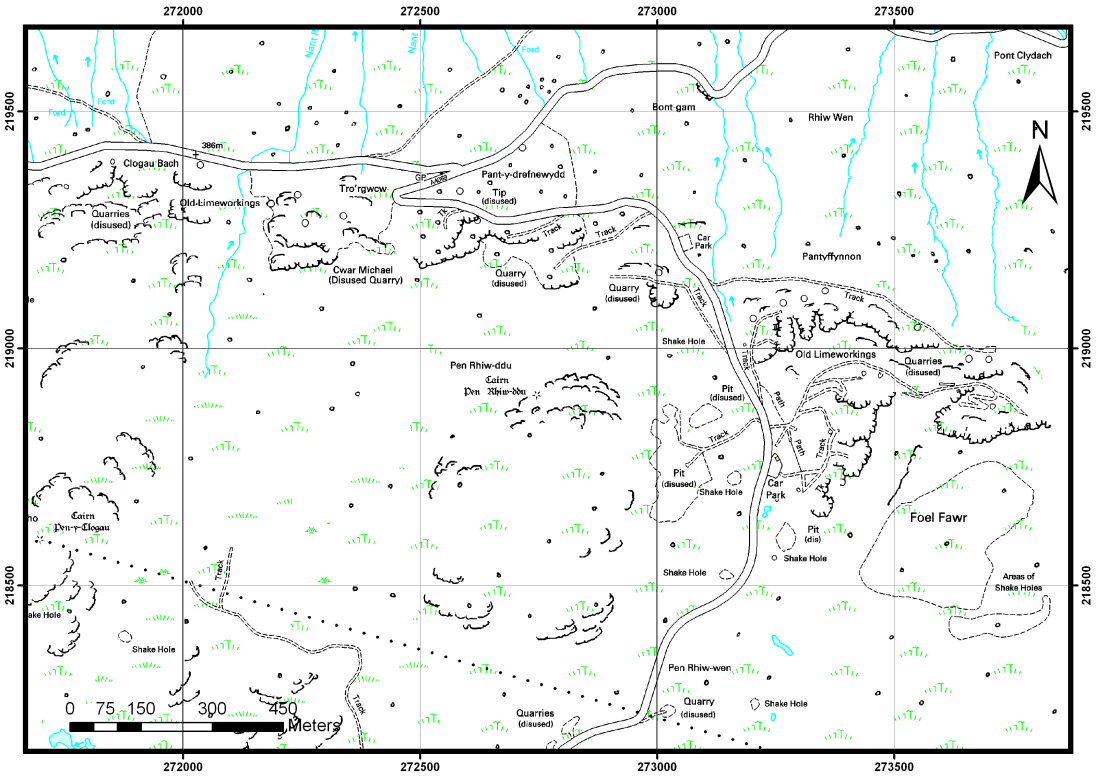

Figure 1.2.2b. The present day extent of quarrying and lime burning at the site. ©Ordnance Survey, 2012.

1.2.3. Geochemistry

Pentecost (1993) found that the tufa deposits at this site were composed of 99.3% calcium carbonate ($CaCO_3$) with low organic and acid-insoluble content (0.18% and 0.22% respectively) compared to other tufa deposits; other constituents were also of low concentrations (Mg: 590ppm, Sr: 140ppm, Fe: 60ppm, Mn: <20ppm, P: 15ppm). This corresponds with Braithwaite's (1979) observation that the deposits are of low Mg calcite. It is unclear exactly which part of the deposits was analysed to generate this data, but it is likely to represent stream crust rather than pisoidal material. Isotopic analysis was carried out by Andrews et al. (1997), who reported significantly light carbon and oxygen isotopic composition of the calcite deposited (approximately -11 $\delta^{18}O‰$, -20 $\delta^{13}C‰$).

The source waters are of very high pH, typically above 11 on emergence and around 9 elsewhere; they are also supersaturated with respect to calcite (Andrews et al., 1997; Pentecost, 2005; Emery, 2008). Baseflow on Foel Fawr is from a karstic system, generating carbonate-bicarbonate waters. Figure 1.2.3a shows the processes of deposition in both natural tufa systems and on Foel Fawr.

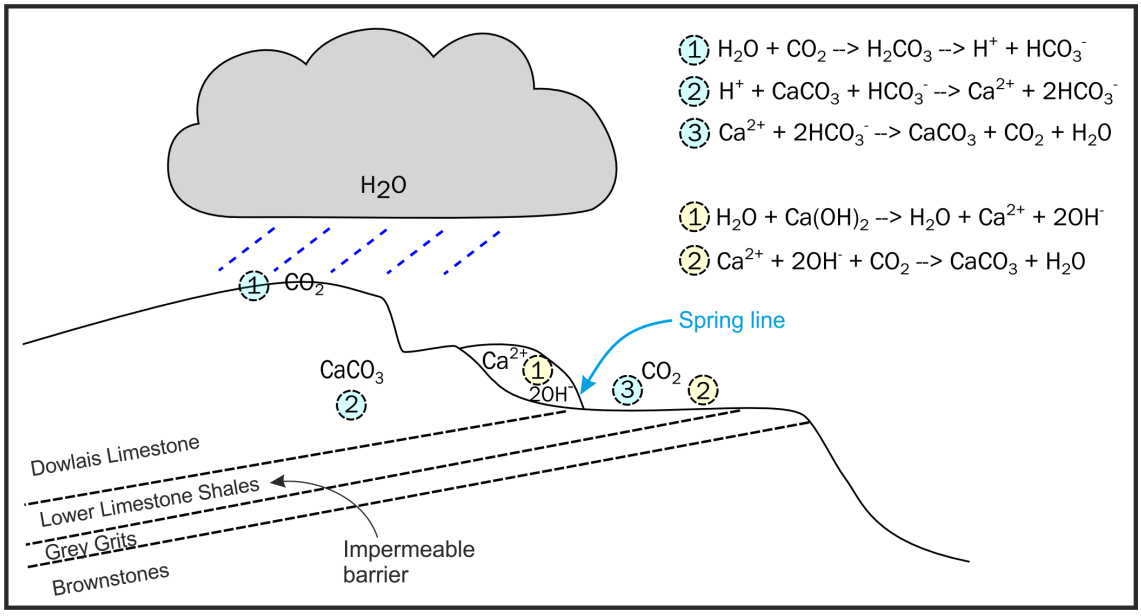

Figure 1.2.3a. A thematic cross section through Foel Fawr. Geochemical processes of natural tufa precipitation are shown in blue; geochemical processes of tufa deposition on Foel Fawr are shown in yellow.

1.2.4. Morphologies and fabrics

The deposits have previously been described by Braithwaite (1979), who made some observations on the spatial distribution of the micro-environments which make up the deposits. Three facies were identified at the site: laminated crusts, pisolitic pools and rimstone pools.

More recent morphological studies were carried out by Emery (2008), who described similar facies to Braithwaite (1979), including: proximal laminated aprons, pools with laminated pisoids, proximal arid pisoidal/oncoidal accretions and marginal biological encrustations. Additionally, Emery (2008) observed the notable lack of vegetation at the site and, consequently, the reduced impact on morphology as compared to natural tufa systems.

Mineralogically, Braithwaite (1979) identified two distinct crystal habits: acicular radial crystals with botryoidal terminations, and prismatic crystals with rhomboidal terminations, which are sometimes rounded or truncated by secondary solution. Acicular crystal habit is typically associated with aragonite (Harris et al., 1985), although it is also known to be a calcitic fabric, albeit less commonly (Kendall, 1985). A brief summary of the crystal habits observed by Braithwaite (1979) is provided in Figure 1.2.4a. The fabric seen in C (figure 1.2.4a) closely resembles fabrics discussed initially by Kendall and Tucker (1973), who suggested that they are formed by recrystalisation of acicular fabrics, and later by Kendall (1985), who revises this theory and suggests they are primary fabrics, which may form from highly supersaturated solutions.

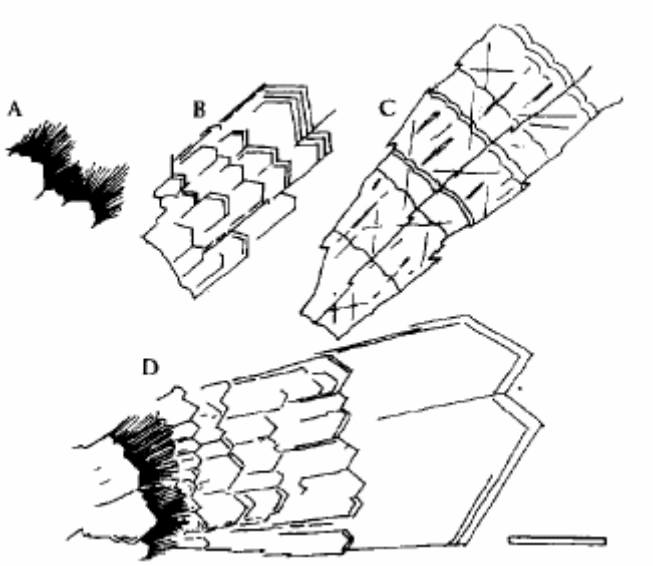

Figure 1.2.4a. Crystal structures observed on site. Bar size = 500 µm. A: Acicular crystals. B: Prismatic crystals with rhombohedral terminations. C: Bladed crystals with linear inclusions and rounded terminations. D: Composite fabric, showing fabrics from A, B and C. After Braithwaite (1979).

1.2.5. MESci thesis

The work contained within this thesis builds upon initial investigations undertaken by the author and reported in Emery (2008). The research reported therein represents a 'snapshot' of one small

part of the site and is summarised here in order to make clear the additional contribution of this thesis.

The work contained in Emery (2008) represents a small scale study, focussed on a small area of the site (figure 1.2.5a). This area was mapped using field sketches and aerial imagery to an accuracy well below that undertaken as part of this thesis. Five distinct facies were mapped, which represent a smaller continuum of morphology than is identified within this thesis (owing to the restricted area considered and the time constraints placed upon an MESci thesis). The facies outlined in Emery (2008) do not correspond directly to the facies considered in this thesis, even if they may be equivalently named. The facies identified within this thesis and Emery et al. (2011) refine and elaborate upon those described in Emery (2008).

The facies identified within Emery (2008) are briefly analysed, utilising both scanning electron microscopy and light microscopy of hand specimens. Two proximal localities (identified as seep and spring in figure 1.2.5a) were analysed geochemically, including 3 days of field data and inductively coupled plasma mass spectrometry (ICP-MS).

While the work undertaken in Emery (2008) significantly impacted the direction in which the research reported in this thesis was progressed, the data reported here represents a far broader and consequently thoroughly revised interpretation of the deposits on Foel Fawr. The facies classification has been revised and expanded significantly and these newly defined facies have been analysed in far greater detail. These facies have been accurately mapped and the spatial relationships between them analysed. Hydrochemical study of the site has been expanded in scale (both spatially and temporally), allowing analysis into the activity of the precipitation processes on Foel Fawr to be tied to observations of facies and facies distribution.

In addition, this thesis has been able to expand on the interpretation and contextualisation of the Foel Fawr deposits, through smaller scale comparative studies with hot spring travertines and several other lime spoil sites (including Harpur Hill, Buxton, UK, where a significant invasive tufa system has formed). Finally, initial observations of the biology (including plants, animals and microorganisms) are reported, providing a stepping stone for any future researchers to consider these aspects of the system.

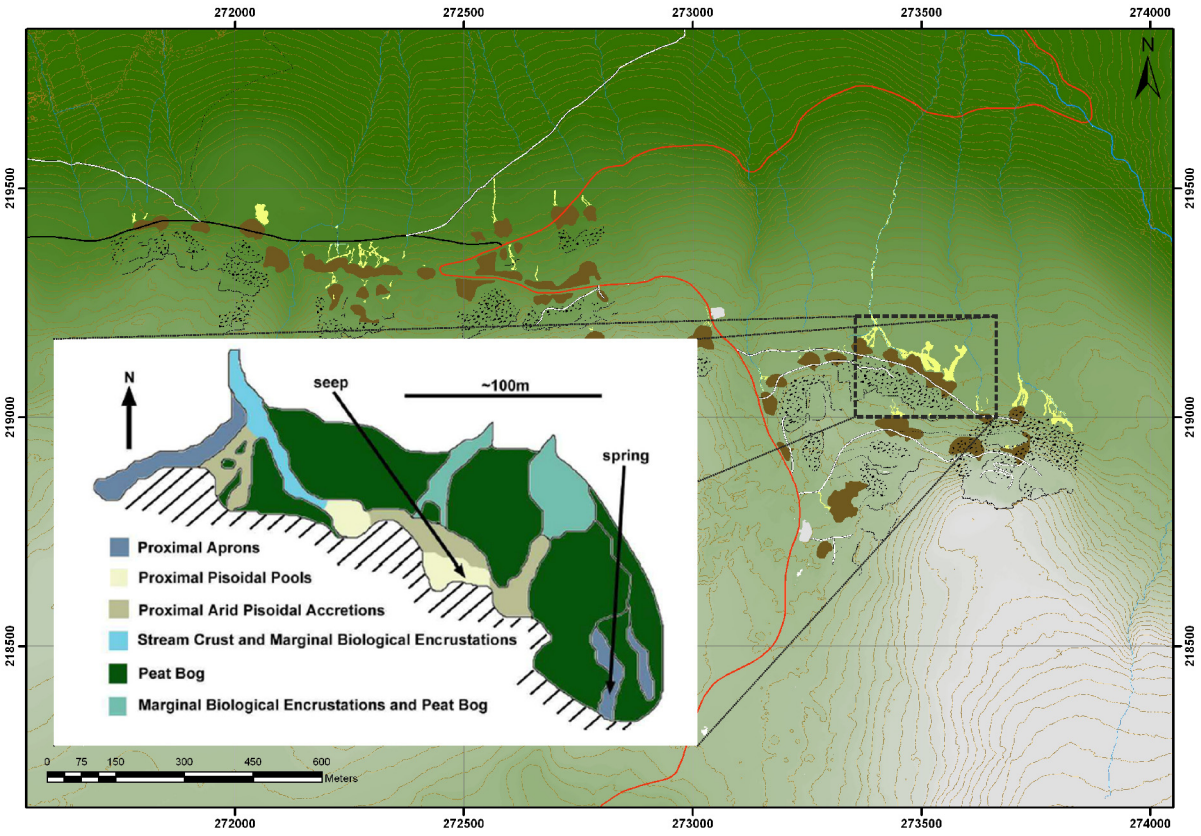

Figure 1.2.5a. Mapped extent contained within MESci thesis. Mapping was based on aerial imagery and limited field sketches. The relative inaccuracy of the MESci mapping can be observed by comparing with maps produced later in this thesis (figures 3.3.5, 3.3.5c, 3.3.5d, 3.3.5e & 3.3.5f)

1.3. Invasive tufa

1.3.1. Overview

Invasive tufa systems are relatively rare and poorly studied. They form by a different process to 'normal' tufa and travertine, the carbonate source being atmospheric and derived from ingassing. Deposits fall into two main subtypes: industrially created systems (e.g. Foel Fawr) and serpentinised systems. Both types form at ambient temperature, but share many morphological similarities with hot spring travertine deposits (Emery, 2008).

1.3.2. Known sites

An exhaustive list of known sites is not provided here, but some comparable sites are listed to provide potential reference sites and to illustrate the rarity of known sites. In the UK, only two sites of any significance are known: Foel Fawr in South Wales (the subject of this thesis) and a smaller site near Buxton, Derbyshire which has not been reported in any detail (Ford and Pedley, 1996). Both sites are industrial in origin. There are also limited serpentinite related travertine deposits in Scotland (Flinn and Pentecost, 1995). Outside the UK, there are sites in California and Oman, which have both been studied geochemically (Barnes and O'Neil, 1971; Neal and Stanger, 1983).

1.3.3. Geochemistry

Source waters derive their geochemistry either from industrially generated quicklime/slaked lime (CaO / $Ca(OH)_2$) or from waters sourced from serpentinised geologies. Both systems produce OH^- buffered waters that have high pH, typically around 9-11 (Boyer, 1994; Pentecost, 2005), as well as high buffer capacity (Mattock, 1961). This buffering system is rare in nature, as the buffer is rapidly consumed upon exposure to CO_2.

The processes leading to deposition are distinct from those of 'natural' tufa systems. Waters emerge with a pCO_2 of close to zero and quickly equilibrate with the atmosphere by the ingassing of CO_2. This then reacts with the $Ca(OH)_2$ in solution (quicklime is rapidly converted into slaked lime on contact with water) to produce $CaCO_3$ and water (equation 1).

$$Ca(OH)_2 + CO_{2(g)} \rightarrow CaCO_3 + H_2O$$

[Equation 1]

This process results in isotopically light tufa (O'Neil and Barnes, 1971; Clark et al., 1992; Andrews et al., 1997; Pentecost, 2005), owing to the atmospheric origin of the carbonate.

Some serpentinised systems form from $Mg(OH)_2$ waters, depositing dolomite as well as calcite (Blank et al., 2009). Industrial deposits are likely to be purer; however, traces of the fuel used to burn the limestone will undoubtedly constitute a large proportion of the tip composition.

1.3.4. Morphologies and fabrics

The morphologies and fabrics of invasive tufa systems have not been described in any great detail. Much of the limited work carried out in the UK has been undertaken at Foel Fawr and is discussed in section 1.2.4.

Several fabrics have been associated with invasive tufa. At Adobe Springs, California, USA, carbonate cements (laminated or massive) are deposited, binding conglomerates together (Blank et al., 2009). Similar morphologies (intraclast tufa) are found at deposits in Shetland, where carbonate cemented breccias occur; cementation is either the result of fine grained intraclast brucite/aragonite/hydromagnesite/calcite deposition or thin aragonite laminations (Flinn and Pentecost, 1995).

1.3.5. Biology

The unusual hydrochemistry of invasive tufa systems results in very high pH environments. These conditions make it impossible for many organisms to survive due to their inability to maintain a near neutral intracellular pH. Typically, prokaryotes are the only organisms represented in environments with the most extreme pH.

The low H^+ activity surrounding cells in high pH environments makes the generation of a proton motive force very difficult, if not impossible (Brock, 2005). In order to overcome this difficulty, alkaliphilic microorganisms living in soda lakes typically utilize a Na^+ driven transporter system instead (Konings et al., 1992; Krulwich and Guffanti, 1992). This system relies on Na^+/H^+ antiporters to maintain Na^+ concentrations on the exterior of the cell wall, and on Na^+/solute symporters to maintain intracellular Na^+ concentrations (Krulwich et al., 2001). Using Na^+ in this manner enables the cell to maintain pH homeostasis and also serves to create the transmembrane electrochemical gradient necessary for ATP synthesis (Krulwich et al., 1998).

Haloalkaliphiles from soda lakes constitute a significant proportion of alkaliphile research, dwarfing freshwater alkaliphile research (López-Archilla, 2004). As a result, many of the processes and adaptations described in alkaliphilic microorganisms often refer to haloalkaliphiles. It is worth noting though that many extremophiles share adaptations, despite their apparently differing environmental pressures; for example, many thermophiles also utilise a Na^+ driven transport system (Konings et al., 1992).

Tiago et al. (2004) showed that microbial communities are able to survive in high pH (pH 11.4) Ca-OH systems. These communities show significant diversity in comparison to other alkaline systems, and it is further suggested that symbiotic interactions are key to their proliferation in such an extreme environment. This is demonstrated by the difficulty in generating laboratory growth at the same pH as in the environment, suggesting that whilst individual species cannot proliferate at such extremes of pH, communities can (Tiago et al., 2006).

1.4. Tufa and travertine

1.4.1. Overview

Despite forming from different hydrochemical systems to invasive tufas, 'normal' tufas and travertines can form a variety of morphologies which are similar to those on Foel Fawr. The differences between tufas and travertines highlight the different stresses on organisms in those environments, and are an analogue for the stresses experienced by organisms in invasive tufa systems.

Tufa systems form extensive calcium carbonate deposits from ambient temperature springs or seeps (the term cold is avoided, as springs can be warmer than hot springs in tropical locations). They are fairly ubiquitous in temperate terrestrial environments where there is a carbonate source (typically limestone), but also form in semi-arid regions and cave systems (Ford and Pedley, 1996). Deposits can be extensive, with some extending over many hundreds of square kilometres (Pentecost, 1995). Young, freshly formed tufa is characterised by relatively high porosity, owing to the macrofloral component preserved within most deposits (Ford and Pedley, 1996).

Hot spring travertines share much in common with tufa systems: they are calcareous and form from carbonate rich waters. The carbonate source in this case is of deeper geological origin (as opposed to meteoric), and so the waters are also geothermally heated (above ambient temperature on emergence). The underlying geology can also generate siliceous hot springs, which share many morphological similarities with calcareous hot springs (Jones and Renaut, 1995; Canet et al., 2005; Pentecost, 2005; Takashima and Kano, 2008).

1.4.2. Geochemistry

Both tufa and travertine form in aqueous, typically alkaline systems, normally buffered by a carbonate-bicarbonate system. This is one of the most common buffering systems for natural water and provides greatest buffering capacity at around pH 7-9 (Mattock, 1961; Langmuir, 1997). Typical pH values for tufa and travertine systems are around 7-8.1 and 6-7 respectively, with almost all systems falling between 6 and 12 (Pentecost, 2005).

The carbonate-bicarbonate buffering system is controlled by the balance of equation 2:

$$CO_{2(g)} + H_2O \leftrightarrow H^+ + HCO_3^- \leftrightarrow 2H^+ + CO_3^{2-}$$

[Equation 2]

The balance of this equation is altered by several inputs and sinks. There are three main inputs to this equation: atmospheric CO_2 (equation 3), meteoric (tufa)/geologic (travertine) CO_2 (equation 4), and geologic HCO_3^- (equation 5).

$$CO_{2(atm)} \leftrightarrow CO_{2(g)}$$

[Equation 3]

$$CO_{2(geo/meteo)} \leftrightarrow CO_{2(g)}$$

[Equation 4]

$$CaCO_3 + CO_{2(g)} + H_2O \leftrightarrow Ca^{2+} + 2HCO_3^-$$

[Equation 5]

Since the systems are closed until emergence, input (or removal) of atmospheric CO_2 is constrained; however, meteoric and geologic CO_2 inputs can still occur, raising the pCO_2. Calcite solubility increases with pCO_2 (equation 2.5; De Silva et al., 2007), and consequently dissolution occurs.

$$Keq = [Ca^{2+}][HCO_3^-]^2 = 10^{-5.97} \cdot pCO_2 \qquad [@25^oC, \text{after Langmuir, 1997}]$$

[Equation 6]

Atmospheric pCO_2 is typically lower than that of the emergent waters (which are in equilibrium with their meteoric/geologic source), and so degassing of CO_2 occurs rapidly upon emergence as the waters tend towards equilibrium with the atmosphere (Dandurand et al., 1982; Appelo and Postma, 2005). This results in a decrease in pCO_2 of the waters, and since calcite solubility therefore also decreases, the saturation state with respect to calcite increases.

In order for precipitation to occur, waters typically need to be heavily supersaturated (5-10 times) with respect to calcite (Dandurand et al., 1982; Chen et al., 2004). This degree of supersaturation is unlikely to be reached throughout a water body; however, isolated variations in saturation may occur. For example, flow accelerates at waterfalls thereby increasing the air-water surface area. It is suggested that this may result in increased degassing and locally focussed precipitation (Zaihua et al., 1995; Zhang et al., 2001; Chen et al., 2004; Pawar and Kale, 2006). Evaporative effects can also alter the saturation state of a solution, acting as a significant driving force for precipitation in some hot springs (Hammer et al., 2005).

Precipitation also occurs away from sites of accelerated flow: lacustrine tufas, for example. Biological processes (specifically photosynthesis) which remove CO_2 from the water have been suggested as one possible explanation for the creation of locally raised saturation indices. While much research focuses on cyanobacteria (Chafetz and Buczynski, 1992; Riding, 2000; Pentecost, 2003a), if photosynthesis is an important factor then plants may also induce carbonate precipitation. The importance of photosynthesis, however, is contentious. Pentecost and Coletta (2007) showed that there is not always variation in precipitation rates between day and night, suggesting that photosynthesis is not necessarily the driving force for CO_2 removal.

More recently, it has been suggested that $CaCO_3$ precipitation is likely dependant on (and driven by) the presence of a microbial biofilm (Rogerson et al., 2008; Shiraishi et al., 2008a; Shiraishi et al., 2008b; Pedley et al., 2009). Aloisi et al. (2006) describe how $CaCO_3$ precipitation can be induced by inoculating a solution (10-15 times super-saturated with respect to calcite) with *Desulfonatronum lacustre*. Precipitation does not occur in solutions which remain sterile. They suggest that "nanoglobules" of amorphous calcium/carbonate/phosphate form on the surface of the bacteria, bound by the extracellular polymeric substances (EPS) which they secrete and that these nanoglobules then act as nucleation sites for $CaCO_3$. The importance of EPS in the precipitation of $CaCO_3$ has previously been suggested by Decho and Kawaguchi (2003); however, they moot that $CaCO_3$ may be directly deposited onto partially degraded EPS.

Tufa and travertine systems are composed primarily of $CaCO_3$, although some systems include a clastic component and/or other minerals, and hot spring systems also commonly form siliceous minerals (Jones and Renaut, 1995; Pentecost, 2005). $CaCO_3$ typically forms either cubic (calcite) or orthorhombic (aragonite) crystals, with calcite being the dominant form. Aragonite does occasionally form in tufa and travertine systems, likely related to high Mg or Sr waters (Spötl, C. et al., 2002; Das and Mohanti, 2005). Amorphous calcite has also been observed forming in hot springs, apparently associated with biofilms (Jones & Peng, 2012). While this is a minor form of calcium carbonate formation, it may be important to the growth of crystalline calcium carbonate.

1.4.3. Biology, morphologies and fabrics

Calcification of terrestrial plants is relatively poorly studied; silicification of vascular plants is a far more common and better documented example of biomineralisation (Raven and Giordano, 2009). Where plants are preserved in calcareous deposits tufas and travertines, they are typically preserved

as external moulds, creating mouldic porosity in the deposited tufa/travertine (Pentecost and Viles, 1994).

Modern and fossil tufas abound with wetland plants and their preserved remains (Koban and Schweigert, 1993), and modern tufa is typically classified either by this macrofloral assemblage or otherwise by the depositional environment (Pedley, 1990). Classifying deposits and attempting to generate models for tufa formation is a useful technique for elucidating the processes of deposition in new deposits quickly. Pedley (1990), Ford and Pedley (1996) and Pedley (2009) provide an extensive classification system based on depositional environment; they suggest several models for tufa environments, which have a variety of fabrics associated with them. Broadly speaking, fluvial tufa systems can be classified with four main types: perched springline, cascade, braided channel and barrage. Alongside this, there are also lacustrine tufa systems, which have some crossover with barrage tufa systems.

Morphologies vary significantly between tufa deposits, owing to variation in the depositional processes and the differing floral assemblages. The most conspicuous macrobiologically influenced morphologies are those constructed by phytoherms (freshwater reefs), such as tufa barrages (Pedley et al., 2003). Bryophytes (terrestrial non-vascular plants) dominate tufa communities, probably due to the porous waterlogged nature of the substrate (Pentecost and Zhang, 2002; Pentecost and Zhang, 2006). While mosses, liverworts and hornworts make up the bulk of research, higher plants are sometimes found (Pentecost, 2005).

Travertine deposits tend to be devoid of mesophilic organisms, owing to the high temperature of the environment, which precludes colonisation by higher plants and bryophytes (Pentecost, 2005). Extremophile microorganisms (typically thermophiles and alkaliphiles in travertine) are still able to live in these environments; however, identifying living microbes from morphological characteristics is fraught with difficulty (Petti et al., 2005), so it is unsurprising that identifying fossilized microbes is also difficult (Konhauser, 2003).

Microbial organisms also play a role in tufa formation, and it is commonly thought that they are required for precipitation (Gradziński, 2010). Diatoms and cyanobacteria dominate the literature on microorganisms in tufaceous environments and form a significant component of the microbial communities in each environment (Winsborough, 2000; Pentecost, 2003a). Cyanobacteria may be

encrusted in highly saturated water bodies. They can also be preserved by sheath impregnation when pCO_2 is low, since bicarbonate is then preferentially used for photosynthesis, thereby leading to calcification (Merz-Preiß and Riding, 1999). Pennate diatoms are by far the most prolific freshwater diatoms, and this is also the case in tufa/travertine systems, however, centric and araphid pennate diatoms have also been observed (Pentecost, 2005).

Microorganisms play an important role in the formation of many hot spring fabrics, but quantifying their importance is still very difficult and attempts to do so represent some of the most current research (Fouke, 2011). The most commonly described tufa/travertine fabrics inferred to be microbial are laminated stromatolitic fabrics, so called because of their resemblance to stromatolites. Stromatolites are perhaps the best studied microbial depositional environments, with fossil examples dating back as far as the Archaean (Riding, 2000; Tice and Lowe, 2004; Allwood et al. 2006; Allwood et al., 2007; Schopf et al., 2007) in addition to numerous modern examples. While there is some controversy over the biogenicity of some fossil stromatolites (Brasier et al. 2006; McLoughlin et al., 2008), there is little doubt that modern stromatolites (both marine and hot spring) form by a repeating sequence of microbial colonisation, followed by lithification (Reid et al., 2000; Jones et al., 2005; Goh et al., 2008; Handley et al., 2008; Takashima and Kano, 2008). Stromatolitic fabrics are commonly observed in hot spring environments, with most terrestrial stromatolites associated with siliceous hot springs; however, there are also stromatolites documented at calcareous hot springs (Canet et al., 2005; Pentecost, 2005; Takashima and Kano, 2008).

1.5. Carbonate speleothems

1.5.1. Overview

Speleothems form in a very different environment to invasive tufas, however, they form similar carbonate deposits. The absence of light creates a stressed environment for many organisms and affects the relative role of biology in the formation of the deposits. This stress is analogous to the stress caused by the high pH environment of invasive tufa systems such as on Foel Fawr. Consequently, morphology may be affected in a similar way.

Whilst speleothems can be formed from a wide range of minerals under a wide range of conditions, the vast majority are formed from calcium carbonate, deposited by the same geochemical processes as tufa (see section 1.4.2.). Carbonate speleothems are most commonly formed from calcite, followed by aragonite and a selection of other minerals which often form in association with either calcite or aragonite (Hill and Forti, 1997a). The subterranean environment in which these formations are deposited creates a set of environmental pressures not experienced by subaerial tufas and travertines.

1.5.2. Geochemistry

The geochemical processes responsible for the precipitation of carbonate speleothems are the same as in subaerially deposited tufa; however, the subterranean nature of the depositional environment affects the rate and distribution of those processes. The partially closed nature of a cave system results in elevated pCO_2 (typically around 10 times) due to the continual degassing of meteoric/geologic waters entering the cave system (Hill and Forti, 1997a; Baldini, 2010). This in turn slows down degassing when compared to similar waters degassing subaerially. Cave systems also have relatively stable temperatures and close to 100% humidity, meaning depositional rates are largely controlled by dripwater composition and flow rates (Lauritzen and Lundberg, 1999).

1.5.3. Morphology and biology

Carbonate speleothems have a wide variety of morphologies, each with specific names. While some of these ‘formations’ are unique to subterranean systems, many are analogous to subaerial travertine morphologies.

The most obvious cave deposits to compare to travertines are gours or gour pools (also referred to as rimstone pools/dams), which are the subterranean equivalents of travertine terraces (Pentecost, 2005); similar morphologies are also found in siliceous sinter and ice environments (Hammer et al., 2010). Other formations are often associated with gour pools, including flowstone, shelfstone and (on the underside of overhanging gours) draperies. Analogous morphologies can be seen in travertine deposits (e.g. Pamukkale, Turkey, figure 1.5.3a).

Figure 1.5.3a. Pamukkale, Turkey. Note terraces forming on slope and draperies forming on the underside.

While the study of microbial influences on tufa and travertine formation is still in its infancy, literature pertaining to speleothems and the role of microbes is even more sparse. It is often very difficult to establish whether microbes are responsible for the precipitation of cave minerals (Northup et al., 1997; Barton et al. 2001; Jones, 2010). That said, research from tufa and travertine systems suggests that precipitation does not occur without the presence of microbes (Rogerson et al., 2008; Shiraishi et al., 2008a; Shiraishi et al., 2008b; Pedley et al., 2009). Whilst equivalent work has not been carried out to reflect subterranean depositional environments, live cells cultured from cave speleothems can induce precipitation of $CaCO_3$ (Banks et al., 2010).

Whilst it is difficult to ascertain the role of microbes in the precipitation of carbonate speleothems, they are definitely present in cave environments (Jones, 2001; Cacchio et al., 2004; Ikner et al.,

2007; Spear, 2007). Many fabrics found in caves can be inferred to be microbial (Jones, 2001), however, their importance and role in this environment is poorly understood.

1.6. Aims and objectives

This thesis aims to contextualize the deposits on Foel Fawr in relation to the broad range of terrestrial carbonates already described. Despite significant differences in the depositional environments, the deposits on Foel Fawr appear to be genetically linked to hot spring travertines and speleothems. It is suggested that this relationship is the result of parallel physico-chemical exclusion of biota within the different environments, resulting in the development of comparable facies. This relationship will be established in several ways:

1. Identify and describe the range of facies present on Foel Fawr.
2. Map the extent of and relationships between these facies.
    a. Monitor the hydrochemistry of the system and identify the hydrological regime in order to understand the physico-chemical processes occuring within the present system. Utilise these data to:characterise the pressures on biota.
    b. identify any historical change in the hydrochemical system.
3. Identify any biological influence on fabrics and the relative importance to each facies.
4. Monitor the growth and/or degradation of deposits in order to understand the temporal context of the current deposits and their future decay.
5. Analyse material from comparable facies in other invasive tufa systems and travertines.

Chapter 2: Methods

2.1. Morphological and facies analysis

2.1.1. Field mapping

Field mapping of facies and biomes forms a major part of this study. Facies were identified and mapped at a sub-metre scale across the site. In total, 12 348 m^2 of tufa, around 142 973 m^2 of quarry and kiln waste, 4 189 m of quarry faces and 7 200 m of paths and tracks were mapped. This level of mapping was undertaken over around thirty days of dedicated field mapping, combined with extra mapping undertaken during the hyrdochemical monitoring (see section 2.2.1). An iterative process was used: initial basemaps were produced from aerial imagery obtained from *getmapping plc* (pixel size: 0.25 m^2, resolvable features ~5 m [50 dpi]) and Ordnance Survey data loaded into a Geographical Information System (*ESRI ArcGIS 10*). Laminated field slips were produced and annotated in the field. These annotations were loaded into ArcGIS in order to produce more detailed maps, and these maps were further annotated to distinguish facies. Facies were distinguished based on field observations of morphology, slope, vegetation, waterways.

Further field observations were recorded, including quarry face locations, footpaths and tracks, kiln locations, kiln spoil tips, quarry spoil tips, waterways and pools. Elevation data was obtained from Natural Environment Research Council (NERC) flight BB11_01, flown on 23rd November 2011. An *Optech ALTM 3033* was used to collect high resolution LiDAR data. LiDAR data was used to produce hillshading on maps, and contours were created using *ArcGIS 10*.

Initial basemaps and field observations were georeferenced using field GPS data collected using a *Magellan eXplorist 210* GPS unit (horizontal accuracy <5 m for all collected data points). Data was incorporated into a geodatabase in *ESRI ArcGIS*, which is provided in the electronic appendix. Polygon and point data was exported into *CorelDRAW X5* and distinguished with custom fill patterns.

2.1.2. Field monitoring

Accretion experiments were run in four localities, recording accretion rates at approximately monthly intervals between 29th April 2009 and 21st April 2010. Nails were affixed using *Araldite*® epoxy resin into holes drilled into laminated crusts at three sites. The fourth site was monitored

where tufa is forming inside a cylindrical pipe; terrace width was measured using a steel rule (with 1 mm divisions). Linear growth rate was calculated utilising the following equations:

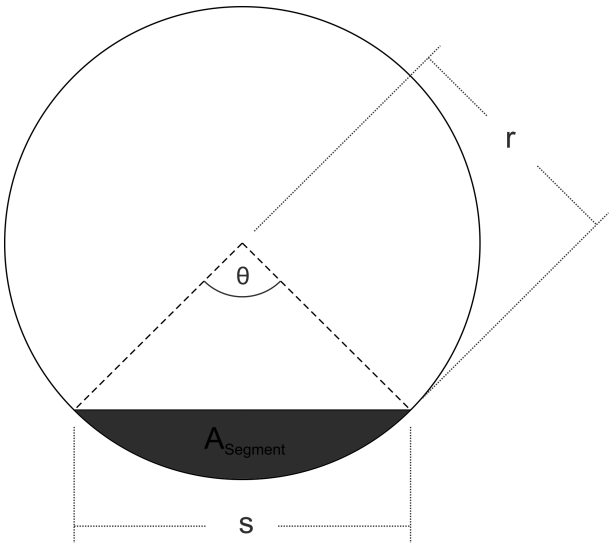

$$\theta = \left(\sin^{-1}\left(\frac{0.5s}{r}\right)\right)\cdot\left(\frac{\pi}{180}\right)$$

Where: θ = angle in radians, s = width of terrace (m), r = radius of pipe (m)

$$A_{Segment} = \frac{r^2}{2}(\theta - \sin\theta)$$

Where: $A_{Segment}$ = area of terrace (m^2), r = radius of pipe (m), θ = angle in radians

Calculated increases in terrace cross-sectional area were converted to notional linear rates of growth (converted to mm/a) based on the width of the channel downstream of the pipe.

$$Accretion = \frac{\delta A_{Segment}}{w}\cdot\frac{365.25}{t}$$

Where: Accretion = Accretion rate (m/a), $\delta A_{Segment}$ = change in area of terrace (m^2), w = width of channel (m), t = time for which $\delta A_{Segment}$ measures (days)

2.1.3. Field photography

Field photography was undertaken using a *Pentax K100D Super* camera, using a *Pentax DA 18-55mm f:3.5-5.6* lens. A *Pentax-A 50mm f:1.7* lens with extension tubes was used for macro photography. Images were auto-corrected in post processing by *Adobe Camera RAW 6.6* to remove geometric distortions and vignetting. Most images were colour corrected using either a scale card or a 60% gray card (manually adjusted colour balances are noted). All photos are by the author, unless otherwise stated. Scale providing objects have been cropped from photographs wherever possible and replaced with scalebars. Approximate scalebars are noted. Broader scale photographs may have scales calculated from field observations.

2.1.4. Light microscopy

Samples were cut, lapped and polished. A *Leica MZ16* stereomicroscope coupled with a *Leica DCF480* camera was used to image samples under reflected light.

2.1.5. Scanning electron microscopy (SEM)

Samples were crushed or broken then sputter coated with Au-Pd and mounted in the SEM. A *Veeco FEI (Philips) XL30 ESEM* (Environmental Scanning Electron Microscope) FEG (Field Emission Gun) was used with an electron beam running at 10 keV or 20 keV; a secondary electron [SE] detector was used to image samples.

The use of SEM was favoured over the use of thin section for several reasons. Previous investigations of the site had revealed the deposits to be predominantly monomineralic (Braithwaite, 1979; Emery, 2008). Consequently, identifying mineralogical differences within samples was not of interest. Owing to this and the friable nature of the material, initial investigations were undertaken using SEM analysis of fracture surfaces. These initial investigations made clear that identifying microbial fabrics by thin section would be limited by the magnification power.

2.2. Geochemical analysis

2.2.1. Hydrochemical field monitoring

An annual field monitoring program was run from 29th April 2009 to 21st April 2010, with sites monitored at approximately weekly intervals. pH, electrical conductivity (EC) and temperature were recorded along two downstream transects and from an apron(see section 3.4.2). Irregular measurements of Acid Neutralising Capacity (ANC) were also recorded from subaqueous facies.

A storm event field monitoring program was run between 1pm on 15th July 2011 and 4pm on 16th July 2011. Hydrochemical parameters (pH, EC and ANC) were monitored along a downstream transect and from a major tributary (see figures 3.4.2c and 3.4.2d).

pH, EC and temperature were measured using a multi parameter field probe (*Hanna Instruments, Model HI 98129*). The probe was two-point calibrated to pH 7 and 10 every fourth site visit (approximately monthly). Between visits, the probe was stored immersed in tap water.

ANC was measured using a digital titrator (*Hach Company, Model 16900*). 50 ml of sample was titrated in the field with 1.600N sulphuric acid (H_2SO_4) and pH was monitored using a field probe (*Hanna Instruments, Model HI 98129*). The volume of acid added and the pH were recorded at every drop of approximately 0.5 pH units. Concentrations of individual ions (OH^-, CO_3^{2-} and HCO_3^-) were calculated (or estimated where necessary) with the *United States Geological Survey Alkalinity Calculator [Version 2.21]* using the inflection point method.

Graphs of geochemical data were produced using *OriginPro 8.5*. Where custom symbols were required, graphs were output into *CorelDRAW X5* and edited manually to produce these. Scatterplots of geochemical data were produced using *Minitab 16*. Data was tested for normality using the Anderson-Darling test combined with a visual analysis of the scatterplot. Where the test was failed, data was ranked in order to use Spearman rank correlation, otherwise pearson's product-moment correlation was used. P-values for pearson's product moment were generated automatically. For Spearman rank, p-values were calculated from a table.

2.2.2. X-ray diffraction (XRD)

Samples were ground to a fine powder using an agate pestle and mortar. XRD analysis was carried out using a *Philips PW1710 Powder Diffractometer* using Cu Kα radiation at 35 kV and 40 mA, between 2 and 70 °2θ at a scan speed of 0.04 °2θ/s. From the analyses, phases were identified using *Philips PC-Identify* Software.

2.2.3. Energy dispersive x-ray spectroscopy (EDX)

Elemental analysis of SEM samples was carried out by Energy Dispersive X-ray spectroscopy (EDX), using an *Oxford Instruments INCA ENERGY* x-ray analysis system.

2.2.4. Meteorological data

RADAR rainfall data (1km resolution) was obtained from the British Atmospheric Data Centre (BADC). Data was extracted using *7-zip* and processed using *Python 2.5.2*, running on *Ubuntu 8.04 LTS*. Custom scripts used for data processing can be found in the appendix.

2.3. Biological analysis

2.3.1. Vegetation sampling

Vegetation was sampled from across the site and analysed both in field and in laboratory. Bryophyte identification was done with the aid of species keys found in Atherton et al. (2010). Vegetation communities were distinguished by visual identification of vegetation change. Judgement sampling was used to sample communities, ensuring that predominant vegetation for the mapped area was sampled.

2.3.2. Microbial imaging

Samples were collected in HDPE containers, and then placed onto glass slides with cover sheet for microscope observation. Images were collected using a *Nikon E4500* digital camera attached to the microscope.

2.3.3. Cell counts

Sediment cores were collected from several localities within a carbonate mud pool (see section 3.5.2) and split into 1 cm segments for sampling. Samples were analysed for total cell counts.

Total cell counts were made following the methodology outlined in Cragg et al. (1998). 1 cm^3 of sediment sampled from each 1 cm segment of core, placed into sterile crimp-top serum bottles, diluted with 10 ml of 0.1 μm filter sterilized formaldehyde solution and agitated for approximately an hour. 10 μl of sample was then vacuum filtered through a 0.2 μm filter. The filter was then stained with a few drops of acridine orange stain and mounted on a glass slide with cover sheet. Samples were observed under UV light with a microscope and bacterial/archaeal cells (on particle/off particle/dividing/divided) counted for each field of view until a minimum of 400 cells had been counted, or 20 fields of view had been counted (whichever came second). Each new field of view was selected randomly by moving the field of view without looking at the microscope.

2.4. Other fieldwork

Additional observations were made at several localities for direct comparison material. The following section contains a summary of the data collected at each site, for information regarding the analytical techniques utilised, refer to sections 2.1, 2.2 and 2.3.

2.4.1. Harpur Hill, Buxton, UK.

A single day was spent in the field, on 8th June 2011. Field observations and photographs were collected, as well as a limited number of samples which proved unsuitable for further analysis due to their friable nature.

2.4.2. Aberthaw Lime Kiln, Aberthaw, UK.

Two days were spent in the field on 28th October 2010 and 21st December 2010. Field observations and photographs were collected as well as a limited number of samples, which were analysed with SEM and XRD.

2.4.3. Pamukkale, Turkey.

A single day was spent in the field on 25th July 2010. Field observations and photographs were collected.

2.4.4. Terme San Giovanni, Rapolano Terme, Italy.

Two trips were made on 18th September 2009 and again on 9th September 2011. Field observations and photographs were collected. A number of samples were collected for SEM analysis.

2.4.5. Bagni San Fillipo, Italy.

A single trip was made on 8th September 2011. Field observations and photographs were collected.

Chapter 3: Results

The following chapter contains a significant volume of interlinked data and is laid out in a narrative fashion. Firstly, the facies which are to be described are defined (section 3.1.1) and then analysed in order to establish the validity of their segregation (sections 3.1.2 to 3.1.11). A summary of these facies and the relevant characters used to identify them is provided in section 3.2. The facies defined within this key are mapped for the entire extent of the site and recorded in section 3.3. For completeness advance references to these maps are made in relevant figure captions throughout section 3.1. These references are to enable the reader to locate sample sites if necessary.

Following this section, a summary of the hydrochemistry of the site is provided (section 3.4). Firstly, as a table outlining typical parameters for the subaqueous facies defined in sections 3.1 and 3.2; secondly, results demonstrating the current spatial relationships of the hydrochemical systems are considered; finally, the influence of high discharge storm events on the hydrochemistry of the system is reported.

The biology of the system is outlined in section 3.5 and the results of accretion experiments demonstrating the activity (or inactivity) of the system are presented in section 3.6. Finally, section 3.7 contains the results of comparative studies from similar invasive tufas, other lime kiln sites, as well as hot-spring travertine systems.

3.1. Facies descriptions and analyses

3.1.1. Overview and general observations

Tufa facies have been distinguished based on a classification that is readily definable in the field. Nine distinct facies are identified: aprons, stream crust, vertical aprons, carbonate mud pools, pisoidal pools, oncoids, carbonate gravel, carbonate mud and fossil tufa channels (sections 3.1.2 - 3.1.9). Facies margins often feature encrustation of plants; these marginal areas are also described (section 3.1.10). Many of the facies have diffuse boundaries, and here there is some crossover between facies. These crossovers are identified within the subsequent facies descriptions and explained (where necessary).

The geographical location of the site creates additional pressures on organisms alongside those generated by the physico-chemical system on Foel Fawr. The northern aspect restricts daylight hours for some areas, especially during the winter when solar elevation angles are low (figure 3.1.1a).

Figure 3.1.1a. The north facing aspect of the slope creates periods of shade when solar elevation angles are low. Note the shade beneath quarry faces. Photo taken October 18th 2007, 12:30, solar declination -9.63° (min -23.44°). Manually Adjusted Colour Balance (MACB). Note person to left of "Quarry" annotation for scale.

The exposed nature of the site combined with its elevation results in extended periods of frost, and the site is commonly snowcapped for weeks at a time (figure 3.1.1b).

Figure 3.1.1b. Snow covered site. Image taken from above quarry face seen in figure 3.1.1a, facing north (6th January 2010). MACB. Note A4069 to the left of image and northernmost car park (see figure 3.3.3.).

During periods of frost and snow cover, the tufa-forming waters may freeze (figure 3.1.1c) or remain liquid despite a covering of snow (figure 3.1.1d).

Figure 3.1.1c. Frozen water on the surface of tufa (24th February 2010). MACB. (Submap: East 10).

Figure 3.1.1d. Spring still flowing through snow cover (6th January 2010). MACB. (Submap: East 6).

3.1.2. Aprons

Aprons (figure 3.1.2a) form proximally to tips. Crystalline crusts are precipitated on gentle to steep (<60^{o}) slopes. They are typically covered in a thin (<1 cm) film of flowing water, but can be temporarily subaerially exposed. Plants and algal mats do not colonise the surface and there is little outflow onto surrounding vegetation.

Figure 3.1.2a. Apron facies. (Submap: East 6).

The surface of the aprons is characterised by the presence of microterracettes (figure 3.1.2b). The pools formed by these microterracettes typically contain granular carbonate mud (silt) and larger crystalline carbonate (sand).

3.1.2b. Apron facies with microterracettes/microgours covering the surface. (Submap: East 3)

Terrace size varies with slope, with larger terraces forming on gentler gradients. These are associated with areas marginal to the main channel (i.e. 1, 2, 3 [figure 3.1.2c]), where flow is discontinuous. Where flow is relatively continuous (i.e. 1a [figure 3.1.2c]), microterracette formation is reduced and a transition towards stream crust facies (see section 3.1.3) occurs.

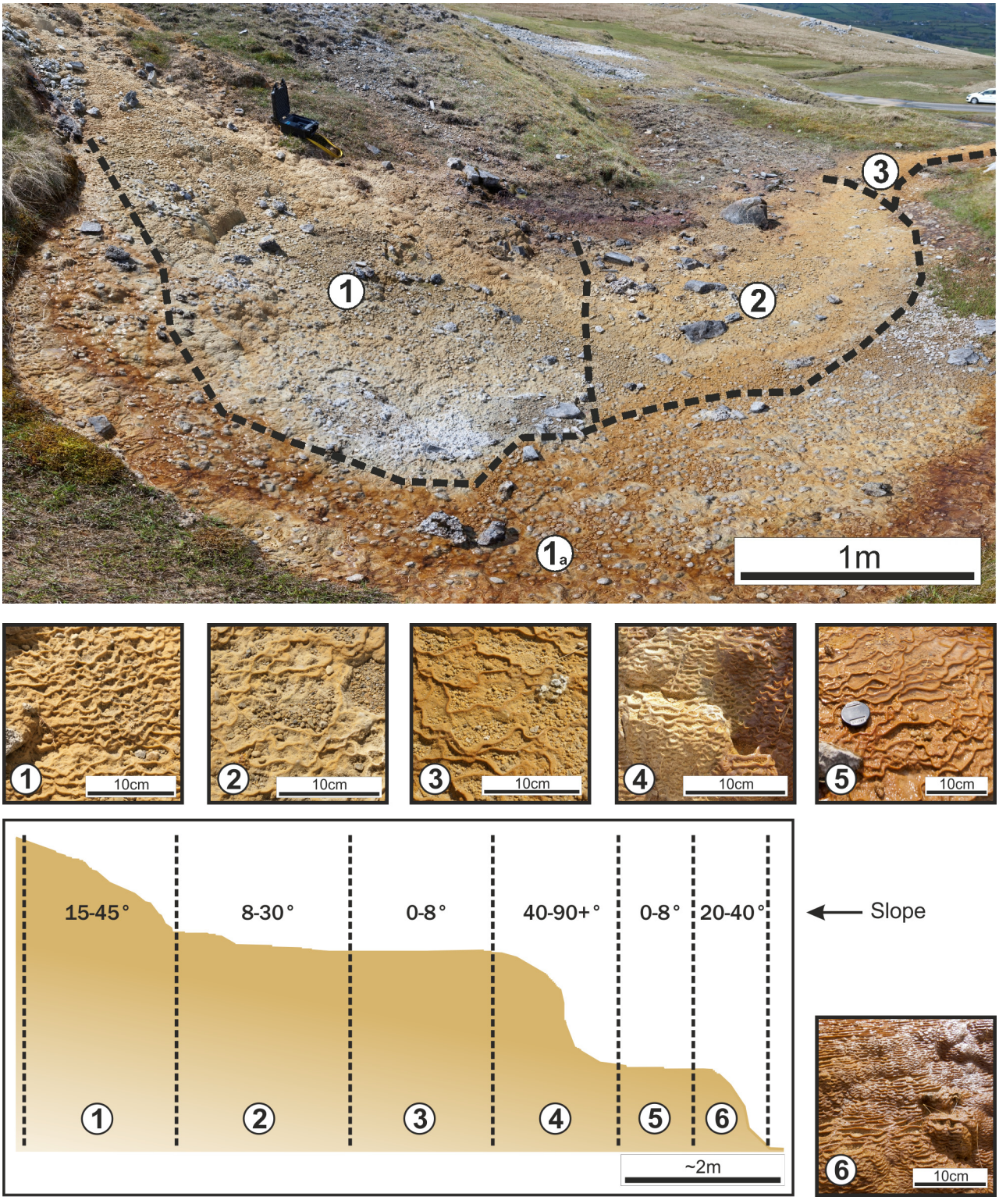

Figure 3.1.2c. Apron cross section showing variation in slope and associated change in terrace morphology. Aspect: West. MACB. (Submap: West 4)

Carbonate rafts sometimes form on the surface of pools created by microterracettes (figure 3.1.2d). The rafts are typically short-lived as they are easily disturbed by strong winds, rainfall or their own weight. Carbonate gravel (see section 3.1.8) may be washed onto the surface of aprons and accumulate in the microterracette pools (figure 3.1.2e).

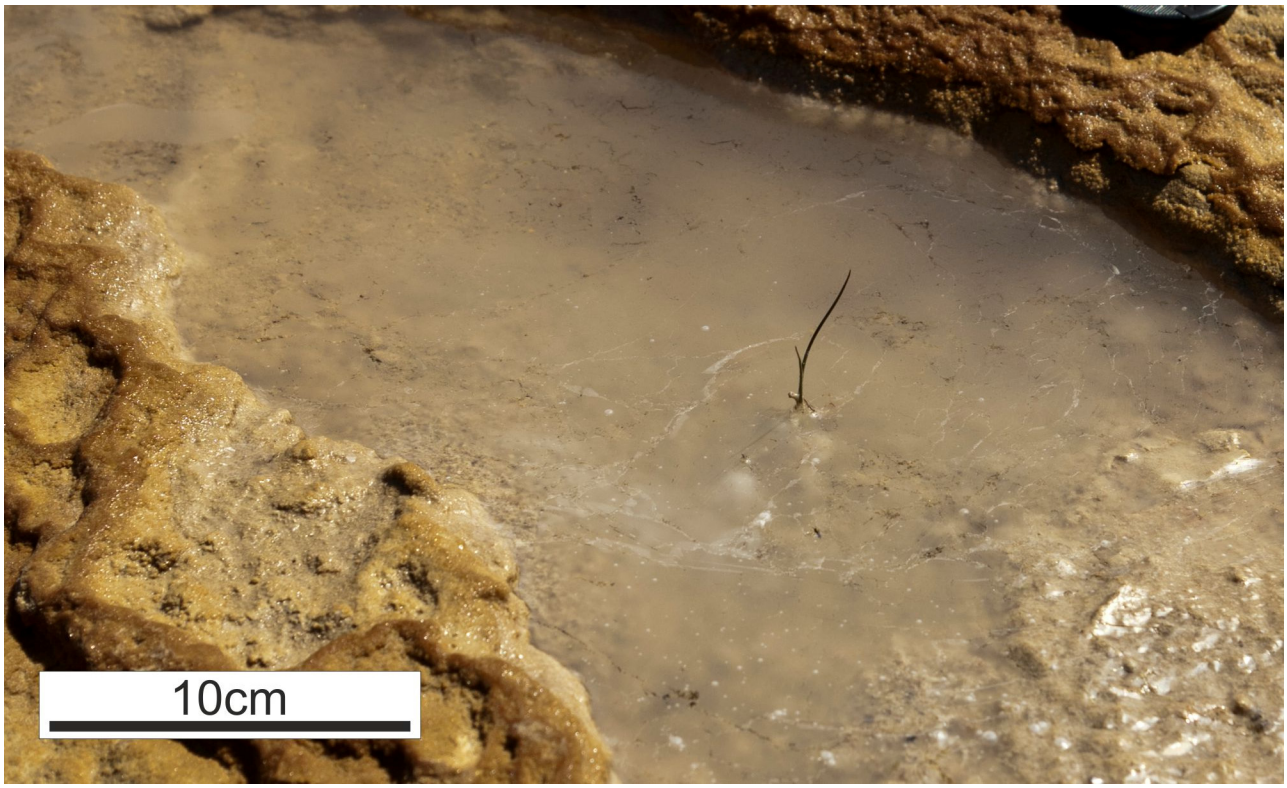

Figure 3.1.2d. Carbonate rafts forming at the air-water interface of a pool created by a microterracette. MACB. (Submap: East 3).

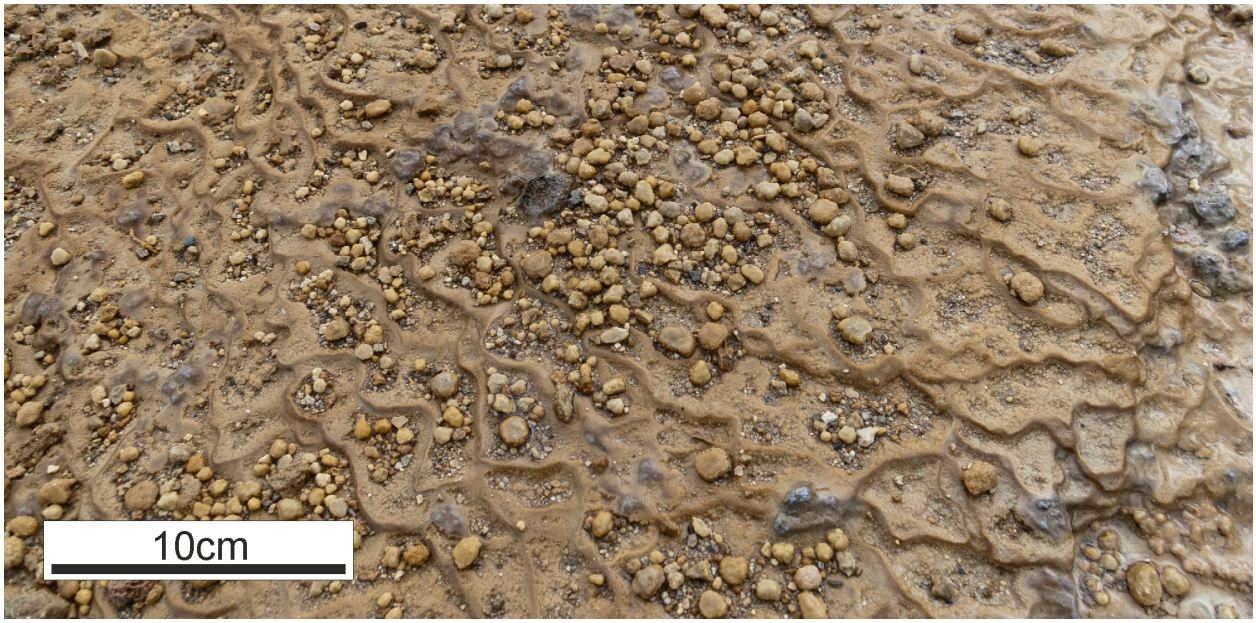

Figure 3.1.2e. Carbonate gravel (see section 3.1.8) accumulating in microterracette pools on Foel Fawr. MACB. (Submap: East 3).

Where submersion is more common, pisoids (see section 3.1.6) may form in the pools and may also become cemented into the apron (figure 3.1.2f).

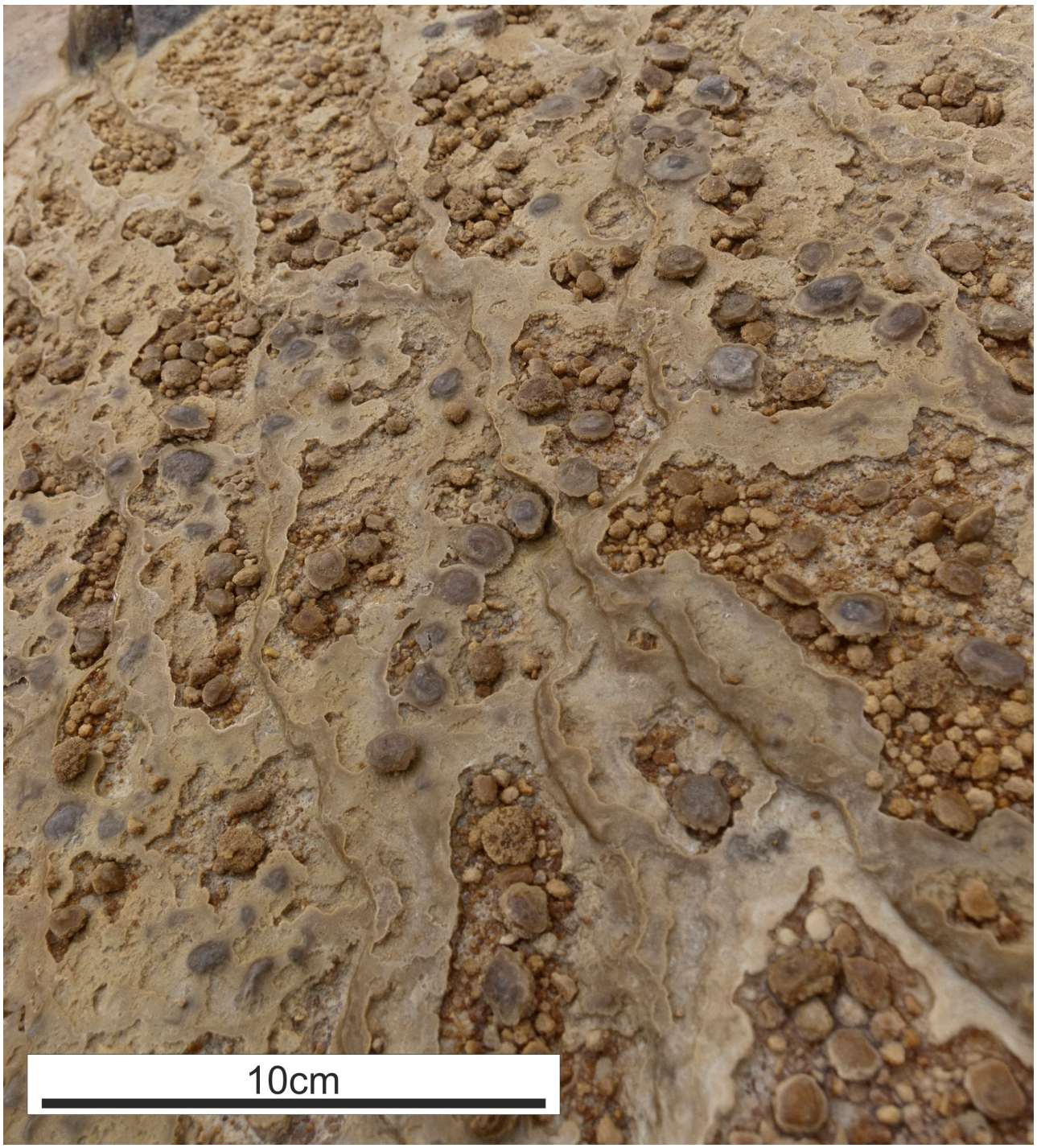

Figure 3.1.2f. Pisoids forming in microterracette pools on Foel Fawr. Note the range of cementation of pisoids into apron laminae. MACB. (Submap: East 3).

Pisoids may be preserved within aprons as they accrete (figure 3.1.2g). Where fracturing and decay of the crystalline crust occurs, small accretions of pisoids may form. The crystalline crusts are laminated, with laminae up to a few mm thick. Away from the actively flowing crusts, endolithic colonisation is evidenced by the presence of a photosynthetic pigment beneath the surface (figure 3.1.2h).

Laminations are commonly formed from anhedral elongate (~100 µm) calcite crystals (figure 3.1.2i). The crystals branch, and smaller (~10 µm) equant rhombs fill the gaps forming shrubby crystal growths. These shrub-like morphologies do not feature micritic areas; in addition EPS is not preserved and there is no direct evidence of microbial life. Of note is the fact that the smaller equant crystals appear to precede the formation of elongate crystals (figure 3.1.2j). These smaller equant crystals are likely from the pools on the surface of the apron.

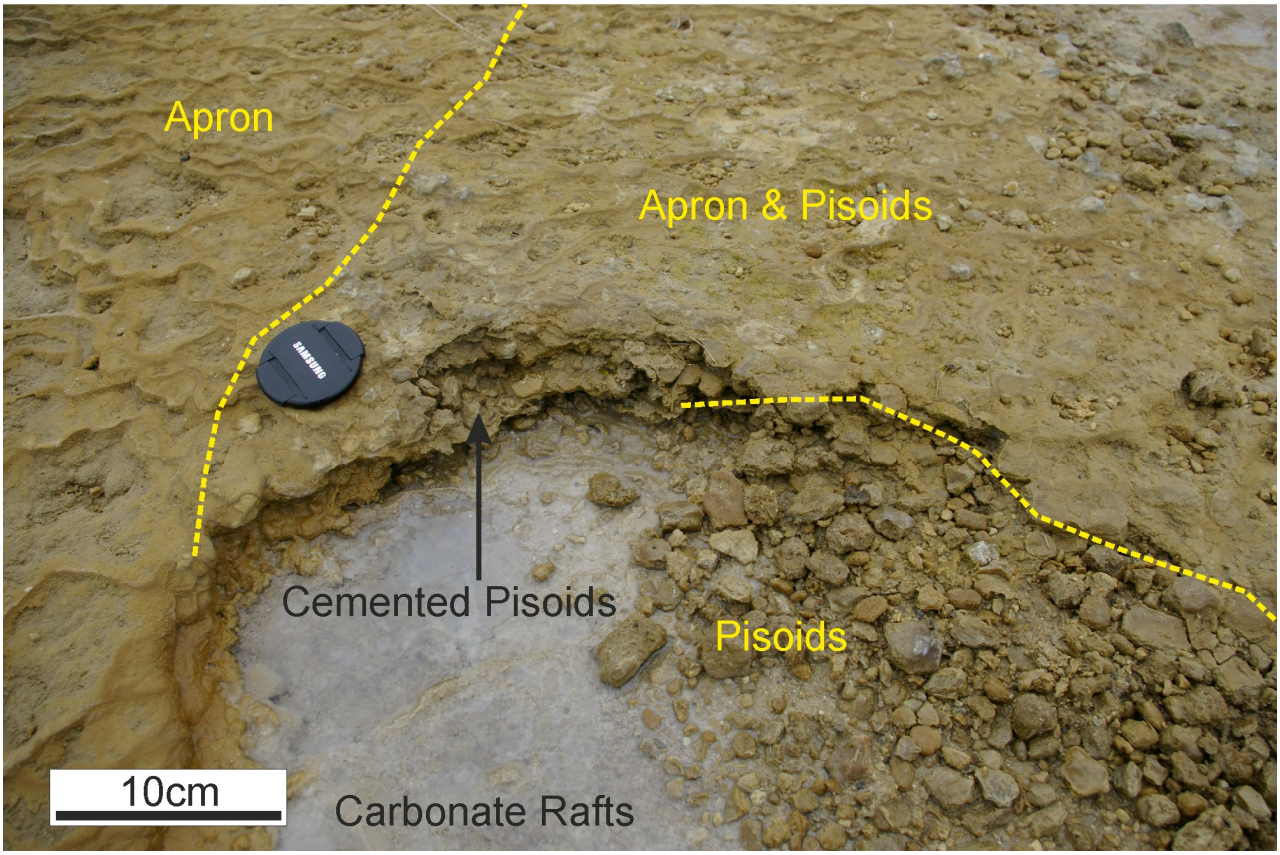

Figure 3.1.2g. Where pisoids are forming on aprons, they are preserved within the laminae (cemented pisoids). Where decay of aprons occurs (bottom right), pisoids decay more slowly, leaving small accretions. MACB. (Submap: East 3)

Figure 3.1.2h. Fracture section of subaerially exposed apron. Note photosynthetic layer absent from active portions of the apron. (Submap: East 6).

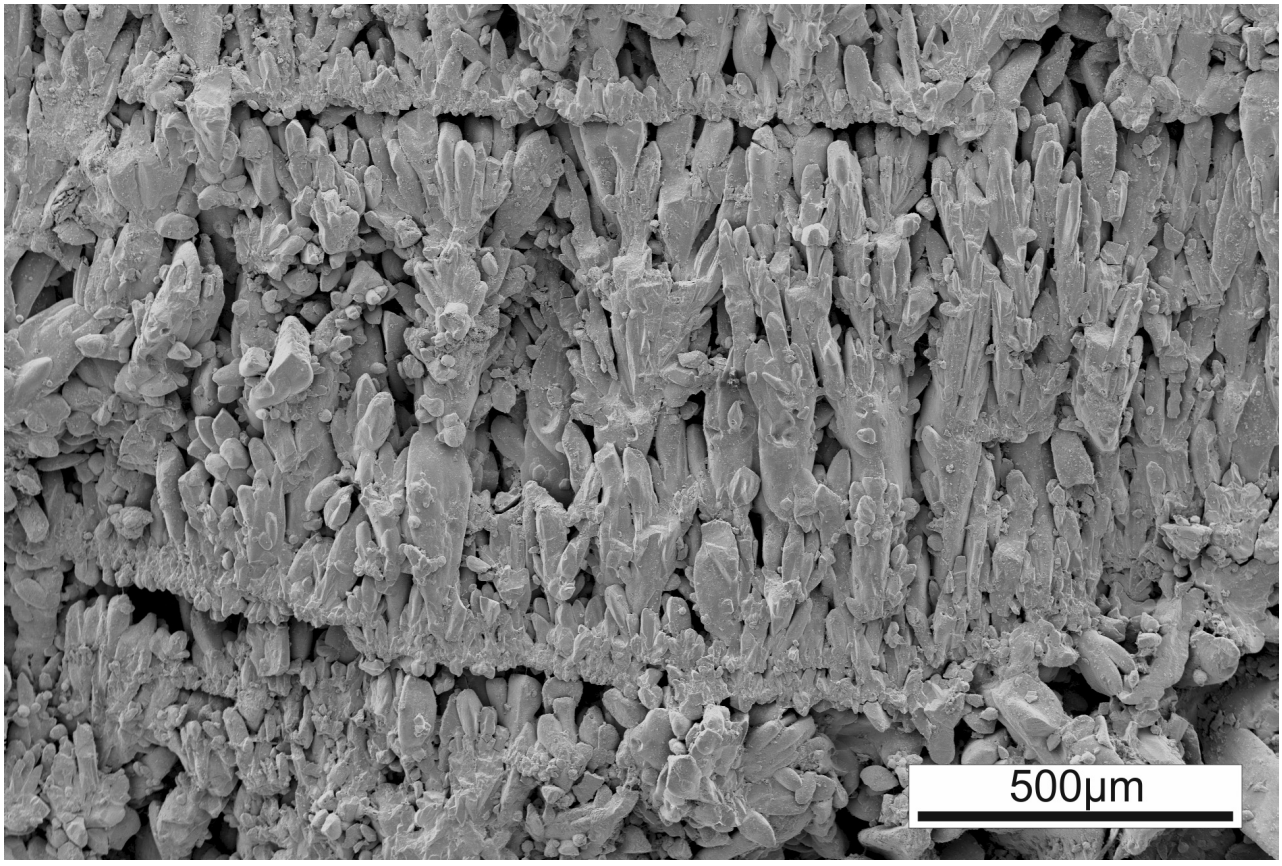

Figure 3.1.2i. Branching 'crystal shrubs'. (Submap: East 6). Stub #01.

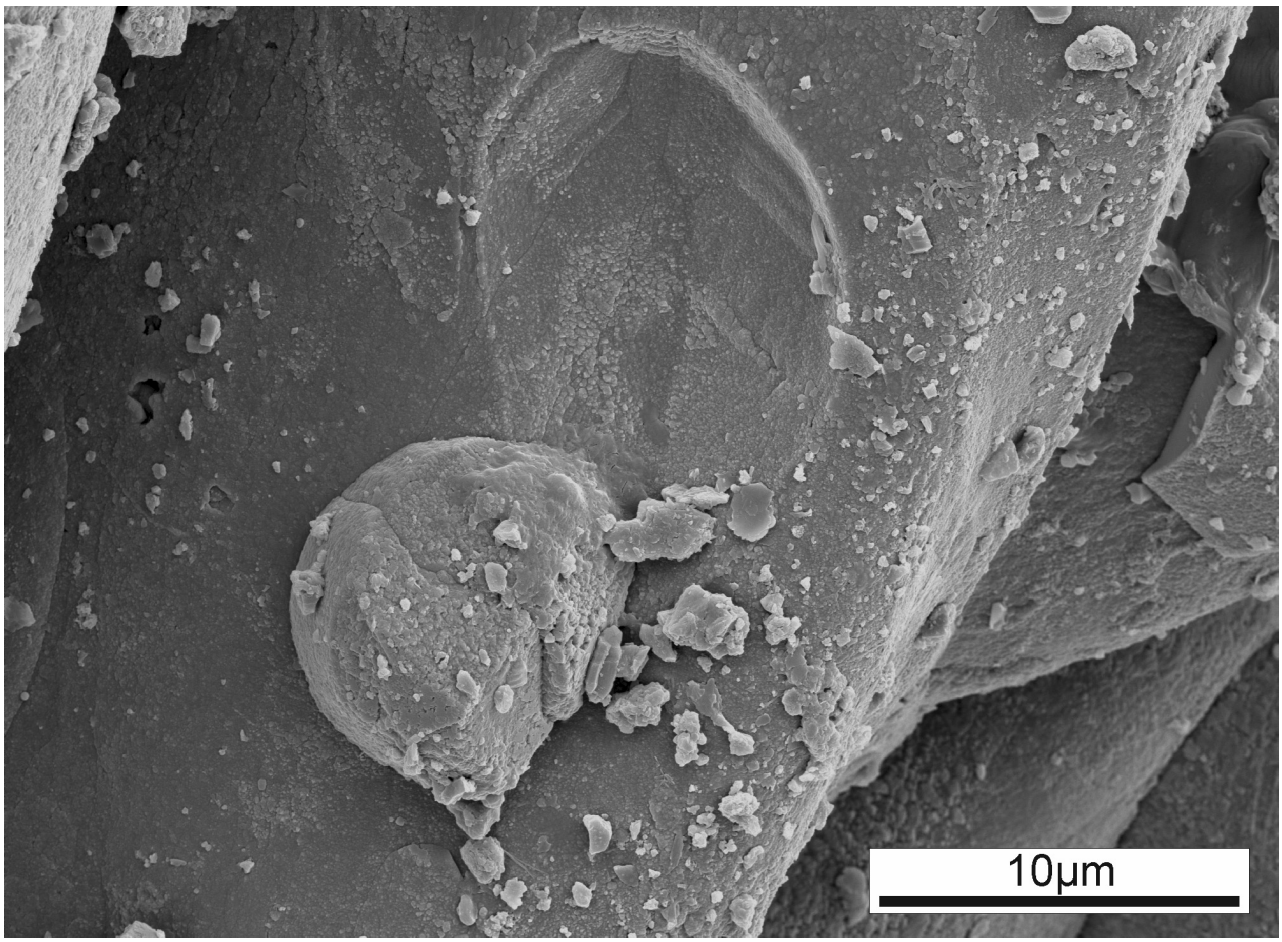

Figure 3.1.2j. Larger elongate crystal has overgrown smaller equant crystal. (Submap: East 6). Stub #01.

3.1.3. Stream crust

Stream crust (figure 3.1.3a) forms further from tips than aprons (see section 3.1.2). Crystalline crusts are precipitated on sub-vertical slopes (0-60^{o}). Water depths are often greater than 1 cm, although shallower and subaerially exposed areas are also common. Increased water depths are invariably the result of channelisation and are also associated with relatively high flow rates.

Figure 3.1.3a. Stream crust facies showing terracettes with associated pools. MACB. (Main Streamway).

The surface of stream crust may feature terracettes (figure 3.1.3b). The pools formed often contain clastic material from sand (0.0625-2 mm) to pebble (4-64 mm) size.

Figure 3.1.3b. Terracettes forming on stream crust. MACB. (Submap: East 3)

Colonisation of the surface by organisms occurs periodically (figure 3.1.3c). The biofilms often contain photosynthetic pigments and do not appear to be linked to active precipitation of tufa.

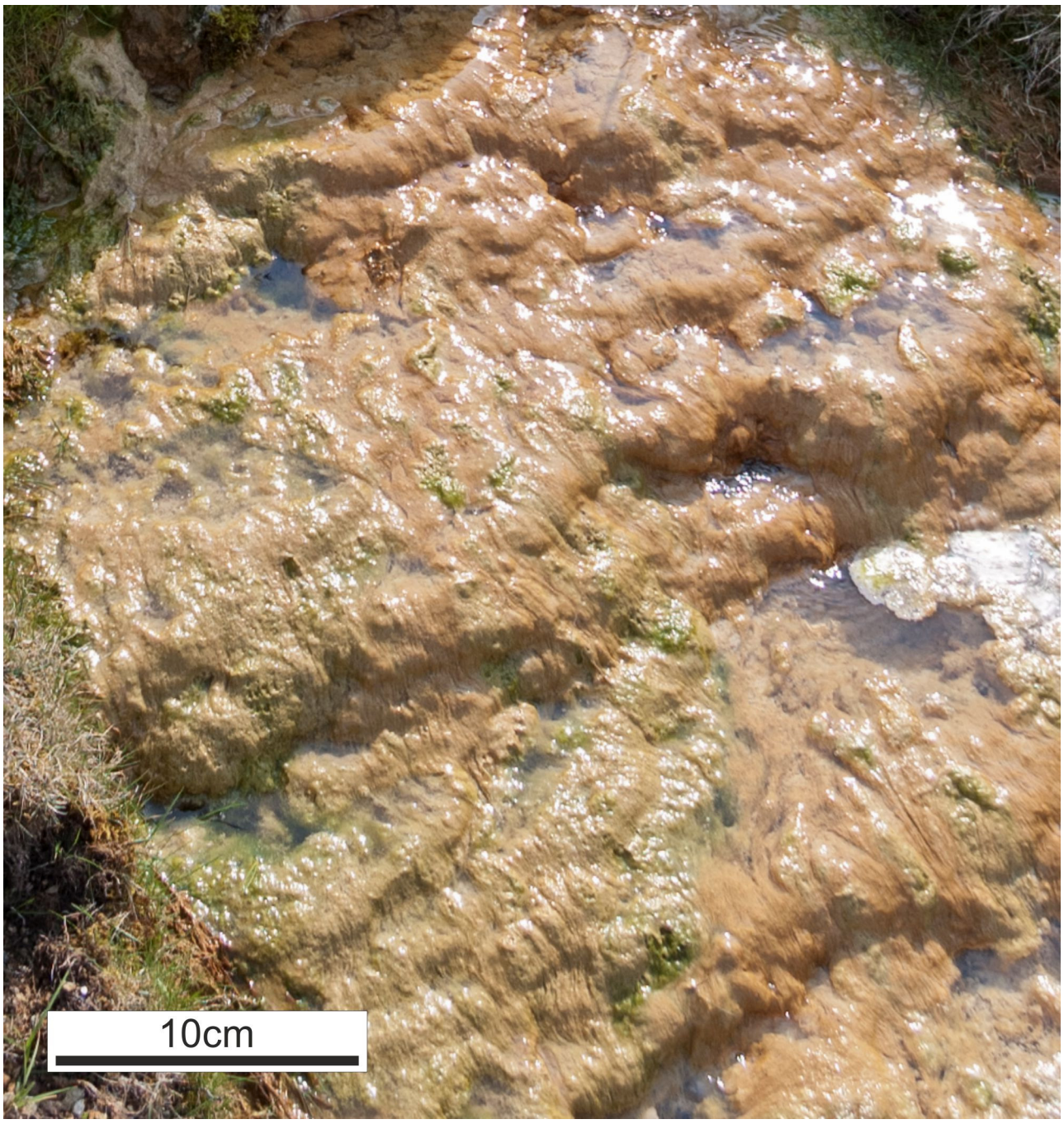

Figure 3.1.3c. Colonisation of stream crust. Note the filamentous growth and green photosynthetic pigment. Following storm events (when precipitation is active), colonisation is inhibited. MACB. (Submap: West 4)

Rapid precipitation after a storm event can generate apron-like morphology on the surface of the stream crust (figure 3.1.3d). This morphology is short-lived (<1 month) and replaced by more typical stream crust morphology as biofilms develop on the surface.

Precipitation occurs throughout the length of a tunnel (see figure 3.1.3d), apparently independent of light (figure 3.1.3e). The tunnel has accreted stream crust to the point of occlusion on two occasions since the project began (it was cleared in the intervening period). When occlusion has occurred, the water accumulates in a carbonate mud pool and overflows the road (figure 3.1.3f), precipitating carbonate mud (see section 3.1.9).

Figure 3.1.3d. Stream crust morphology varies temporally. 1: Typical morphology of smooth laminated crusts, coated by a biofilm (16/07/11). 2: Apron-like morphology with microterracettes (01/03/09). MACB. (Submap: West 4).

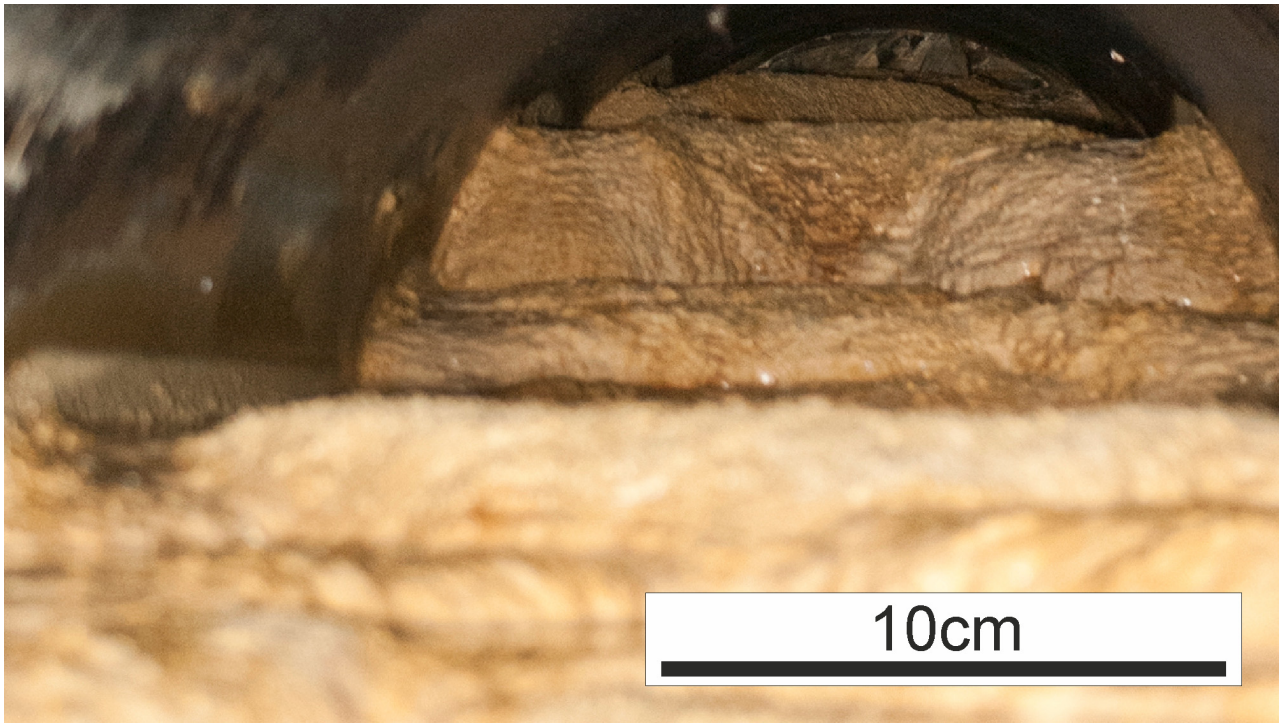

Figure 3.1.3e. Precipitation occurring throughout the length of a plastic tunnel under the road. MACB. (Submap: West 4).

Figure 3.1.3f. Overflowing of carbonate mud pool generated by occlusion of tunnel normally precipitating stream crust (see figure 3.1.3d). (Submap: West 4)

In more distal areas, decay becomes a prominent feature. Undercutting of the crust occurs, allowing erosion of the underlying sandstone. Exfoliation of the sub-aerial surface removes material and thins the crust (figure 3.1.3g).

Figure 3.1.3g. Exfoliation of laminae on stream crust becomes more common in distal areas. (Main Streamway).

Where the crust is too thin to support itself above the underlying streamway, large-scale (cm-m scale) fractures occur, ultimately resulting in the crust breaking up into large blocks (figure 3.1.3h).

Figure 3.1.3h. Breakdown of distal stream crust. Stream flows beneath the fractured crust. (Main Streamway).

Where fractured crust exposes the laminated surface, colonisation occurs between harder laminae (figure 3.1.3i), demonstrating the long-term repeated alternation between hard prismatic laminae (see figure 3.1.3k) and porous micritic laminae (see figure 3.1.3l).

Figure 3.1.3i. Fractured stream crust at the downstream end of the deposits. (Main Streamway).

Downstream, there is a change in the deposits (figure 3.1.3j). Proximally aprons often feature dense prismatic laminae. Downstream, alternating micritic laminae become more prominent.

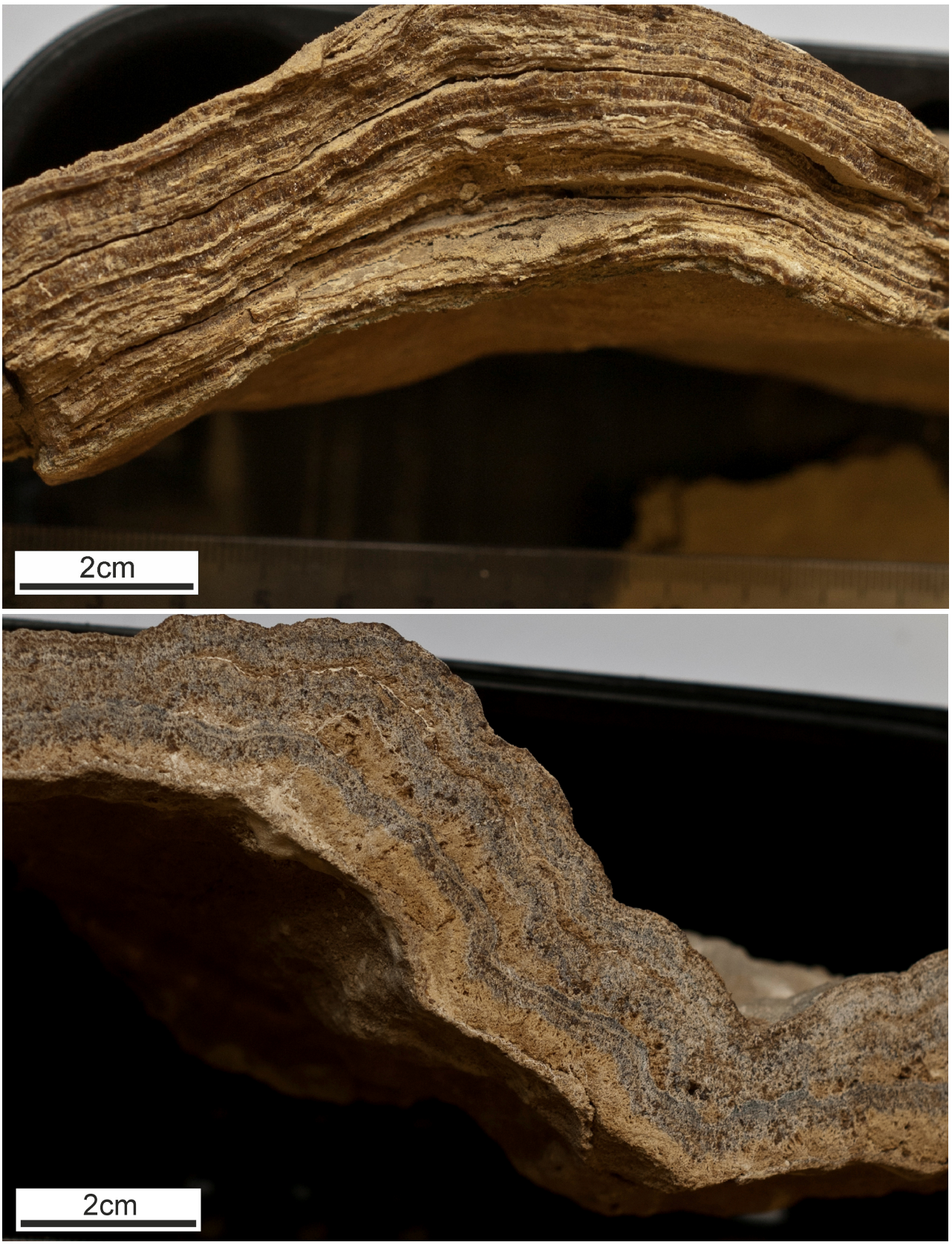

Figure 3.1.3j. Lamination of stream crust, showing repeated prismatic laminae from proximal crust (top) and alternating prismatic and micritic laminae downstream (bottom). MACB. (Main Streamway).

Laminations are typically formed from prismatic calcite with rhombohedral terminations (figure 3.1.3k). Crystals are aligned perpendicular or sub-perpendicular to the laminae. The terminations are commonly rounded suggesting rapid growth, and there are significant (10s-100s μm thick) layers of micrite and microspar interspersed between laminae.

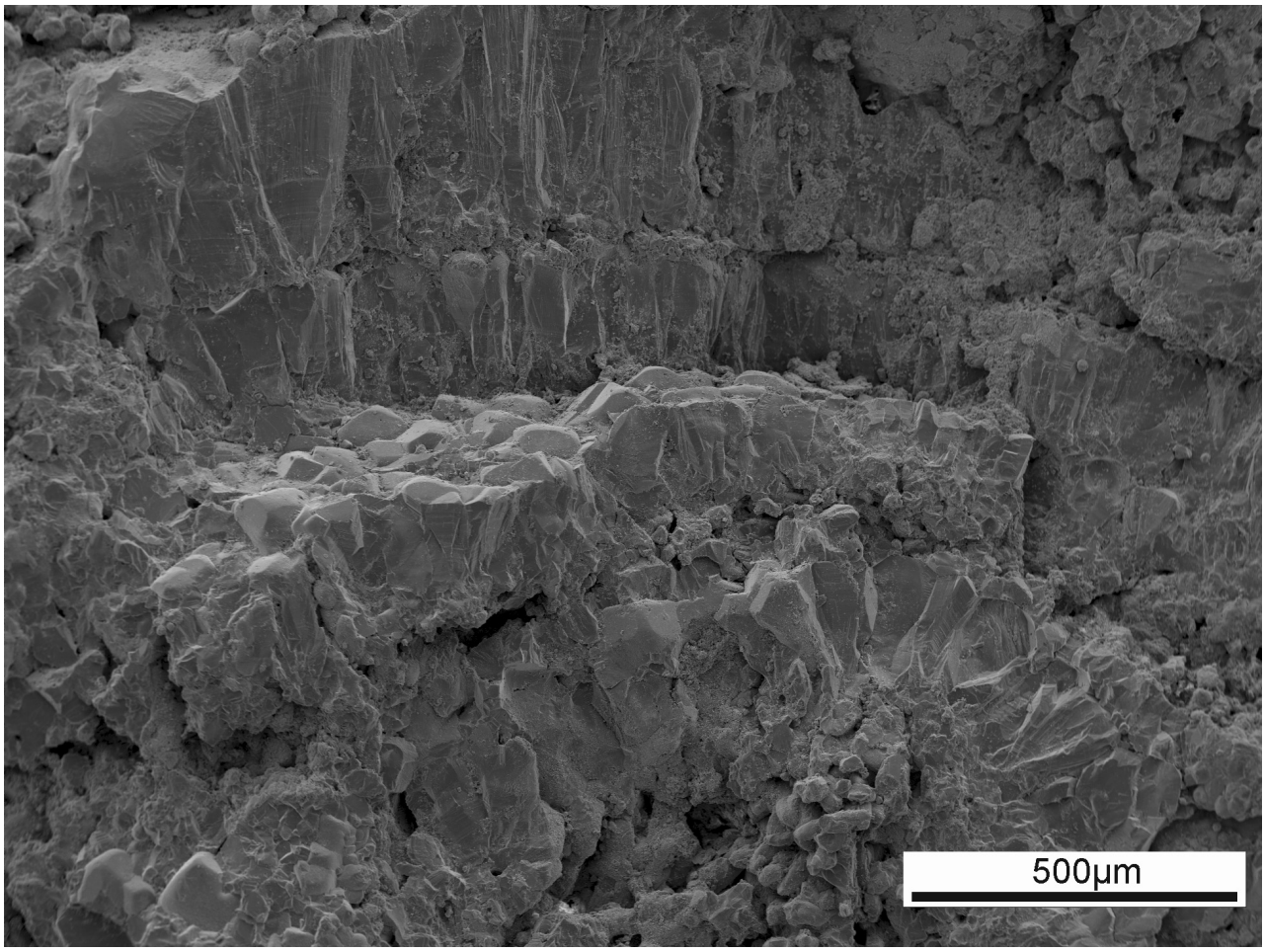

3.1.3k. Prismatic calcite laminae, with rounded rhombohedral terminations visible along the centre of the image. (Main Streamway). Stub #02.

In some parts, micrite and microspar are more extensive and not confined to thin layers between laminae (figure 3.1.3l). They are typically associated with organic filaments, pennate diatoms and extracellular polymeric substances (EPS).

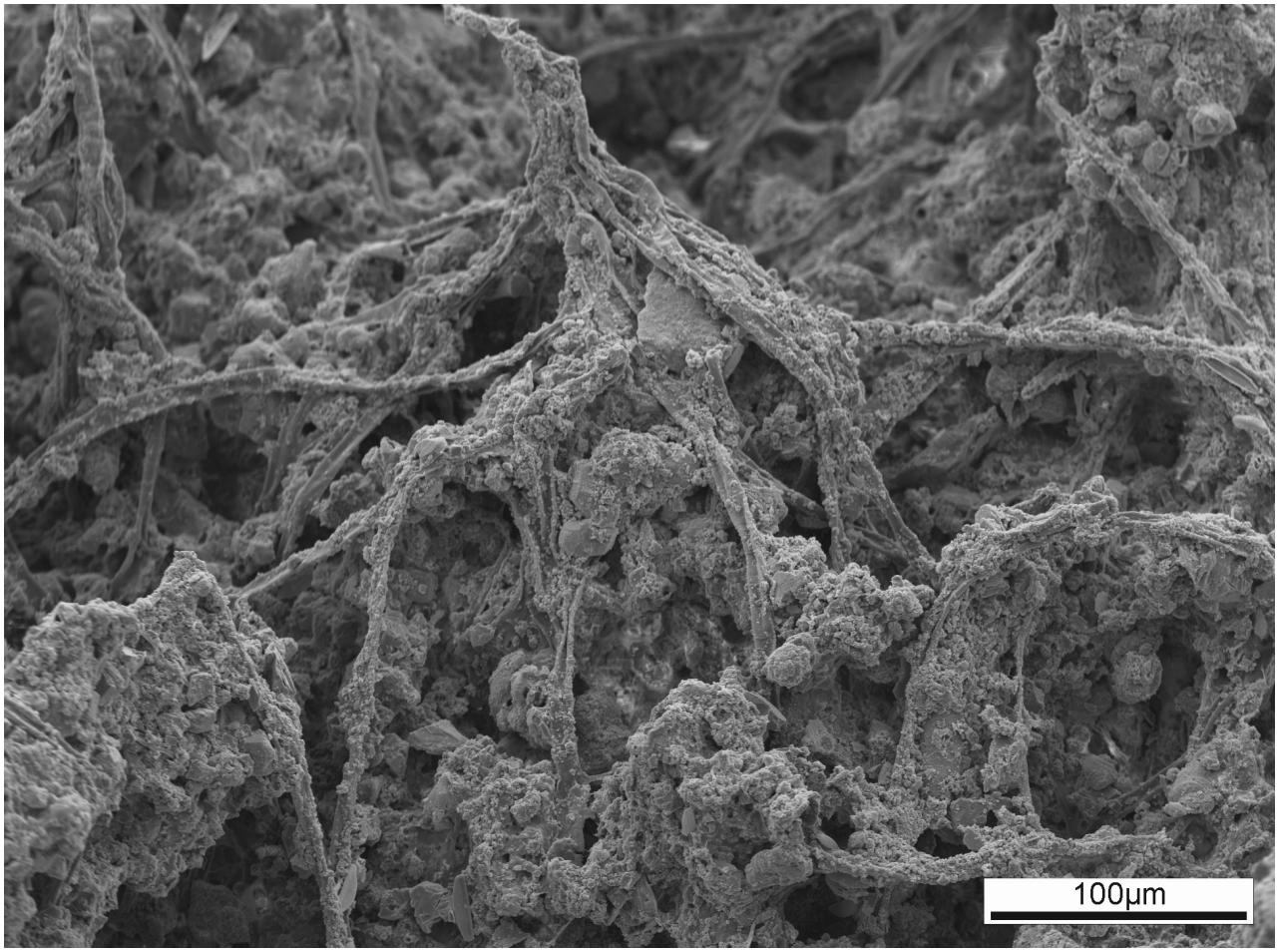

3.1.3l. Micrite, microspar and organic filaments. (Main Streamway). Stub #03.

Where rapid deposition occurs, generating apron-like morphology (see 3.1.3d.), laminations of equant euhedral/subhedral calcite rhombs are formed (figure 3.1.3m). These fabrics are not found in older deposits. Crystal terminations are rounded, likely as a result of rapid precipitation.

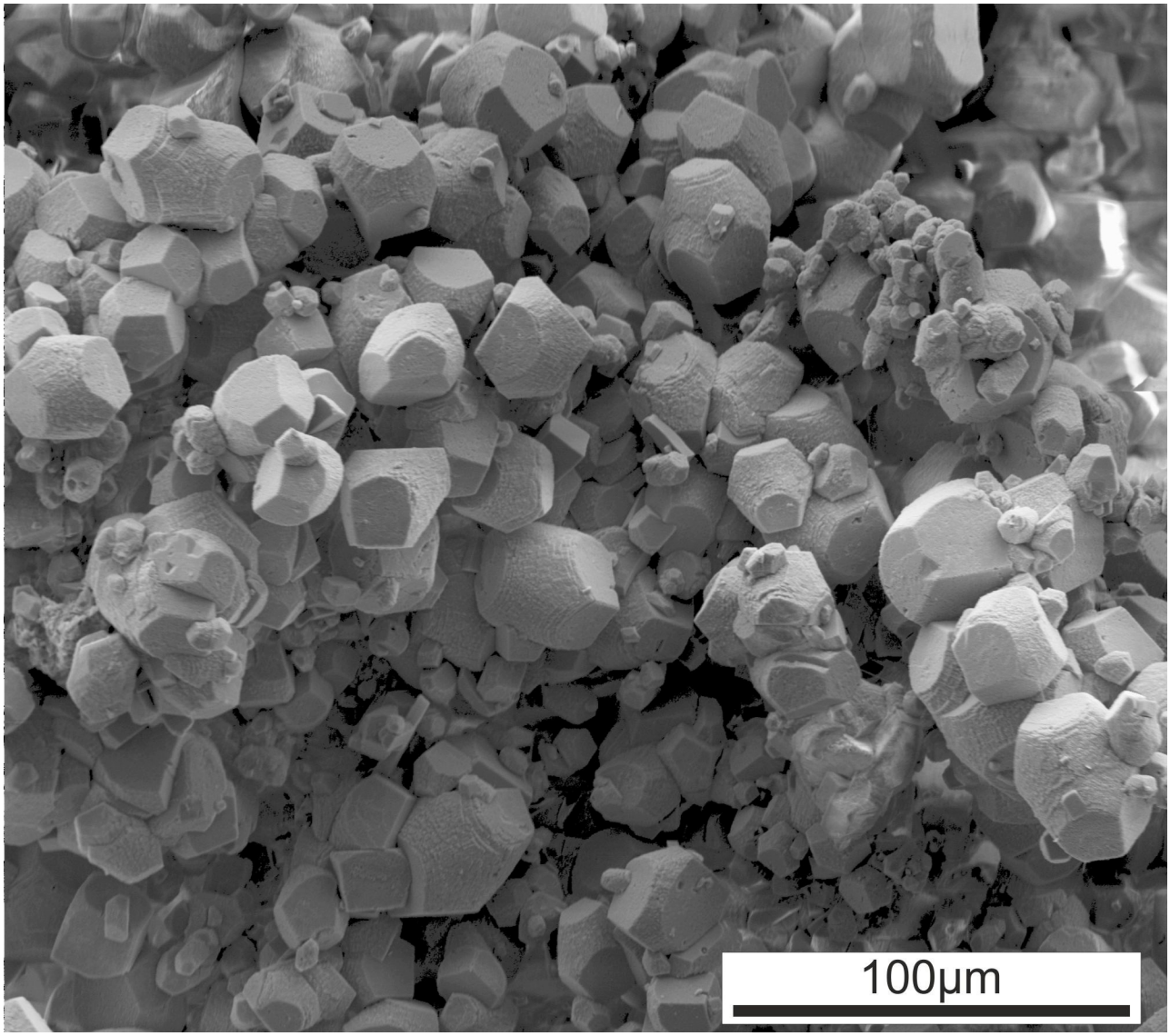

3.1.3m. Equant calcite rhombs from temporary apron-like lamina. (Submap: West 4). Stub #04.

Overgrowing trigonal crystals are common (figure 3.1.3n), forming in both recent and older deposits. These may feature euhedral crystal faces, indicative of periods of slower growth.

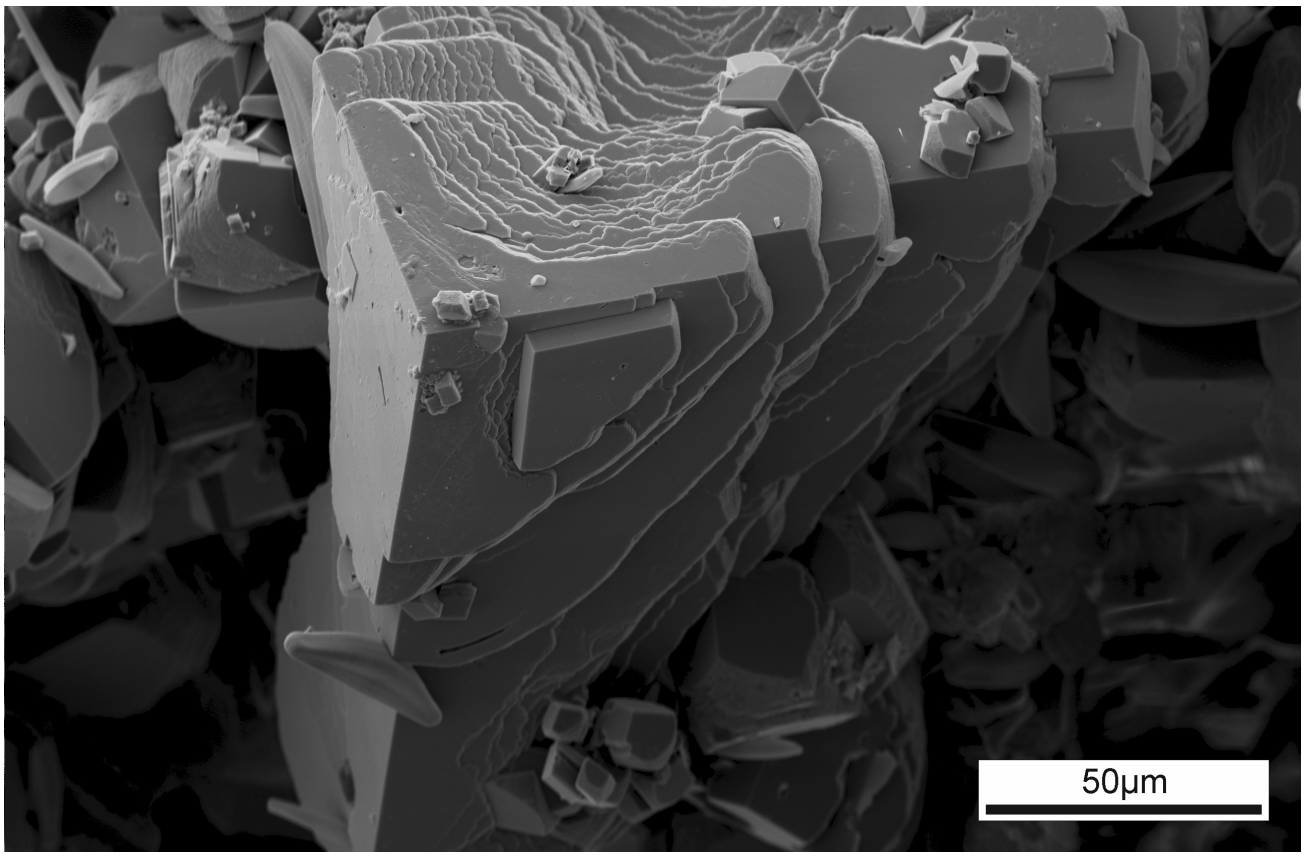

Figure 3.1.3n. Overgrowing trigonal calcite crystals. (Submap: West 4). Stub #05.

Pennate diatoms are common, especially in fresh (weeks old) deposits, although they are also preserved in older (years old) deposits. A selection of the most common species is shown in figure 3.1.3o. Centric diatoms (figure 3.1.3p) are less common, but not entirely absent. They are only observed in fresh deposits, but their apparent absence in older deposits is likely due only to scarcity. In young deposits, diatoms are found extensively and appear to interfere with crystal growth, collecting in small stepped depressions on a crystal face to form ‘diatom jacuzzis’ (figure 3.1.3q).

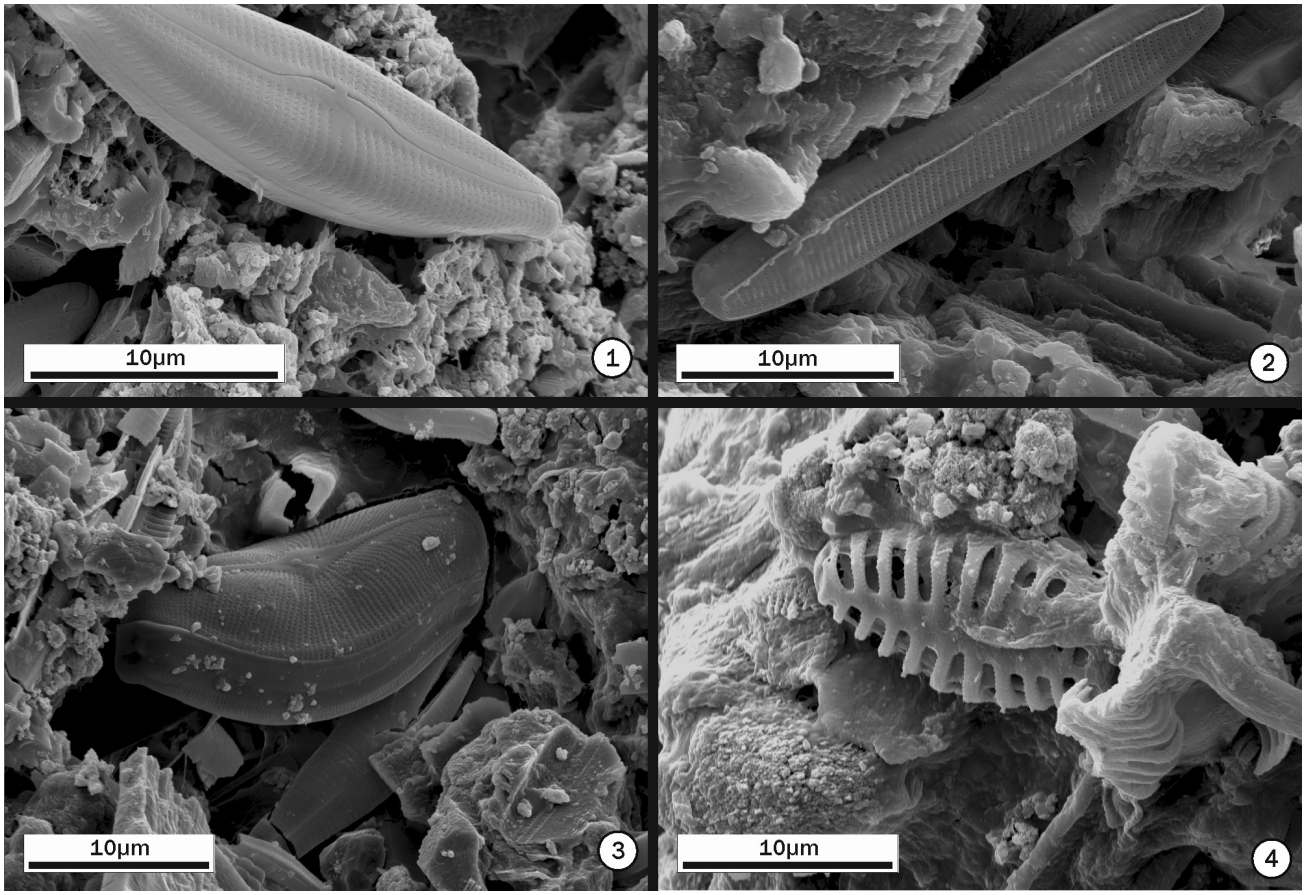

3.1.3o. Pennate diatoms. 1: Achnanthes sp. 2: Pennate diatom 3: Euccoconeis sp. 4: Planothidium delicatulum. Stubs: #03, #06, #07, #03.

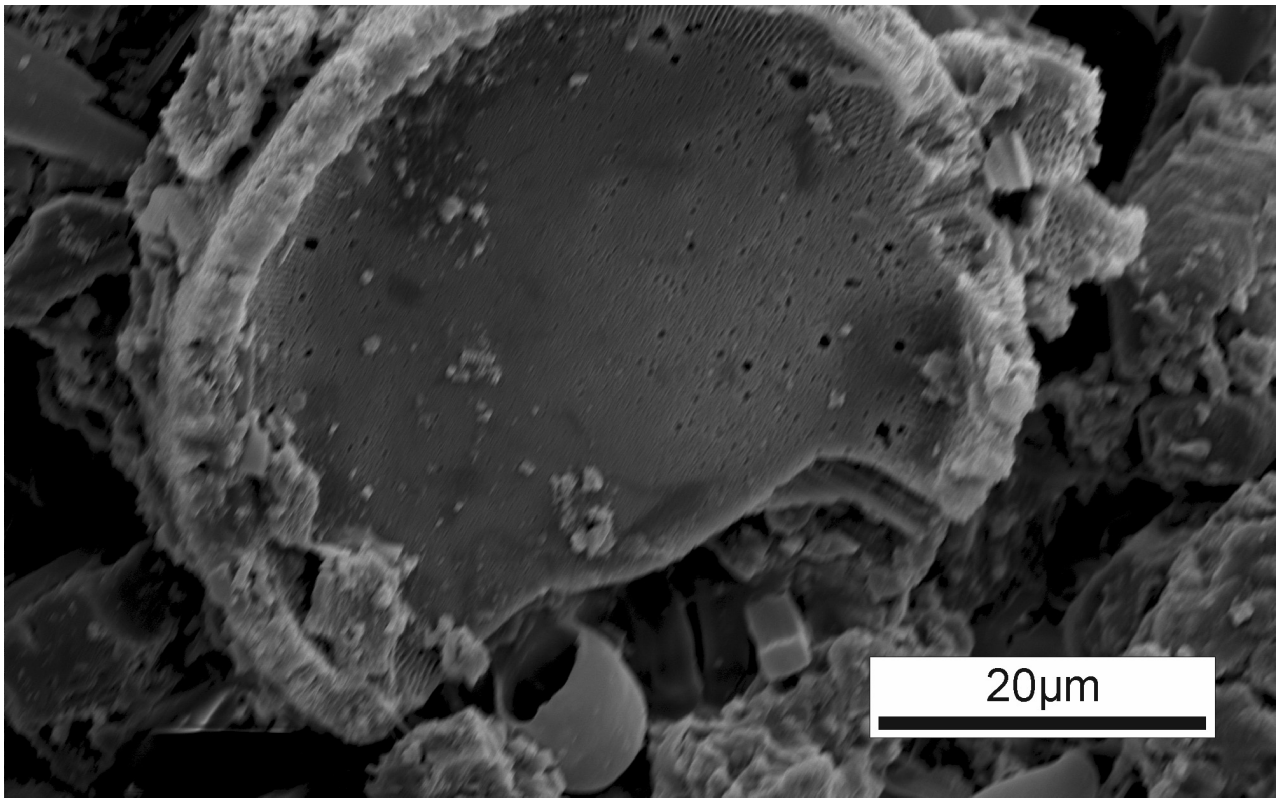

3.1.3p. Centric diatom. (Submap: West 4). Stub #07.

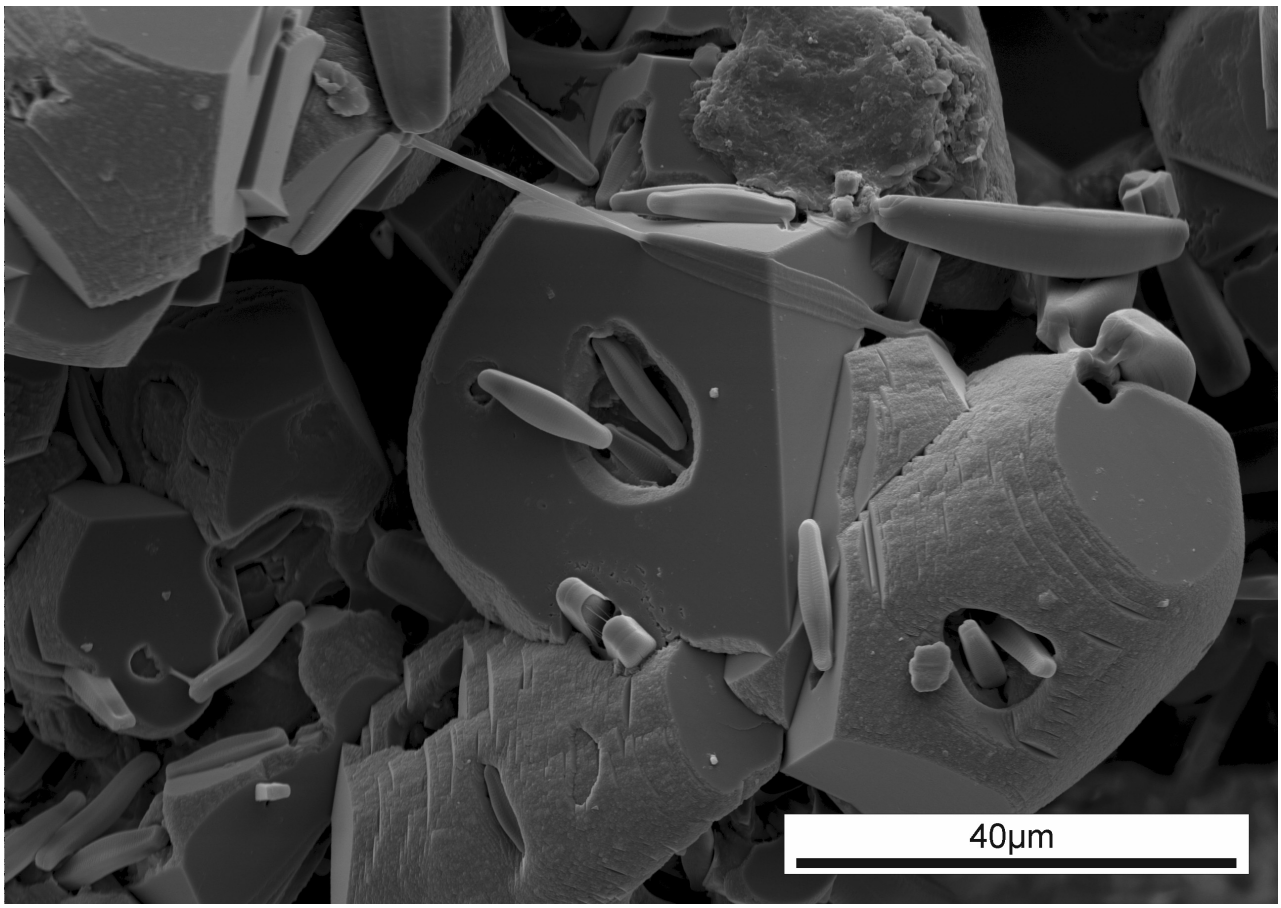

Figure 3.1.3q. 'Diatom jacuzzis' with crystals forming around diatoms. (Submap: West 4). Stub #05.

Moulds of stoma are preserved on crystal faces in young deposits (figure 3.1.3r). They are not observed in older crust. Pollen is found in micritic layers associated with stream crust, and is often well-preserved (figure 3.1.3s).

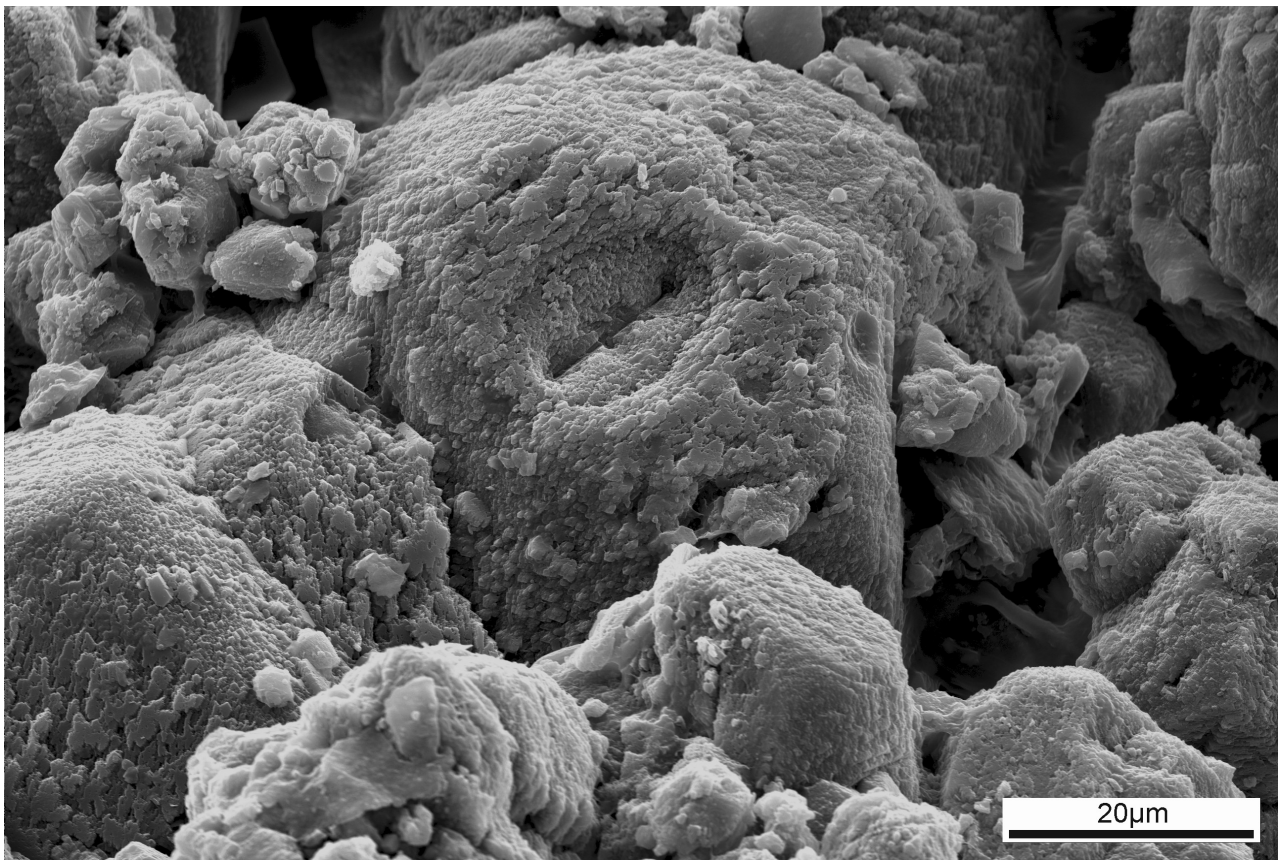

3.1.3r. Stoma preserved in young (<1 week old) stream crust. (Submap: West 4). Stub #08.

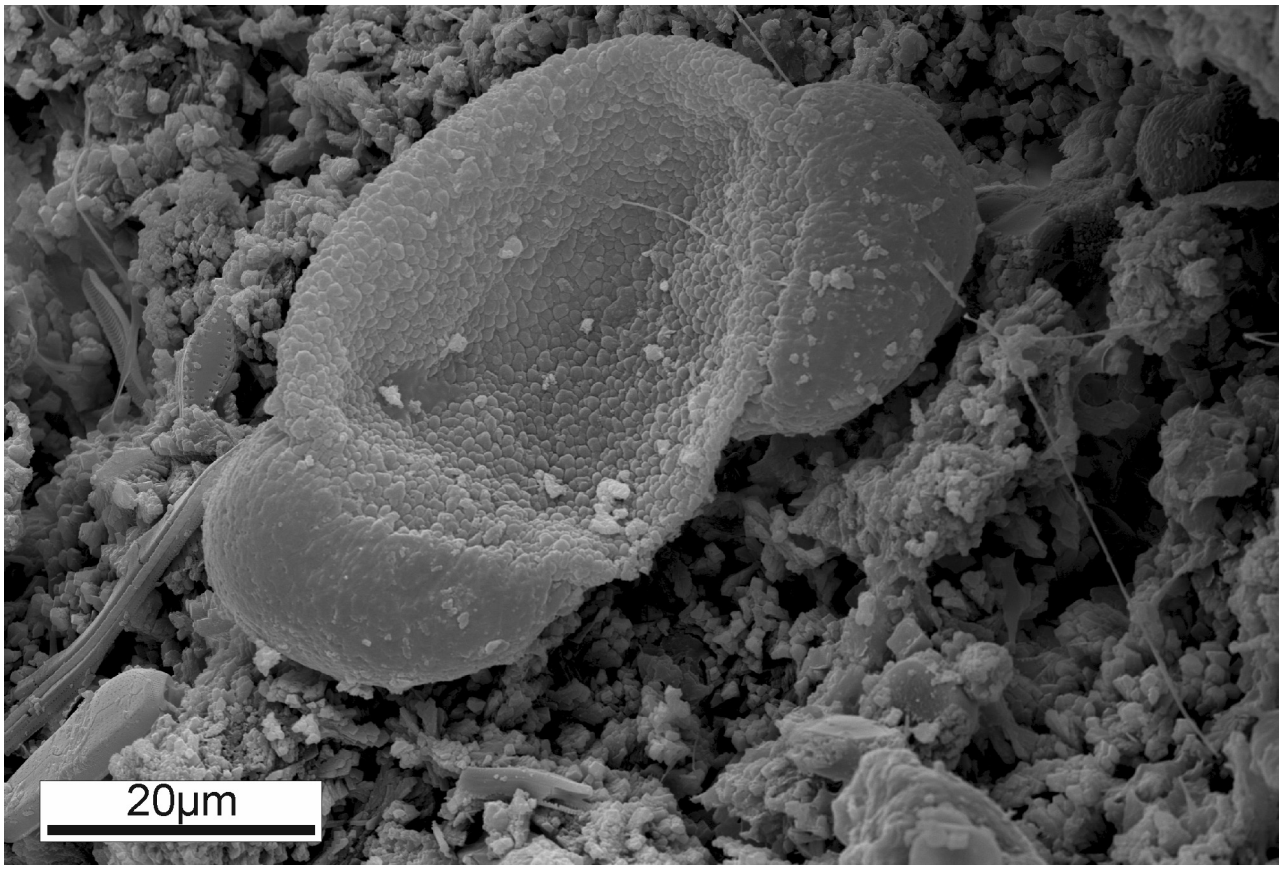

Figure 3.1.3s. Bisaccate pollen grain preserved within stream crust. (Main Streamway). Stub # 09.

3.1.4. Vertical aprons

Vertical aprons (figure 3.1.4a) form on vertical (>60^{o}) quarry faces. Crystalline crusts, sometimes featuring microterracettes or stalactitic formations, are precipitated on vertical and overhanging surfaces. They are often covered in a thin (<1 cm) film of flowing water, but can be temporarily subaerially exposed. Plants and algal mats do not colonise the surface, and marginal plants are typically not encrusted.

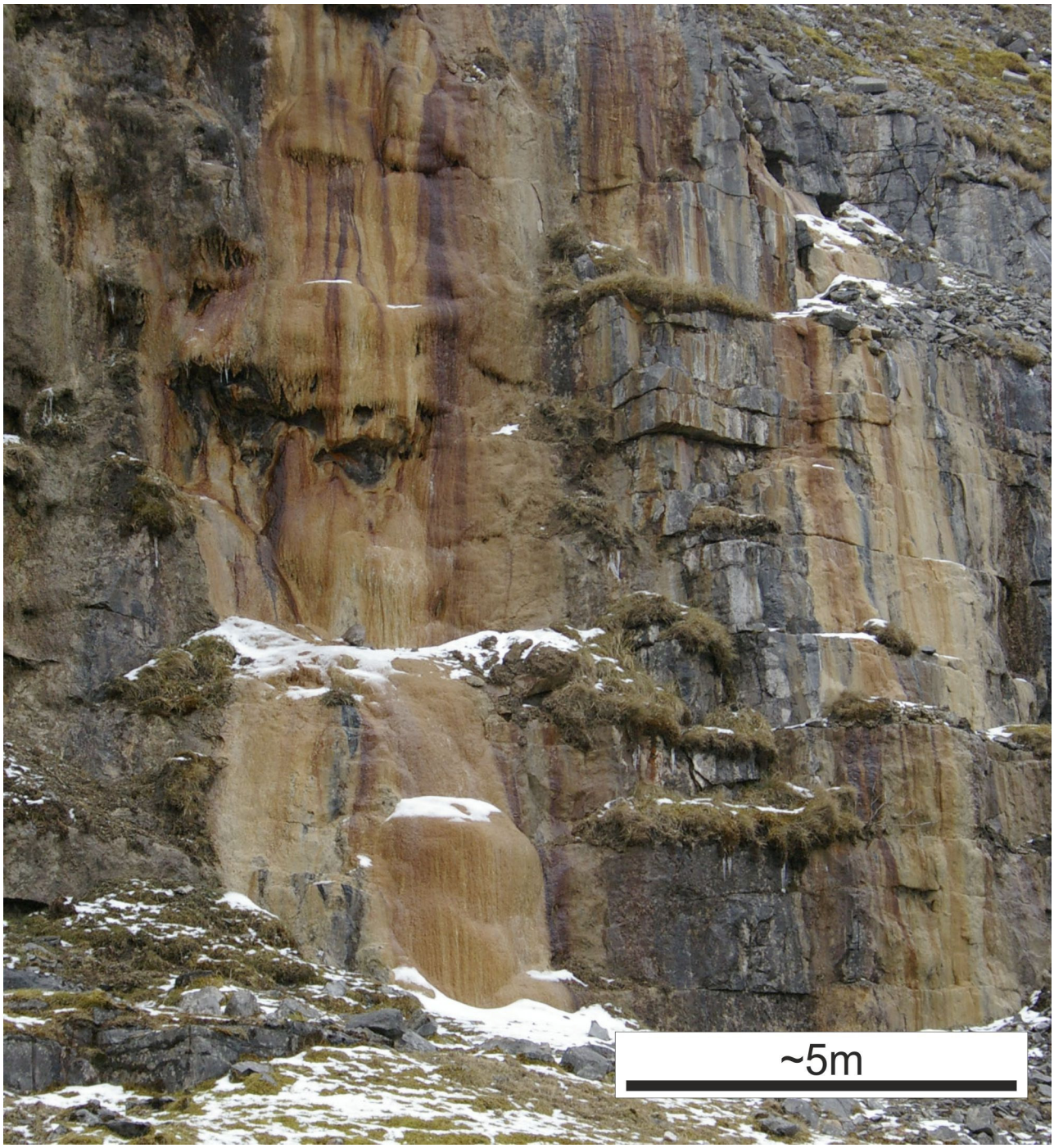

Figure 3.1.4a. Vertical apron facies. MACB. (Submap: East 10).

Often, the crust is only a few mm thick and covers a layer of detrital gravel and mud (figure 3.1.4b). This crust is readily broken, especially away from active areas; here, biofilm development accelerates the decay of the crust.

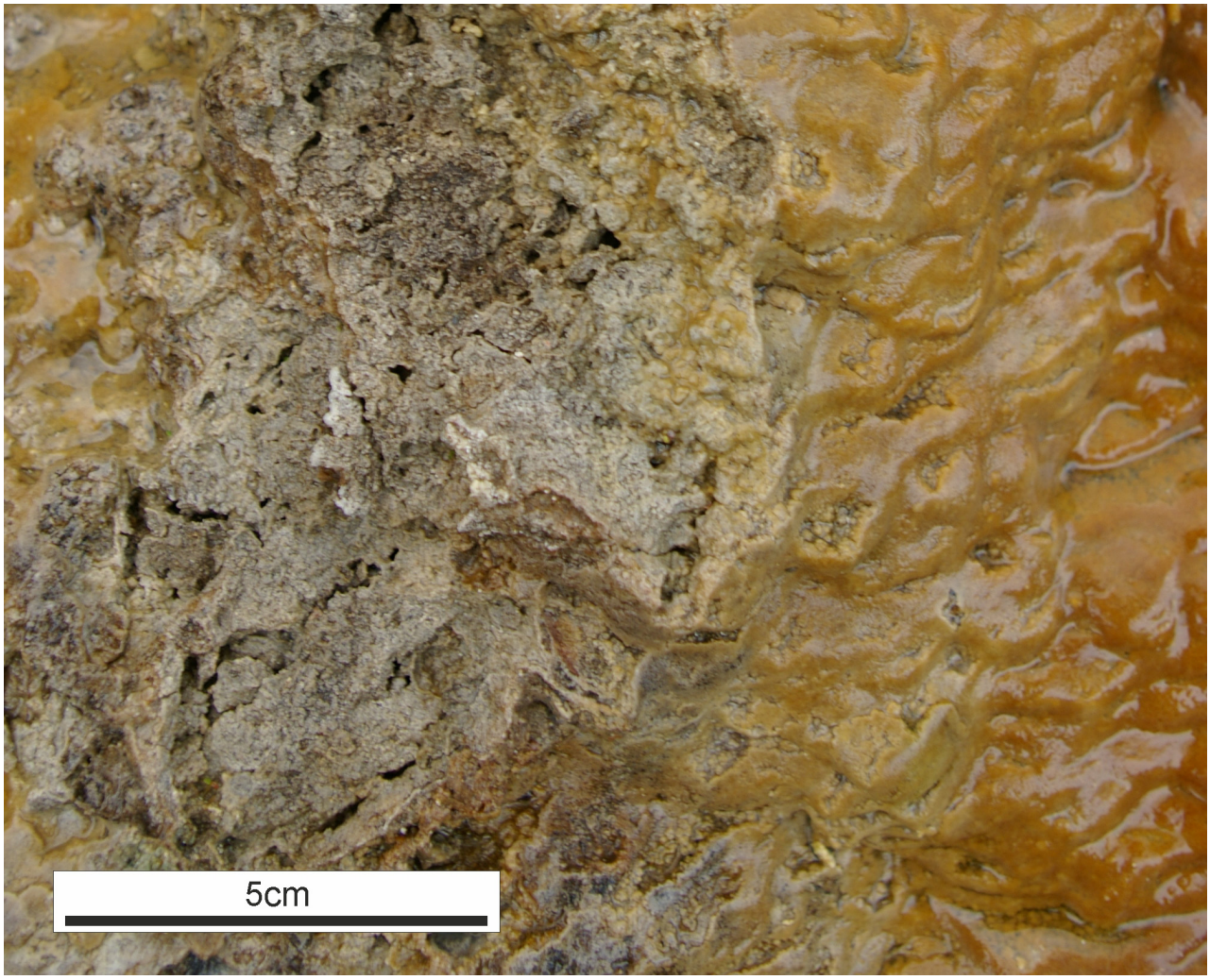

Figure 3.1.4b. Laminated surface of vertical apron. Note exposed subsurface (image left). (Submap: East 10).

The surface of the crust is typically covered with microterracettes, which are more defined on subvertical faces and transition into flatter laminations on steeper faces (figure 3.1.4c).

Figure 3.1.4c. Microterracettes forming on the surface of a vertical apron. (Submap: West 4).

Beneath overhanging parts of the cliff, stalactites form (figure 3.1.4d). The absence of large overhangs precludes the growth of large stalactites; however, they are ubiquitous where vertical aprons meet overhangs.

Figure 3.1.4d. Straw stalactites forming on the underside of an overhang. Note stalagmite forming beneath. (Submap: East 10).

Draperies also form at overhangs on vertical faces (3.1.4e). They are often associated with stalactites, which form at the base.

Figure 3.1.4e. Draperies forming on the underside of an overhang. (Submap: East 10).

3.1.5. Carbonate mud pools

Carbonate mud pools form proximally to tips (figure 3.1.5a). Carbonate mud is precipitated on level ground (~0^{o}) at the base of shallow pools (<20 cm). Plants occasionally colonise small areas and can be encrusted on the margins.

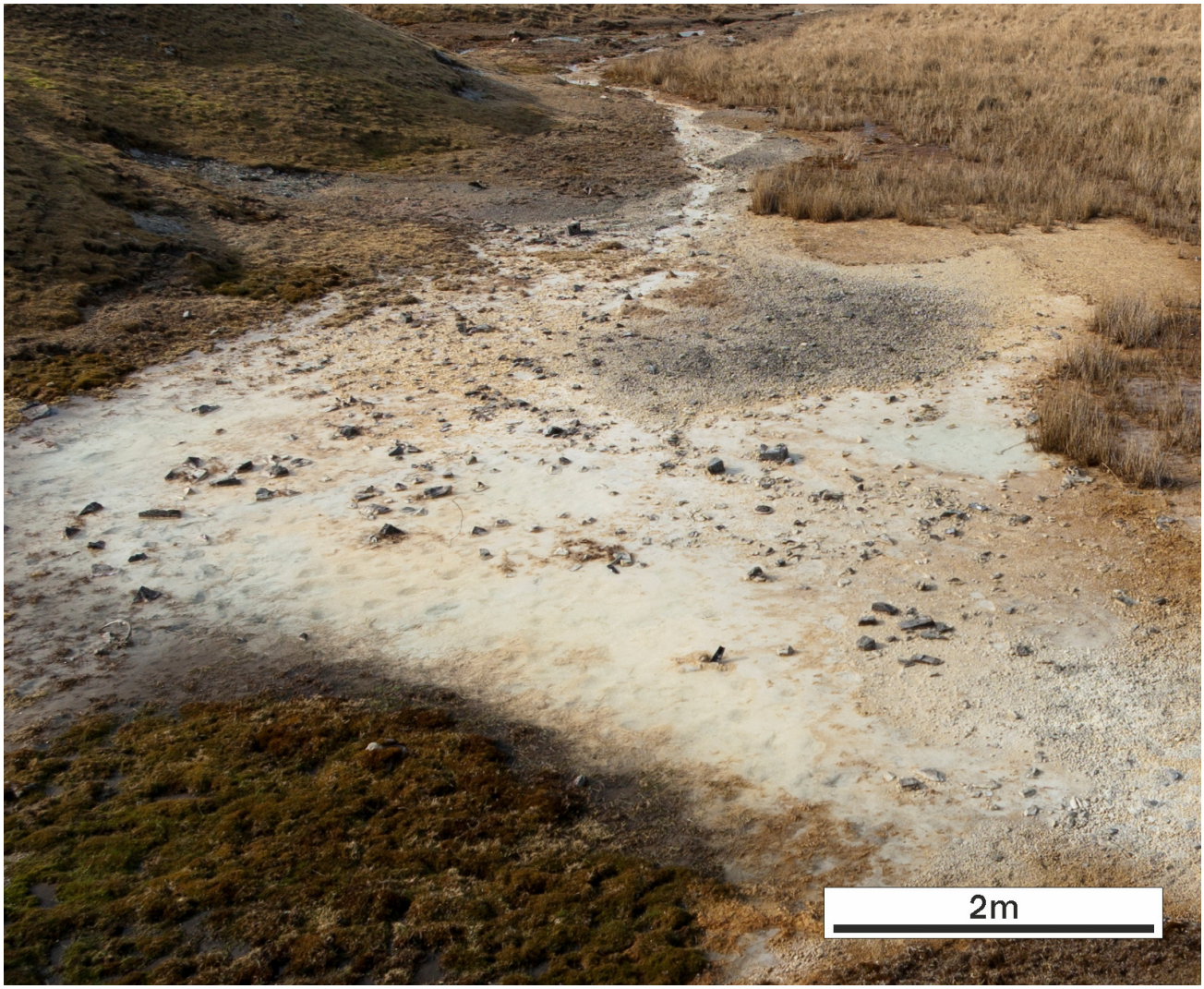

Figure 3.1.5a. Carbonate mud pool facies. (Submap: East 4).

Carbonate rafts are precipitated at the air-water interface, often coalescing into a complete covering of a pool (figure 3.1.5b).

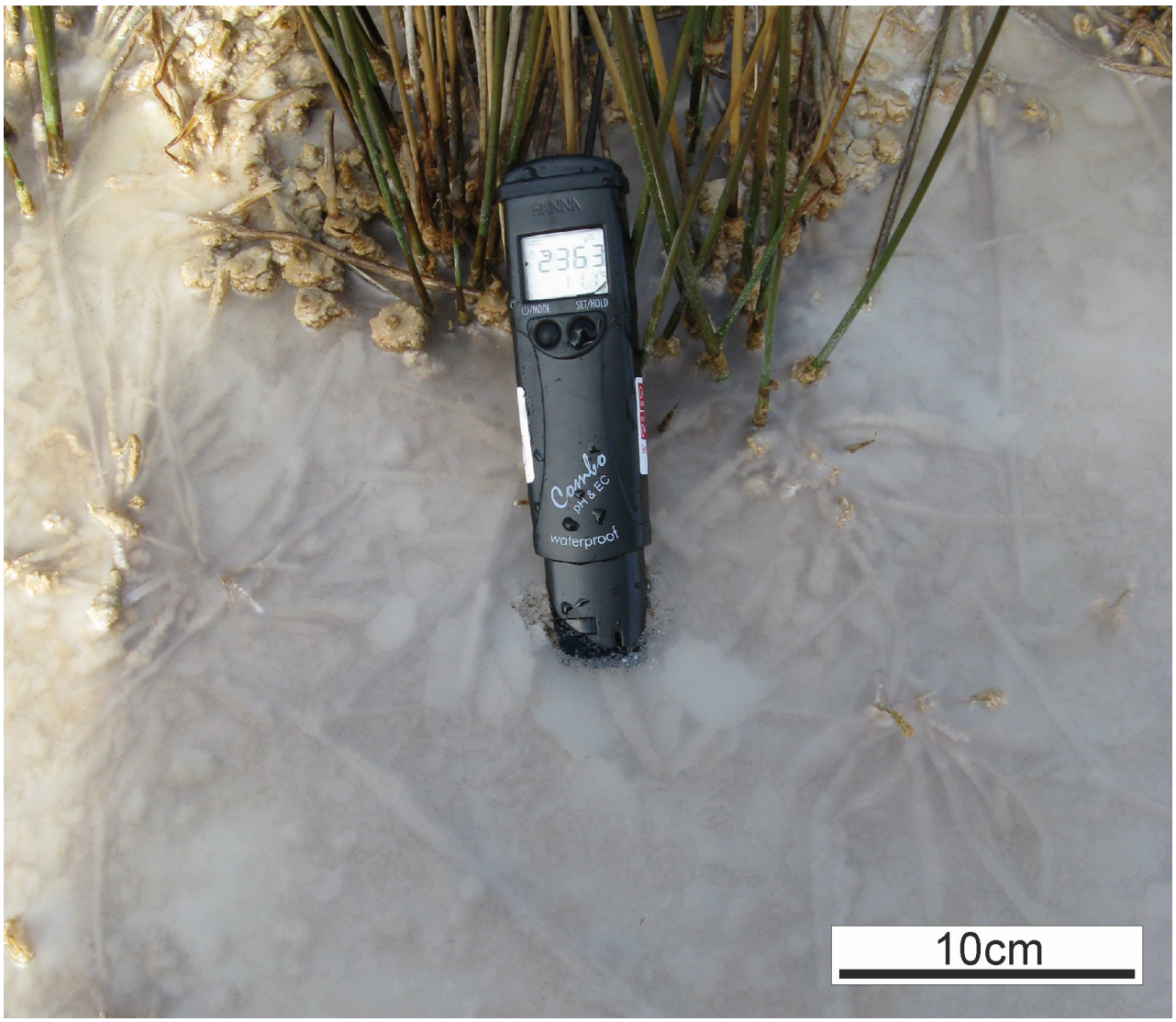

Figure 3.1.5b. Carbonate rafts forming at the air-water interface in a carbonate mud pool. Note fracturing where pH meter has broken the surface and encrusted *Juncus* stems on pool margin. Note electrical conductivity on meter: 2363 µS.cm^{-1} (moderately elevated for this site [see figure 3.4.1f]) (Submap: East 4).

Sediment at the base of carbonate mud pools appears to be micritic (figure 3.1.5c).

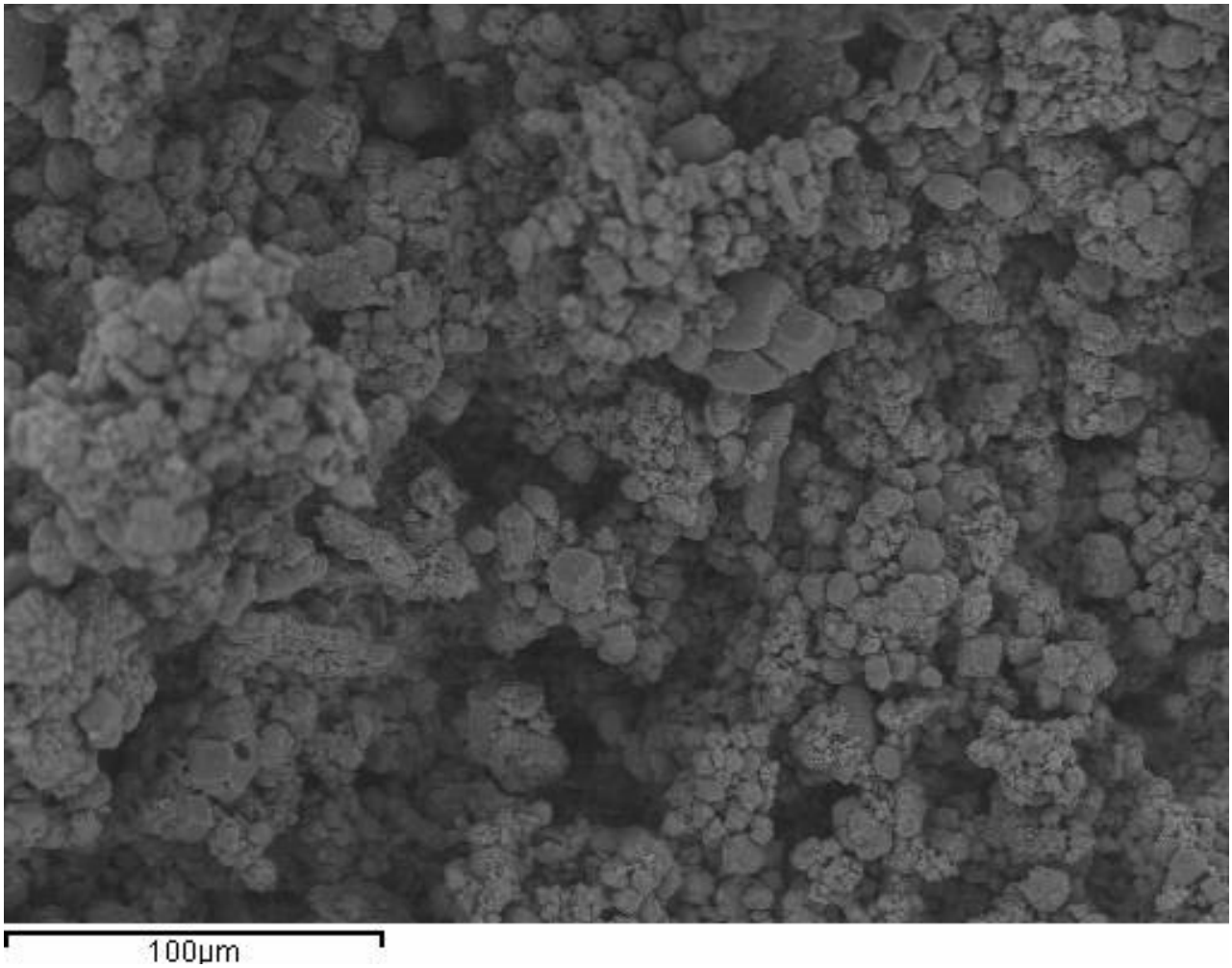

Figure 3.1.5c. Micrite precipitated in a carbonate mud pool. (Submap: East 4). Stub #10.

Fragments of carbonate rafts may be preserved within the micrite (figure 3.1.5d). Note the radial growth of crystals, growing in a single plane.

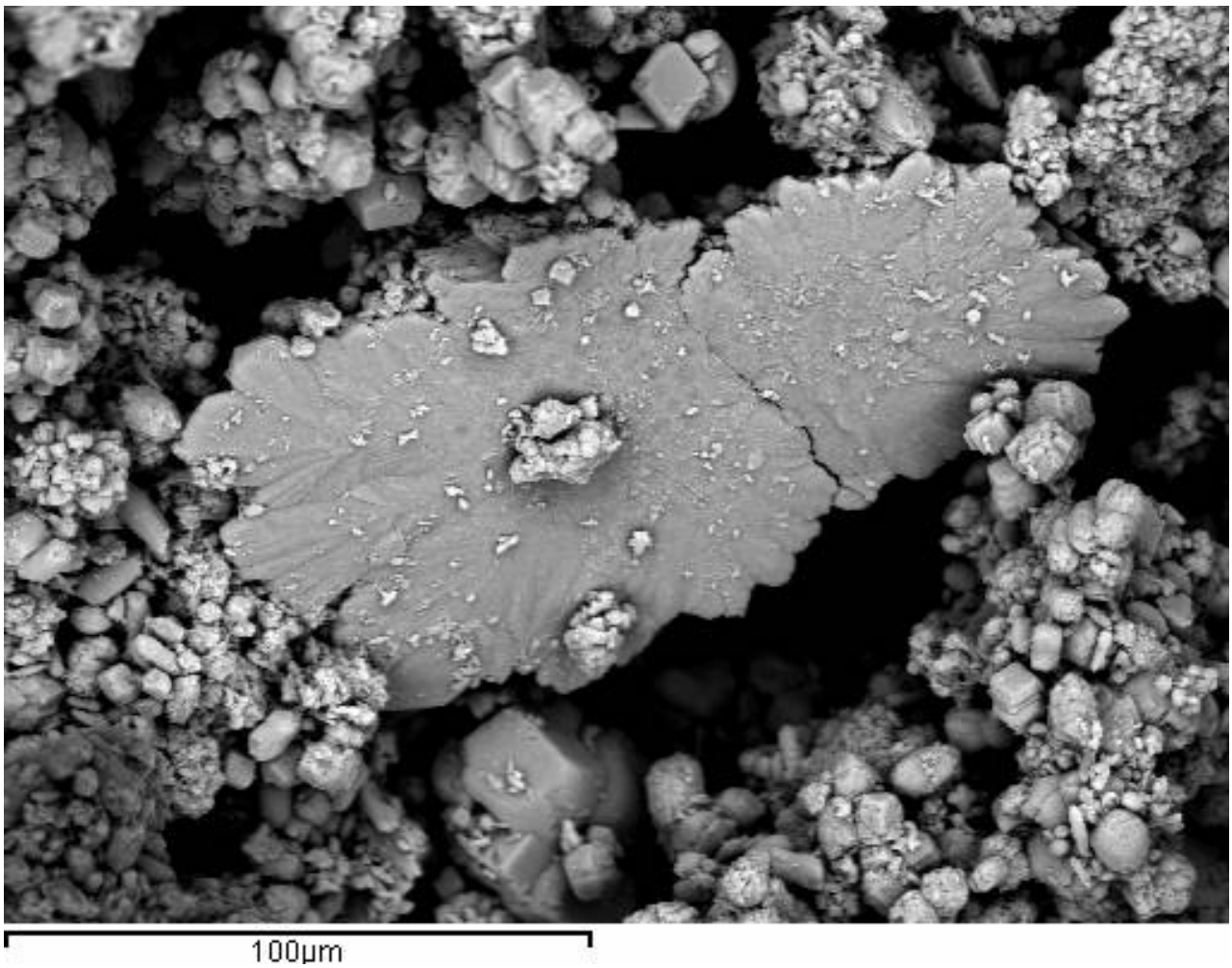

Figure 3.1.5d. Carbonate raft and micrite from carbonate mud pool. (Submap: East 4). Stub #10.

3.1.6. Pisoidal pools

Pisoidal pools (figure 3.1.6a) form proximally to the tips on level ground (~0^{o}). Small (<5 cm), typically disk-shaped, sometimes spheroidal grains featuring a regular laminated cortex are formed in the pools. Laminated crusts form around the edges and base of the pools, often cementing the grains in place. Pools are typically stagnant and ephemeral, up to a few cm deep (although typically <1 cm deep). Plants and algae do not colonise the pools and carbonate mud is generally absent from the base of the pools. Carbonate rafts are common, and fragments of submerged rafts often settle at the base of pools.

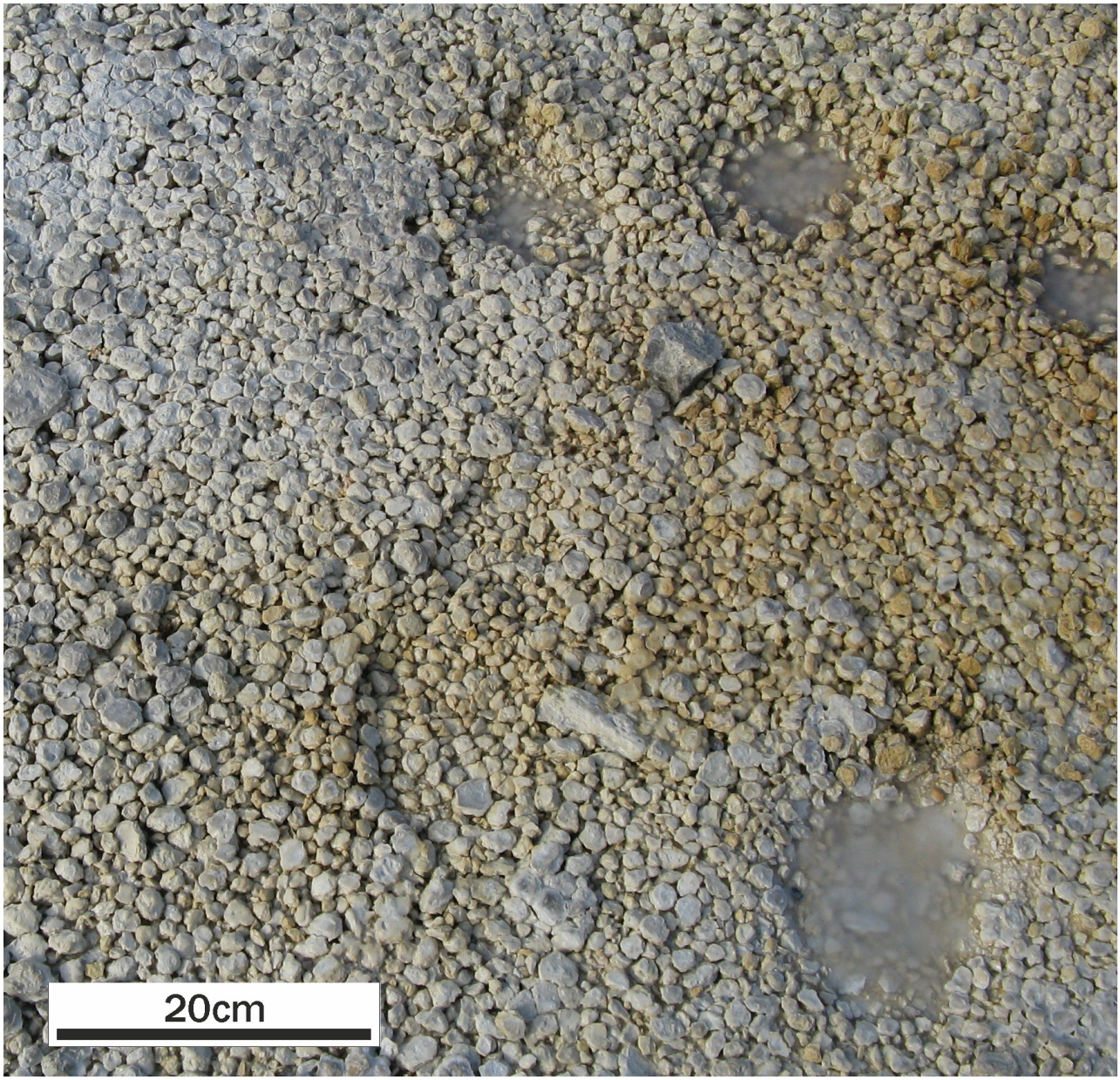

Figure 3.1.6a. Pisoids. Note cementation at top left, and pools which show the water level just below surface. (Submap: East 4).

Shelfstone commonly forms around the edge of both pools and pisoids. Growth is aligned with the air-water interface and typically extends 1-5 mm (figure 3.1.6b).

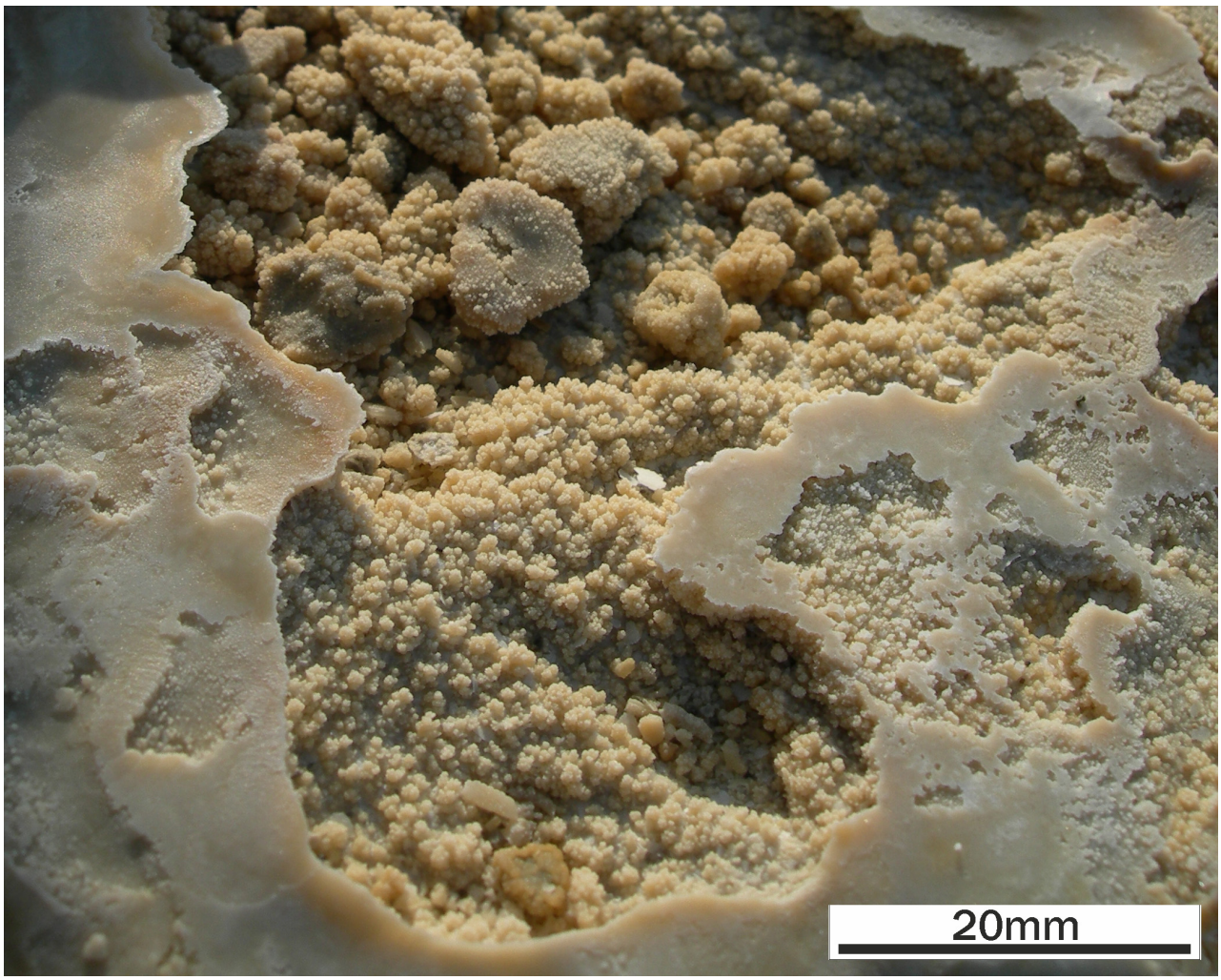

Figure 3.1.6b. Shelfstone lining the periphery of a pool (temporarily dry). (Submap: East 4).

Where pisoids are commonly submerged in the ephemeral pools, spicular growth occurs (figure 3.1.6c).

Figure 3.1.6c. Spicular growth occurring below the surface of the water in an ephemeral pool. (Submap: East 8).

Pisoids feature a core, typicall containing encrusted plant fragments, and a laminated cortex (figure 3.1.6d).

Figure 3.1.6d. Fractured cross section through a pisoid. Note encrusted plant fragments in centre and laminated cortex.

A variety of pisoid morphologies and compositions are observed (figure 3.1.6e). Highly porous cores of lime spoil, calcified plant or a fractured segment of a pisoid are coated by concentric laminations of either prismatic calcite or micritic laminae. Where the pisoids are partially submerged in pools (even if submersion is discontinuous), shelfstone forms around the waterline. This creates a rim, which is responsible for the commonly found 'biscuit' morphology.

Vertical cross-section	Description
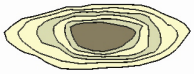	1. Pisoid with core of either lime spoil or calcified plant. Cortex mostly of crystalline calcite laminae with some micritic laminae.
	2. Pisoid with core formed from a fragment of a pisoid. Cortex mostly of crystalline calcite laminae with some micritic laminae.
	3. Pisoid (compostion as 1 or 2), with shelfstone ridges formed at the air-water interface generating 'biscuit' morphology.
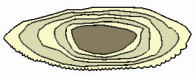	4. Pisoid (composition as 1 or 2), with 'shrubby' texture on underside, typically submerged (see 3.4.3d.).

Figure 3.1.6e. Pisoid compositions on Foel Fawr.

Laminated crusts commonly surround pools. These crusts form either between pisoids collected on the surface (see figure 3.1.6a) or as laminated crusts between and around pools. Beneath the water surface, spicular textures may form on both pisoids and the pools themselves (figure 3.1.6f).

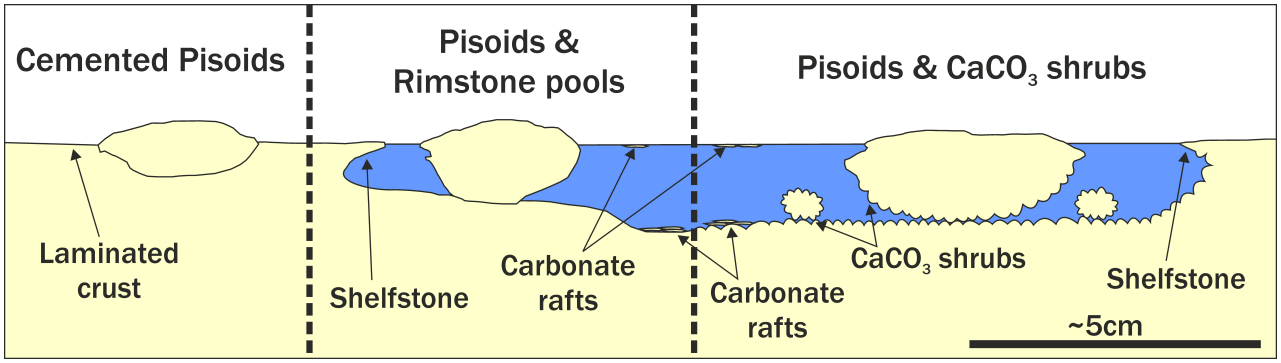

Figure 3.1.6f. Thematic cross-section through pisoidal pool showing the variety of morphologies observed.

Prismatic calcite crystals growing perpendicular to the surface form the majority of laminae (figure 3.1.6g).

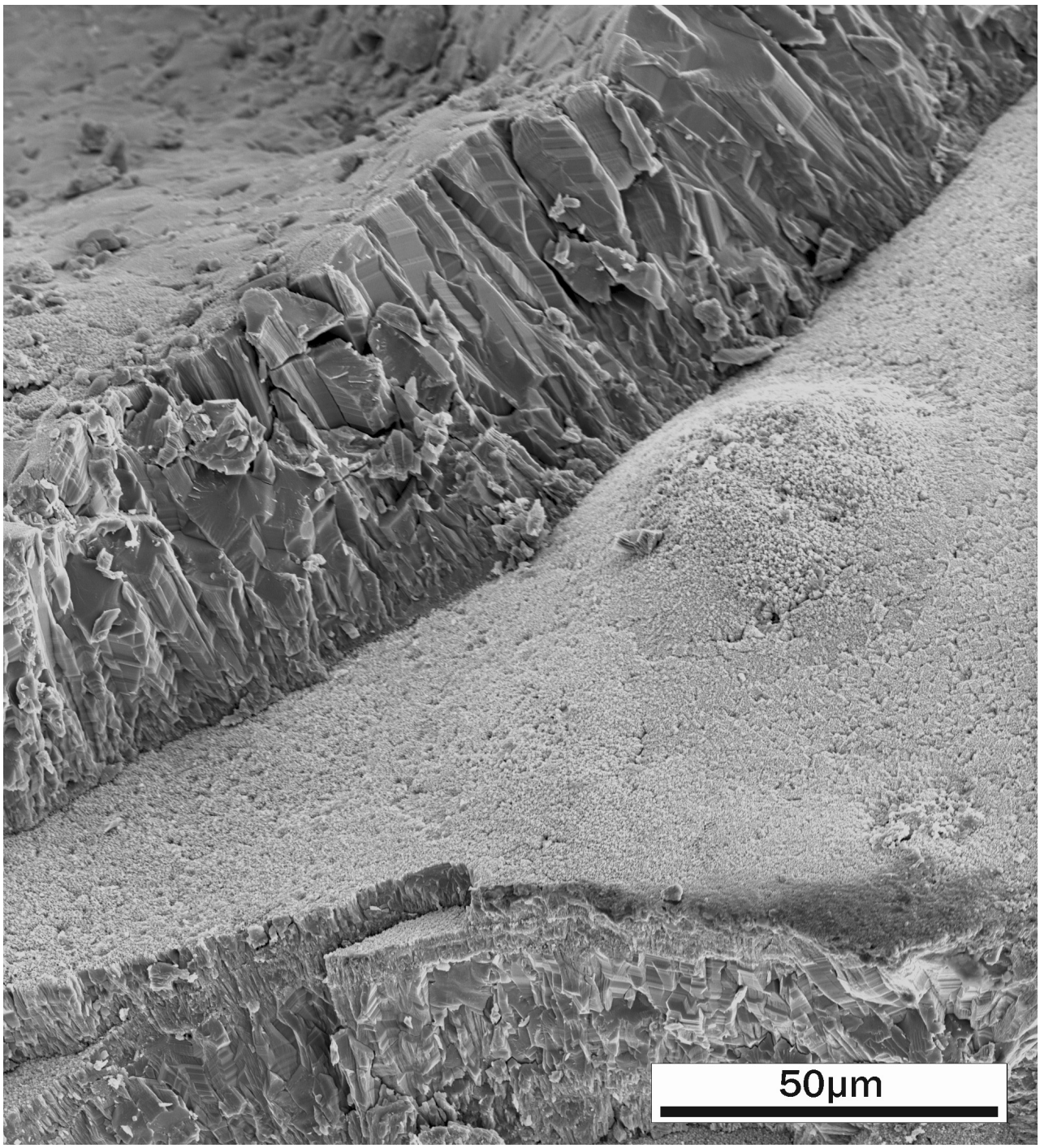

3.1.6g. Prismatic calcite lamina from pisoid cortex. (Submap: East 4). Stub #11.

Repeated laminae of prismatic calcite may form dense crusts around pisoids, apparently devoid of biological material (figure 3.1.6h).

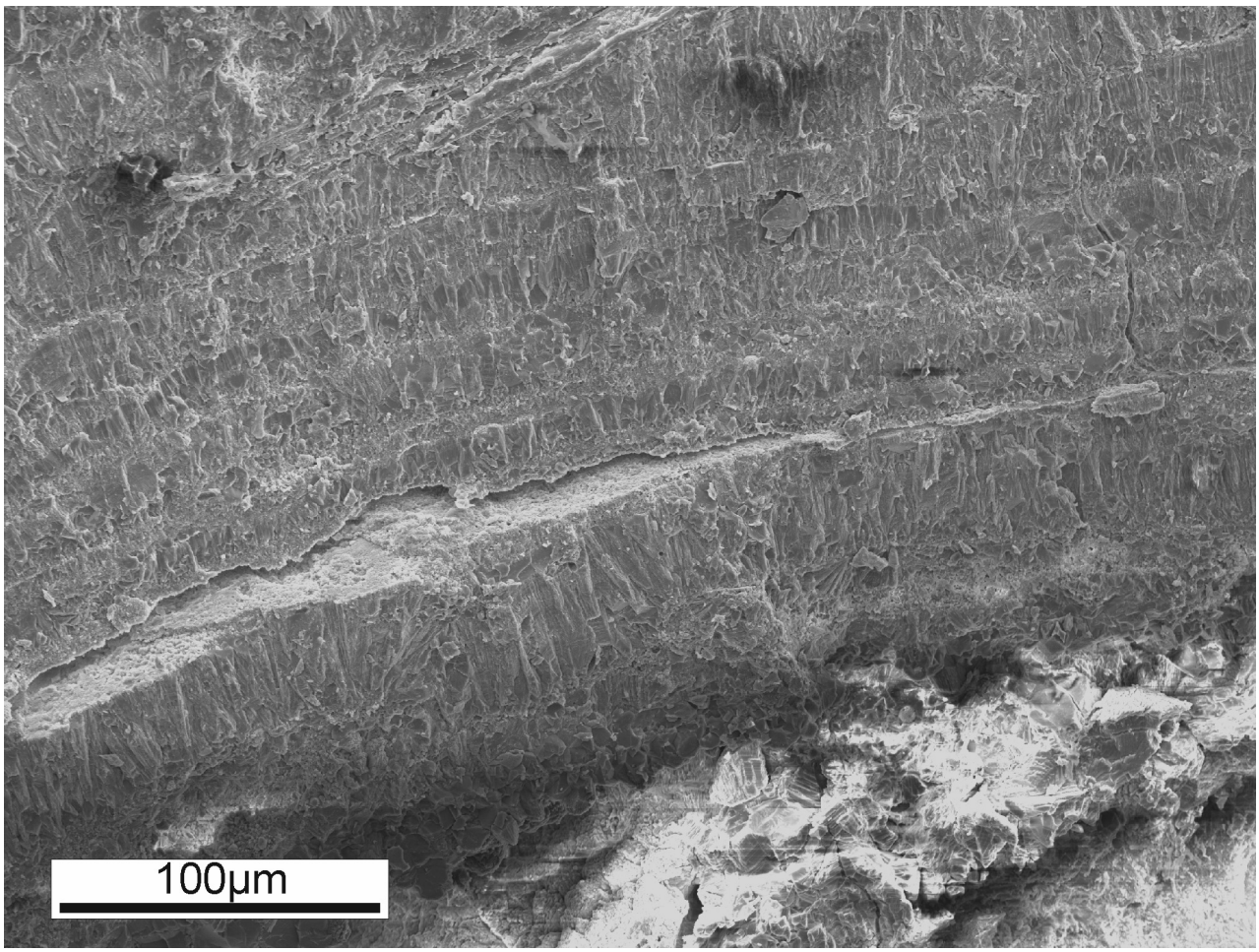

Figure 3.1.6h. Dense prismatic calcite laminae forming around a pisoid on Foel Fawr. (Submap: East 4). Stub #11.

Radial crystals may form in the core of a pisoid (figure 3.1.6i), possibly the result of void filling by abiogenic precipitation following submersion of allochthonous material (see figure 3.1.6d).

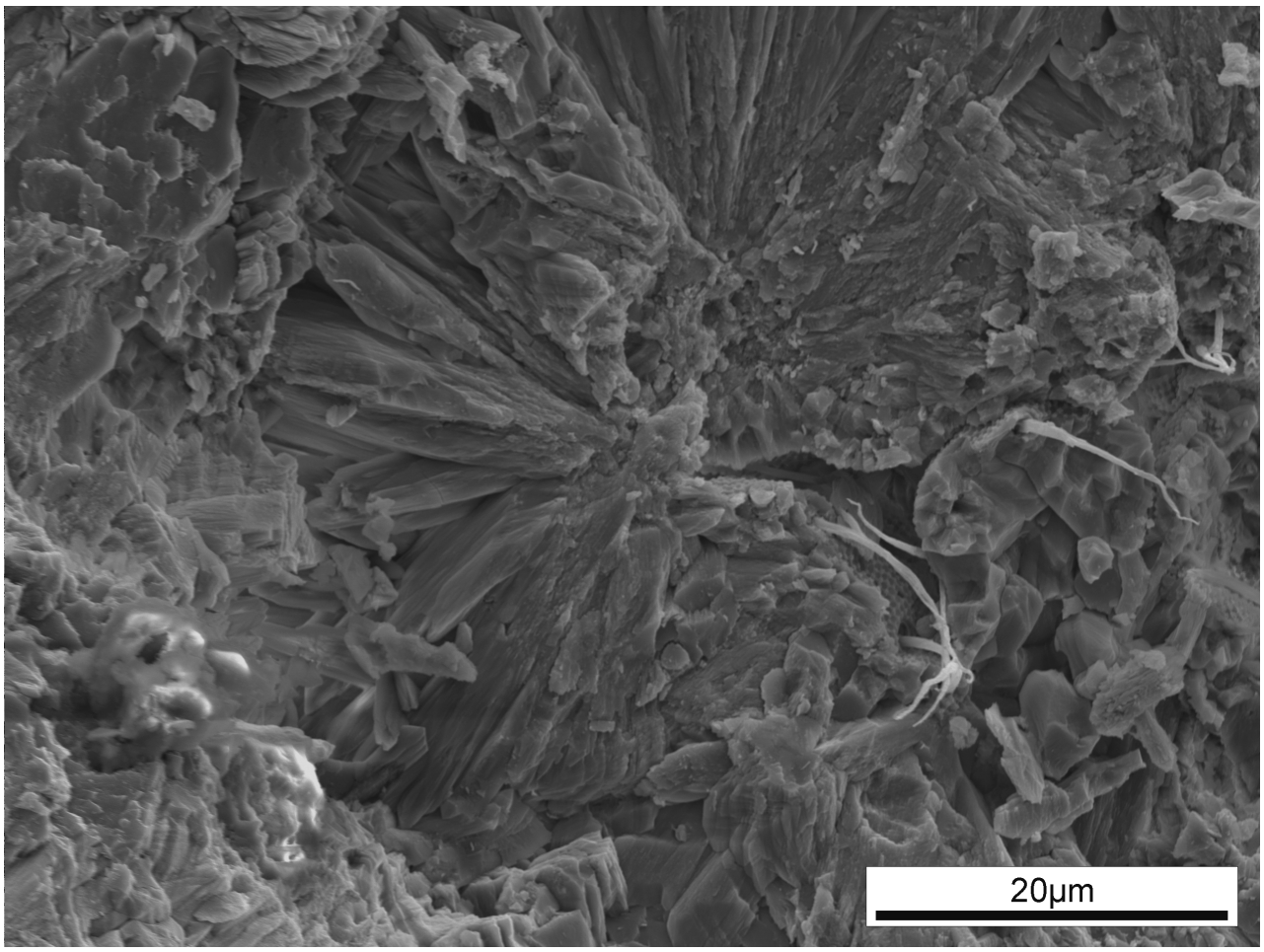

Figure 3.1.6i. Radial crystals in a pisoid core. (Submap: East 4). Stub #11.

Within the core of pisoids, diatoms, EPS and filamentous organisms may be found (figure 3.1.6j). These are conspicuous in their absence from the prismatic laminae forming the cortex, and are likely allochthonous.

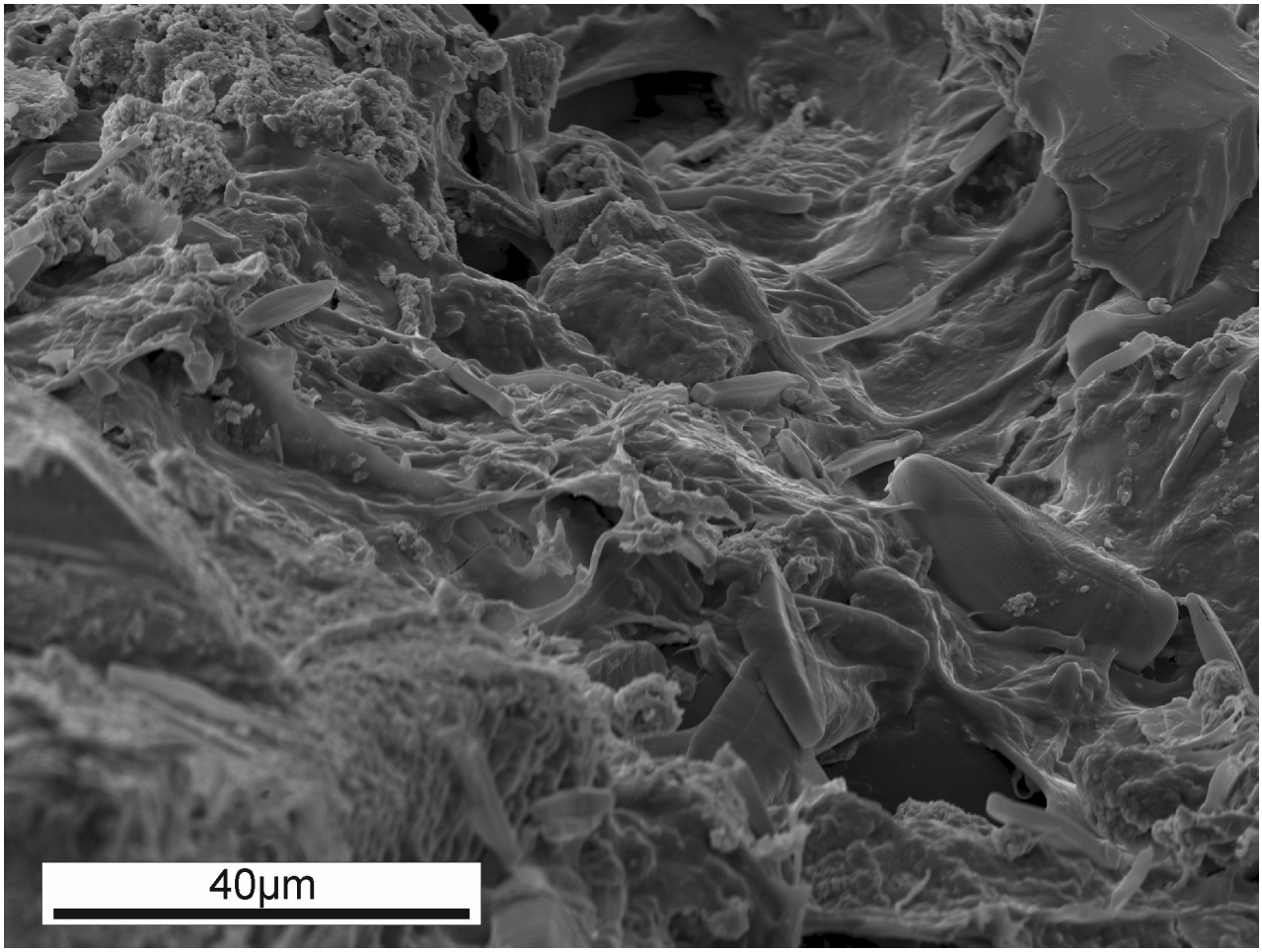

Figure 3.1.6j. Diatoms, EPS and filaments from a pisoid core. Note Euccoconeis sp. (image right). Stub #12.

3.1.7. Oncoids

Oncoids are often adjacent to carbonate gravel, but typically further from the tips. They form on flat ground or occasionally on gentle slopes (<10^{o}), and may form in pools up to ~5 cm deep or be subaerially exposed. Small and large grains (<20 cm) with an irregular surface and typically a spheroidal or sub-spheroidal shape are precipitated. Oncoids are found in both vadose and phreatic conditions. The vadose oncoids appear to be associated with depressions, which likely held water previously.

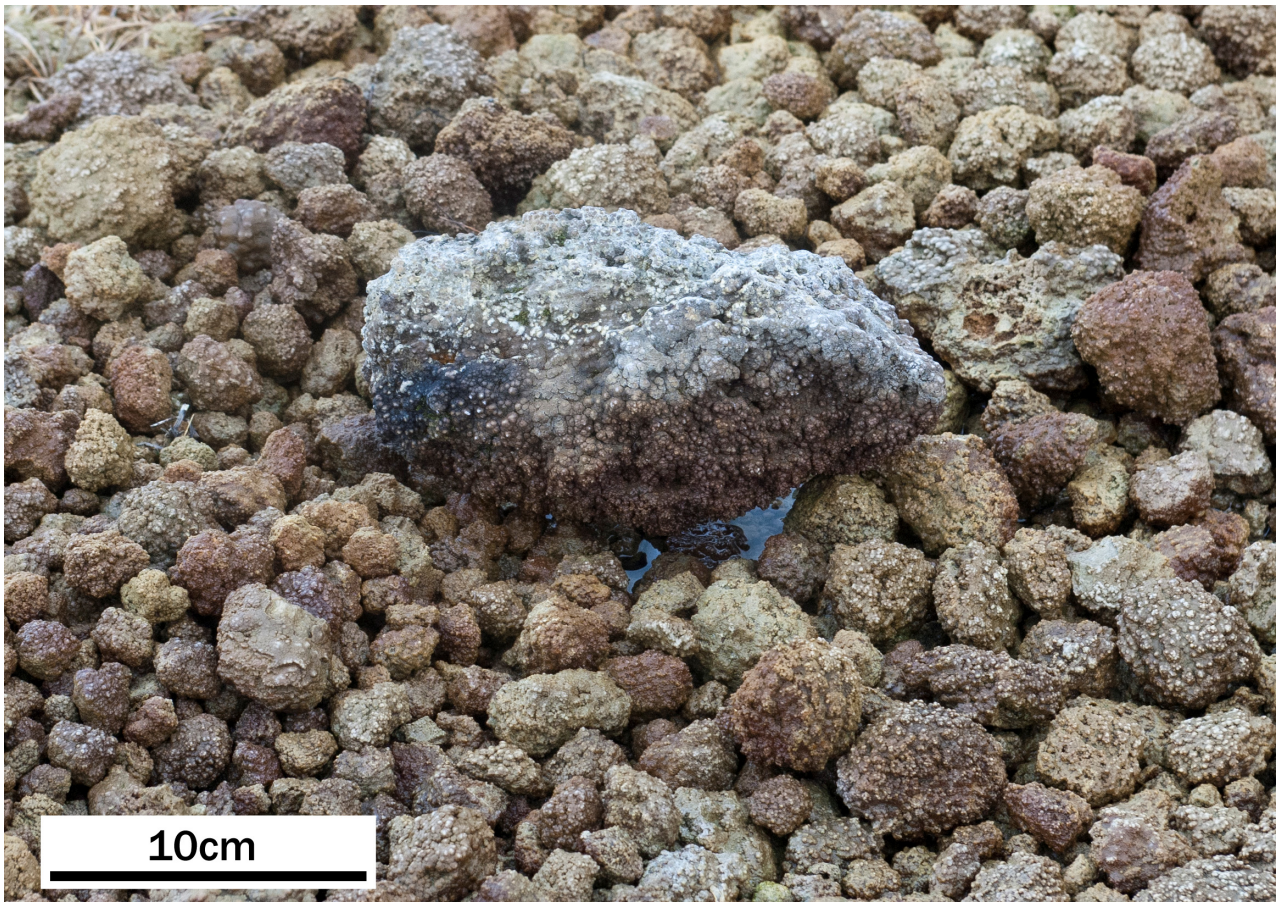

3.1.7a. Oncoids. Note water level visible just below large oncoid in the centre. (Submap: East 4).

Laminations within oncoids often form from prismatic calcite crystals growing perpendicular to the lamina (figure 3.1.7c).Some laminations are formed from branched elongate calcite crystals (figure 3.1.7d). This fabric is comparable to those forming in aprons (see figure 3.1.2i). Radial crystals are often found within oncoids, typically growing around a spherical (organic?) nucleus (figure 3.1.7e).

Where oncoids are sub-aerially exposed, bryophytes colonise the surface (figure 3.1.7f). They do not appear to be linked to actively accreting oncoids and are not observed within the oncoids. Plant moulds are common and are typically formed of radial prismatic calcite (figure 3.1.7g). Stoma moulds are well preserved in some oncoids (figure 3.1.7h).

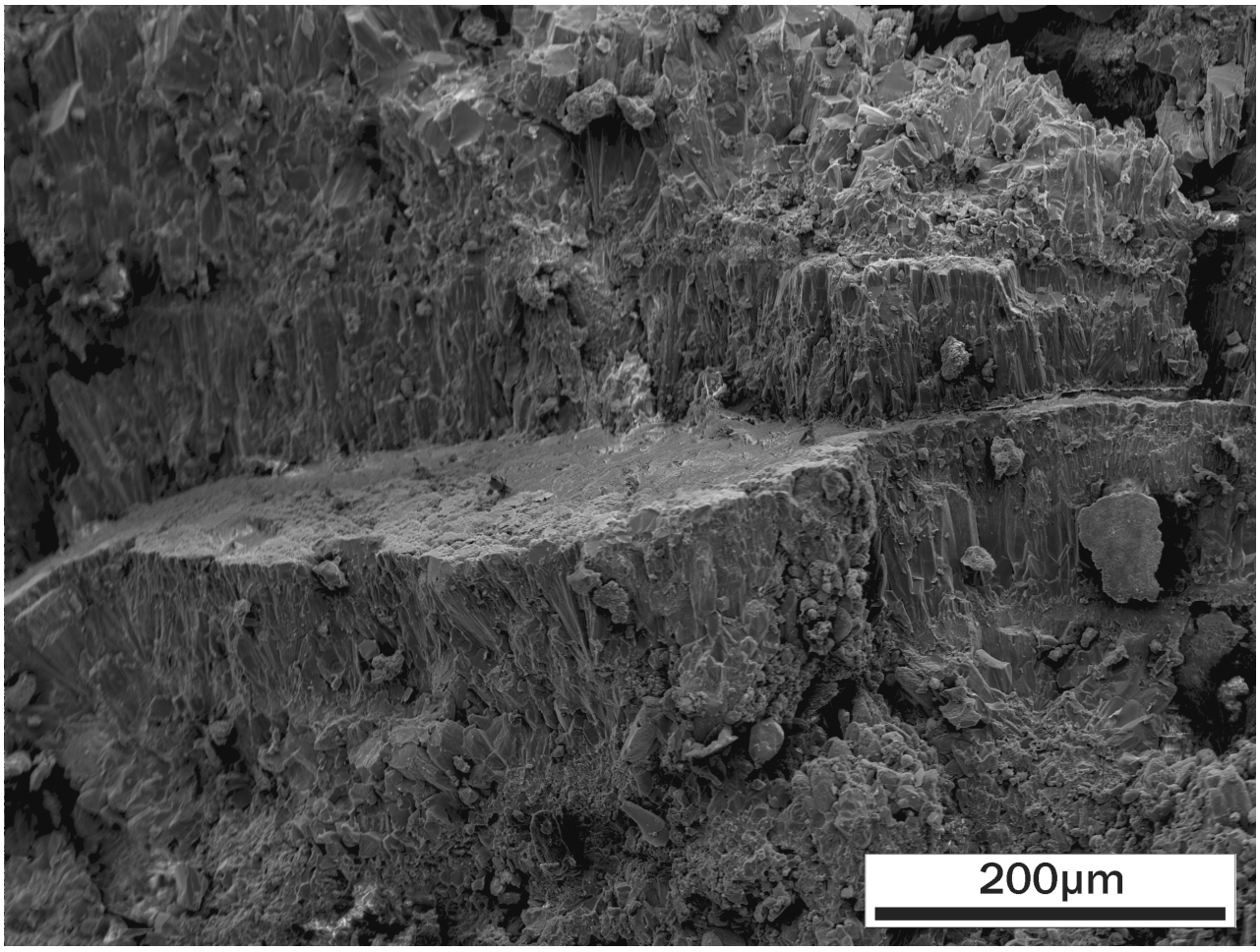

Figure 3.1.7c. Lamination of prismatic calcite within an oncoid. (Submap: East 4). Stub #13.

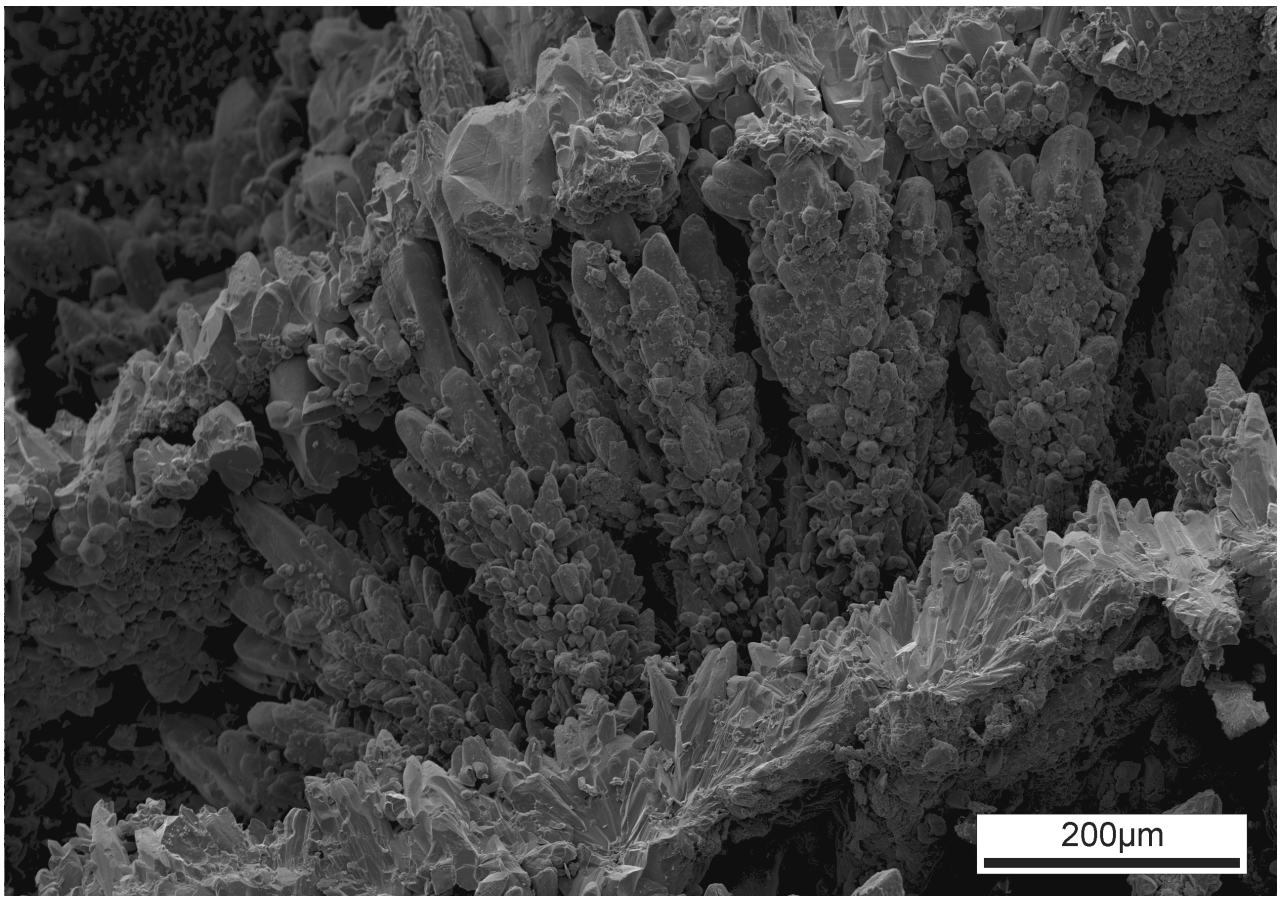

Figure 3.1.7d. Branching 'crystal shrubs' forming laminae within an oncoid. (Submap: West 2). Stub #14.

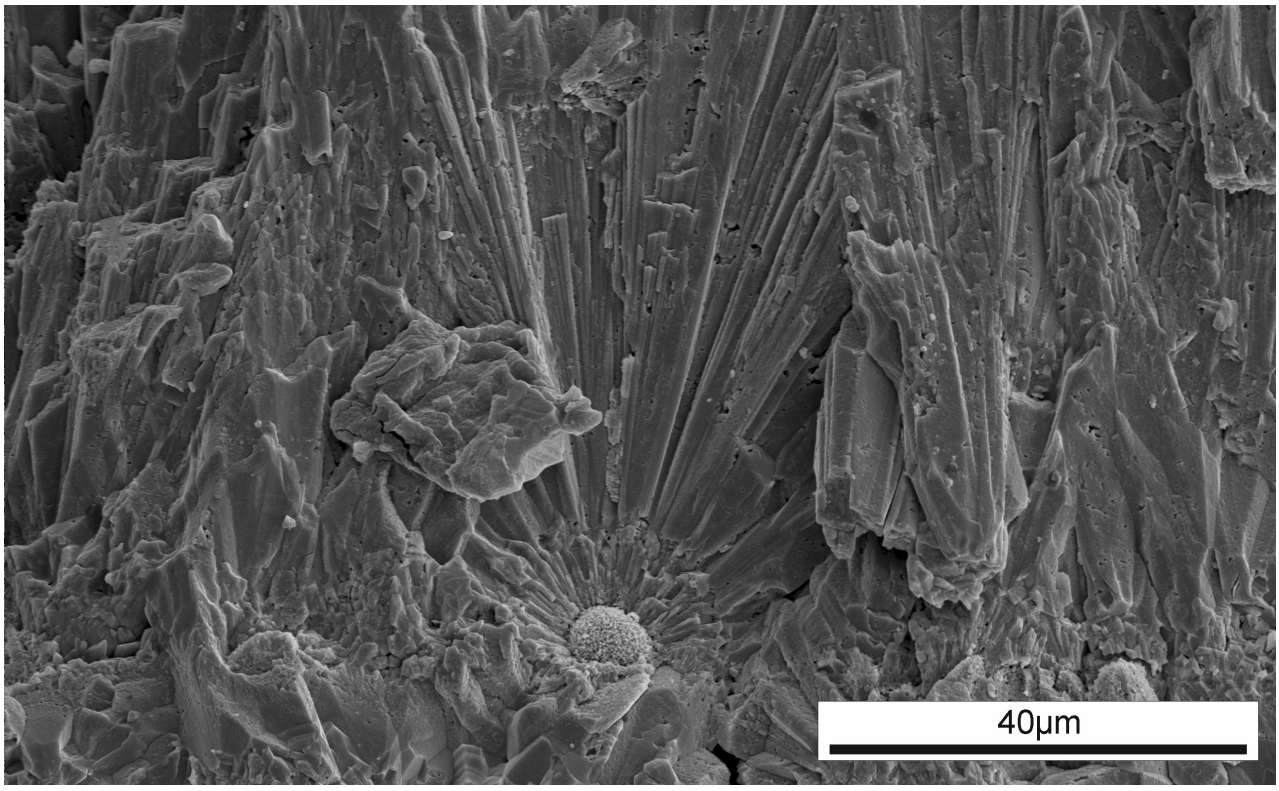

Figure 3.1.7e. Radial crystals within an oncoid (Submap: East 4). Stub #15.

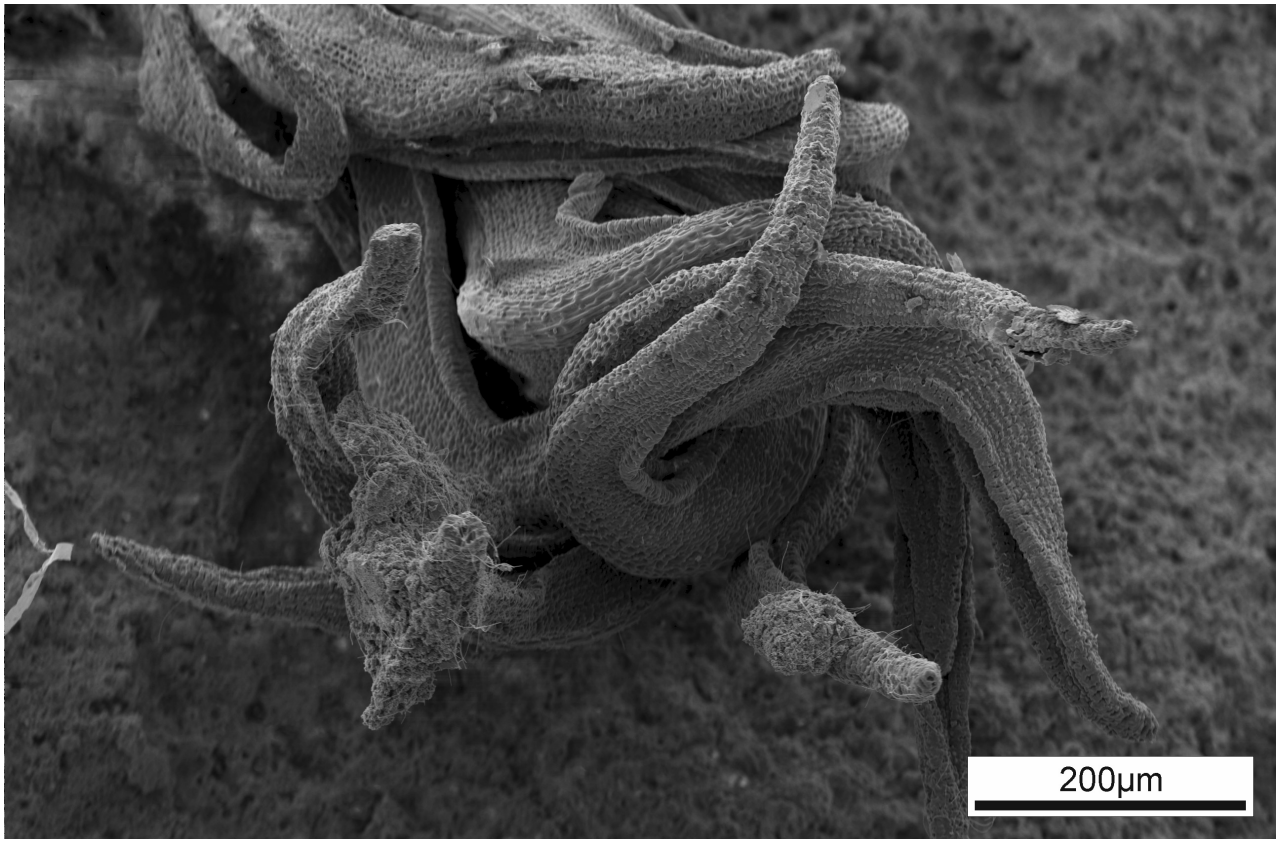

Figure 3.1.7f. Bryophyte leaves on the surface of an oncoid, Foel Fawr. (Submap: West 2). Stub #16.

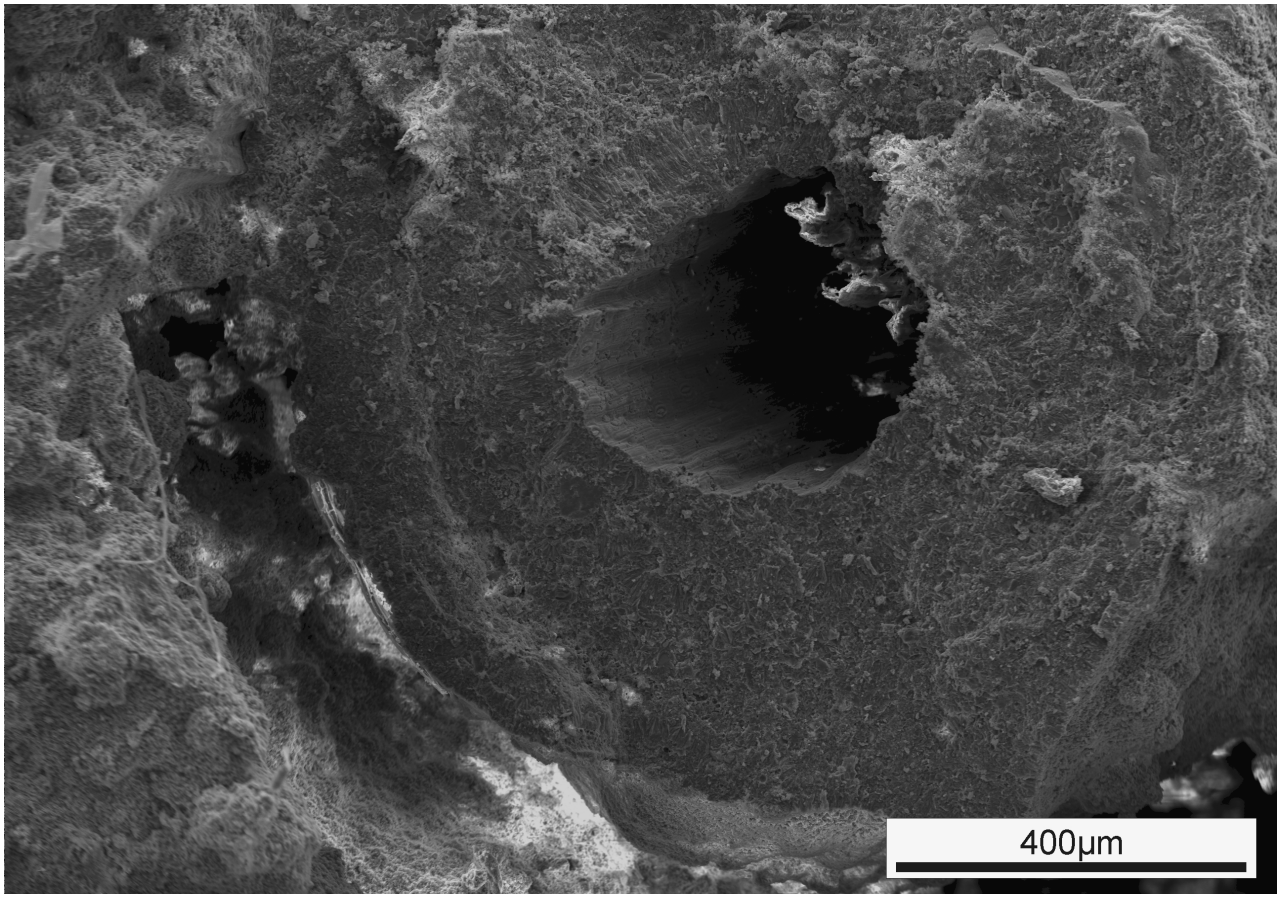

Figure 3.1.7g. Mould of a stem preserved within an oncoid. (Submap: West 2). Stub #17.

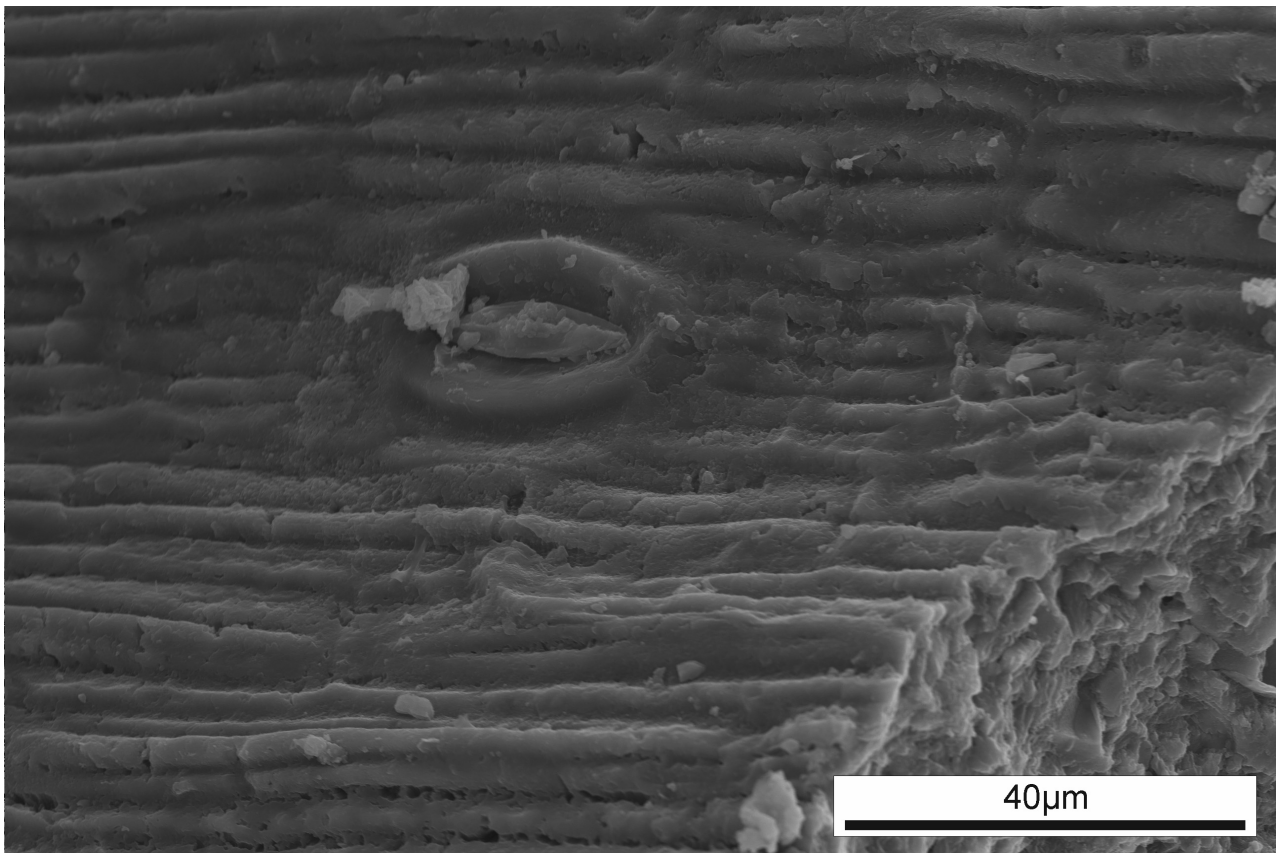

Figure 3.1.7h. Stoma mould from within an oncoid. (Submap: West 2). Stub #17.

Areas of EPS, typically associated with micrite, are common (figure 3.1.7i).

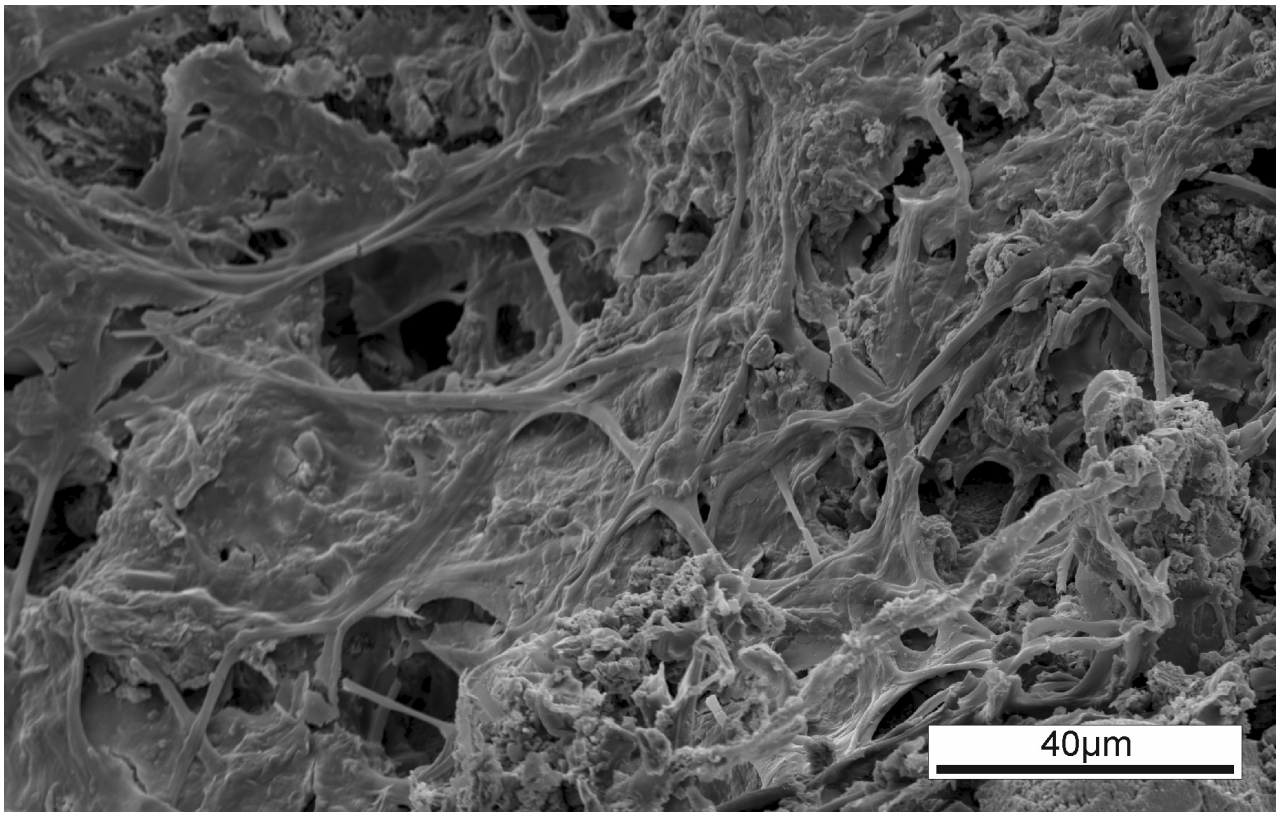

Figure 3.1.7i. EPS, filamentous organisms and micrite within an oncoid. (Submap: West 2). Stub #18.

3.1.8. Carbonate gravel

Carbonate gravel (figure 3.1.8a) forms proximally to tips on gentle slopes (<20^{o}). Small (<5 cm), approximately spheroidal grains with a smooth coating accrete sub-aerially. Despite this, the water level is typically only a few cm below the surface. Plants occasionally colonise, but are limited to isolated patches.

Figure 3.1.8a. Carbonate gravel facies. MACB. (Submap: East 5).

Grain size varies from gravel (2 mm – 4 mm) through to cobble-sized (25.6 cm) sized particles, with gravel and small pebbles being by far the most common. Larger particles are usually formed from cemented accretions of smaller particles (figure 3.1.8b).

3.1.8b. Carbonate gravel with small pebble-sized cemented accretion (image left). (Submap: East 4).

Carbonate gravel is often associated with other clastic material, most notably quarry spoil (figure 3.1.8c).

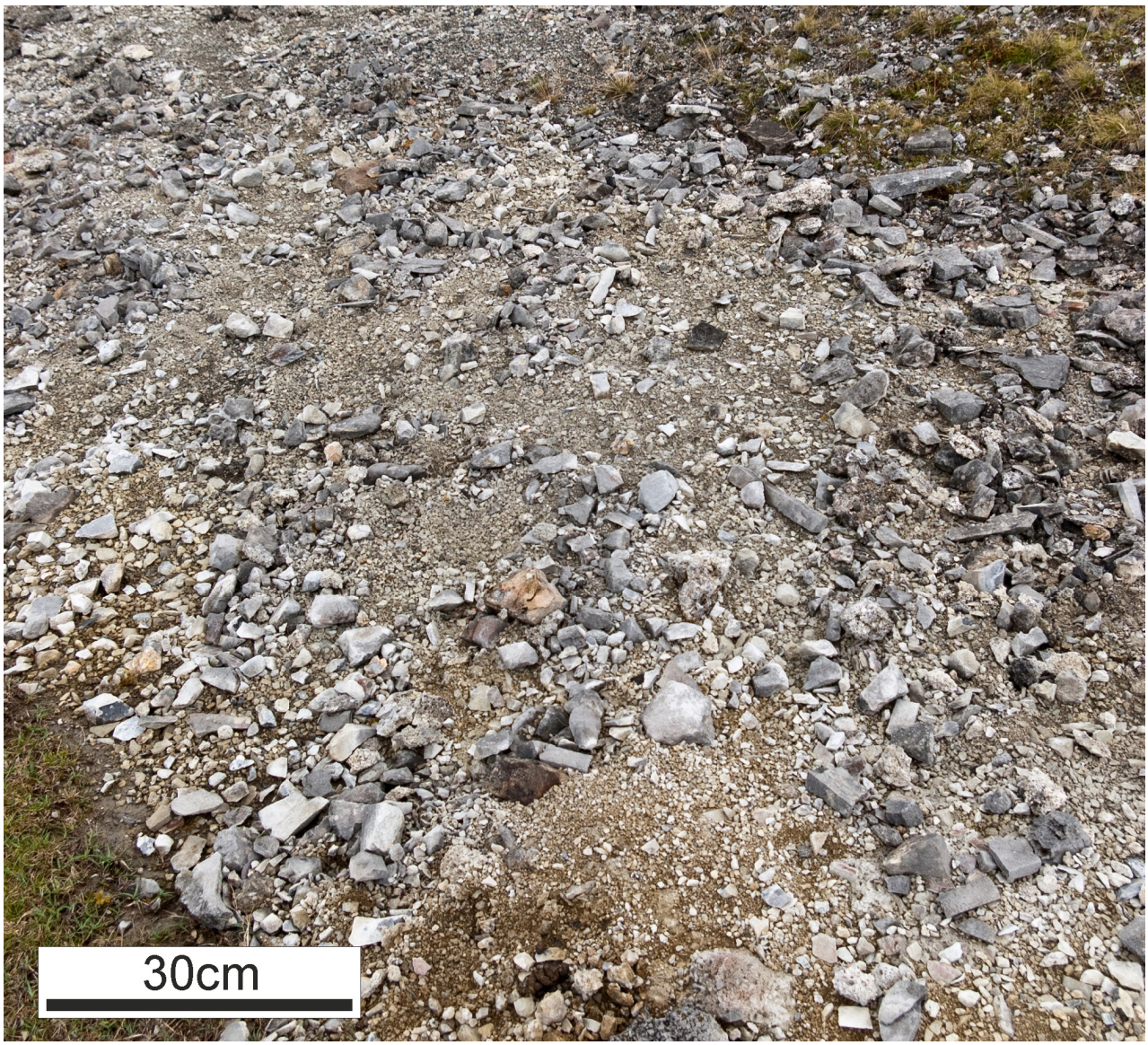

Figure 3.1.8c. Carbonate gravel and quarry scree. MACB. (Submap: West 4)

Gravel is typically formed from a core of kiln waste, with a thin cortex of calcite (figure 3.1.8d).

Figure 3.1.8d. Carbonate gravel grain. Note black sooty area in core and laminations visible (image bottom).

The core of carbonate gravel sometimes contains encrusted plant material (figure 3.1.8e).

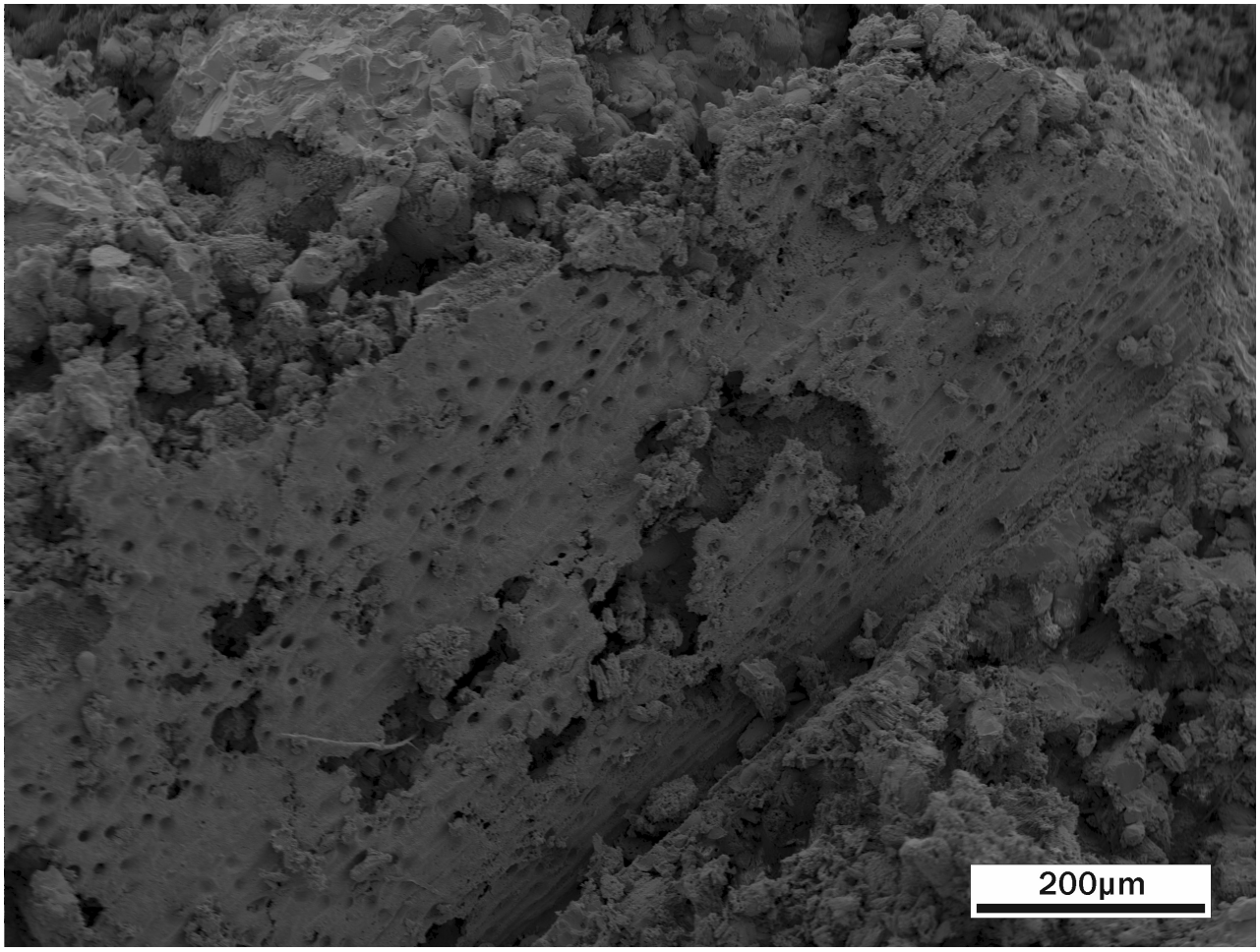

Figure 3.1.8e. Plant mould from carbonate gravel core. (Submap: East 3). Stub #19.

3.1.9. Carbonate mud

Carbonate mud forms on gentle slopes (<20^{o}) away from tips (figure 3.1.9a). Carbonate mud is precipitated in broad 'channels' flowing away from the tips. They are subaerially exposed, but often waterlogged. Plants frequently colonise the surface, although vegetation is always sparse and stunted.

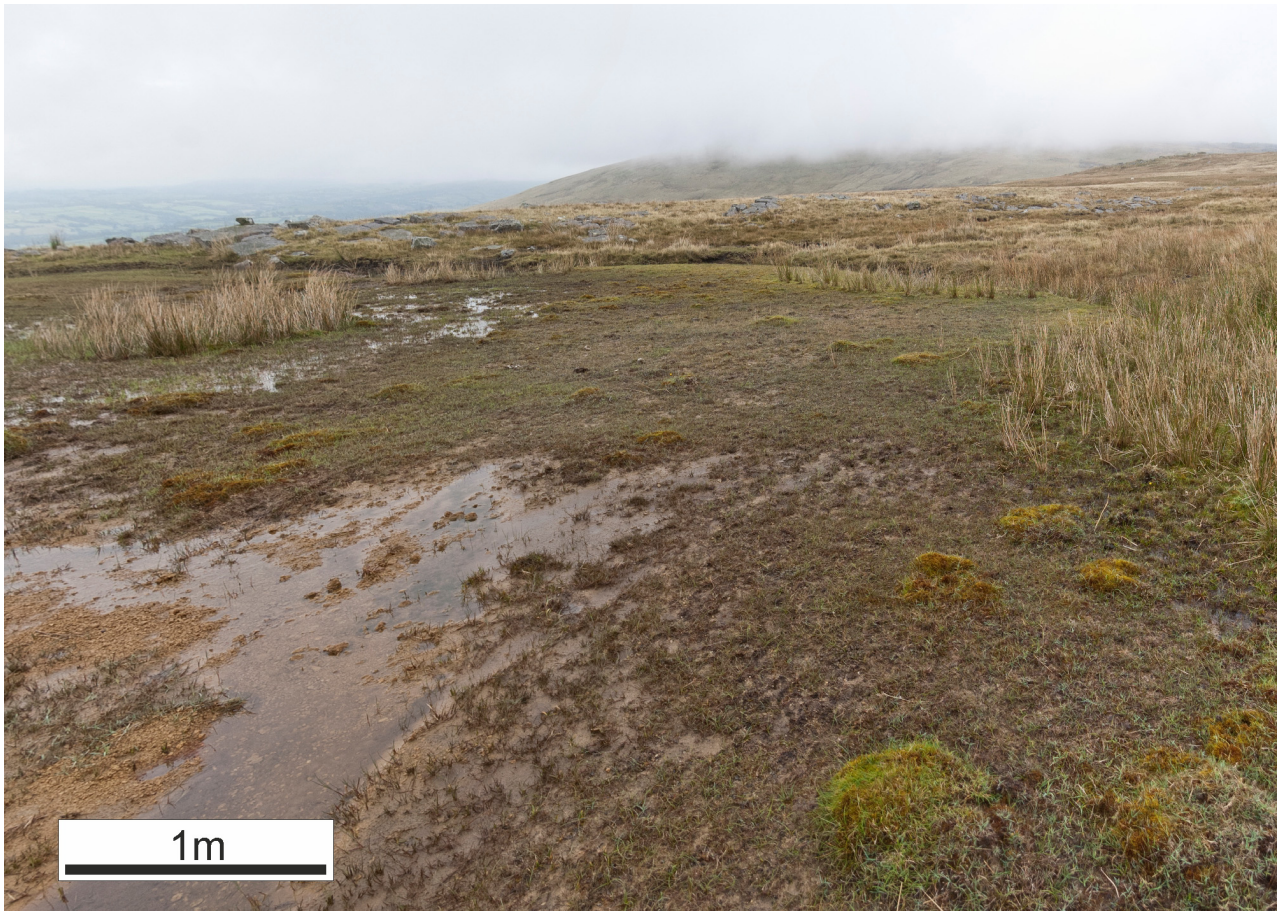

Figure 3.1.9a. Carbonate mud precipitating from an outwash on Foel Fawr. Note absence of plants at the lower left and stunted plants elsewehere. MACB. (Submap: East 5).

Where water regularly flows over the surface of the mud, microterracettes may begin to form (figure 3.1.9b). These microterracettes are morphologically similar to those forming on aprons (section 3.1.2); however, they are friable and easily fractured upon subaerial exposure.

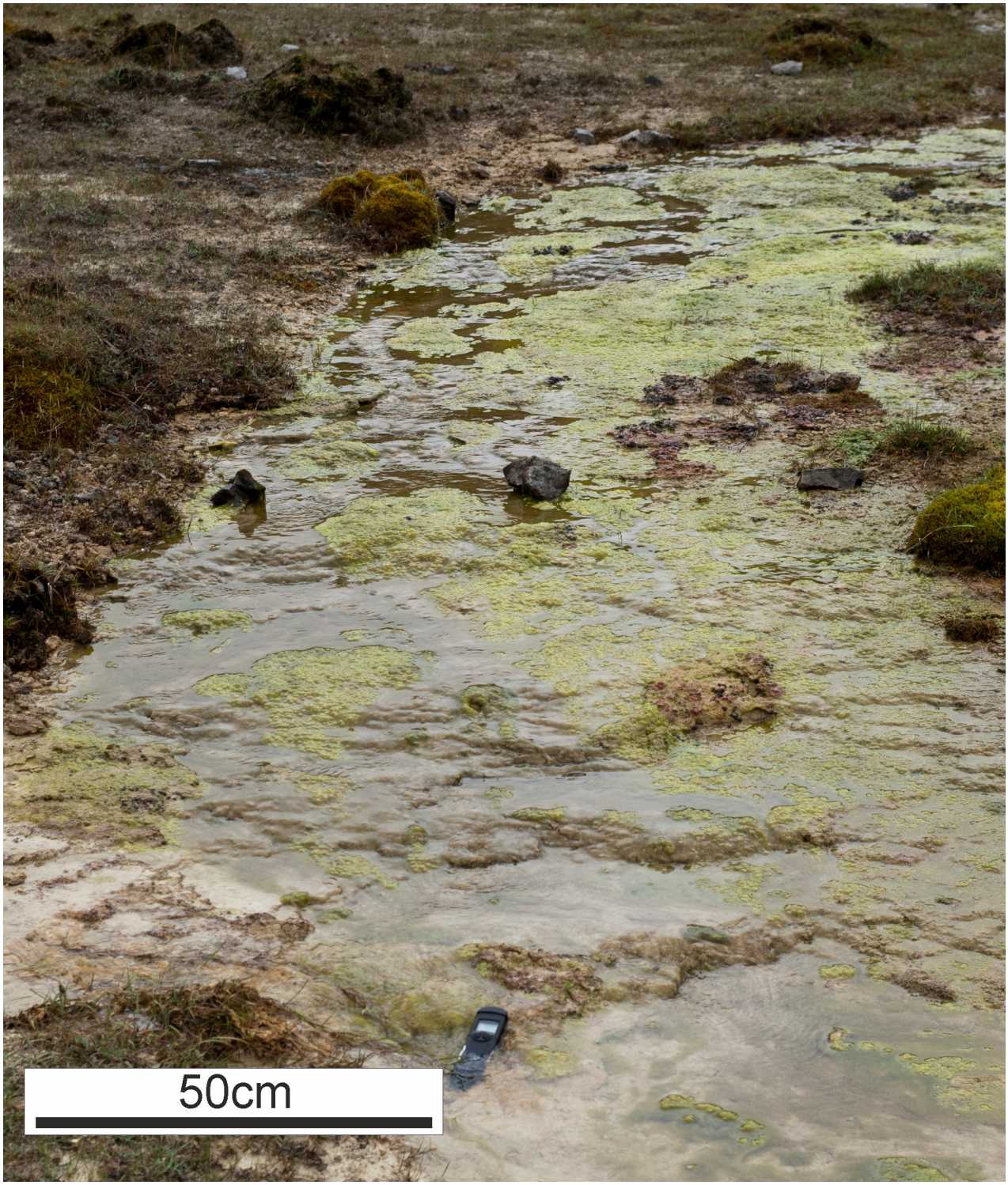

Figure 3.1.9b. Microterracettes forming on the surface of carbonate mud deposits. MACB. (Submap: East 3).

3.1.10. Marginal plant encrustations

Plants and detrital material are encrusted primarily in marginal areas (figure 3.1.10a). However, they are also found as small (10's cm^2) isolated areas within other facies.

3.1.10a. Marginal plant encrustations forming in a small outwash channel. MACB. (Submap: East 2).

Encrustation occurs at different rates depending on proximity to waters. Figure 3.1.10b shows the variation in encrustation relative to proximity to streamway. Encrustation is primarily by large prismatic calcite crystals, which form radially to the stem or root being encrusted (figure 3.1.10c). Smaller, subhedral to anhedral equant crystals also form encrustations. These are commonly associated with diatoms (figure 3.1.10d).

Pennate diatoms (figure 3.1.10e) are common, especially in deposits forming in frequently submerged areas. In older samples forming in less alkaline (circa. pH 8) streams, diatoms often completely cover the surface of the encrusting calcite (figures 3.1.10f and 3.1.10g). In fresh encrustations, diatoms interfere with crystal growth and form ‘diatom jacuzzis’ (figure 3.1.10h), similar to those observed in stream crust (figure 3.1.3q). Extracellular Polymeric Substances (EPS) are often associated with diatoms and may be preserved (figure 3.1.10i). Filamentous strands, associated with micrite are also observed (figure 3.1.10j). Stomata from undecayed tissue is preserved in fresh encrustations, highlighting the speed of precipitation (figure 3.1.10k).

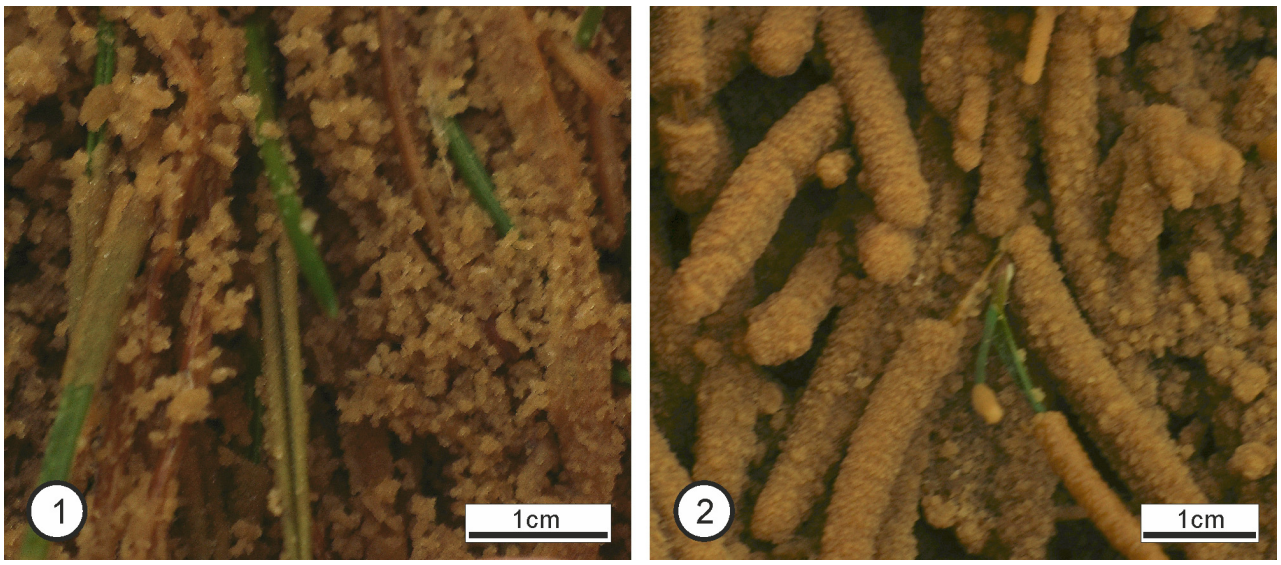

Figure 3.1.10b. Encrustation of stems on margins of outwash. 1: Further from streamway - granular carbonate and thin micritic coating of leaves and stems. 2: Closer to streamway - consolidated coating of stems and leaves by equant calcite crystals (see figure 3.1.10d). (Submap: West 4).

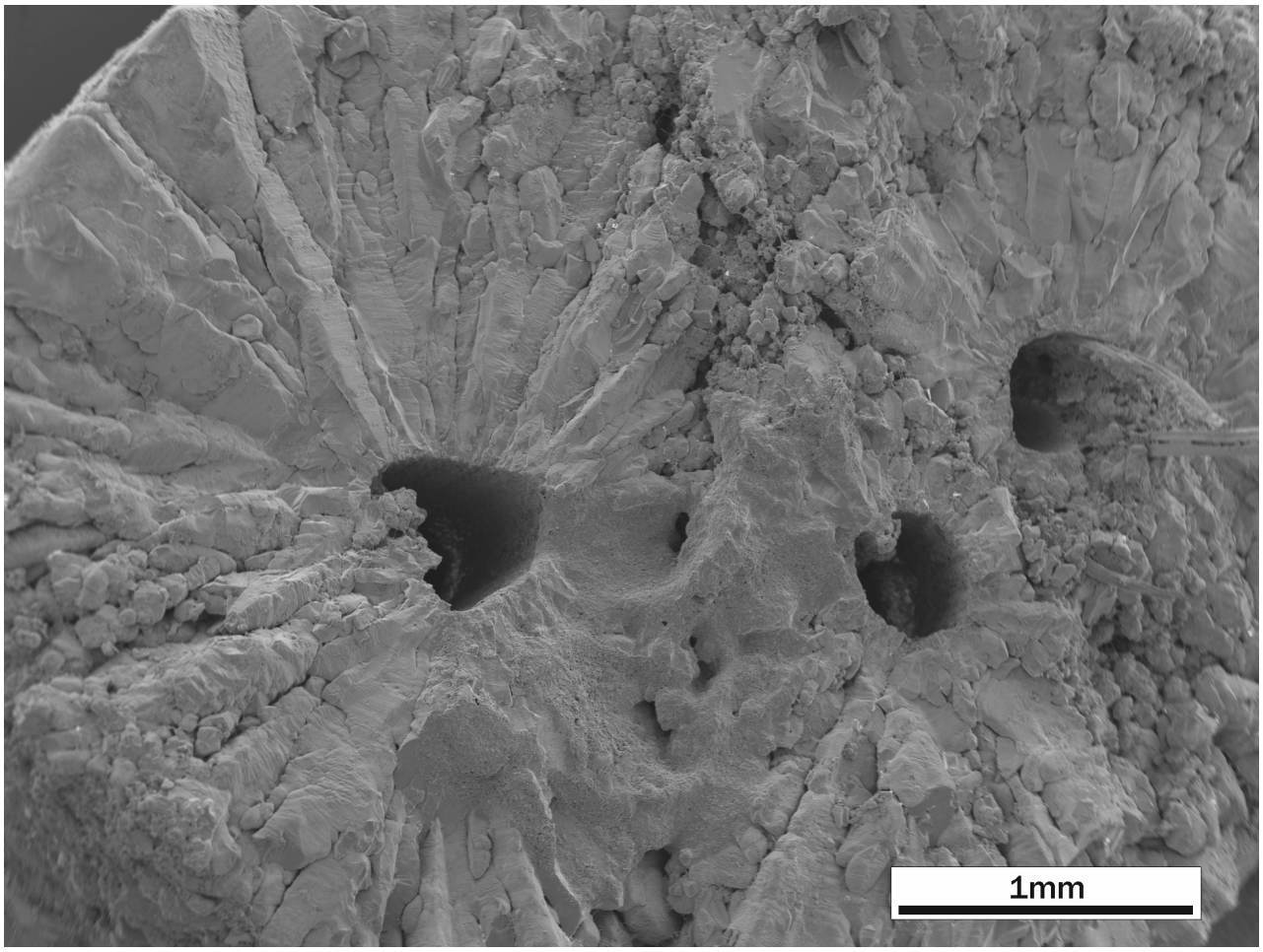

Figure 3.1.10c. Radial prismatic crystals forming mould around (now absent) root/stem. (Submap: West 4). Stub #20.

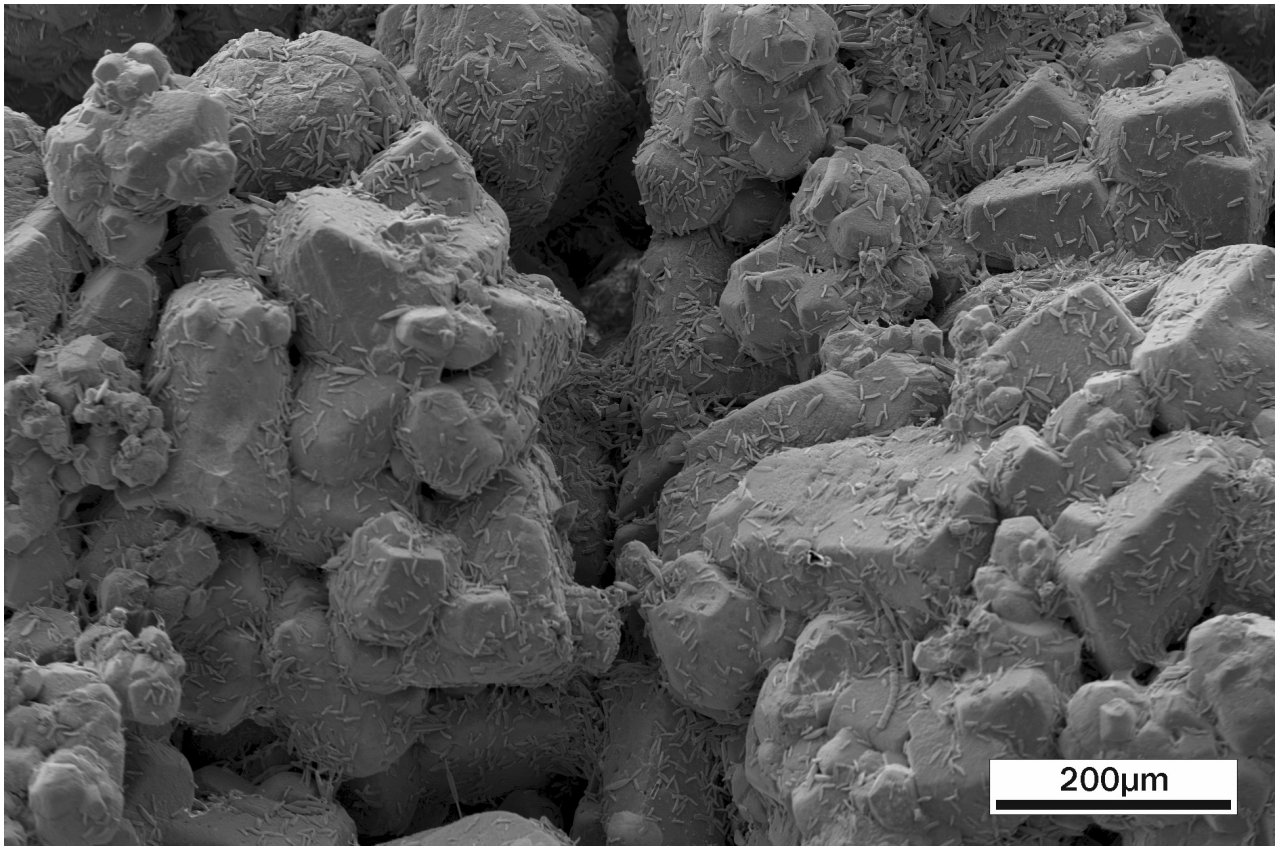

Figure 3.1.10d. Anhedral, equant calcite encrusting stem. Note abundance of diatoms. (Submap: West 4). Stub #20.

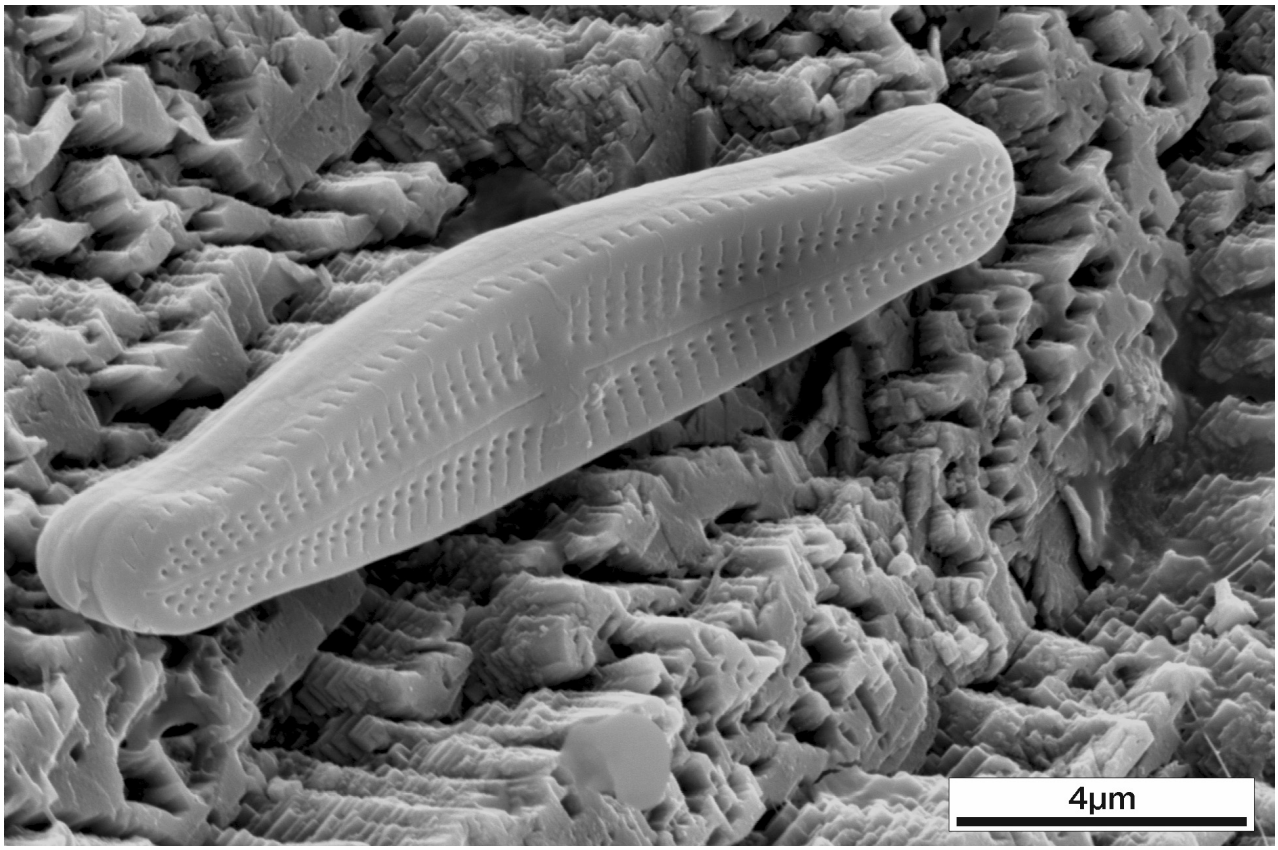

Figure 3.1.10e. *Achnanthidium catenatum*. (Submap: West 2). Stub #21.

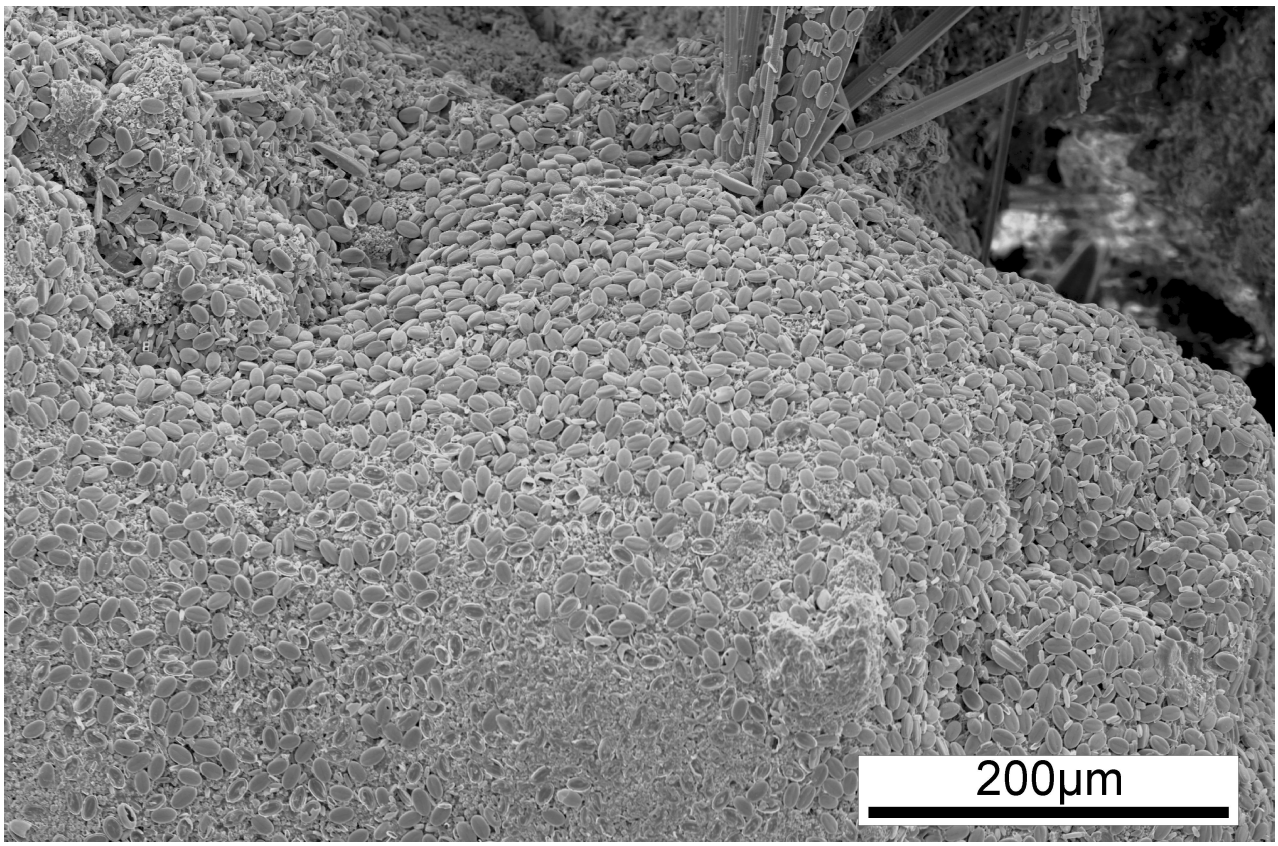

Figure 3.1.10f. Diatoms cover the surface of calcite crystals encrusting Juncus stem in streamway. (Submap: East 7). Stub #22.

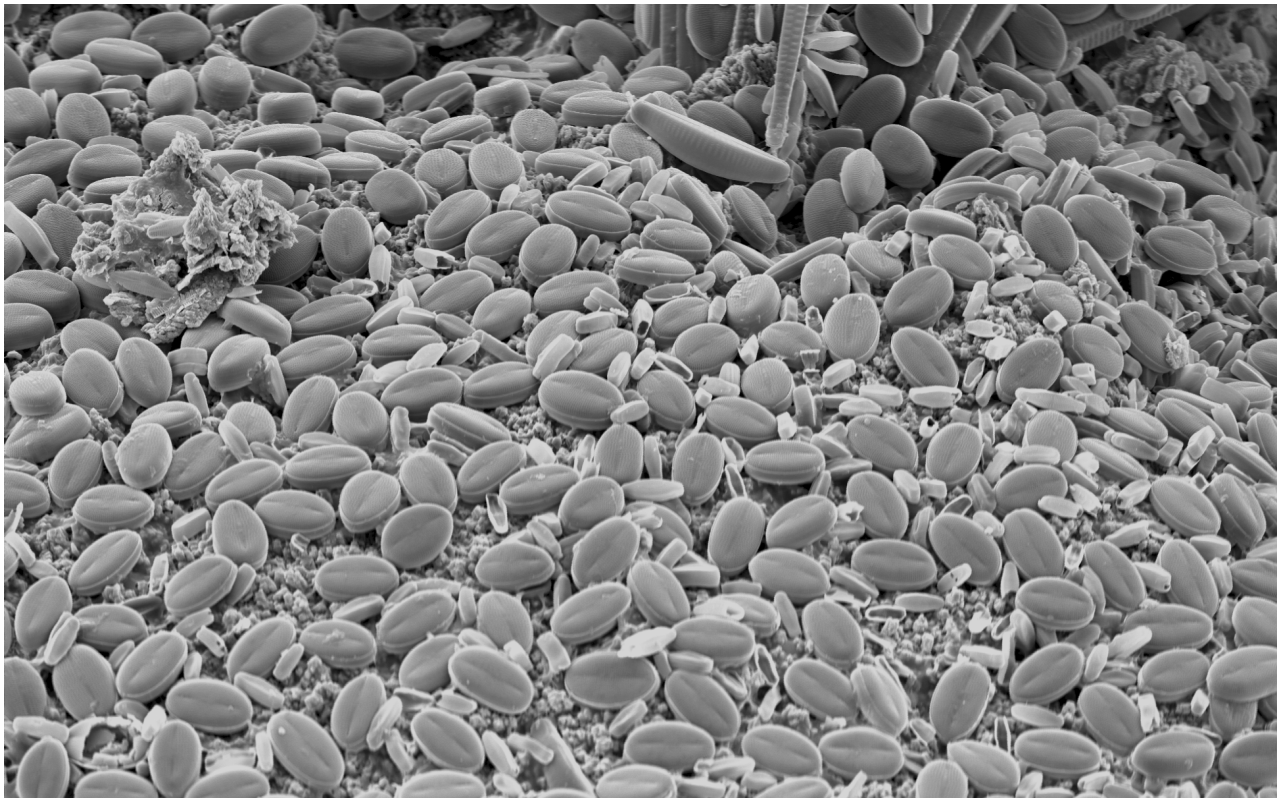

Figure 3.1.10g. Close-up of figure 3.1.10f. (Submap: East 7). Stub #22.

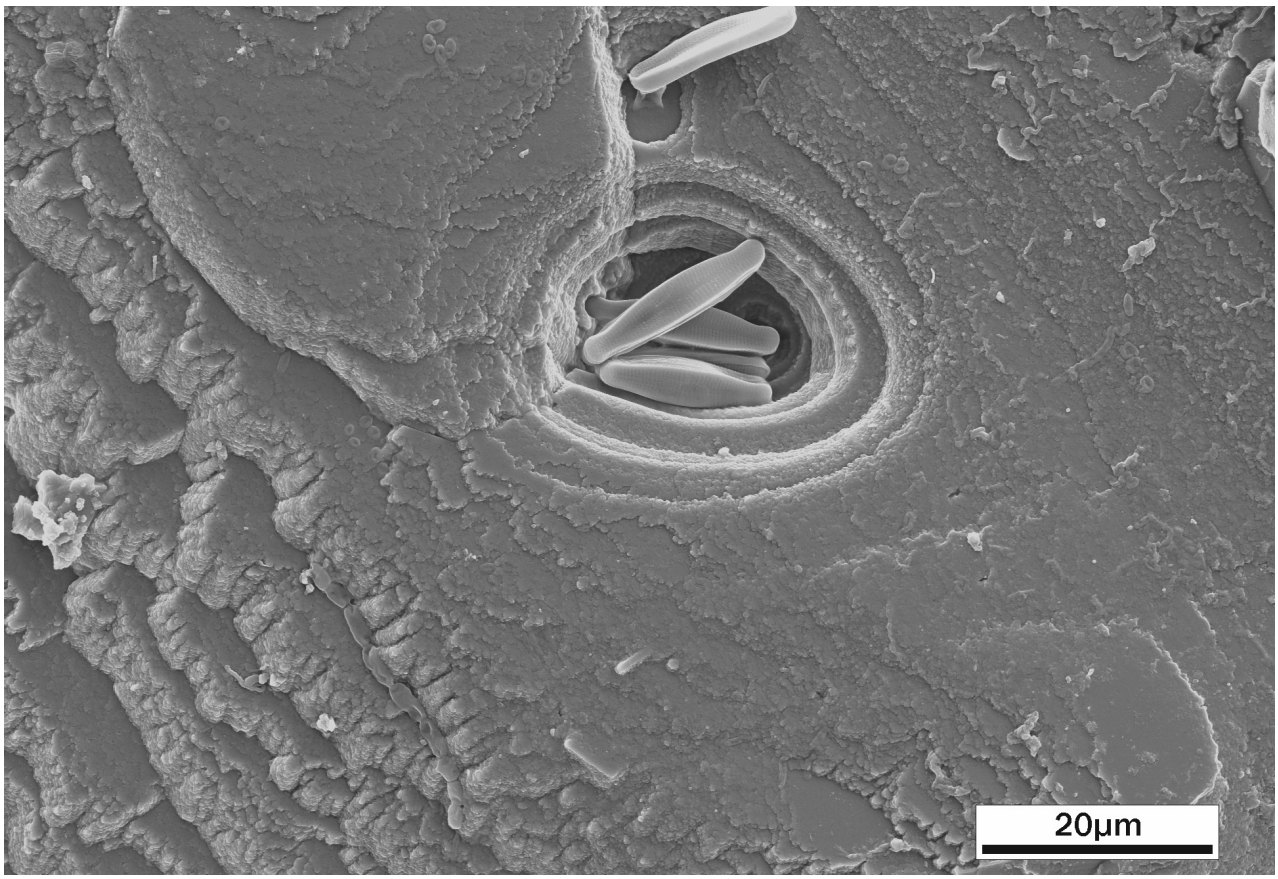

Figure 3.1.10h. 'Diatom jacuzzis' forming in freshly precipitated tufa encrustations on Foel Fawr. Note mucilage stalk of lone diatom. (Submap: West 2). Stub #21.

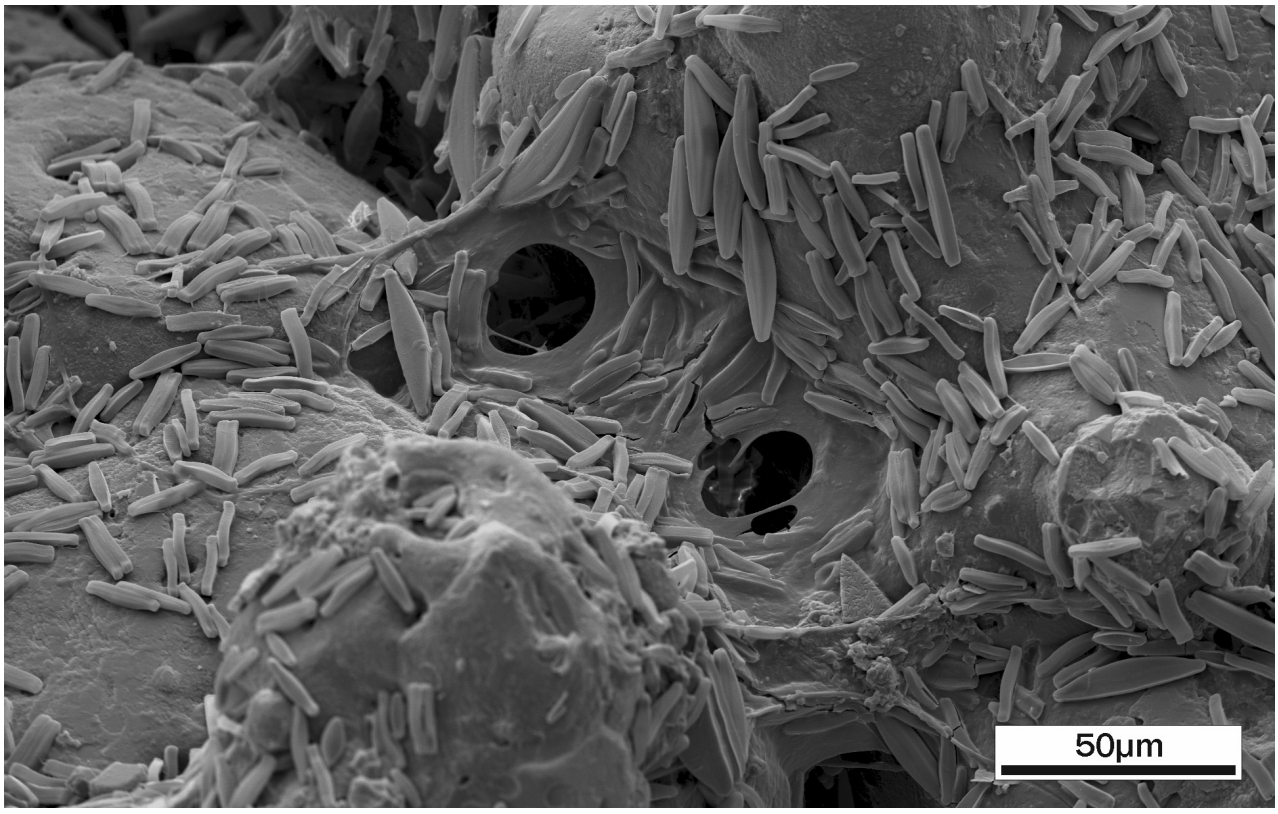

Figure 3.1.10i. EPS associated with diatoms on a tufa encrustation, Foel Fawr. (Submap: West 4). Stub #20.

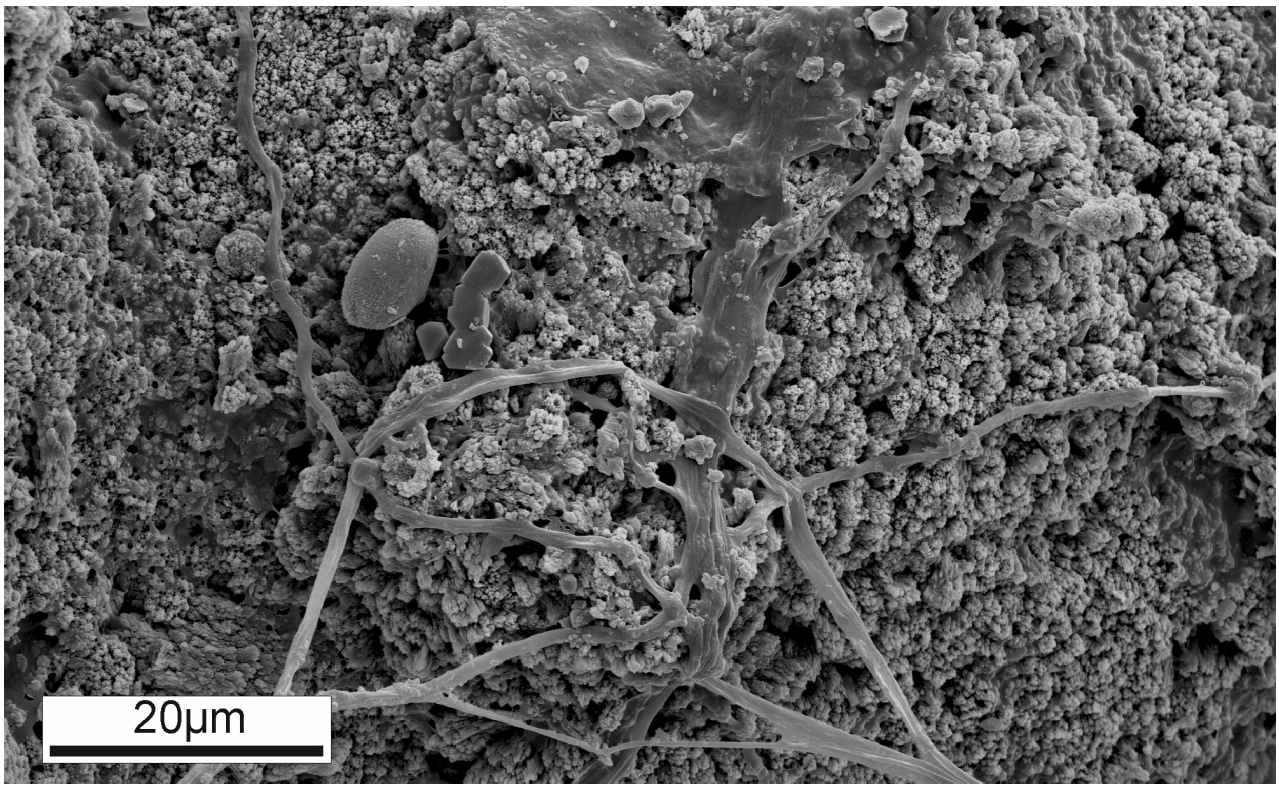

Figure 3.1.10j. Filamentous strands, EPS and micrite forming in marginal areas on Foel Fawr. (Submap: East 8). Stub #23.

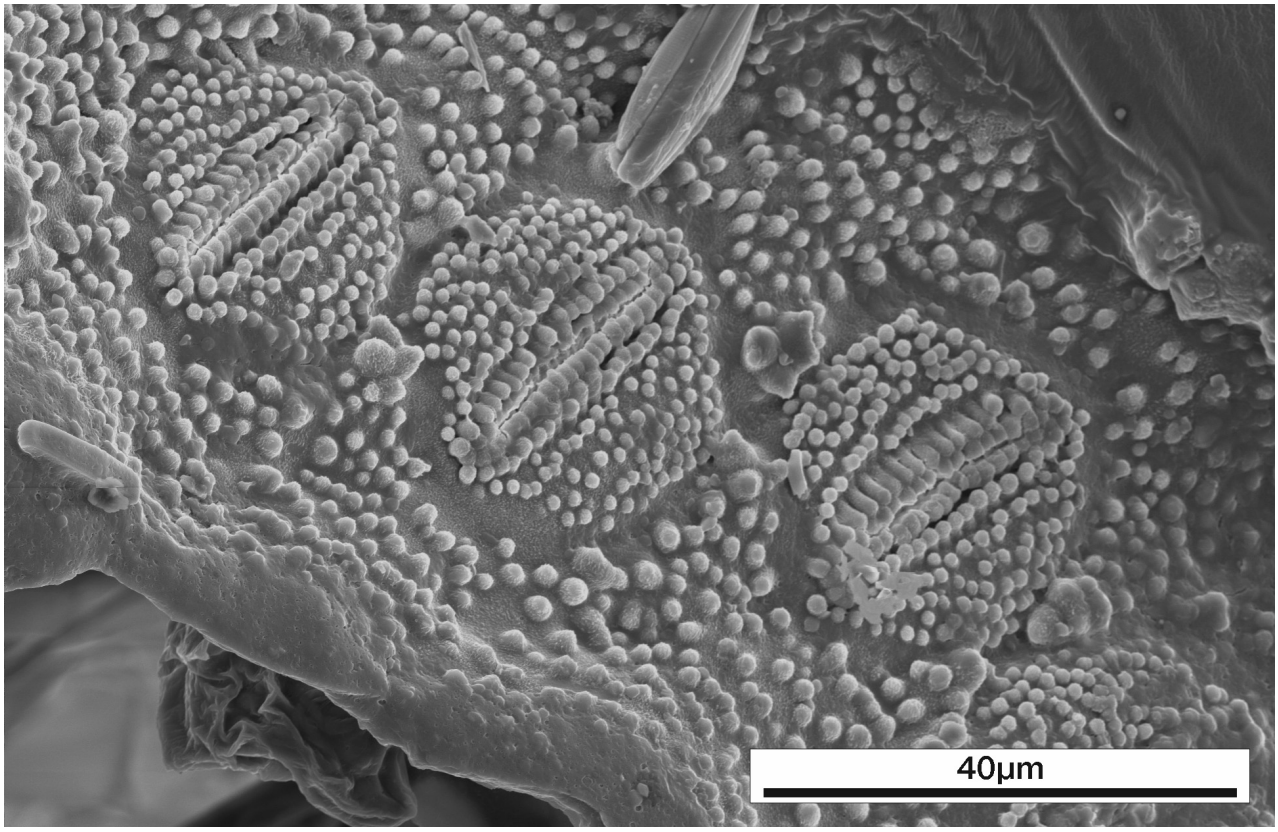

Figure 3.1.10k. Equisetum sp. stoma preserved in fresh marginal encrustation on Foel Fawr. Note silica papillae covering the epidermis and stomatal cover cells. (Submap: West 2). Stub #21.

Pollen is also preserved, often associated with diatoms and micrite, suggesting areas where sub-aerial exposure may have lasted longest (figure 3.1.10l).

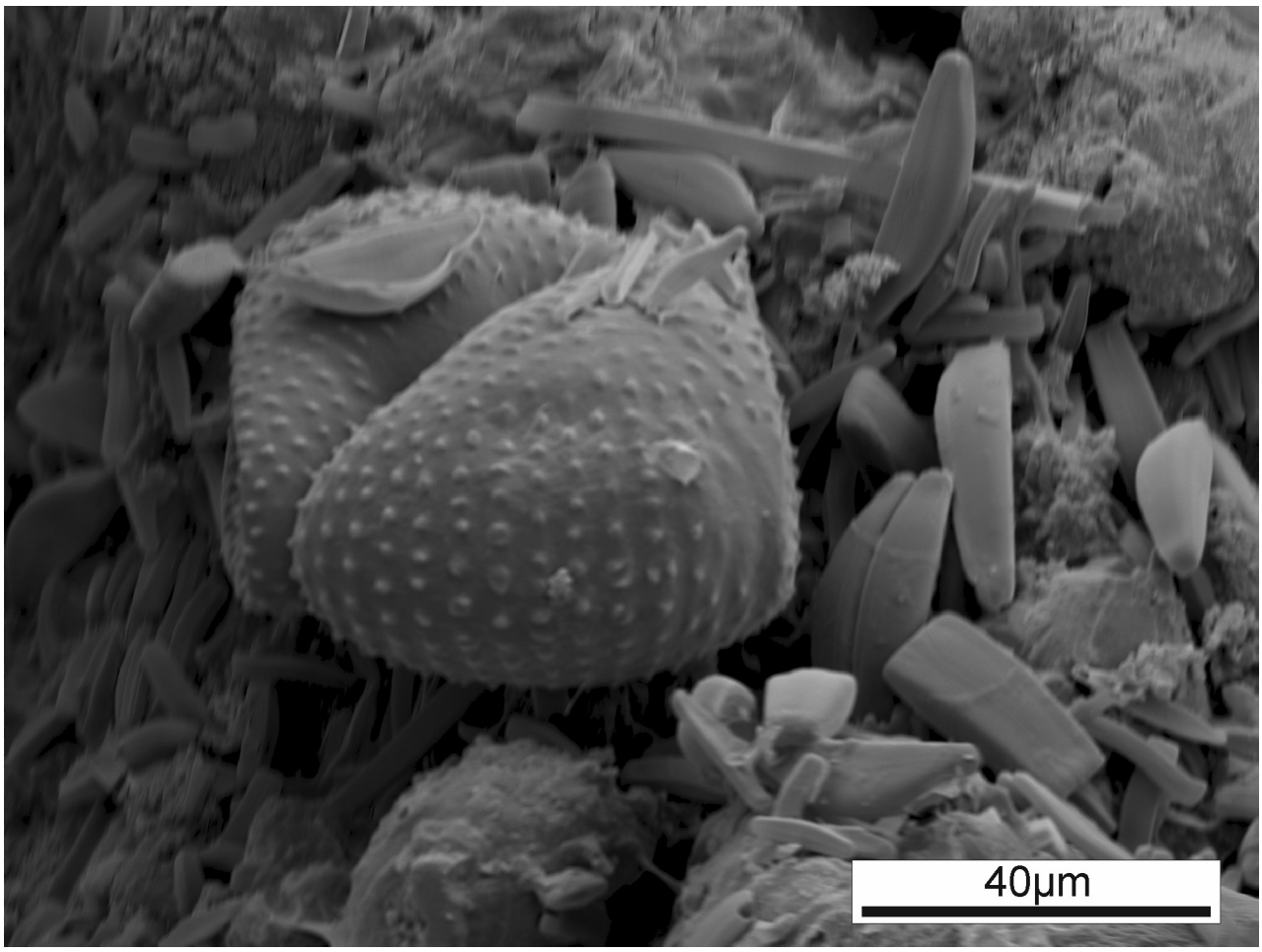

Figure 3.1.10l. Pollen grain. (Submap: East 8). Stub #24.

3.1.11. Fossil tufa channels

Fossil tufa channels form raised linear structures on slopes (<60^{o}) proximally to the tips (figure 3.1.11a). They are subaerially exposed and colonised by bryophytes and plants. They are formed from laminated crusts; however, this can be obscured by fracturing and vegetation.

3.1.11a. Fossil tufa channel forming on Foel Fawr. (Submap: East 7).

3.2. Facies key

The following key provides a quick reference for the characters present within each facies. It is not essential for all characters to be present to positively identify each facies. As most of the facies represent an end member of a continuum of morphology, the characters here are typically representative of those expected of that end member. Where facies transition between one another, the distinction of a boundary is somewhat arbitrary and has been determined by considering the relative dominance of adjacent facies.

						Slope			Terraces		Grains				Other Features				
Facies	Submerged (<1cm)	Submerged (>1cm)	Subaerial	Proximal[1]	Distal[1]	<20°	20-60°	60°<	Microterracettes (cm-scale)	Terracettes (m-scale)	Small Spheroidal[2]	Small Disk Shaped[2]	Large[2]	Irregular	Crystalline Crusts	Calcareous Mud	Carbonate Rafts	Marginal Plants Encrusted	Plants/Algae Colonising
Apron	×		×	×		×	×		×						×		×		
Stream Crust	×	×	×		×	×	×			×	×				×			×	×
Vertical Apron	×		×	×				×	×						×			×	
Carbonate Mud Pool	×	×		×		×										×	×	×	×
Carbonate Mud			×		×	×										×			×
Pisoidal Pool	×	×	×	×		×					×	×			×		×		
Carbonate Gravel			×	×	×	×					×			×		×			×
Oncoids	×	×	×		×	×					×		×	×			×	×	×
Fossil Tufa Channels			×	×		×	×												×

Table 3.2a. Facies key.

1: Proximal is defined as <10m from the spring/seep, distal as >10m from the spring/seep.

2: Small grains: maximum measurement <5cm. Large grains >5cm.

3.3. Facies maps

3.3.1. Introduction

Tufa is deposited in streams along a 2.5 km stretch of the northern side of Foel Fawr, South Wales. Maps of the deposits are organised west to east, and descriptions can be found below each map. A broad scale overview map is provided (figure 3.3.3), along with three general maps (figures 3.3.4, 3.3.5 and 3.3.6), showing the distribution of quarries, lime spoil, and tufa across the site. Submaps are provided at approx. 1:750 scale, outlining the extent of facies described in section 3.1 and summarised in section 3.2. A facies key is provided at the front and back of the maps sections for use with submaps. The table of contents overleaf is provided to aid navigation between maps.

Overview data regarding the extent of the deposits on Foel Fawr is provided in table 3.3.1a. Carbonate gravel is by far the most expansive facies, however, this observation must be tempered by the consideration that there are many small outwashes which are very thin and thus represent a very small volume of tufa. Conversely, the relative area covered by vertical aprons likely underplays their significance as the horizontal area they take up does not represent the vertical area they occupy.

Facies	Total area (m^2)	Individual areas (m^2)		
		Smallest	Largest	Mean
Total	12 348	-	-	-
Apron	1 922	4.7	228.3	48
Stream Crust	976	4.9	771.0	98
Vertical Apron	107	5.6	52.4	27
Carbonate Mud Pool	211	6.6	133.0	70
Carbonate Mud	1 769	15.8	517.6	161
Pisoidal Pool	129	1.7	50.5	21
Carbonate Gravel	6 958	6.2	733.9	109
Oncoids	221	12.5	108.5	44
Fossil Tufa Channel	55	0.8	8.1	3

Table 3.3.1a. Overview of horizontal extent of facies on Foel Fawr.

Table of contents: facies maps

3.3.2. Facies key

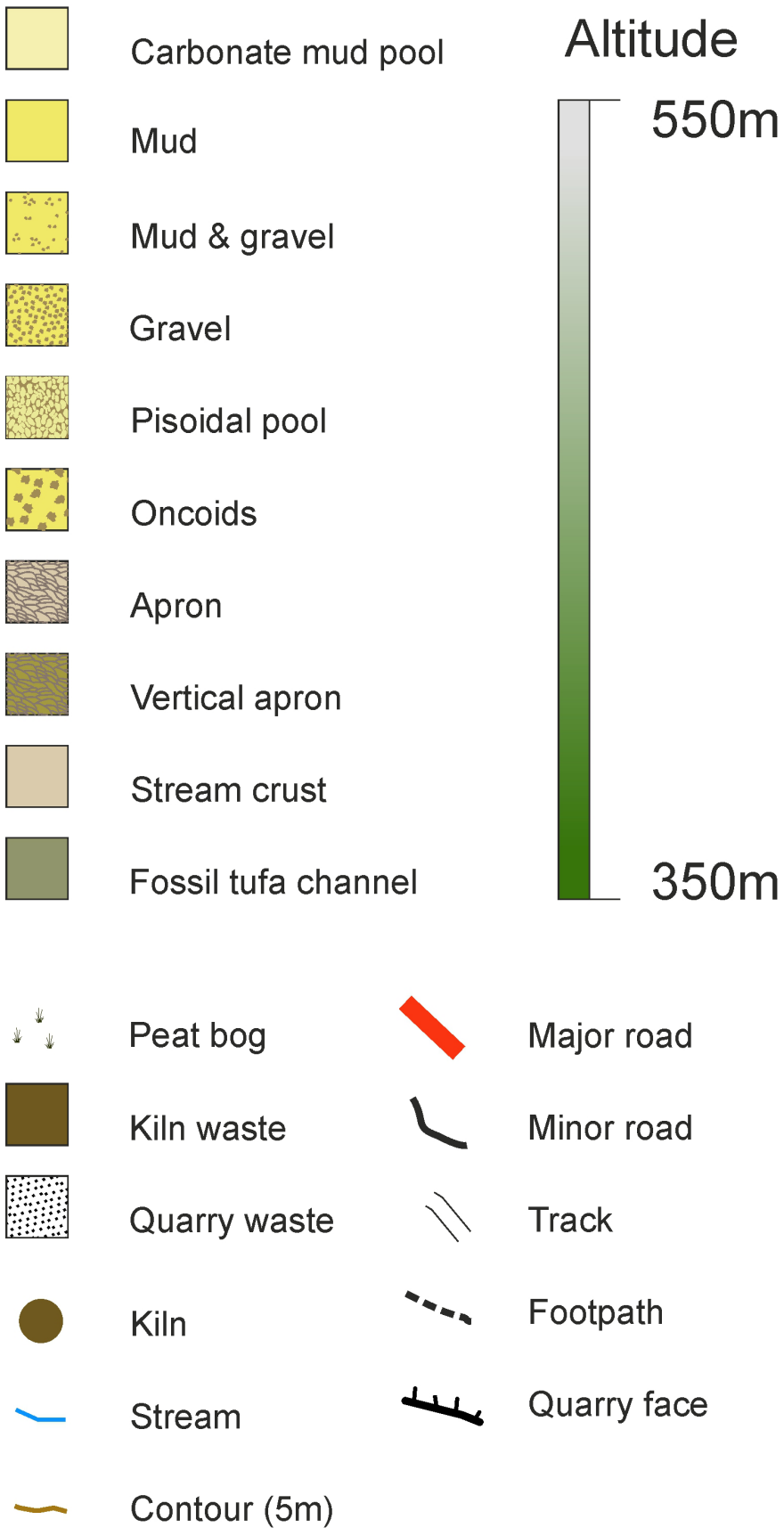

3.3.3. Overview map

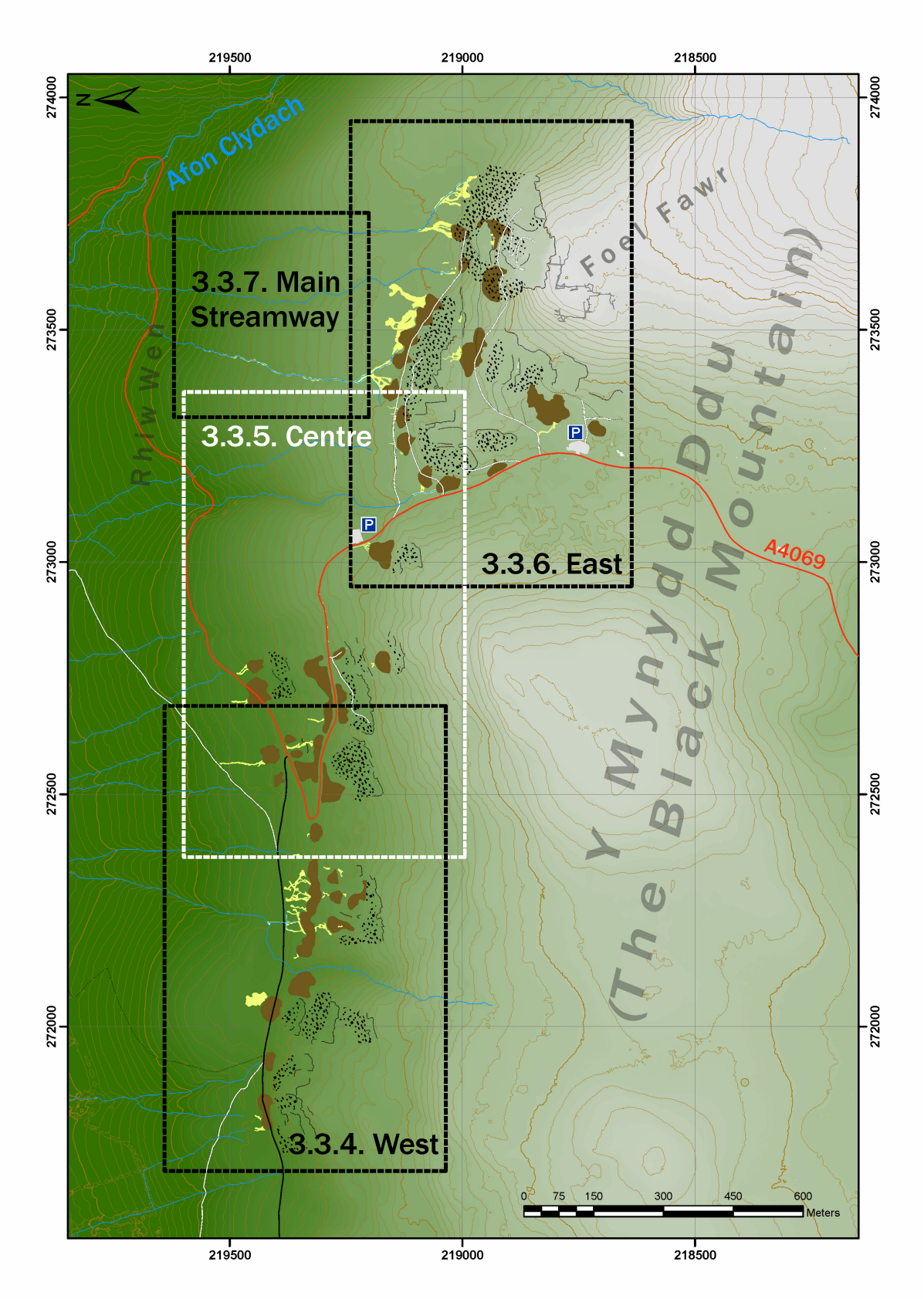

Figure 3.3.3. Overview map of Foel Fawr. Dashed boxes denote submap extents.

3.3.4. West

The westernmost tufa deposits consist predominantly of small aprons and gravel outwashes. They are formed mostly amongst the tips, above the natural springline at the base of the spoil tips. Typical discharge is generally lower than the deposits further east, and natural runoff streams are smaller. There are some small areas of peat bog onto which tufa has formed, however, these areas are limited compared with the eastern deposits (see section 3.3.6.). Typical altitude is around 400 m. Submaps are shown in figures 3.3.4a, 3.3.4b, 3.3.4c, 3.3.4d, 3.3.4e, 3.3.4f, 3.3.4g and 3.3.4h.

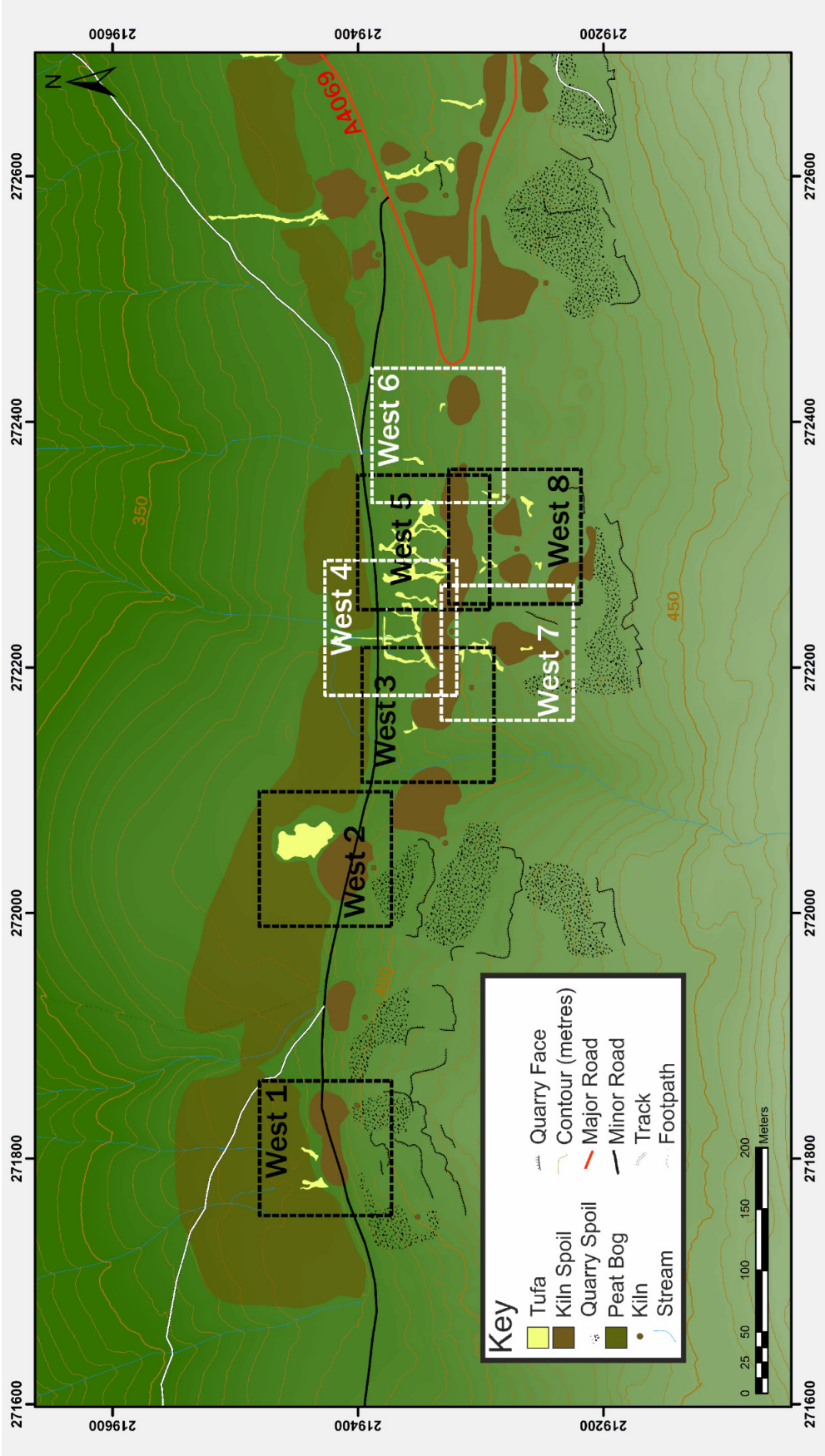

Figure 3.3.4. Western deposits

3.3.4a. Submap: West 1

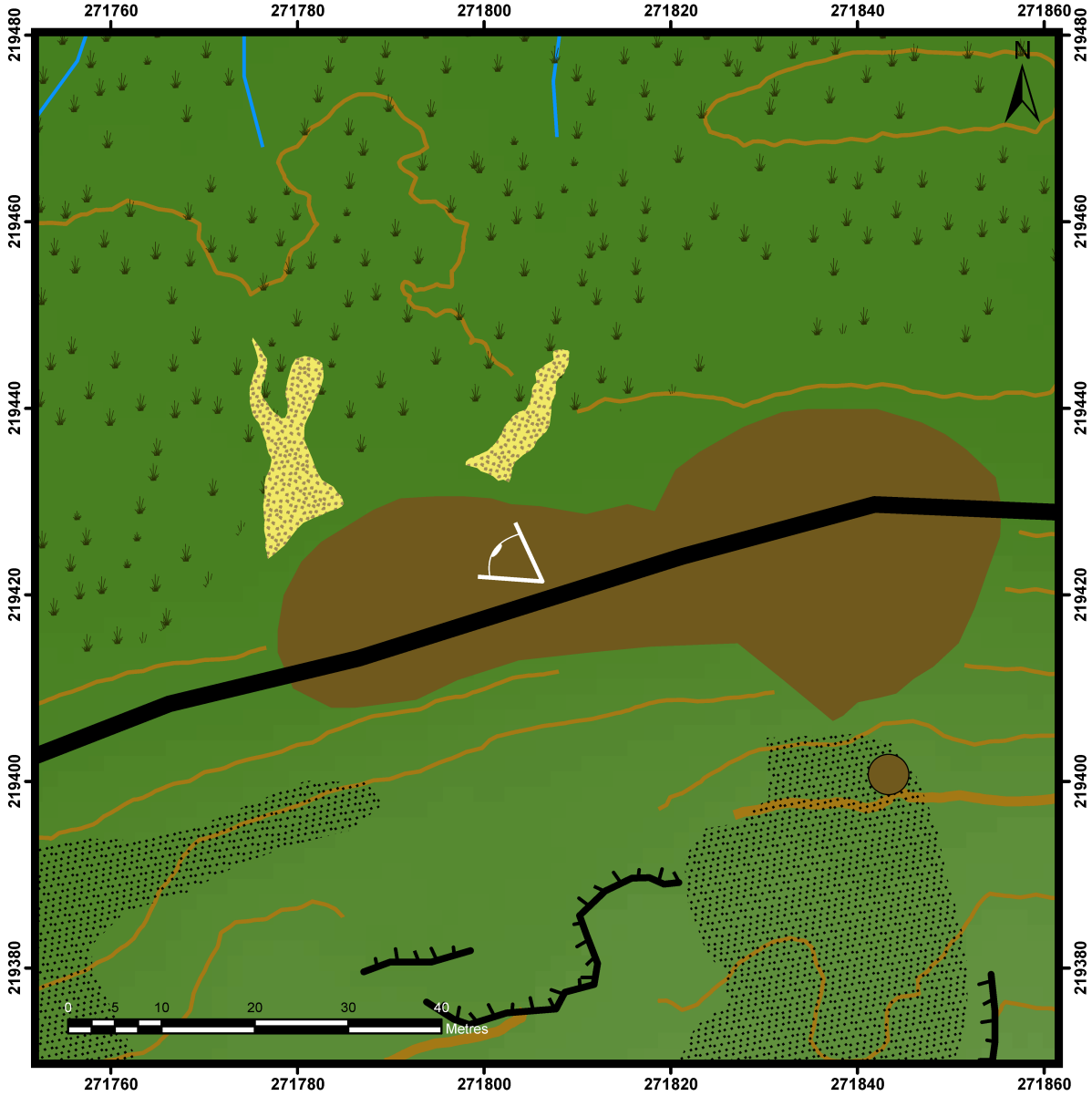

Figure 3.3.4a. Submap: West 1 and image (above) Two isolated outwashes of carbonate gravel at the extreme western end of the site.

3.3.4b. Submap: West 2

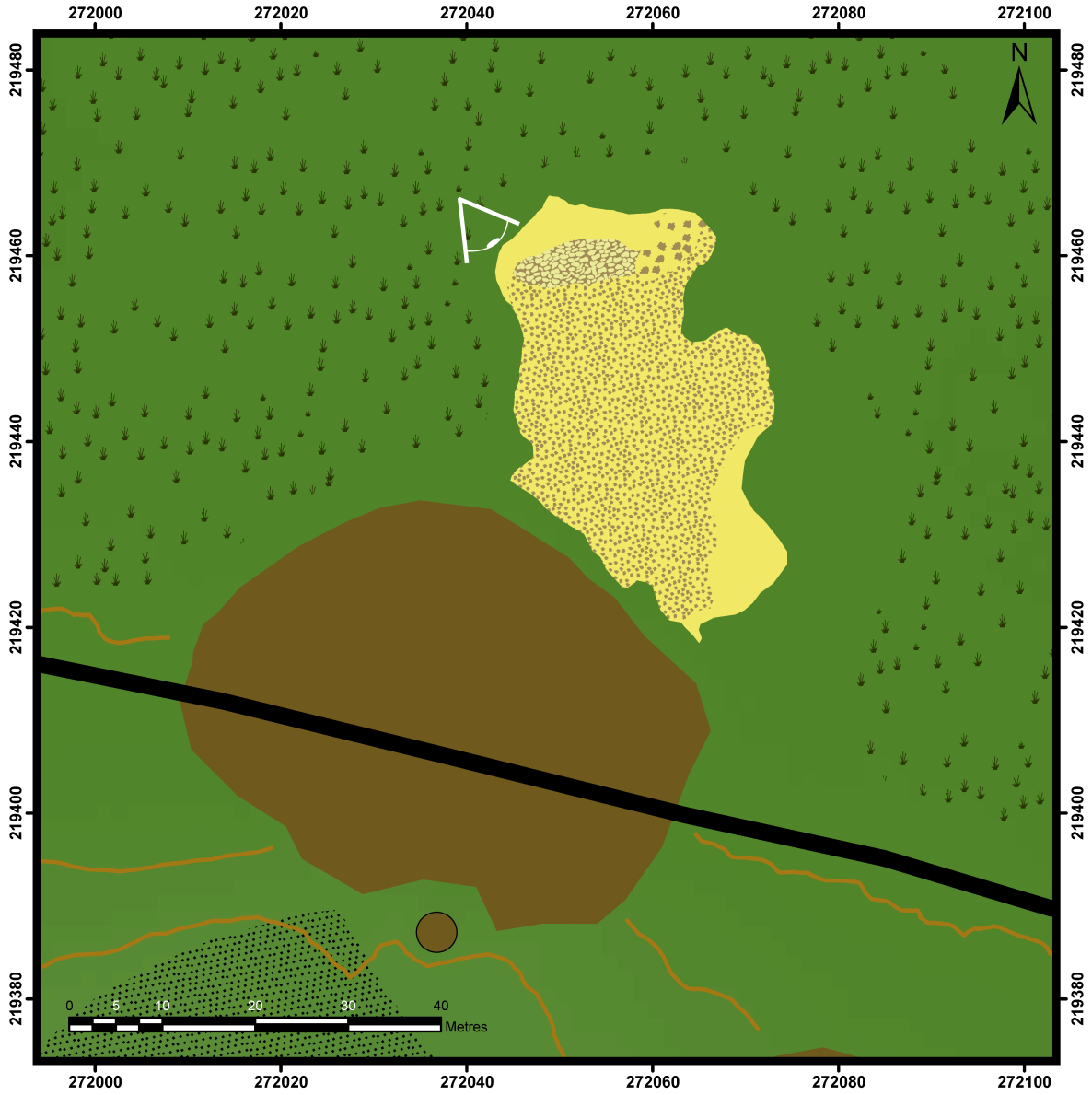

Figure 3.3.4b. Submap: West 2 and image (above). Large, flat carbonate gravel outwash, flanked by carbonate mud on the east and an ephemeral pool containing pisoids and oncoids to the north.

3.3.4c. Submap: West 3

Figure 3.3.4c. Submap: West 3 and image (above). A small, isolated outwash of carbonate gravel.

3.3.4d. Submap: West 4

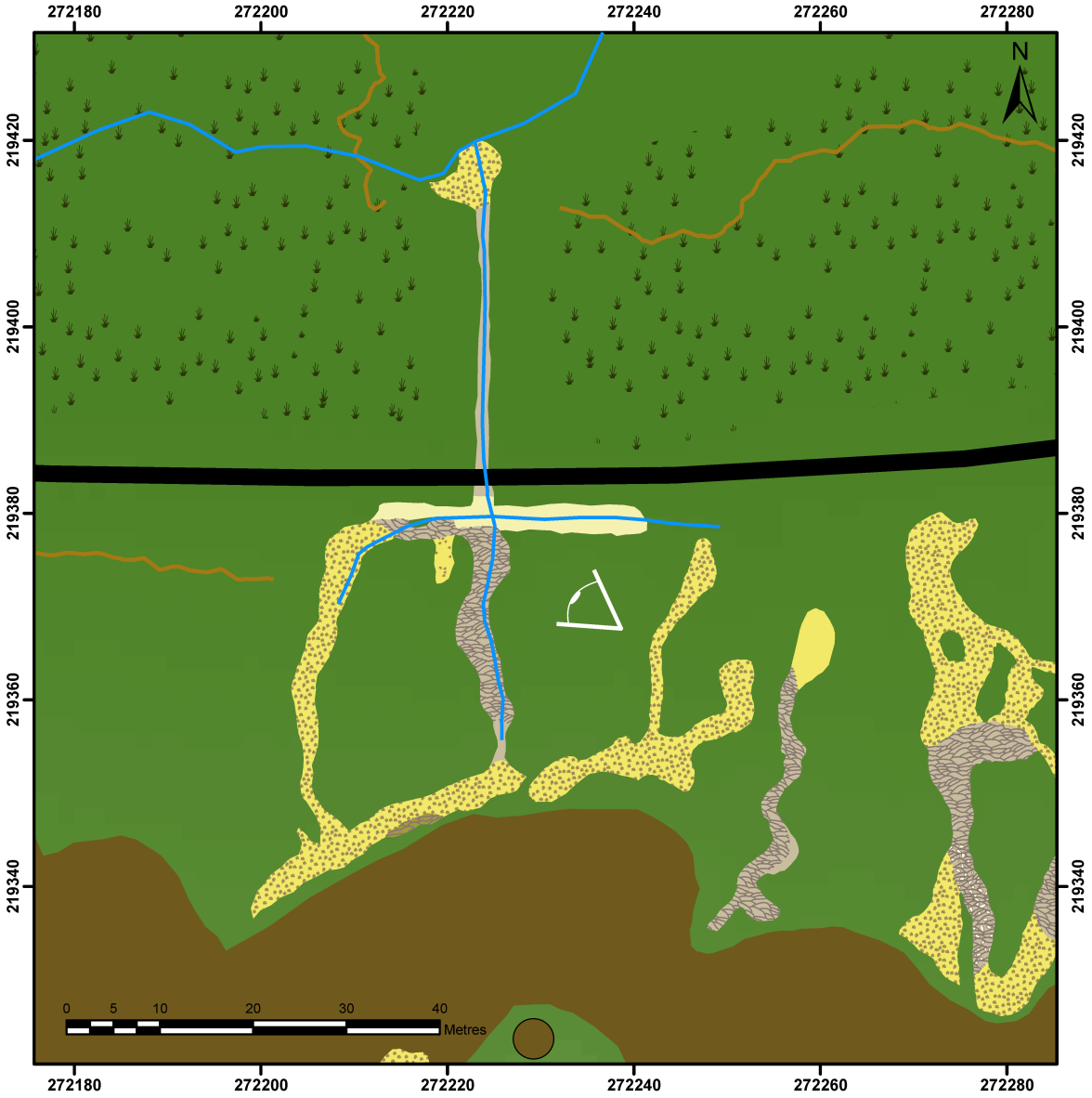

Figure 3.3.4d. Submap: West 4 and image (overleaf). Apron and gravel outwashes draining north into a carbonate mud pool (ditch), which drains through a tunnel into a channel, forming stream crust with a gravel outwash at the base. Below this, input from uncontaminated streams precludes precipitation. To the east, an (inactive) apron drains northwards with a carbonate mud outwash at its base. Deposits at the far east of the map are described in figure 3.3.4e.

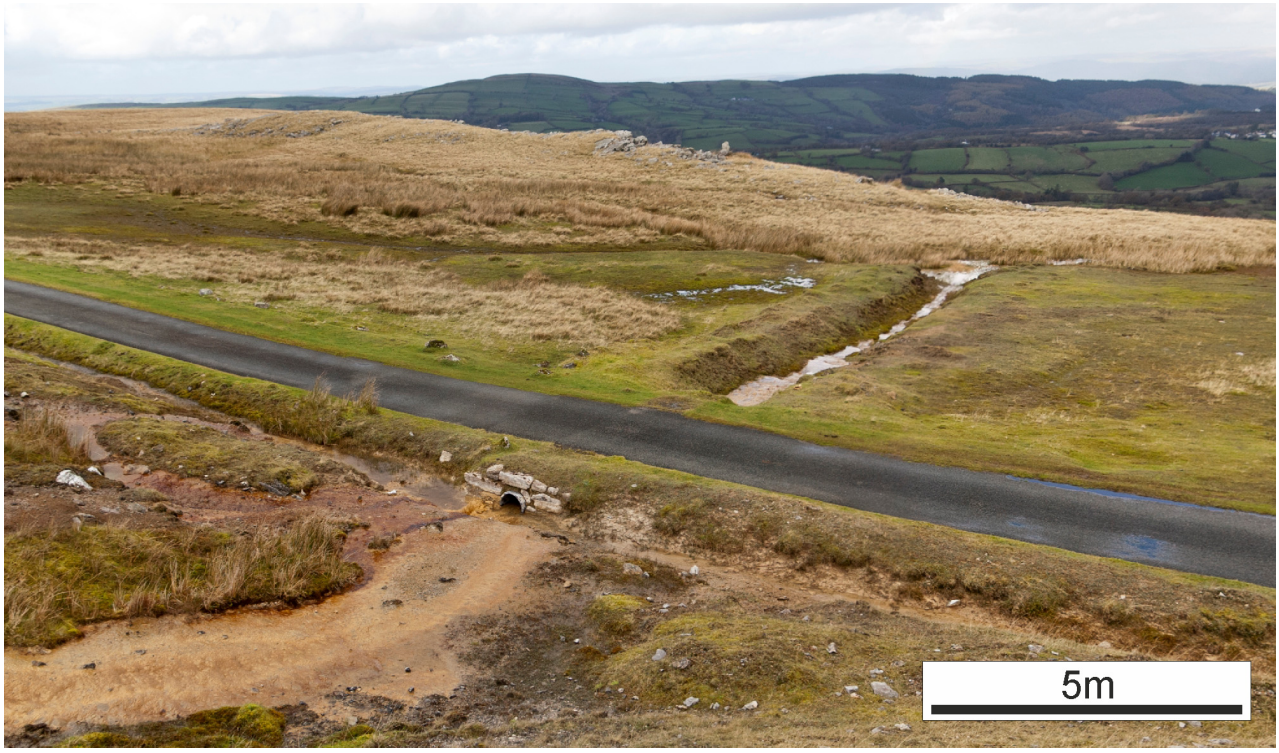
5m

3.3.4e. Submap: West 5

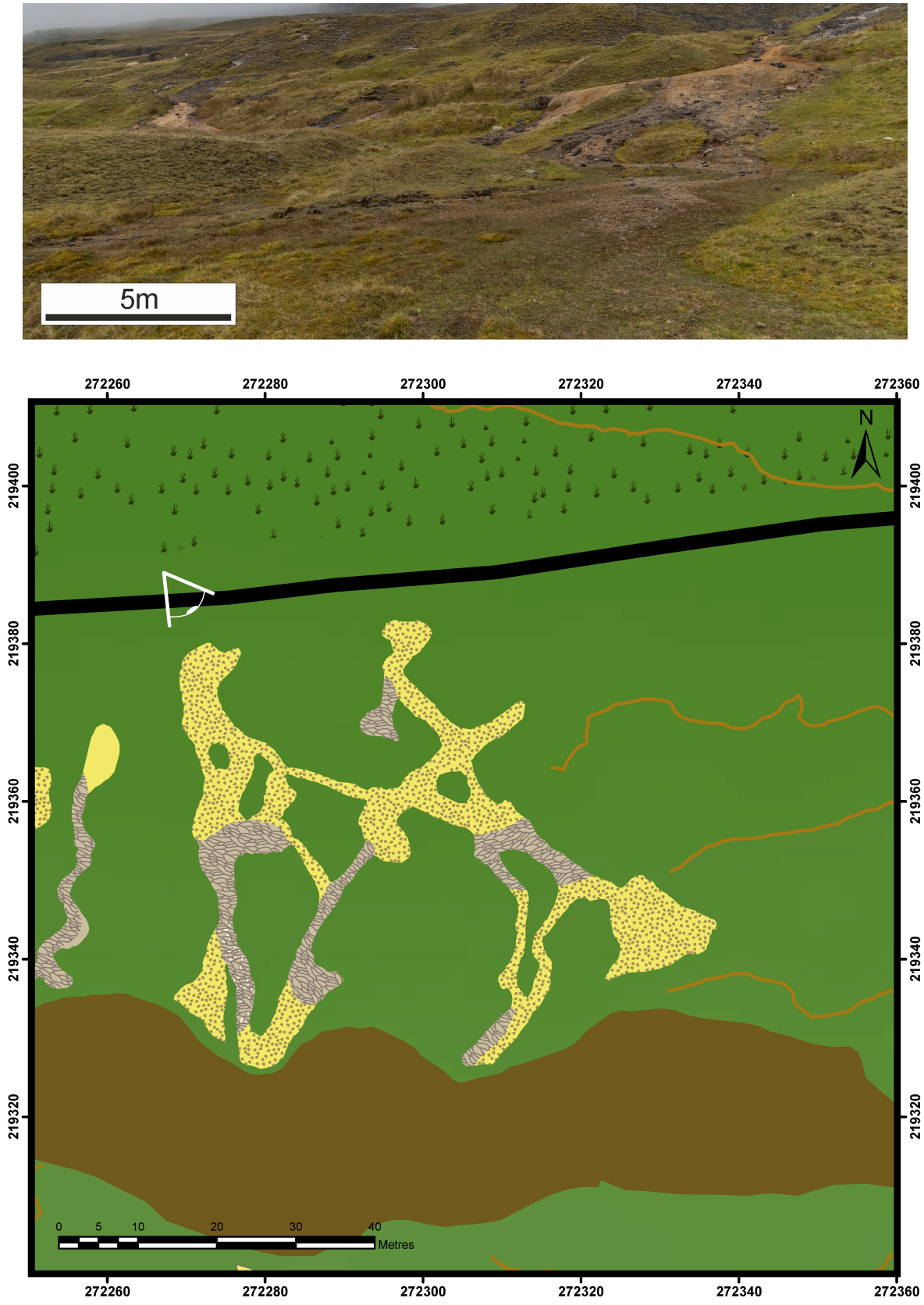

Figure 3.3.4e. Submap: West 5 and image (above). Aprons and gravel outwashes with (mostly inactive) aprons on steeper sections and carbonate gravel on gentler slopes.

3.3.4f. Submap: West 6

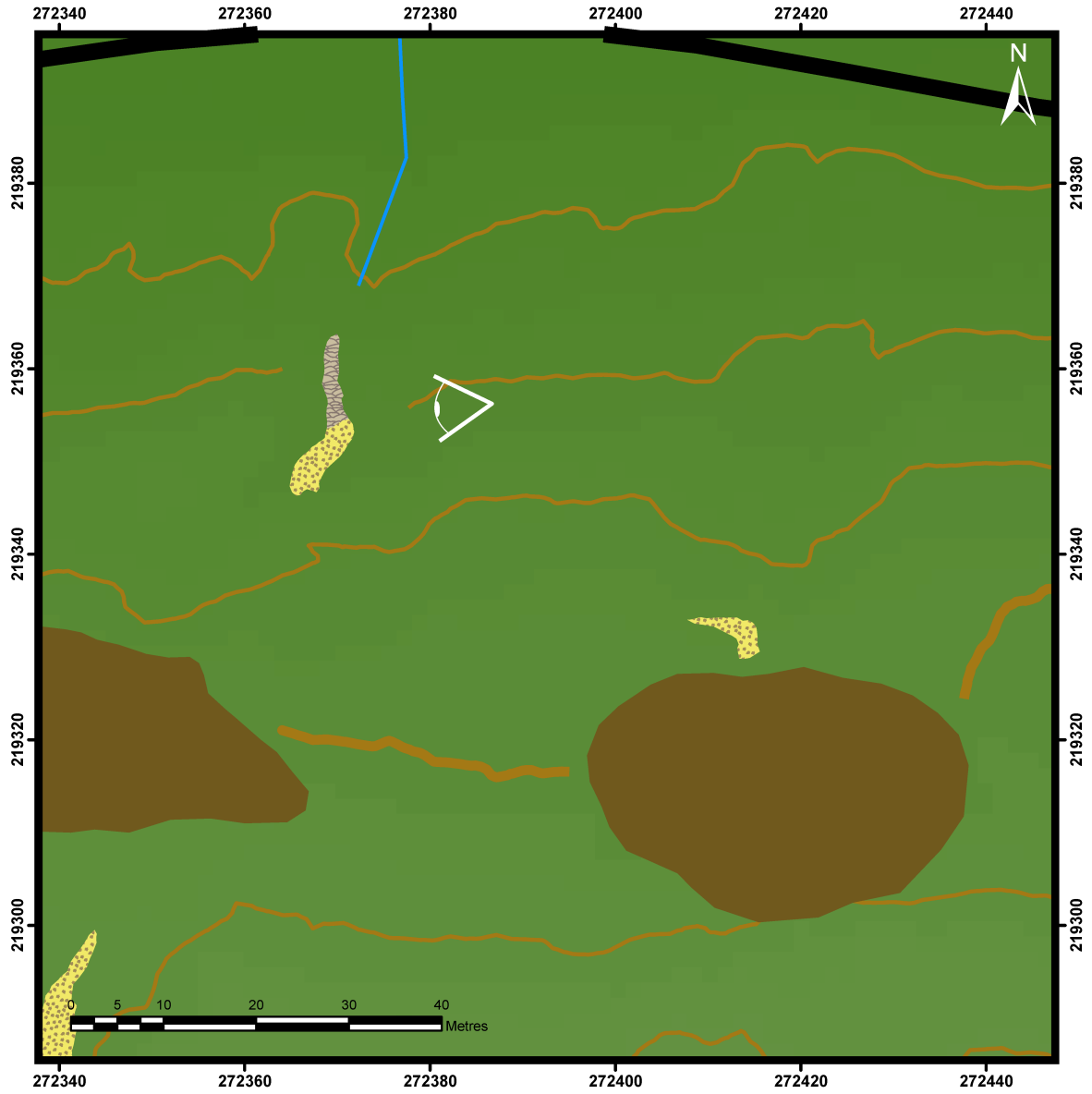

Figure 3.3.4f. Submap: West 6 and image (above). Two isolated gravel outwashes with a small (inactive) apron at the base of the westernmost outwash where the slope increases.

3.3.4g. Submap: West 7

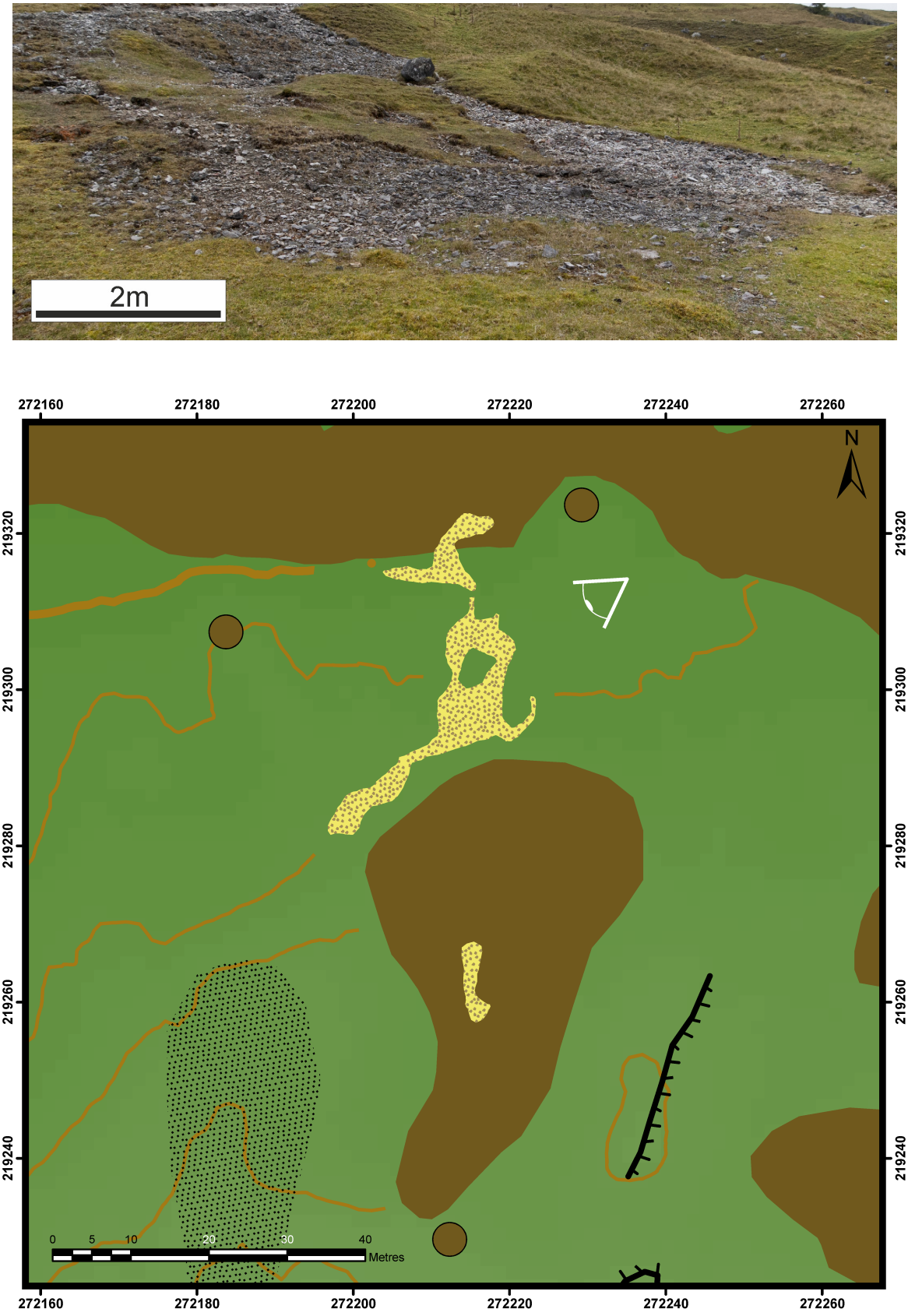

Figure 3.3.4g. Submap: West 7 and image (above). Two isolated gravel outwashes in amongst the lime tips.

3.3.4h. Submap: West 8

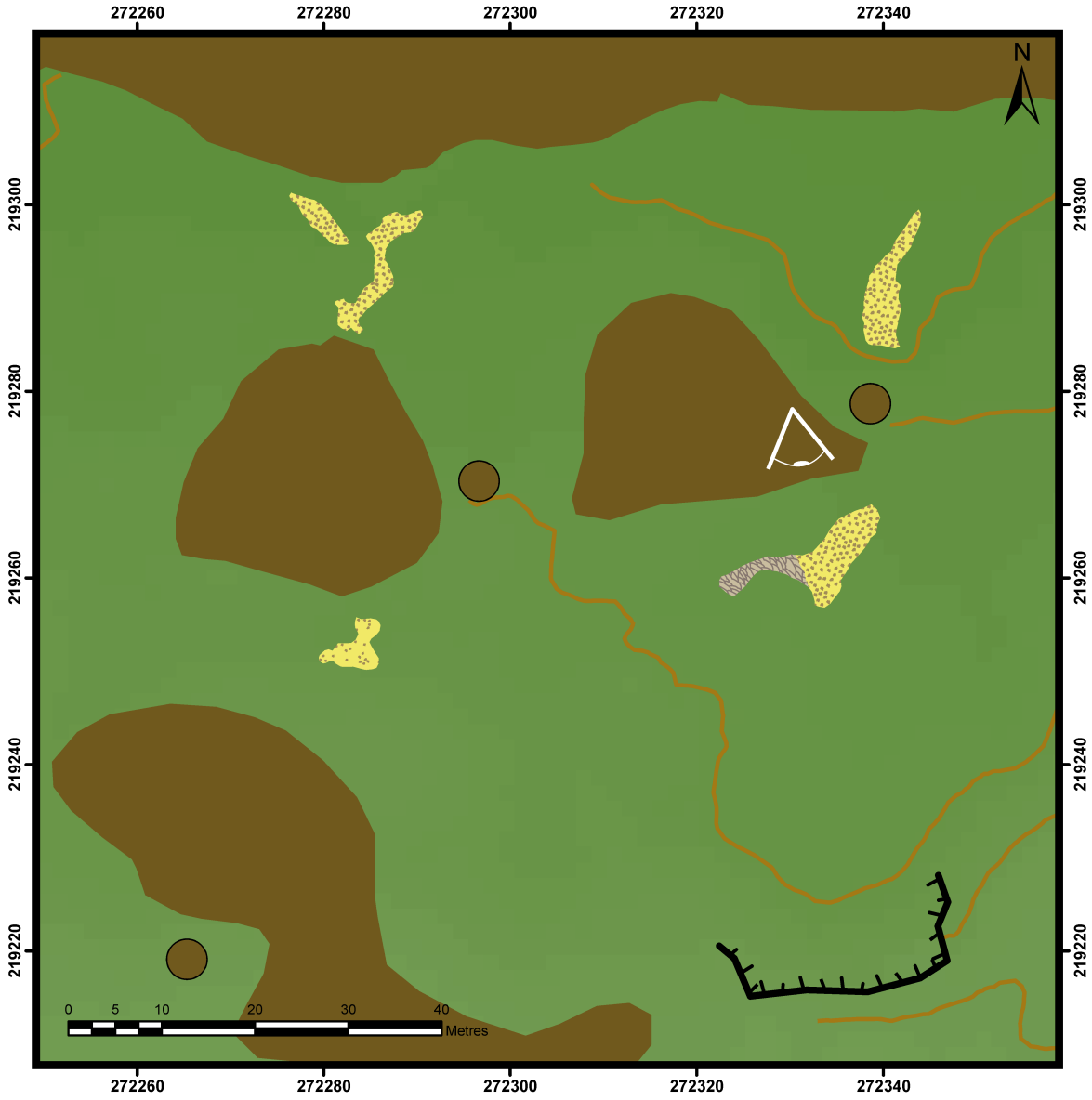

Figure 3.3.4h. Submap: West 8 and image (above). Several small, isolated gravel outwashes with a small (inactive) apron. All are forming above the lower lime tips.

3.3.5. Centre

The central deposits consist of several isolated outwashes, mostly consisting of springs forming aprons. Most of the streams are of relatively low discharge, forming small stream compared with the eastern deposits (see section 3.3.6). Typical altitude is around 400m. Submaps are shown in figure 3.3.5a, 3.3.5b, 3.3.5c, 3.3.5d and 3.3.5e.

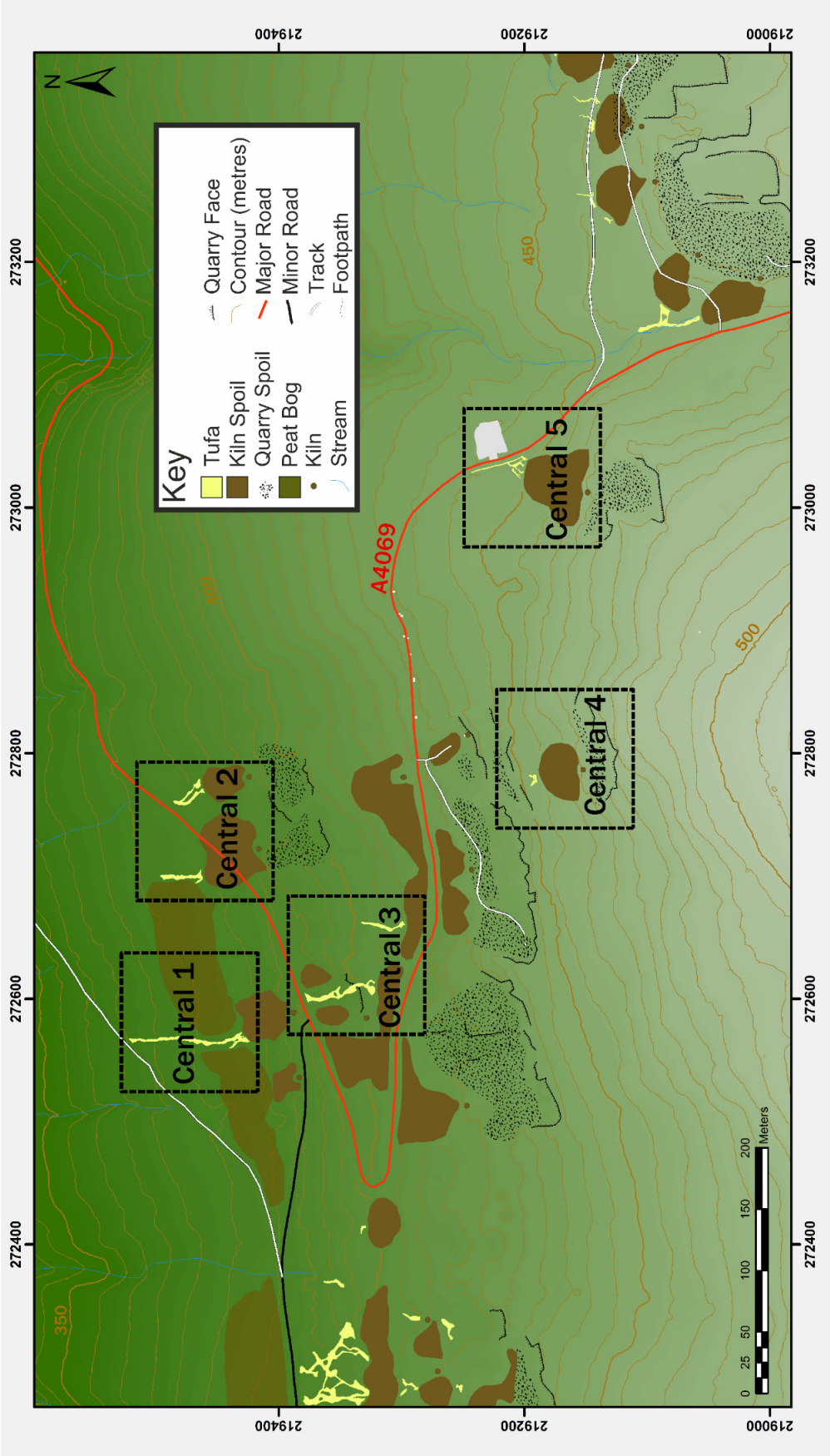

Figure 3.3.5. Central deposits

3.3.5a. Submap: Centre 1

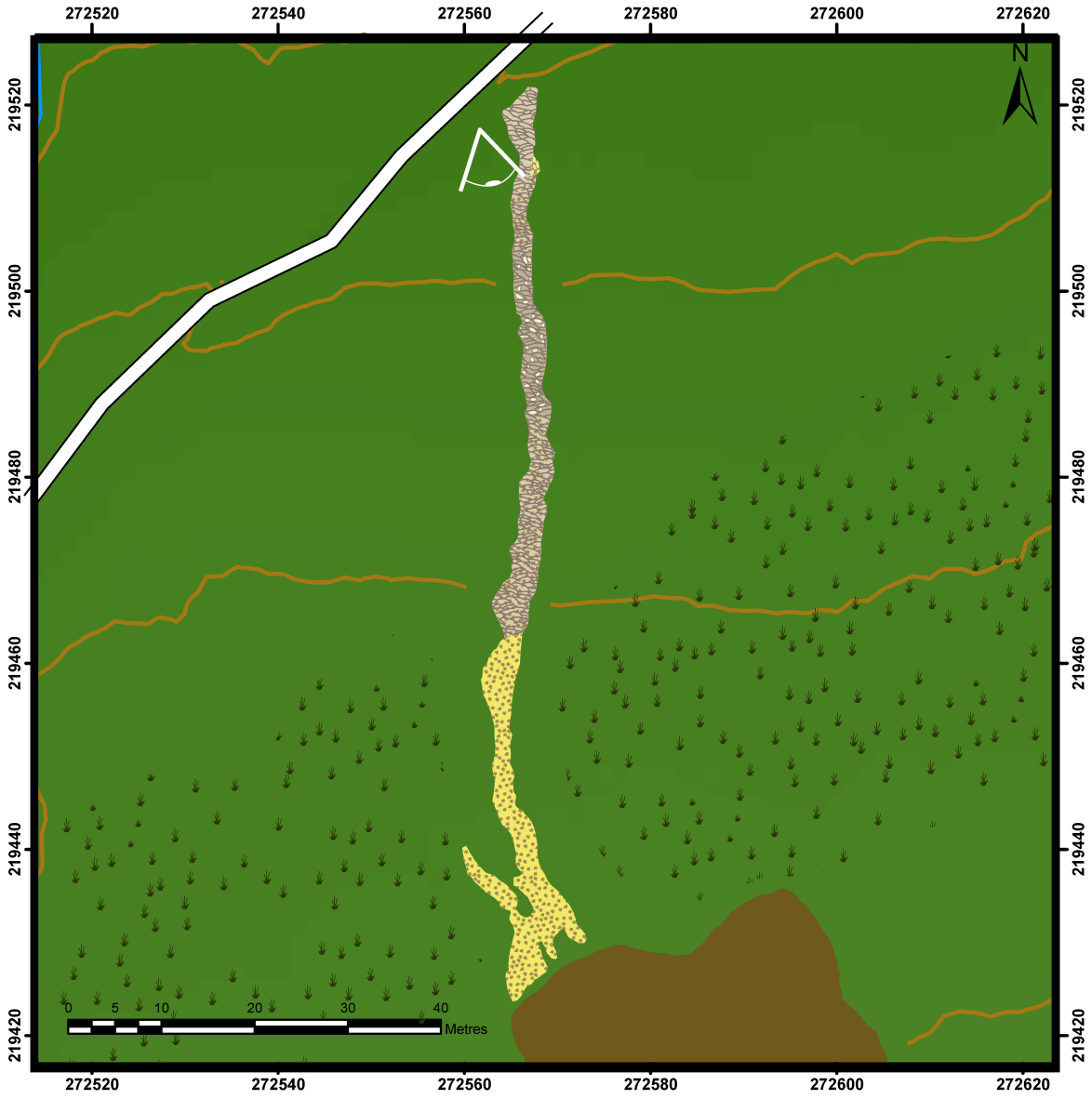

Figure 3.3.5a. Submap: Centre 1 and image (overleaf). A single outwash, with gravel facies, transitioning to apron facies (with gravel or pisoids on the surface in places) as the slope increases away from the tips.

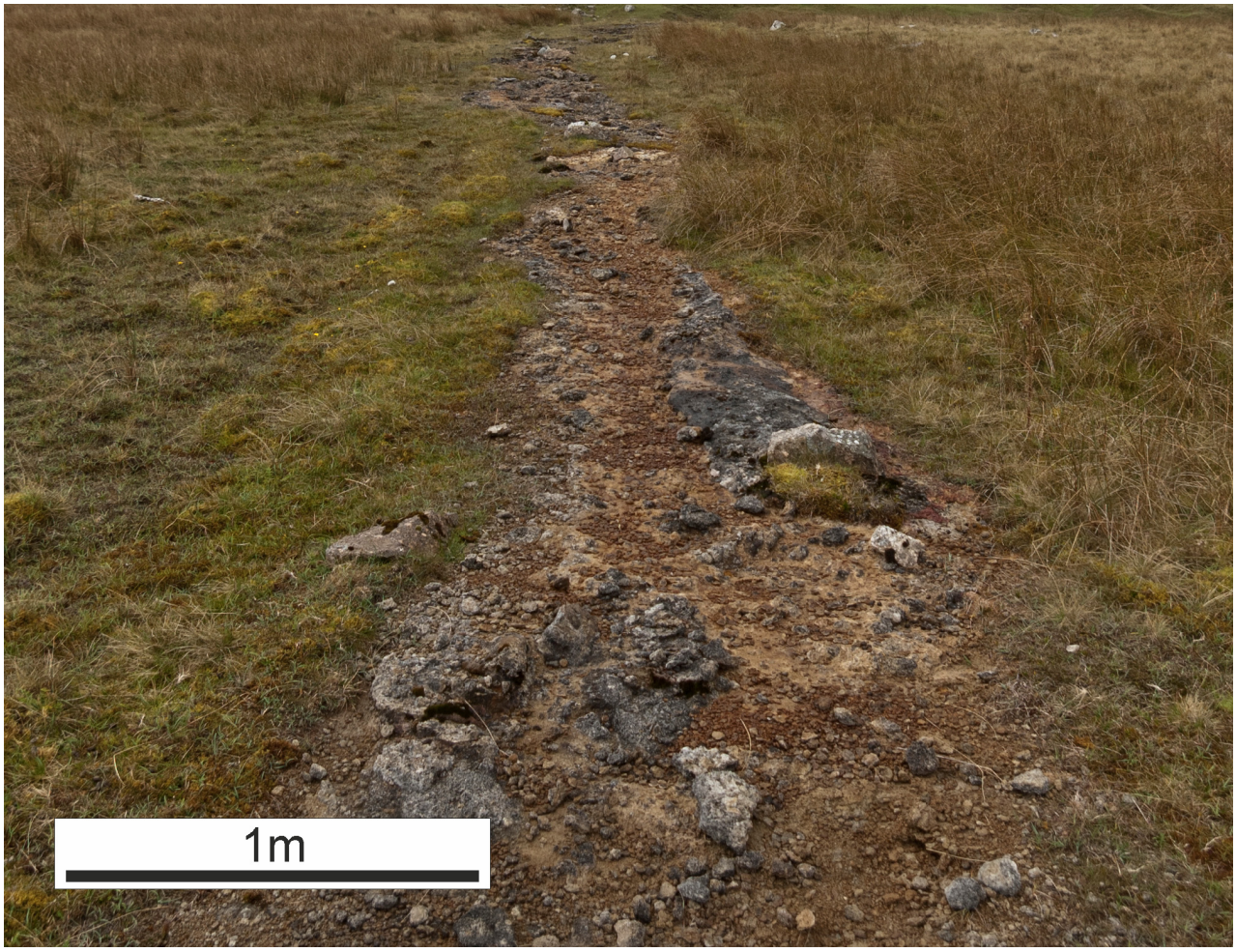
1m

3.3.5b. Submap: Centre 2

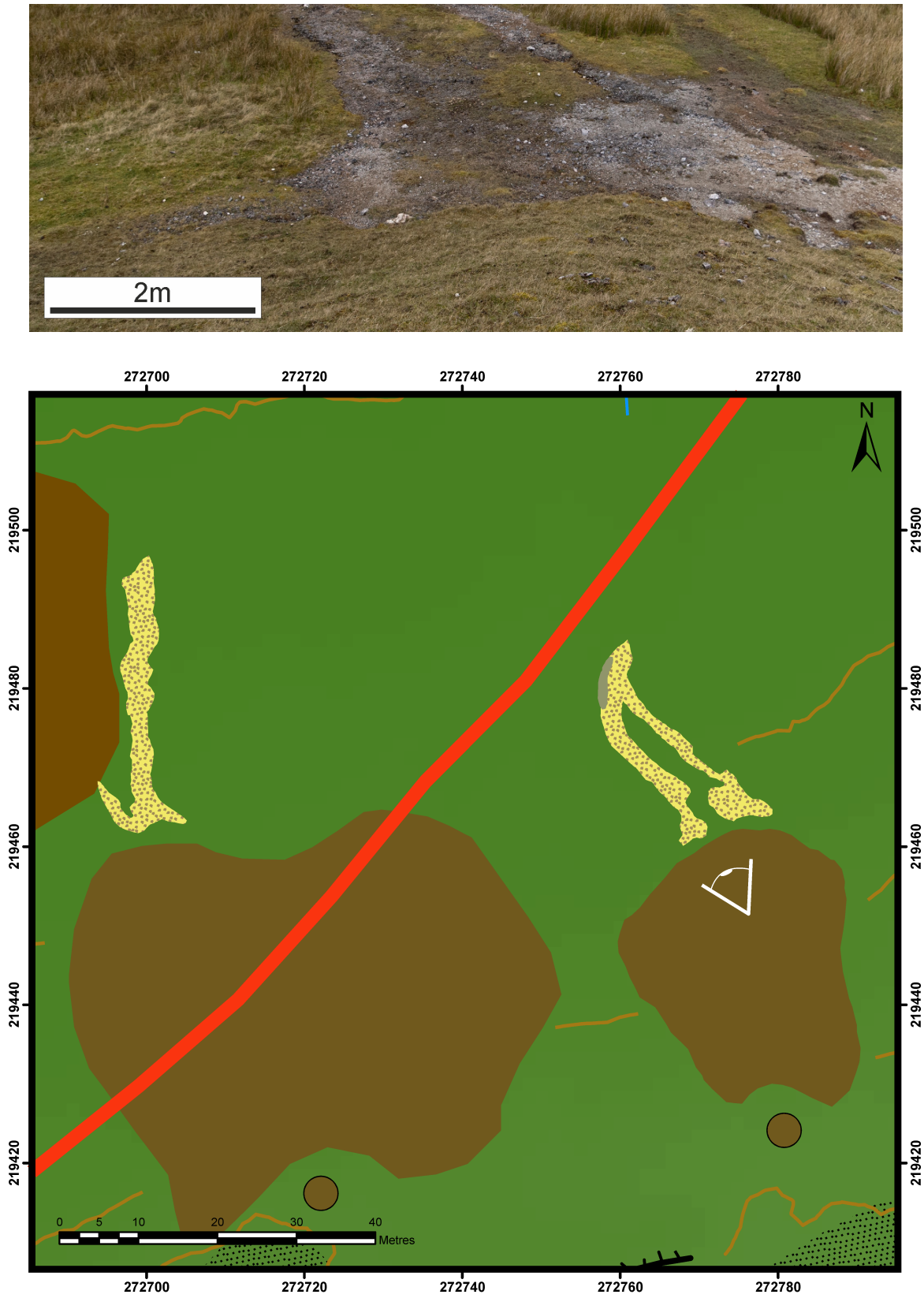

Figure 3.3.5b. Submap: Centre 2 and image (above). Two small, isolated carbonate gravel outwashes with remnants of a small fossil tufa channel.

3.3.5c. Submap: Centre 3

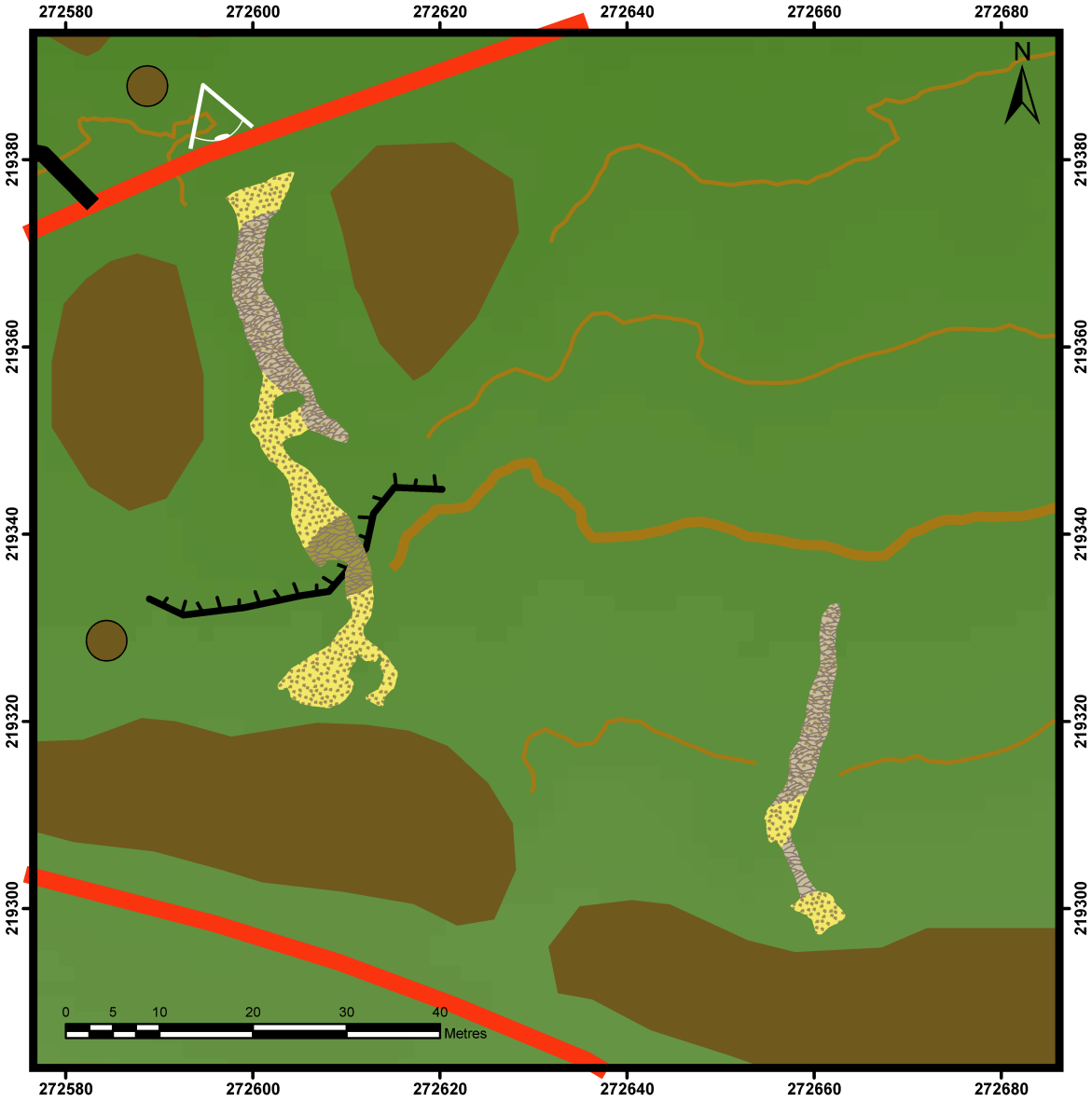

Figure 3.3.5c. Submap: Centre 3 and image (overleaf). Aprons and carbonate gravel outwashes, with a vertical apron forming where the western outwash channel transects a vertical quarry face.


2m

3.3.5d. Submap: Centre 4

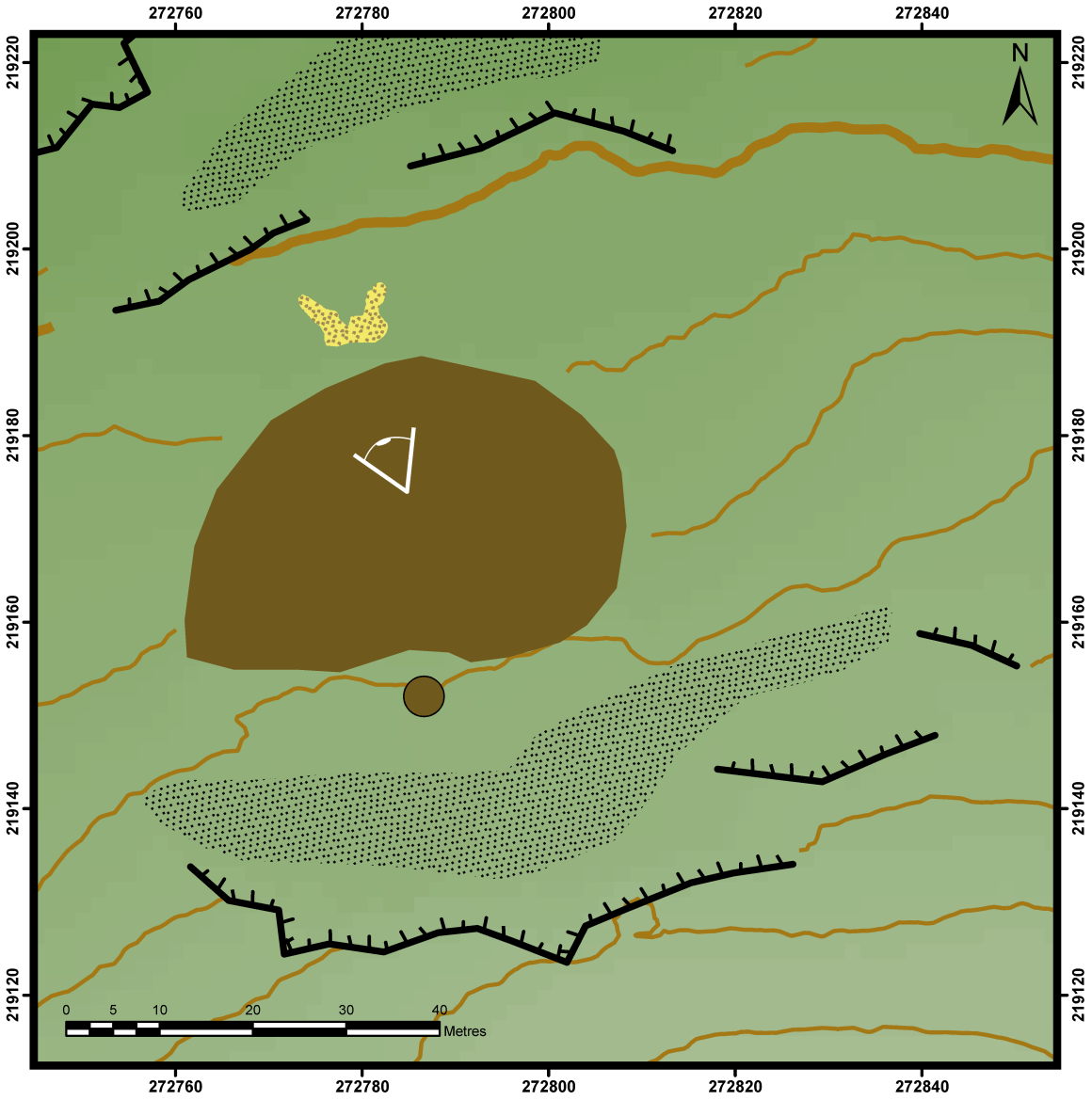

Figure 3.3.5d. Submap: Centre 4 and image (above). A small, isolated carbonate gravel outwash.

3.3.5e. Submap: Centre 5

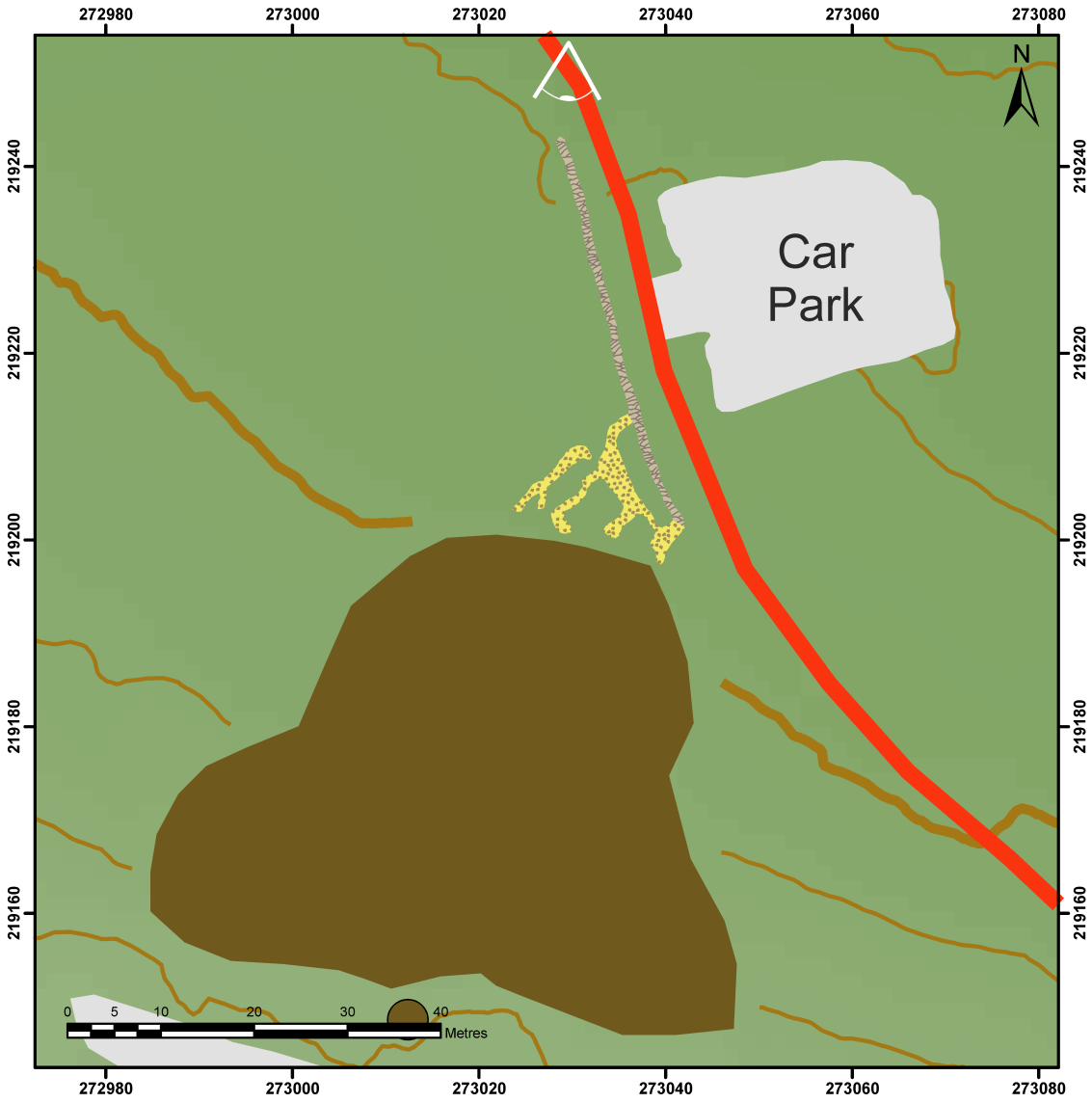

Figure 3.3.5e. Submap: Centre 5 and image (above). Carbonate gravel outwashes, leading into a small ditch containing apron until confluence with a 'natural' runoff channel.

3.3.6. East

The eastern deposits are more varied than those to the west (see sections 3.3.3. and 3.3.4). There are extensive areas of carbonate gravel and carbonate mud forming over the background peat bog system. Several aprons form proximally and a large carbonate mud pool at a seep. There are also large vertical aprons, owing to the multi-level nature of the kilns and associated waste at this location. The discharge is generally higher in this area, with several sizeable streams discharging north; one of the streams (section 3.3.6) contains an extensive amount of stream crust. The site is at a greater elevation than the deposits further west, owing to a fault running between them, and is mostly at around 450m. Submaps are shown in figures 3.3.6a, 3.3.6b, 3.3.6c, 3.3.6d, 3.3.6e, 3.3.6f, 3.3.6g, 3.3.6h, 3.3.6i, 3.3.6j and 3.3.6k.

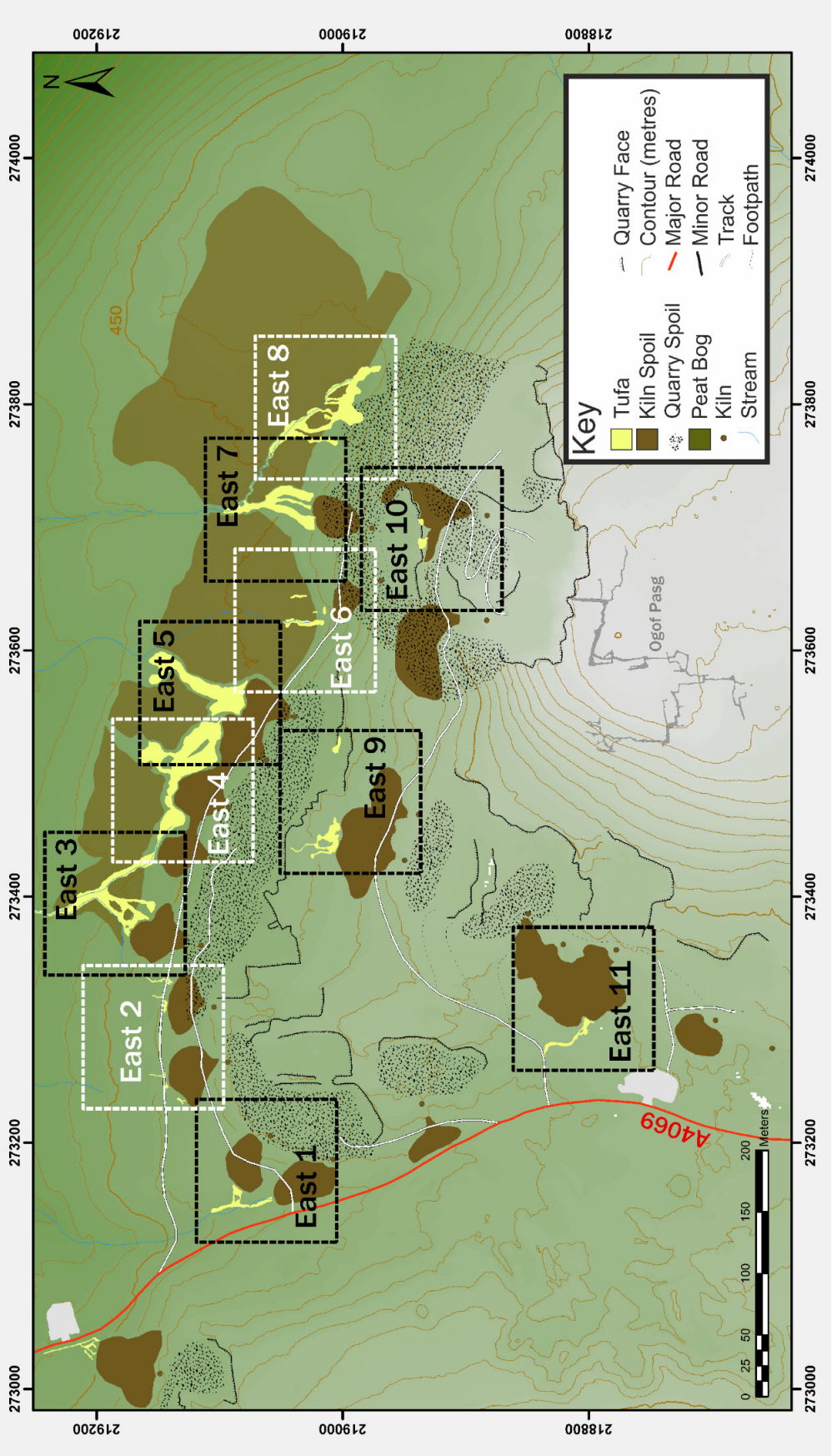

Figure 3.3.6. Eastern deposits

3.3.6a. Submap: East 1

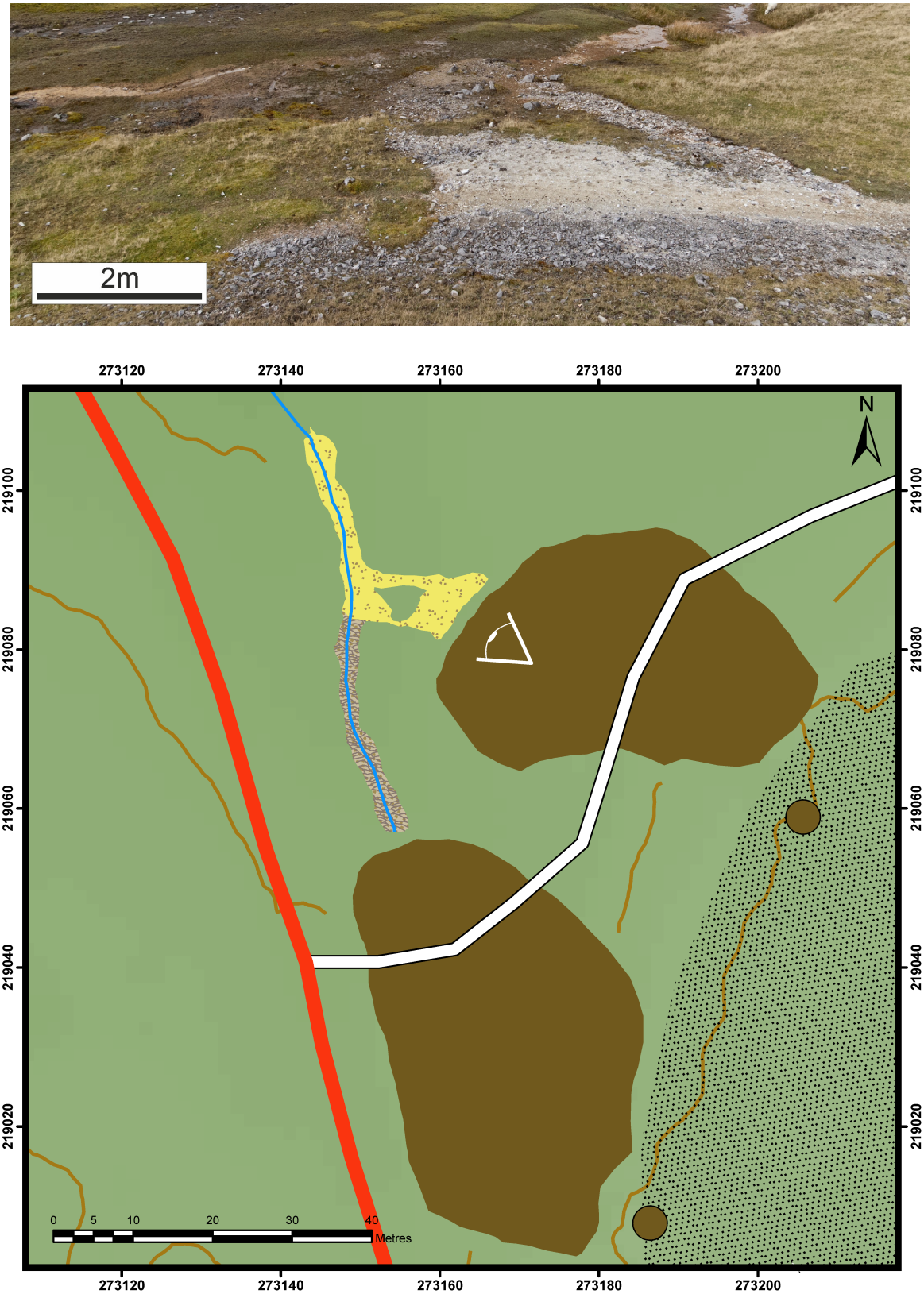

Figure 3.3.6a. Submap: East 1 and image (above). Apron and carbonate gravel/mud outwash forming from a small stream.

3.3.6b. Submap: East 2

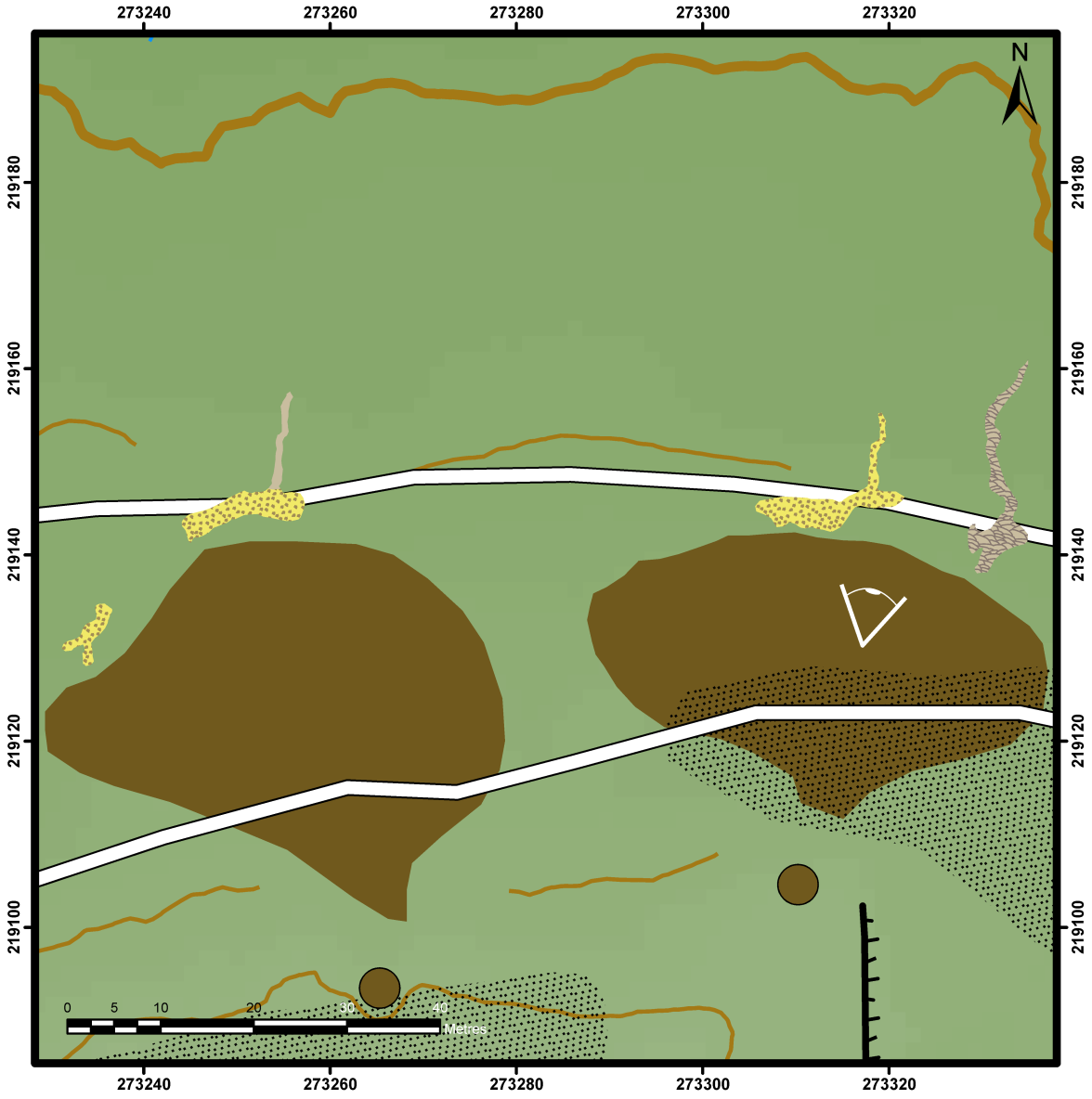

Figure 3.3.6b. Submap: East 2 and image (above). Several small carbonate gravel outwashes and a small apron.

3.3.6c. Submap: East 3

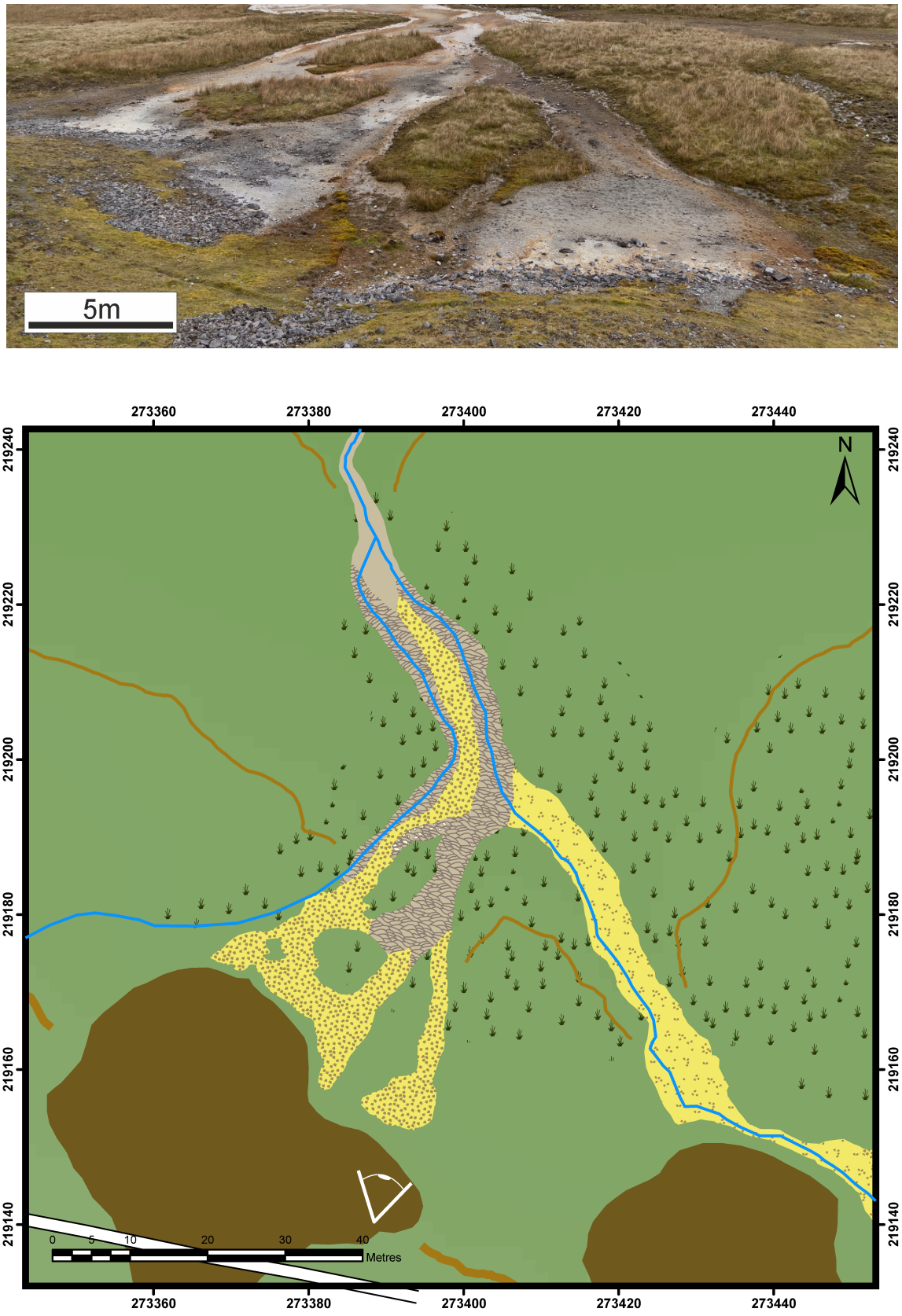

Figure 3.3.6c. Submap: East 3 and image (above). Carbonate gravel and aprons forming from small streams below the tips. Downstream, the aprons transition into stream crust facies.

3.3.6d. Submap: East 4

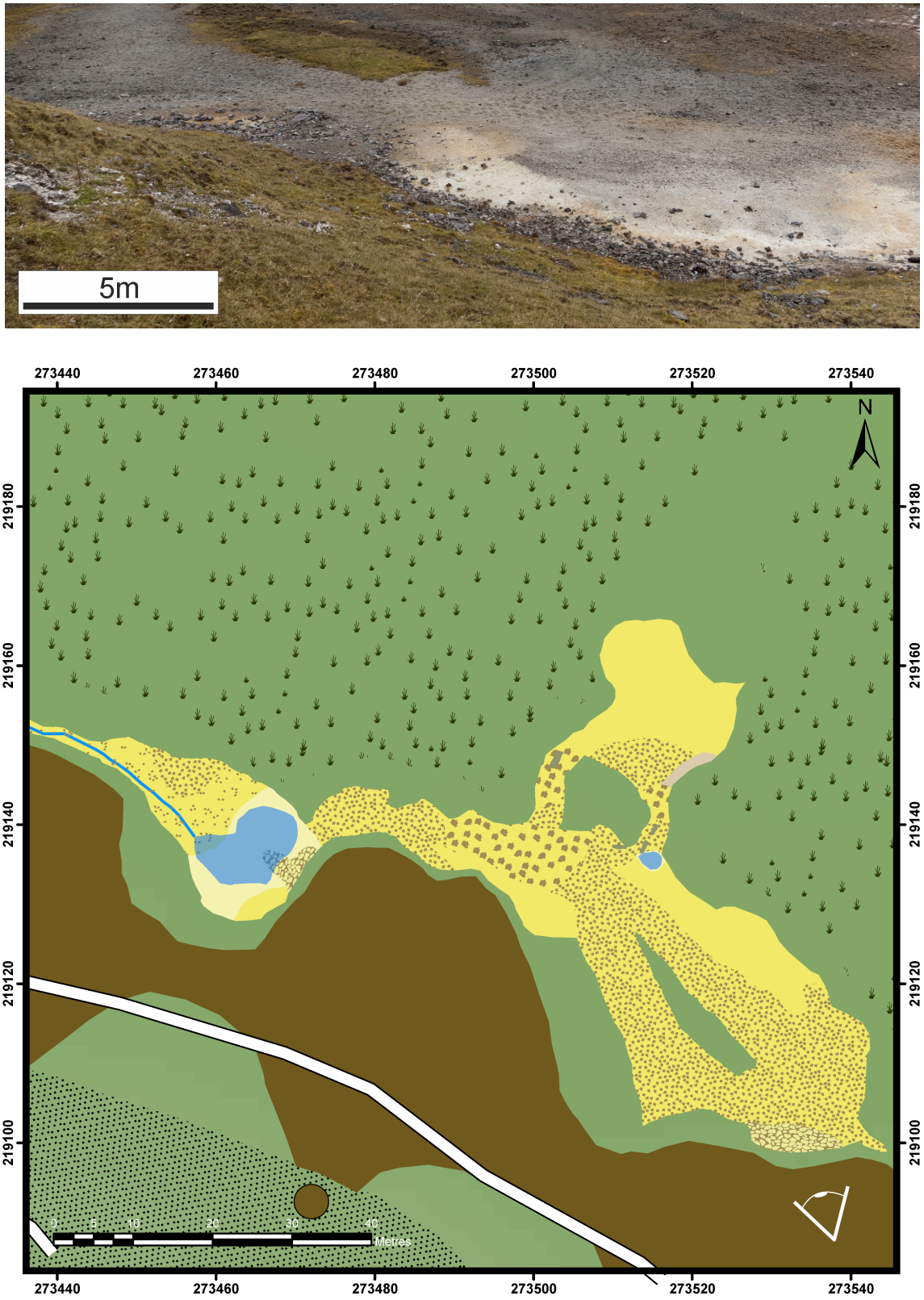

Figure 3.3.6d. Submap: East 4 and image (above). Proximal carbonate mud pools and pisoidal pools are surrounded by carbonate gravel outwashes. Distally, small patches of oncoids and stream crust form amongst carbonate mud outwashes.

3.3.6e. Submap: East 5

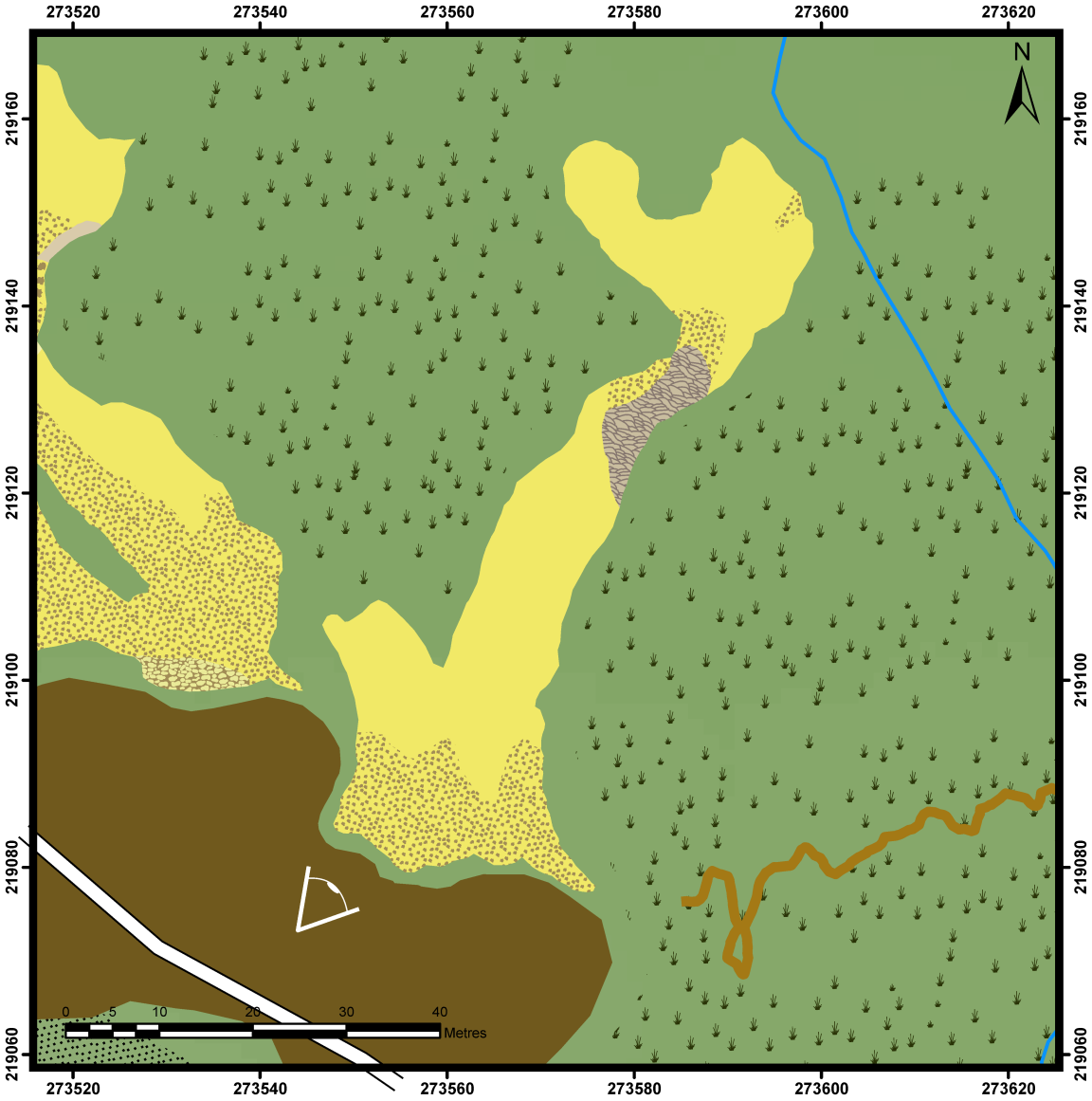

Figure 3.3.6e. Submap: East 5 and image (above). Proximal carbonate gravel outwash, with carbonate mud further from the tips. Where the slope increases briefly, apron and pisoids form, before returning to carbonate mud outwashes below where slopes are reduced.

3.3.6f. Submap: East 6

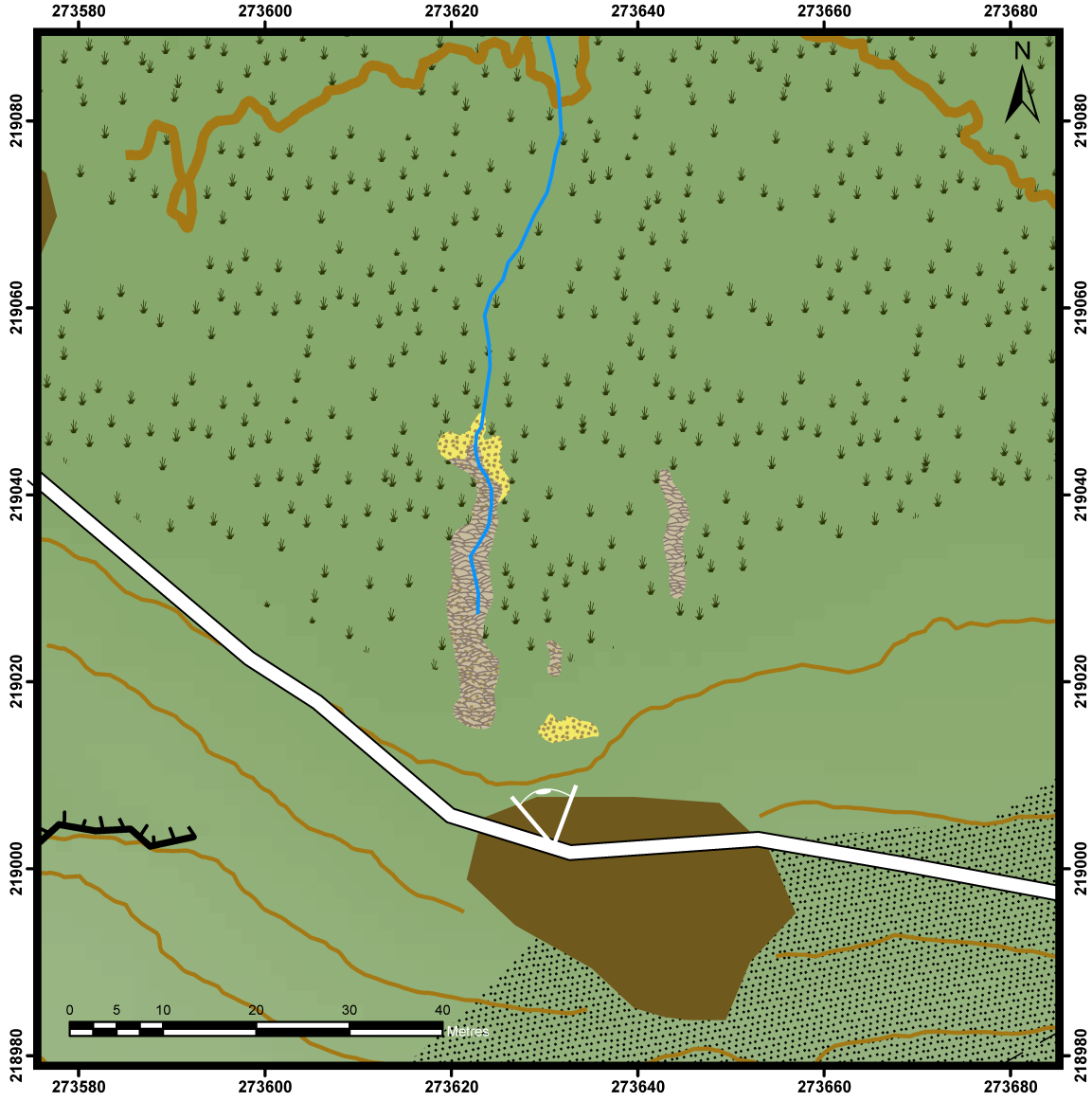

Figure 3.3.6f. Submap: East 6 and image (overleaf). Several isolated aprons and carbonate gravel outwashes.


2m

3.3.6g. Submap: East 7

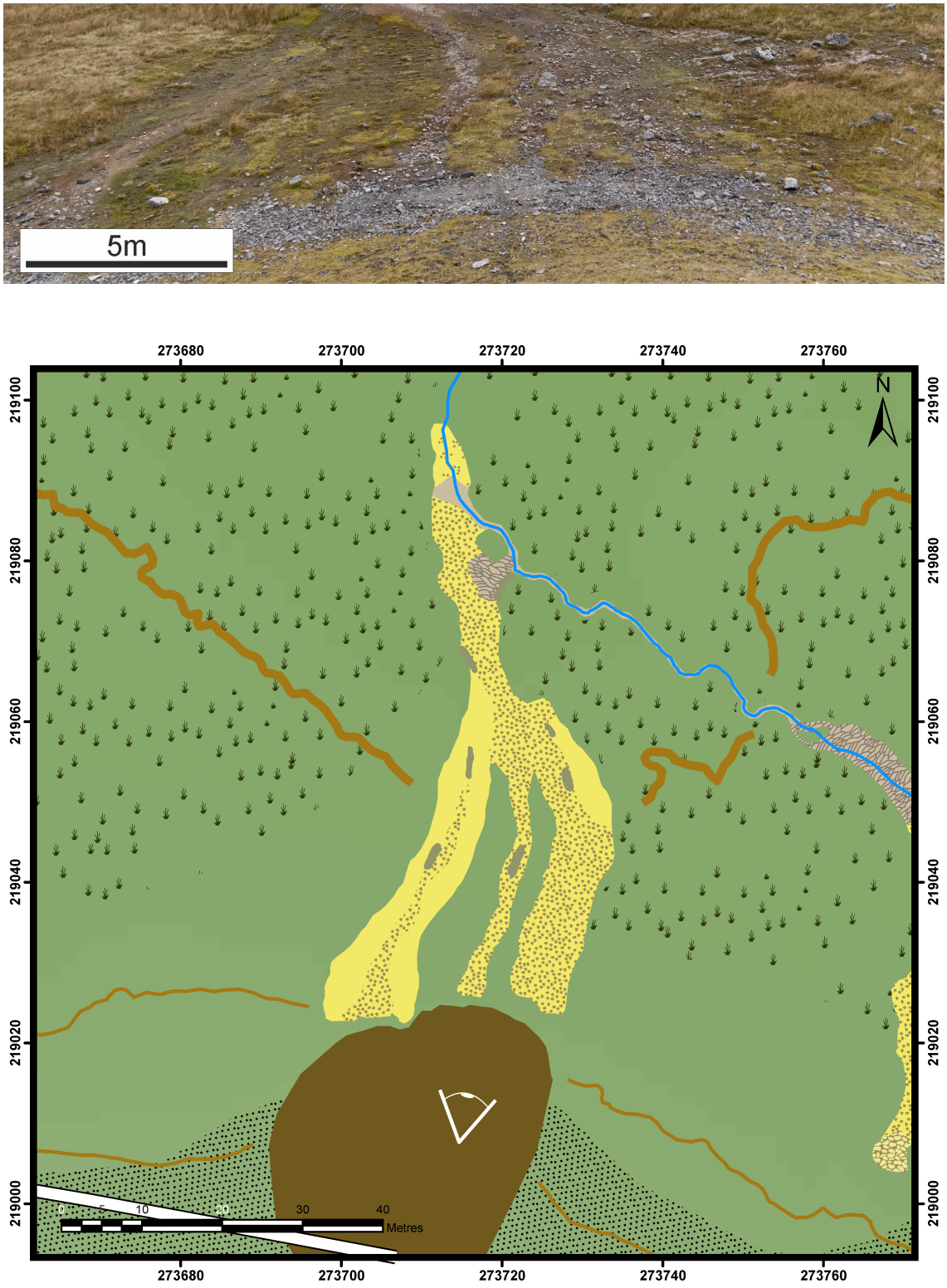

Figure 3.3.6g. Submap: East 7 and image (above). Gravel and mud outwashes, with oncoids forming at the base of the slope and apron and carbonate gravel on the slopes below. All outwashes join a stream flowing from the east containing stream crust, which a short way downstream is replaced by carbonate gravel. Discontinuous remains of fossil tufa channels are common along the outwashes.

3.3.6h. Submap: East 8

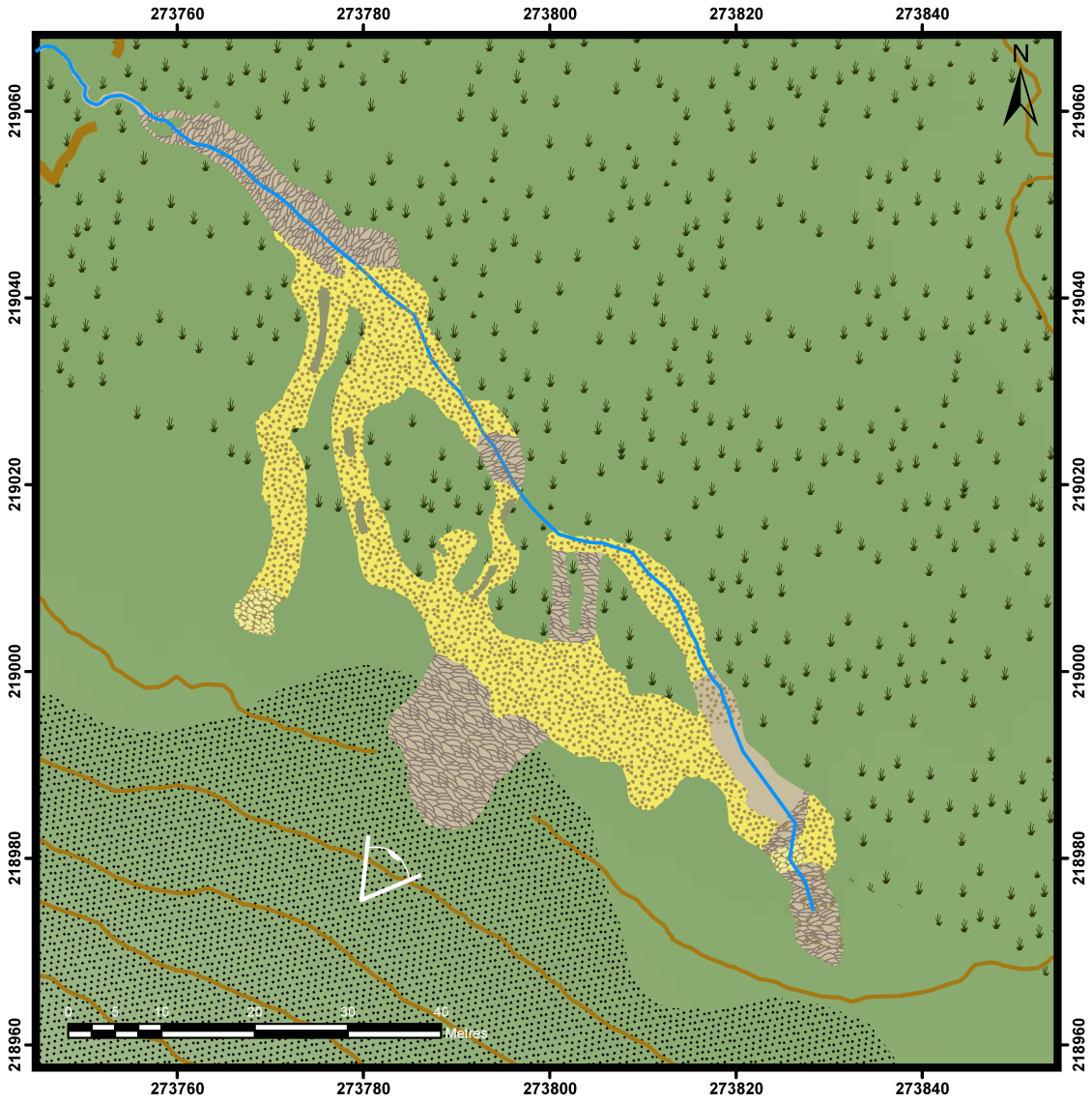

Figure 3.3.6h. Submap: East 8 and image (above). Proximal aprons and pisoids flow out into carbonate gravel, with aprons or stream crust forming where slope increases. Where outflows converge (approximately 273780 219040), apron facies form, transitioning to stream crust facies as the water becomes channelised.

3.3.6i. Submap: East 9

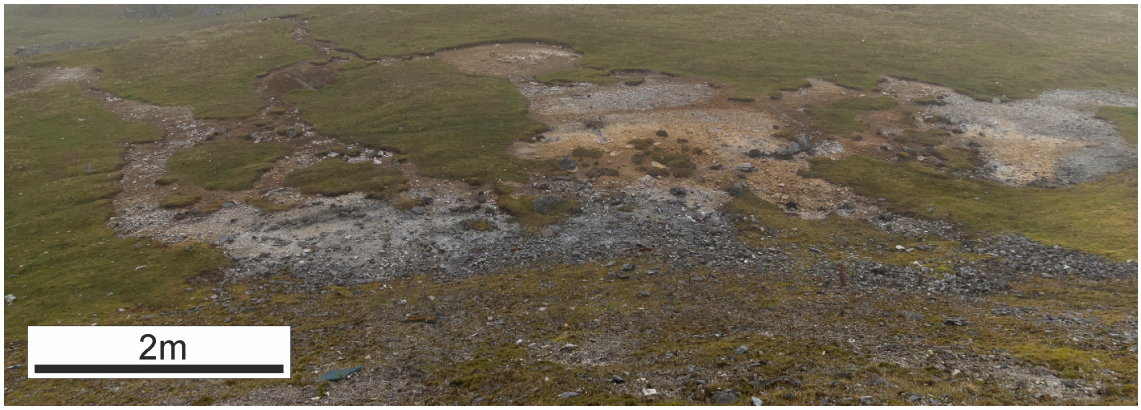

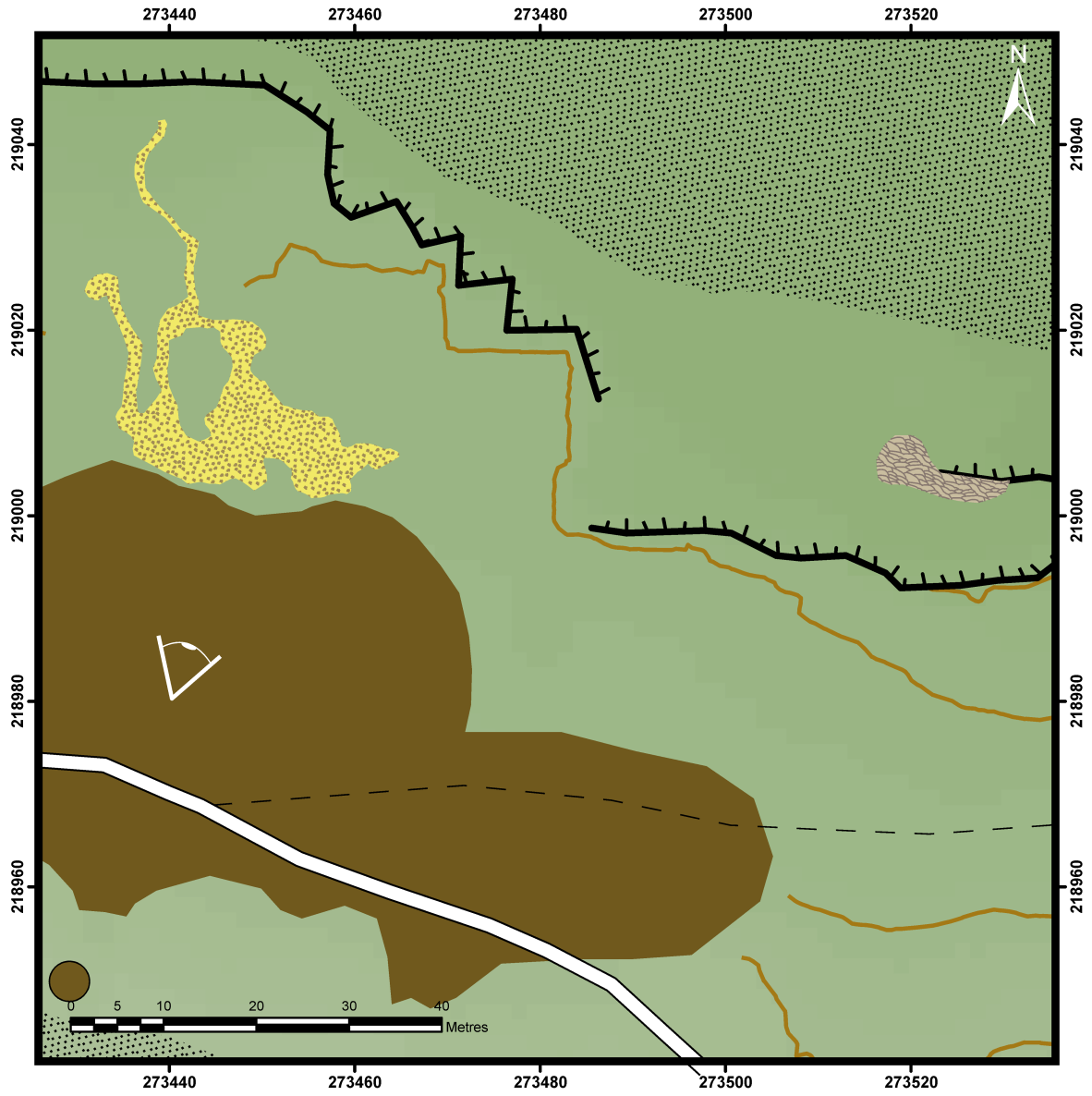

Figure 3.3.6i. Submap: East 9 and image (above). Isolated carbonate gravel outwash and a small apron.

3.3.6j. Submap: East 10

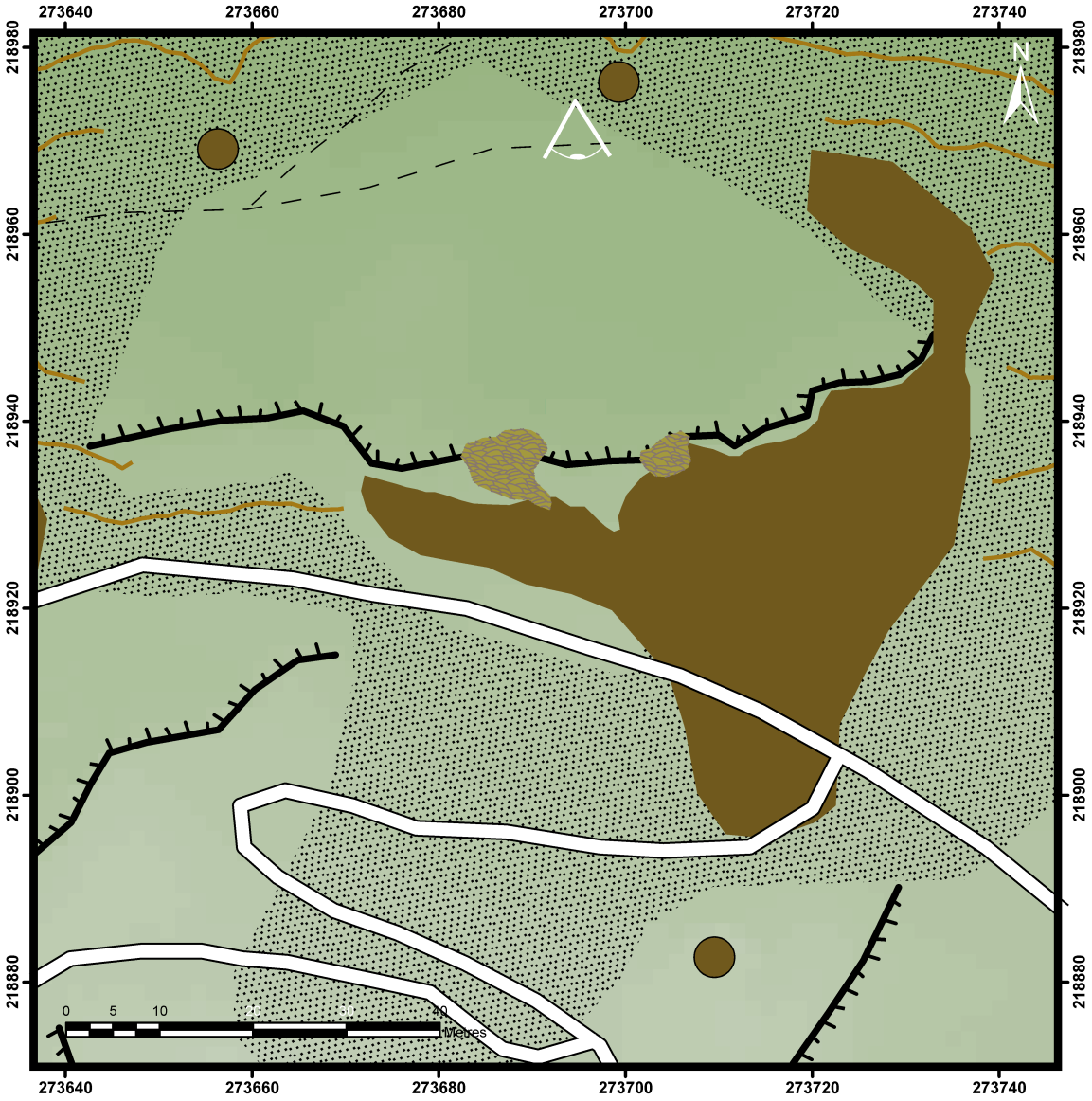

Figure 3.3.6j. Submap: East 10 and image (above). Isolated vertical aprons forming on a cliff face below a lime spoil tip.

3.3.6k. Submap: East 11

Figure 3.3.6k. Submap: East 11 and image (above). Carbonate gravel outwash, changing to apron facies as slope increases, returning to carbonate gravel and mud as slope reduces.

3.3.7. Main streamway

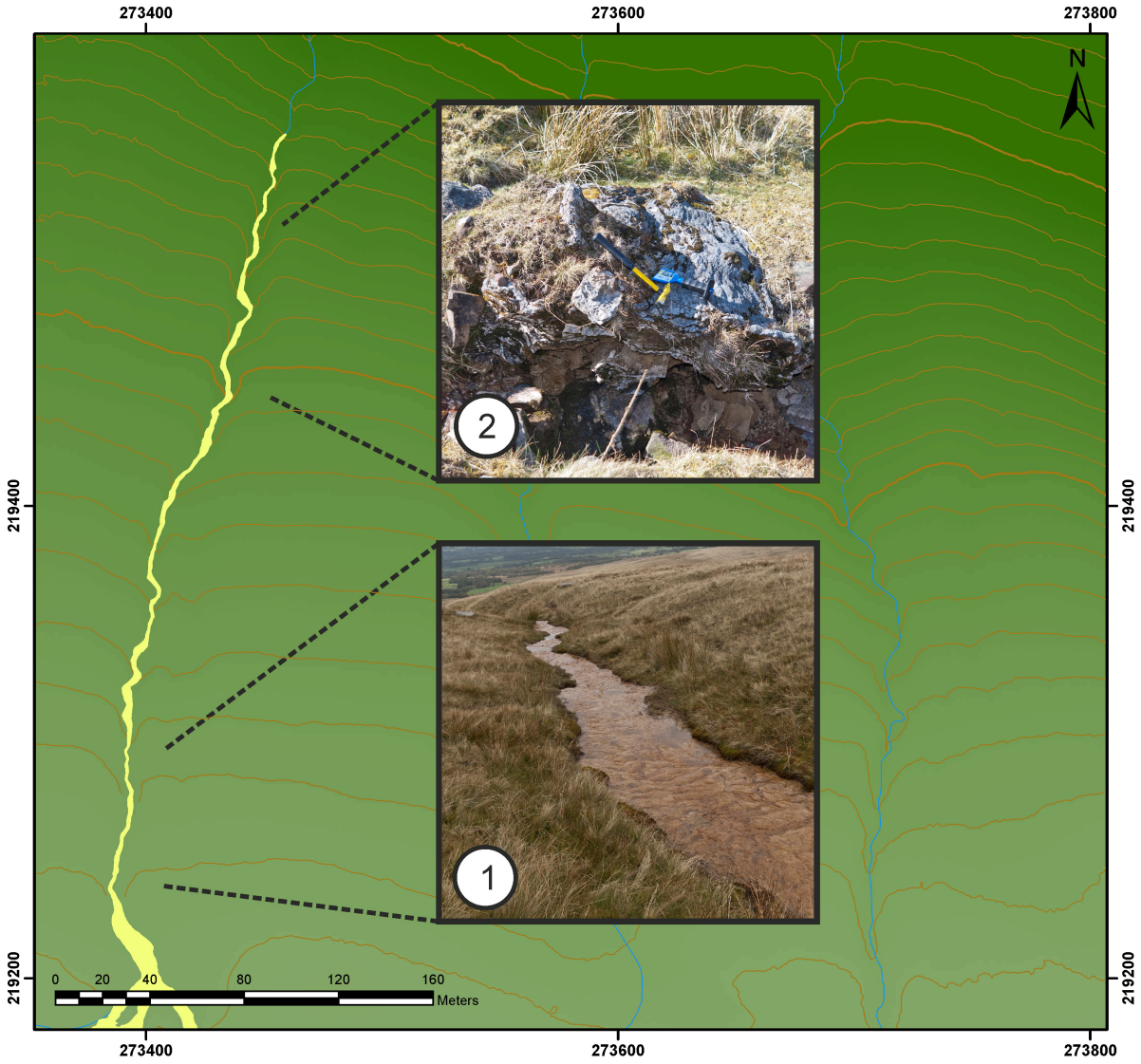

Figure 3.3.7. Main streamway. Stream crust lining a steeply descending stream bed. Upstream reaches (1) are intact, but are not actively accreting (see section 3.7.2). Decay becomes progressively greater downstream (2).

3.3.8. Facies key

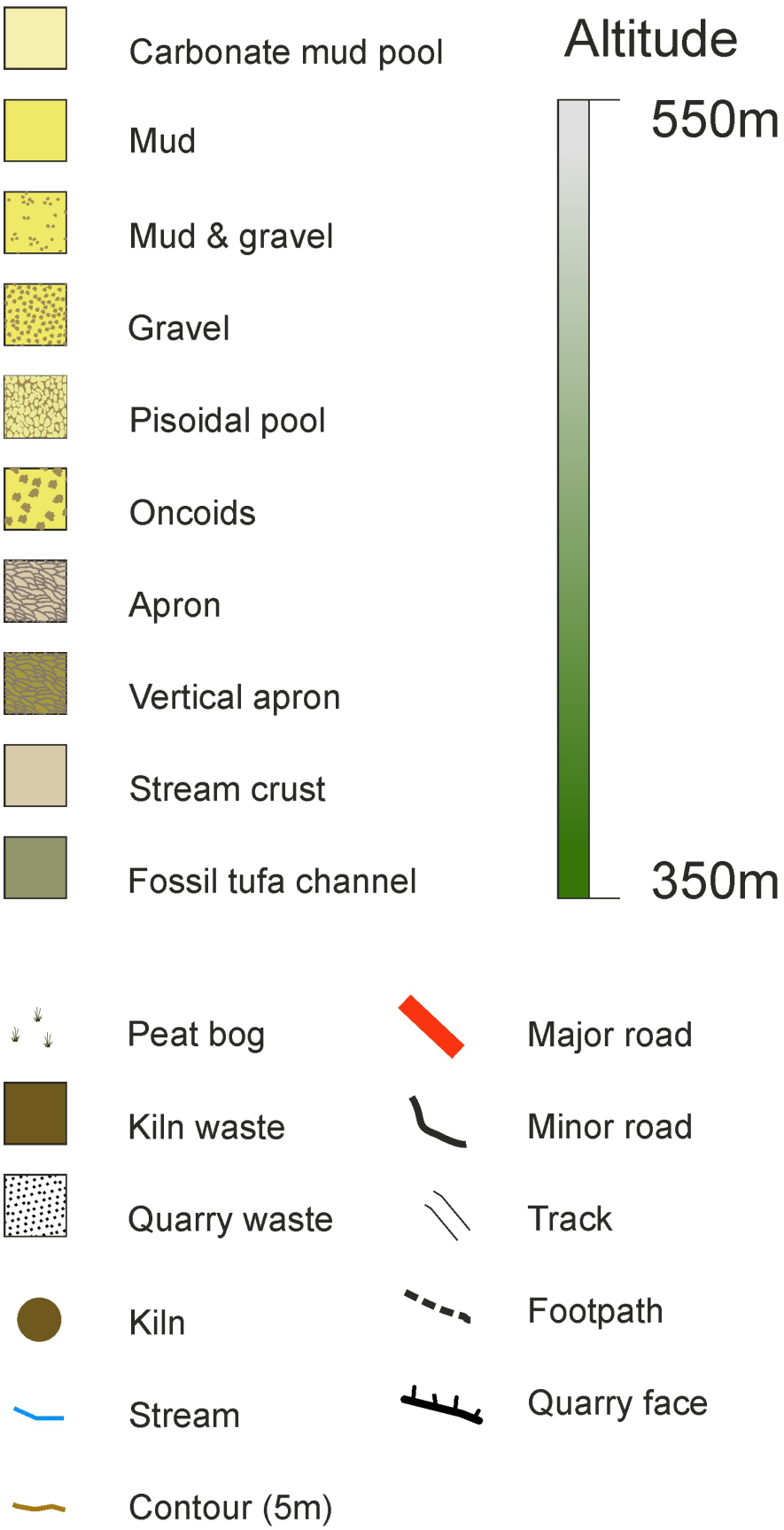

3.4. Geochemistry

3.4.1. pH meter calibration and accuracy

The manufacturers stated precision (erroneously described as accuracy in the associated literature) of the field meter (Hanna Instruments 98129) is outlined in table 3.4.1a. No data is provided on the expected accuracy of the probe when new; however, it is assumed that when using a new, calibrated probe, the accuracy matches the precision. For pH this accuracy is only valid at the point(s) of calibration.

Parameter	Range	Resolution	Precision
pH	0.00 - 14.00	0.01	± 0.05
EC ($\mu S.cm^{-1}$)	0 - 3999	1	± 2%
T (°C)	0.0 – 60.0	0.1	± 0.5

Table 3.4.1a. Manufacturer claimed pH, electrical conductivity (EC) and temperature specifications for Hanna Instruments 98129 meter.

Analysis of the probe following calibration revealed no appreciable deterioration in accuracy (figure 3.4.1a). There is, however, a systematic error (in comparison with the laboratory pH meter), which is symptomatic of the meter's limited ability to calibrate accurately (table 3.4.1b). Figure 3.4.1b demonstrates the linear deviation from the bench meter following calibration. This deviation is a result of the probe automatically calibrating before a stable pH has been achieved. Consequently, once the probe has calibrated at pH 10 the pH continues to rise to around pH 10.2, resulting in the error observed.

Since this error is the result of the meter failing to reach a stable pH quickly enough (which is itself a function of probe age), this systematic error is likely to increase throughout the life of the probe. The analysis of the probe was undertaken after the monitoring period; consequently it is likely that the error measured represents the maximum error throughout the dataset. However, due to the uncertainty regarding any change in error within the dataset, a correction is not applied to the data.

Parameter	Precision	Accuracy
pH	± 0.04	-0.20 (@ pH 7.23) 0.00 (@ pH 8.60) +0.20 (@ pH 10.01)

Table 3.4.1b. Measured pH specifications for Hanna Instruments 98129 meter.

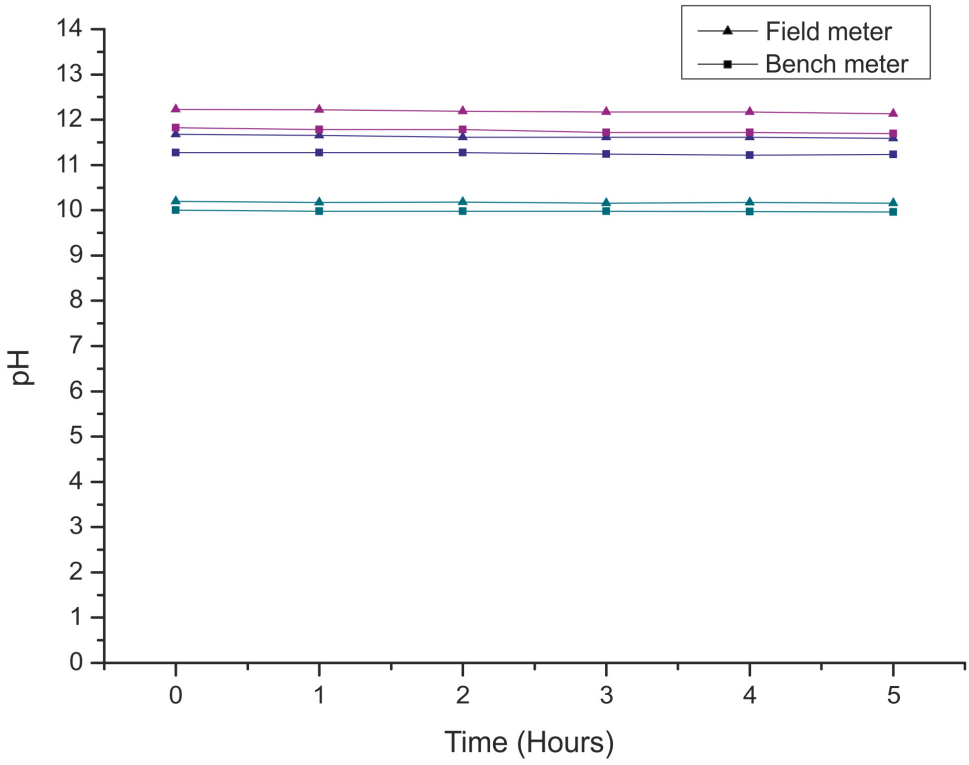

Figure 3.4.1a. No deterioration of pH readings with time at pH 10 (turquoise), pH 11 (dark blue) or pH 12 (violet).

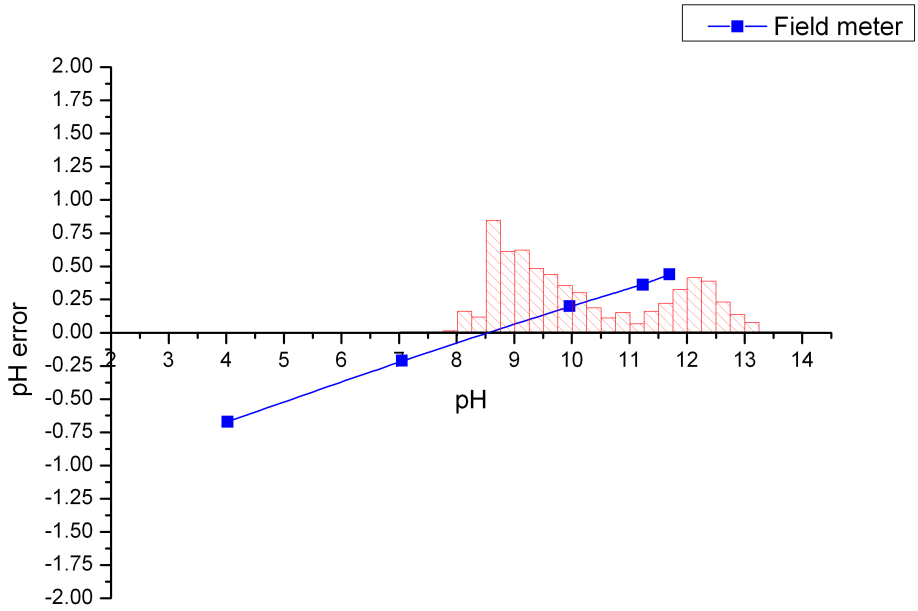

Figure 3.4.1b. Systematic error of Hanna 98129 probe (blue). The distribution of pH within the dataset suggests the maximum impact of this error is likely less than 0.66 pH units, with the majority of data affected significantly less.

3.4.2. Hydrochemistry overview and annual trends

A summary of the hydrochemical parameters of each facies is given in table 3.4.2a. Data spans the time between 29th April 2009 and 19th April 2010, with pH and EC (electrical conductivity) monitored weekly and alkalinities monitored irregularly throughout the period. The table shows that proximal facies have extremely high pH, in excess of 11 (on average), with greatest variability in proximal pools (carbonate mud pool and pisoidal pool facies). Distal stream crust is associated with more neutral pH levels, although the maximum pH levels are high, associated with temporary shifts in morphology (see section 3.1.3).

	pH			EC			OH^-			CO_3^{2-}			HCO_3^-		
				$\mu S.cm^{-1}$			$mmol.L^{-1}$								
Facies	Min	**Mean**	Max	Min	**Mean**	Max	Min	**Mean**	Max	Min	**Mean**	Max	Min	**Mean**	Max
Carbonate Mud Pool	8.62	**11.26**	13.24	111	**831**	3999+	0.00	**3.51**	19.93	0.00	**0.56**	3.76	0	**0.89**	6.34
Apron	10.92	**12.08**	12.85	341	**774**	2177	2.54	**4.32**	5.18	0.00	**0.34**	1.38	0	**0.02**	0.07
Pisoidal Pool	8.47	**11.67**	12.45	224	**1476**	2315	-	-	-	-	-	-	-	-	-
Stream Crust	7.86	**9.18**	12.06	58	**192**	351	0.00	**0.01**	0.02	0.05	**0.16**	0.39	2.04	**5.92**	9.79

Table 3.4.2a. Summary hydrochemical data for different facies on Foel Fawr. Data collected from multiple sites sampled weekly for one year. Data has been binned according to the corresponding tufa facies forming at the locale. Carbonate mud pool data are comprised of data from hydrochemical monitoring sites 1, 1a, 1b, 1c & 11 (see figures 3.4.2b, 3.4.2c and 3.4.2d); apron data are comprised of data from hydrochemical monitoring sites Apron & 10 (see figures 3.4.2c, 3.4.2d and 3.4.2e); pisoidal pool data is summarised from Emery (2008) [12 data points, sampled 18/10/07, 13/12/07 & 04/02/08]; stream crust data are comprised of data from hydrochemical monitoring sites 5, 6, 7, 8, 9, 13 & 14 (see figures 3.4.2a, 3.4.2b, 3.4.2c & 3.4.2d).

Hydrochemical locations 1-9 (figure 3.4.2a) represent a downstream transect of the eastern deposits (see section 3.3.6).

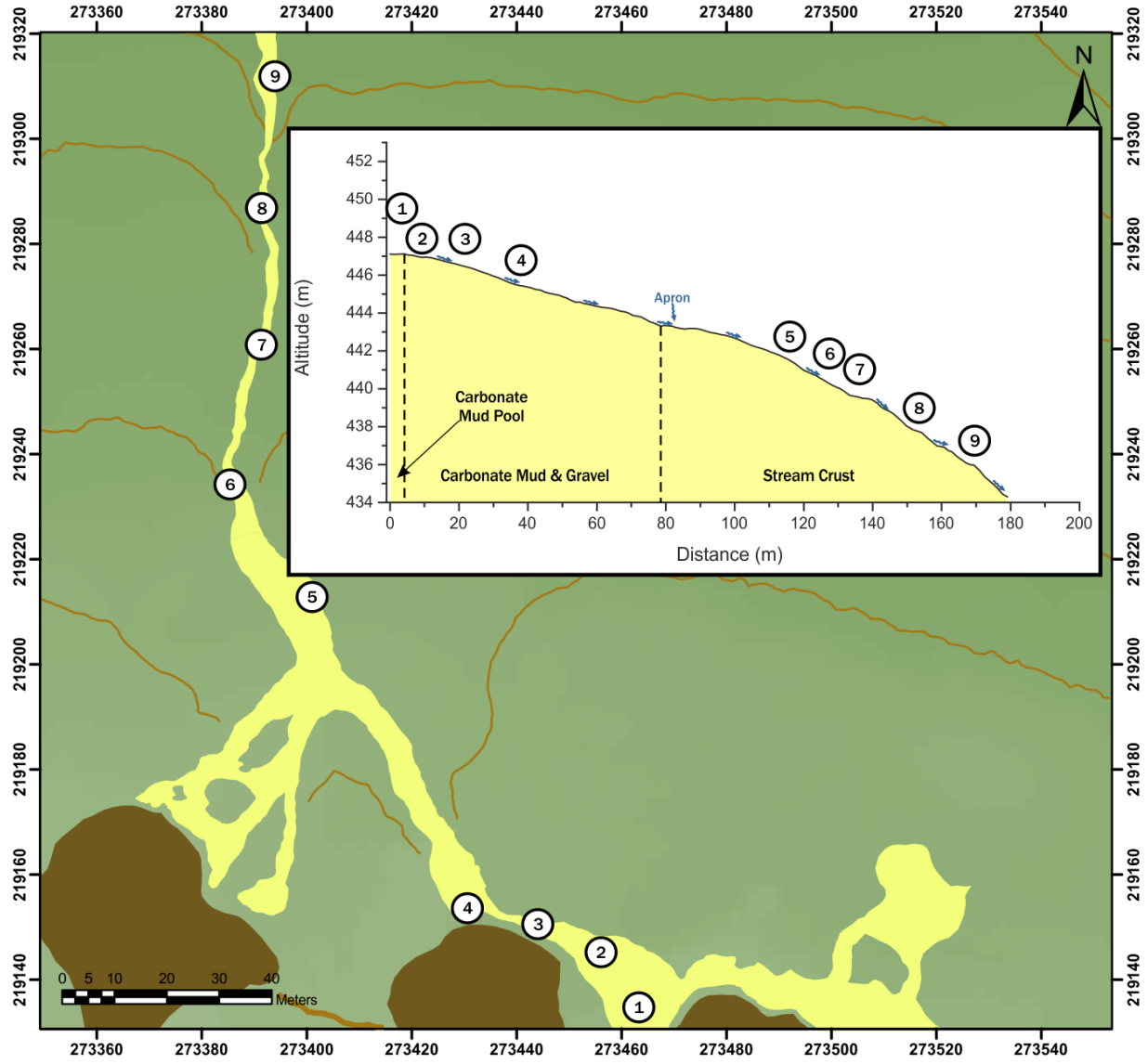

Figure 3.4.2a. Hydrochemical sampling map 1.

The downstream transect includes several samples from a carbonate mud pool (1, 1a, 1b, 1c & 1d) and a downstream transect to site 9 (figure 3.4.2b).

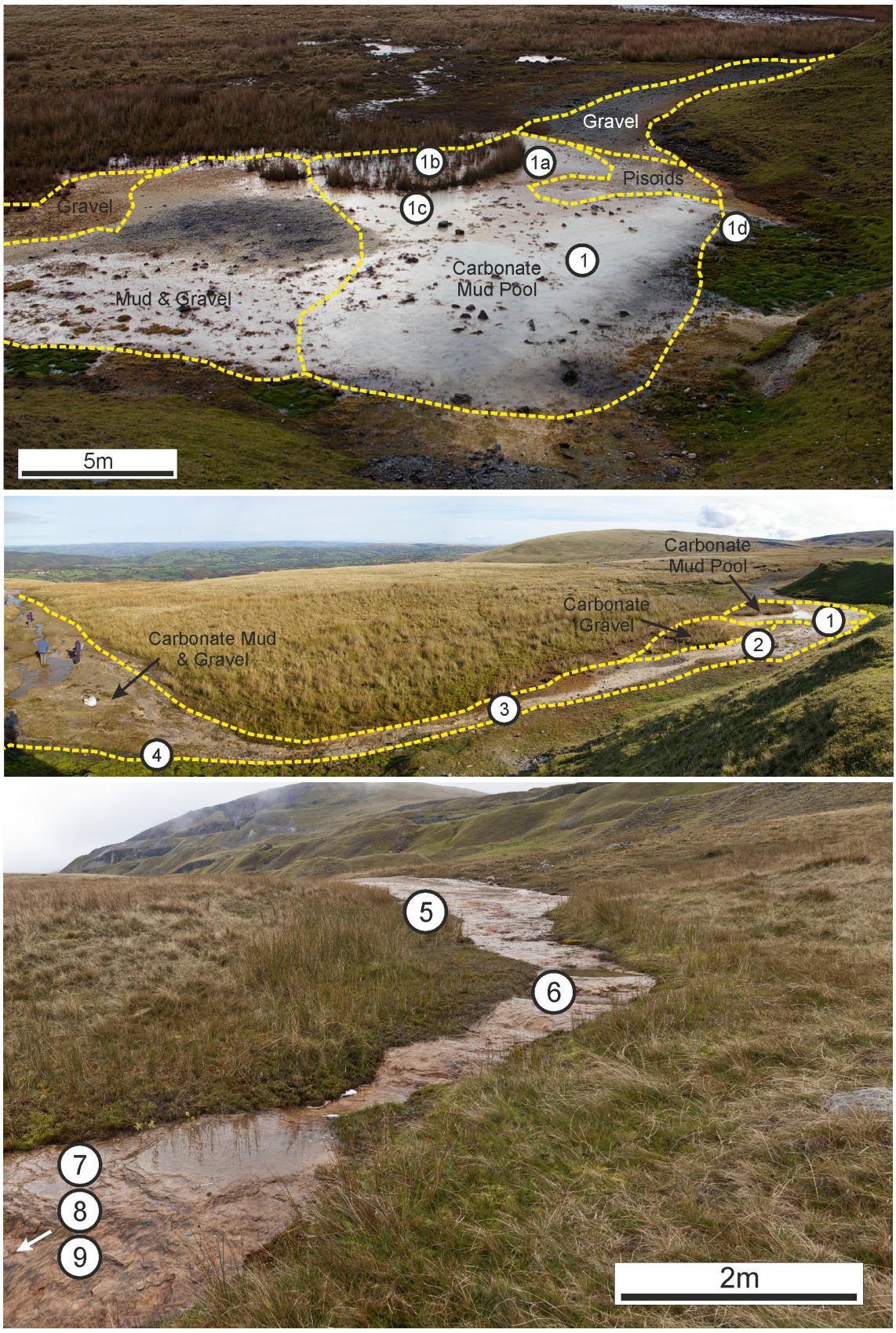

Figure 3.4.2b. Hydrochemical sampling sites 1-9.

Hydrochemical locations 10-14 (figure 3.4.2c) represent a downstream transect of the western deposits (see section 3.3.4). Sample location 12 represents major input from a tributary, which does not actively precipitate tufa.

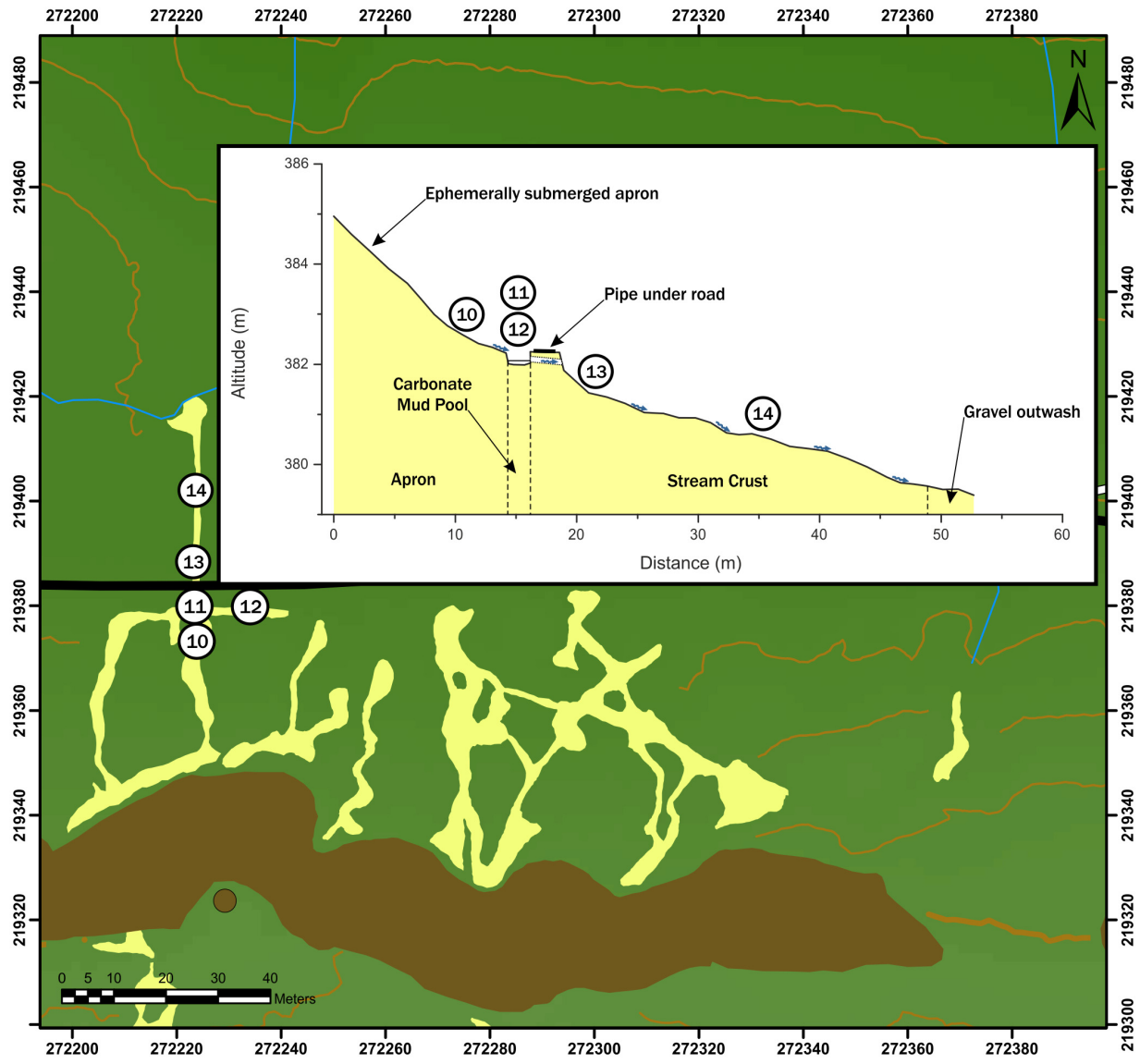

Figure 3.4.2c. Hydrochemical sampling map 2.

The image in figure 3.4.2d shows the transect represented in figure 3.4.2c.

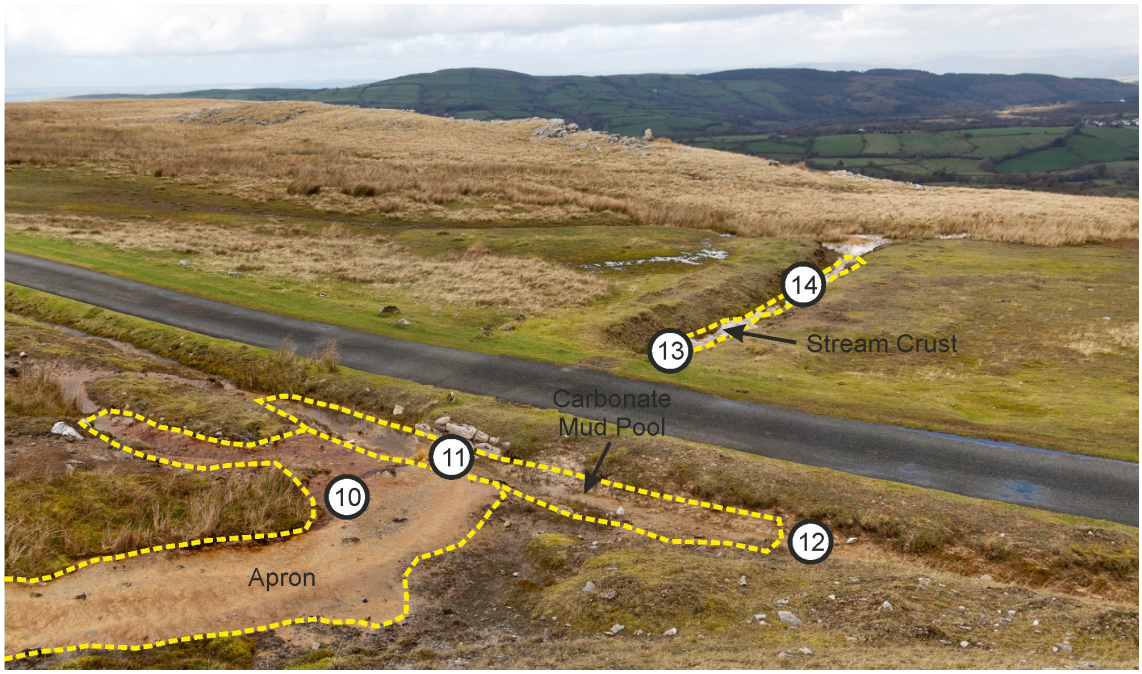

Figure 3.4.2d. Western deposits on Foel Fawr showing hydrochemical sampling points 10-14.

Hydrochemical location ‘Apron’ is shown in figure 3.4.2e.

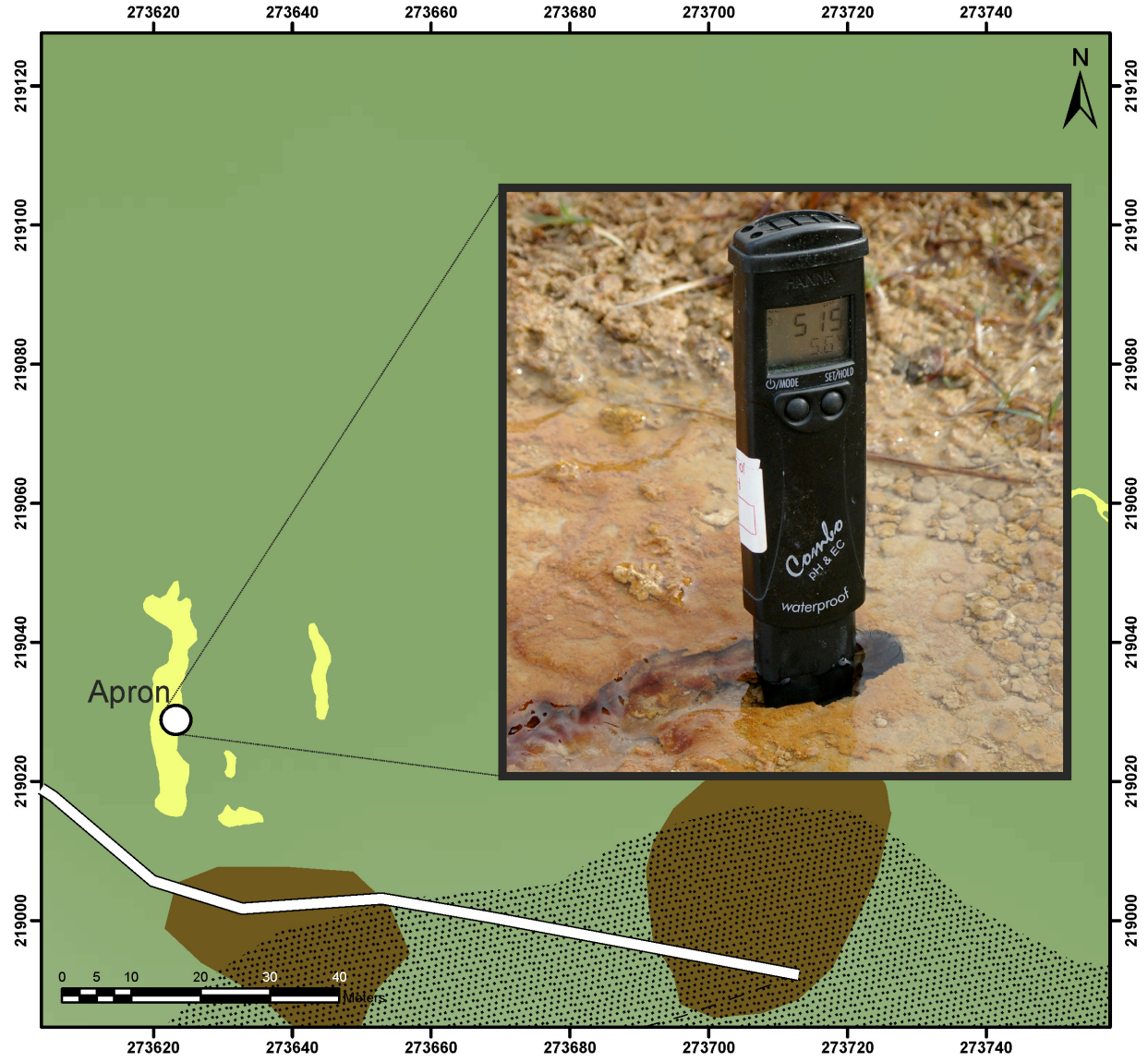

Figure 3.4.2e. Hydrochemical sampling map 3

The graphs presented on the following pages demonstrate the present-day variability of hydrochemistry over the site. Figure 3.4.2f shows the relationship between pH and electrical conductivity (EC) across all hydrochemistries sampled. Proximal environments demonstrate both higher pH and higher EC; distal environments feature lower values and a different relationship between pH and EC. A proximal seep (forming a carbonate mud pool) is considered in detail and compared to two proximal springs (forming aprons). Three distal hydrochemistries are analysed, each representing a different difference from source in order to consider any downstream change in distal environments.

Figures 3.4.2g, 3.4.2h and 3.4.2i represent data from sites 1a, 1b and 1 respectively (see figure 3.4.2b). All three sites are from a pool formed by a proximal seep. These sites all have a strong positive correlation between pH and EC, and feature the highest extremes of EC and pH across the site. Site 1 sometimes features pH and EC more comparable to distal environments (see figure 3.4.2f); this is likely due to the input of surface runoff coming from site 1d (see figure 3.4.2b).

Figures 3.4.2j and 3.4.2k represent data from sites 10 and 'Apron' respectively (see figures 3.4.2c and 3.4.2e). While the proximity of these sites to the spoil tips is comparable to the seep previously described, they are evidently different in their hydrochemistry. Variability and magnitude of both pH and EC are lower, and the correlation between them is marginally weaker. This difference is likely due to the difference in hydrology between these two environments. The higher discharge at the seep produces deeper water, compared to the thin film of water covering aprons. The result is a reduced air-water interaction (i.e. ingassing) in the pool due to the reduced surface: volume ratio.

Figures 3.4.2l, 3.4.2m and 3.4.2n are from distal sites forming stream crust (sites 13, 5 and 9 respectively; see figures 3.4.2a and 3.4.2c). All sites show relatively little variation in EC compared to proximal sites; however, there is significant variation in pH, both temporally and between sites. The sites vary in distance from source, with the range of pH observed decreasing with increased distance from source with site 13 closest (c.20 m from source), and sites 5 (c.120 m) and 9 (c.170 m) further away. NB: There is a minor apron precipitating spring c.40 m above site 5, however discharge is very low and it unlikely it has a large impact on the observed decline of pH.

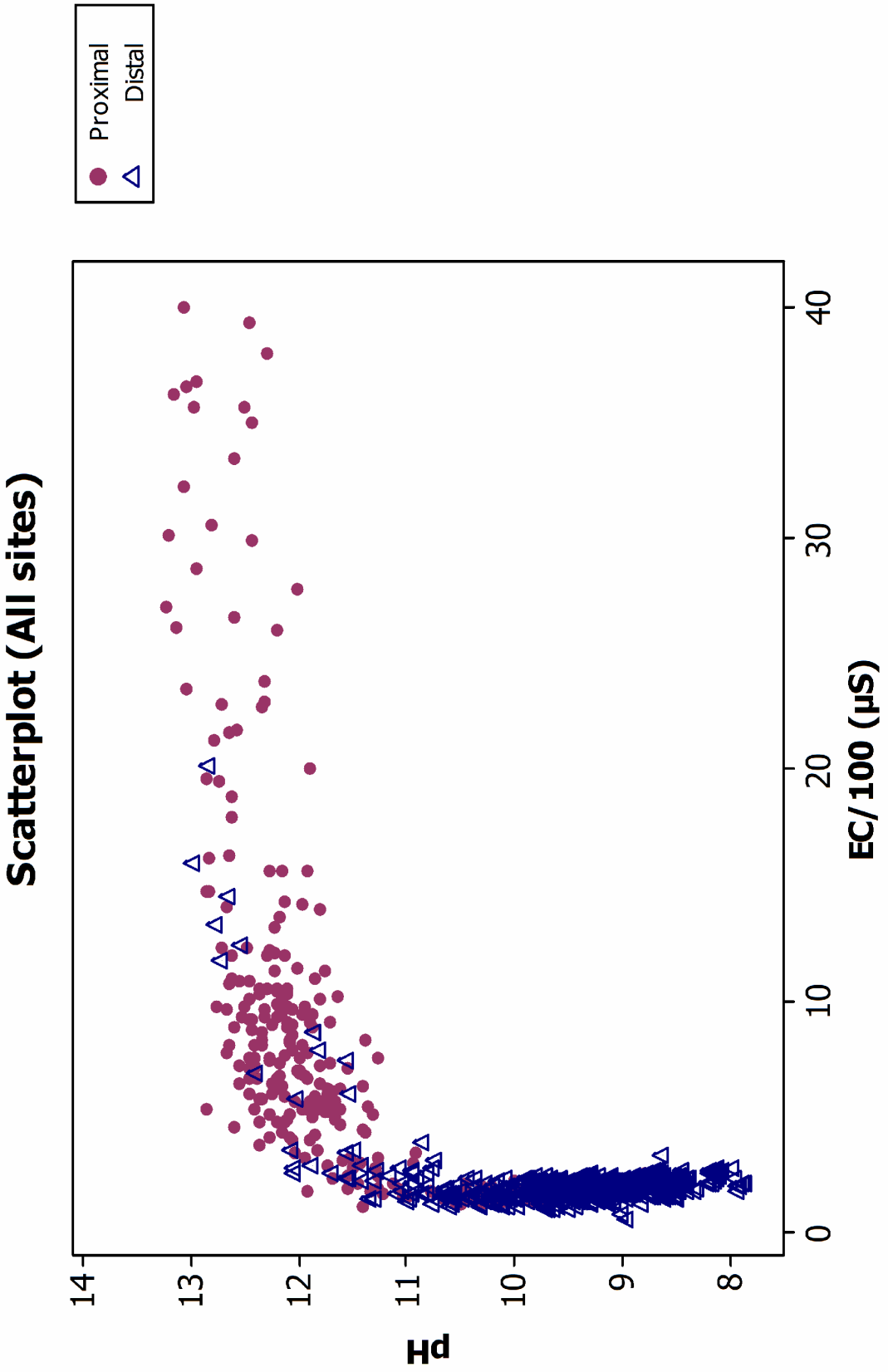

Figure 3.4.2f. Scatterplot of pH and electrical conductivity (EC) observed on Foel Fawr. Data is segregated into proximal (purple dots) and distal environments (blue triangles).

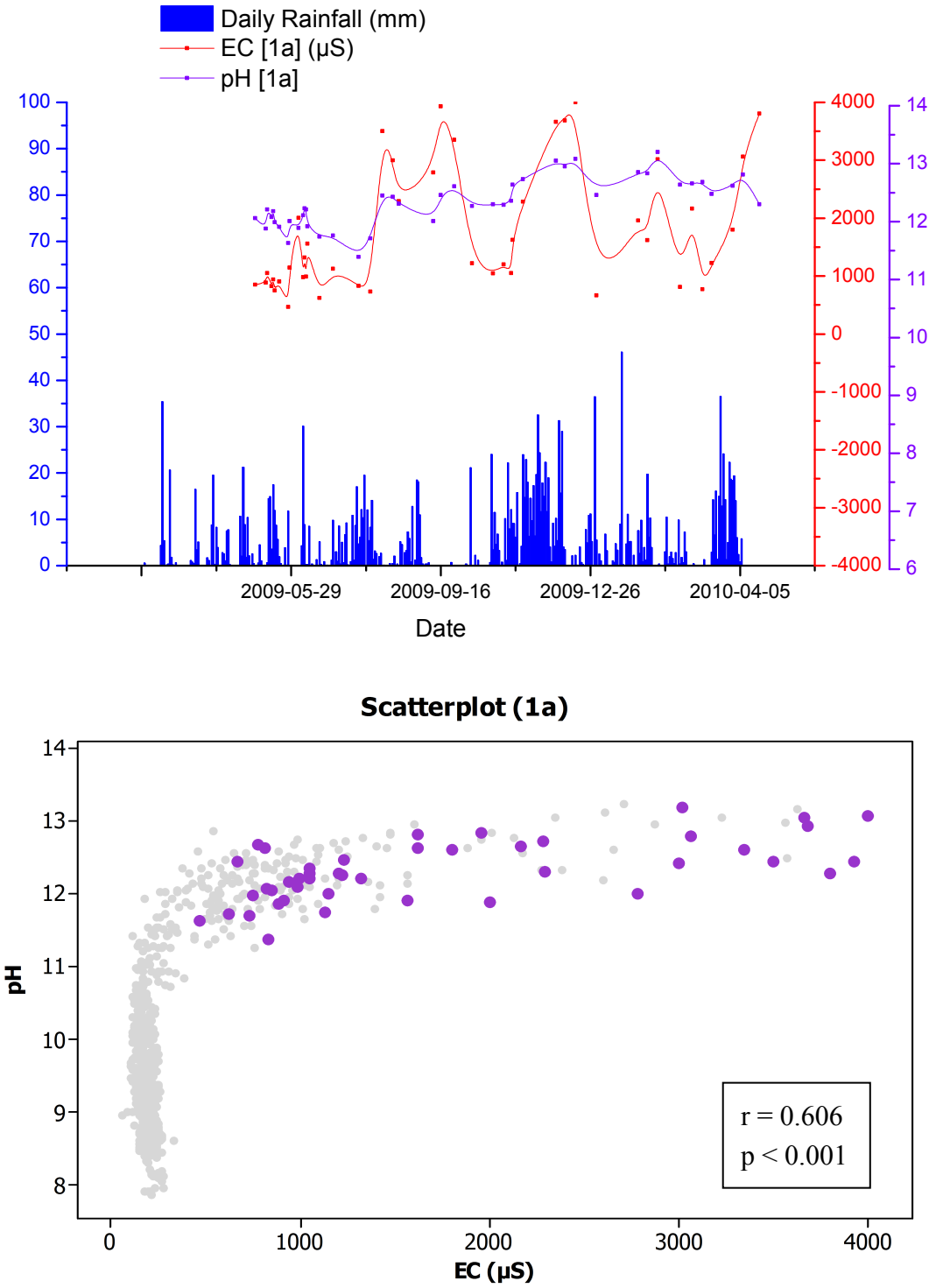

Figure 3.4.2g. [Above] Annual variability in rainfall, pH and electrical conductivity (EC) for geochemical site 1a. [Below] Scatterplot of pH and EC for site 1a (purple) and the whole site (light grey). Spearman's rank correlation values (r) and confidence level (p) for site 1a are inset.

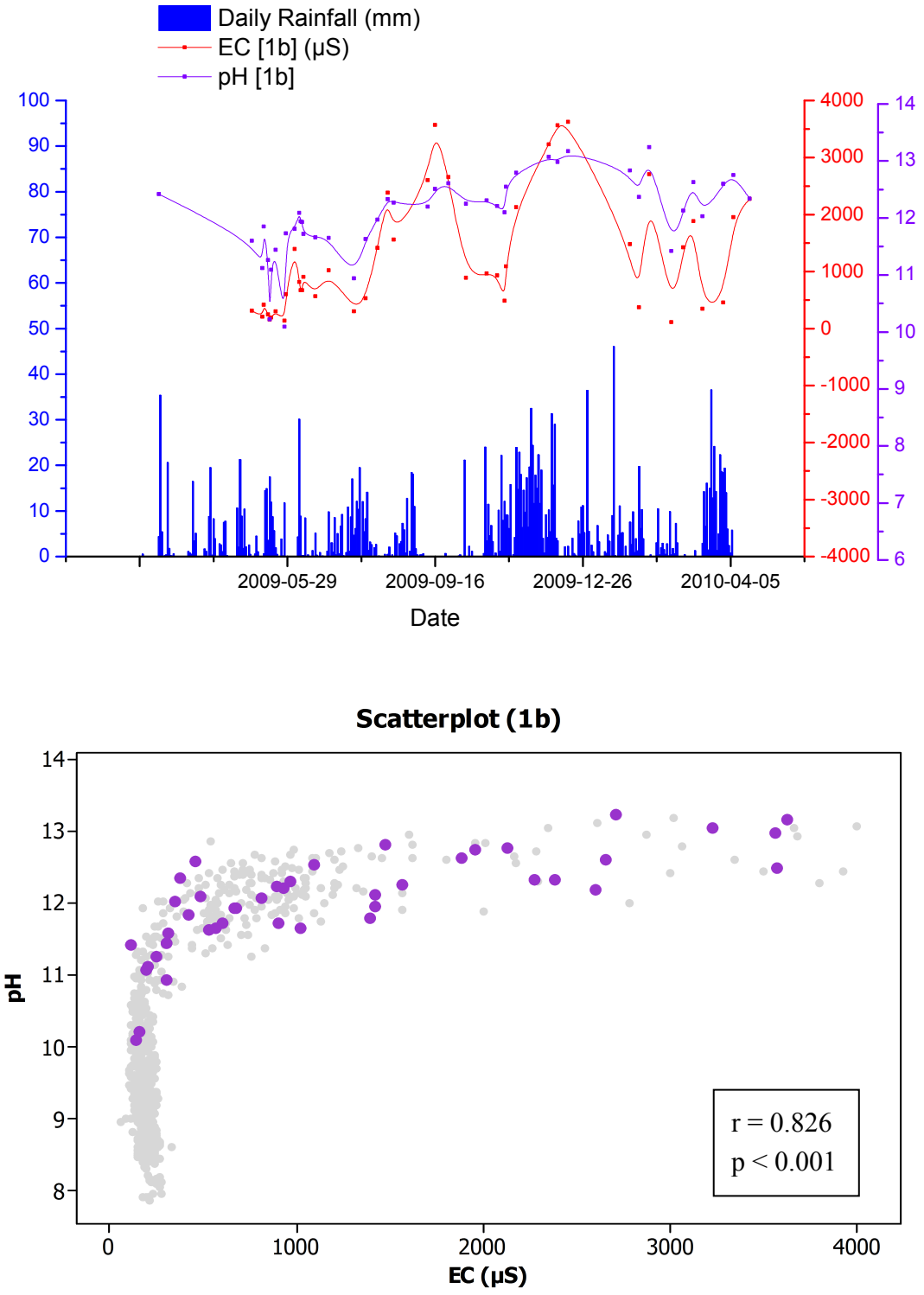

Figure 3.4.2h. [Above] Annual variability in rainfall, pH and electrical conductivity (EC) for geochemical site 1b. [Below] Scatterplot of pH and EC for site 1b (purple) and the whole site (light grey). Spearman's rank correlation values (r) and confidence level (p) for site 1b are inset.

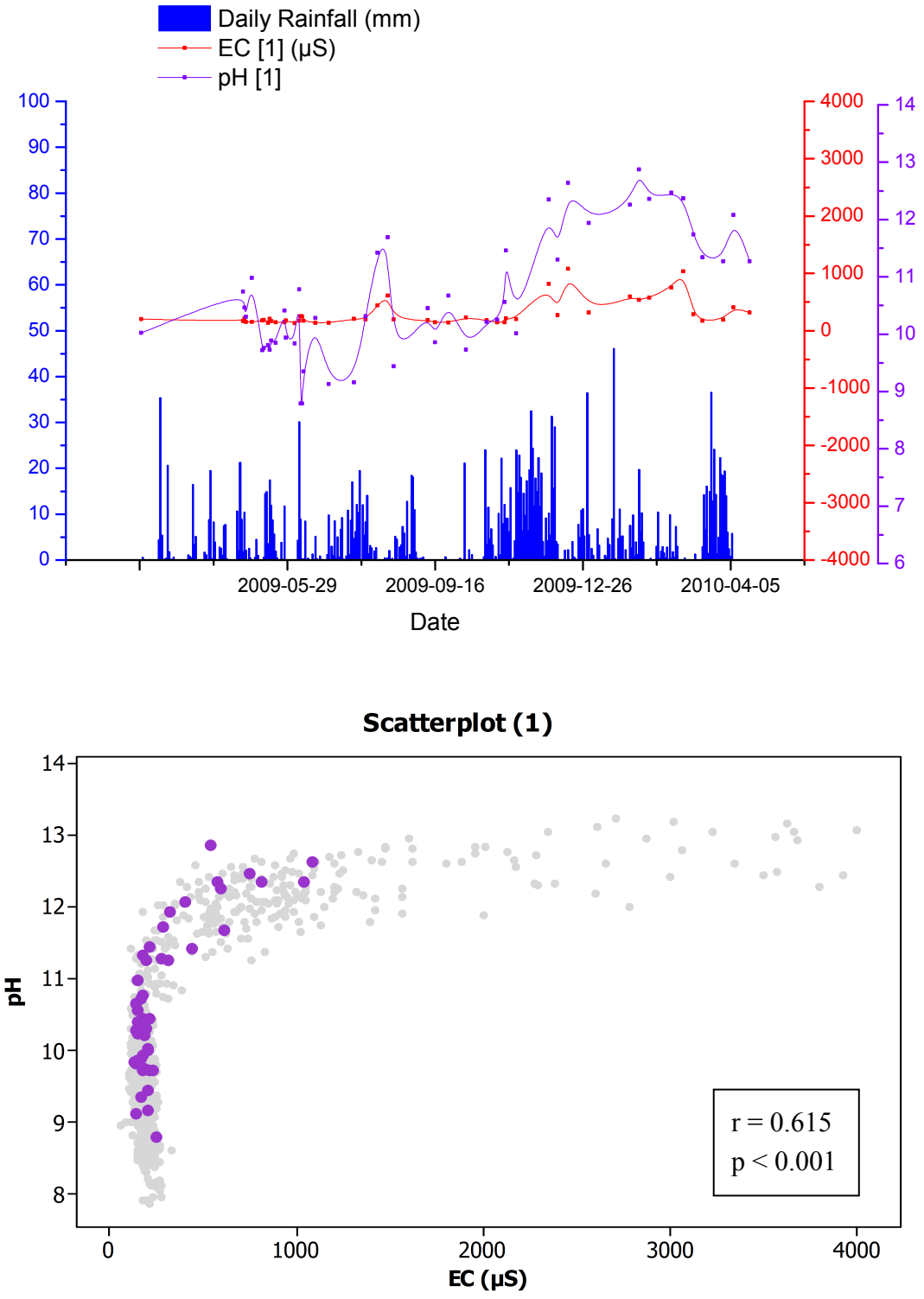

Figure 3.4.2i. [Above] Annual variability in rainfall, pH and electrical conductivity (EC) for geochemical site 1. [Below] Scatterplot of pH and EC for site 1 (purple) and the whole site (light grey). Spearman's rank correlation values (r) and confidence level (p) for site 1 are inset.

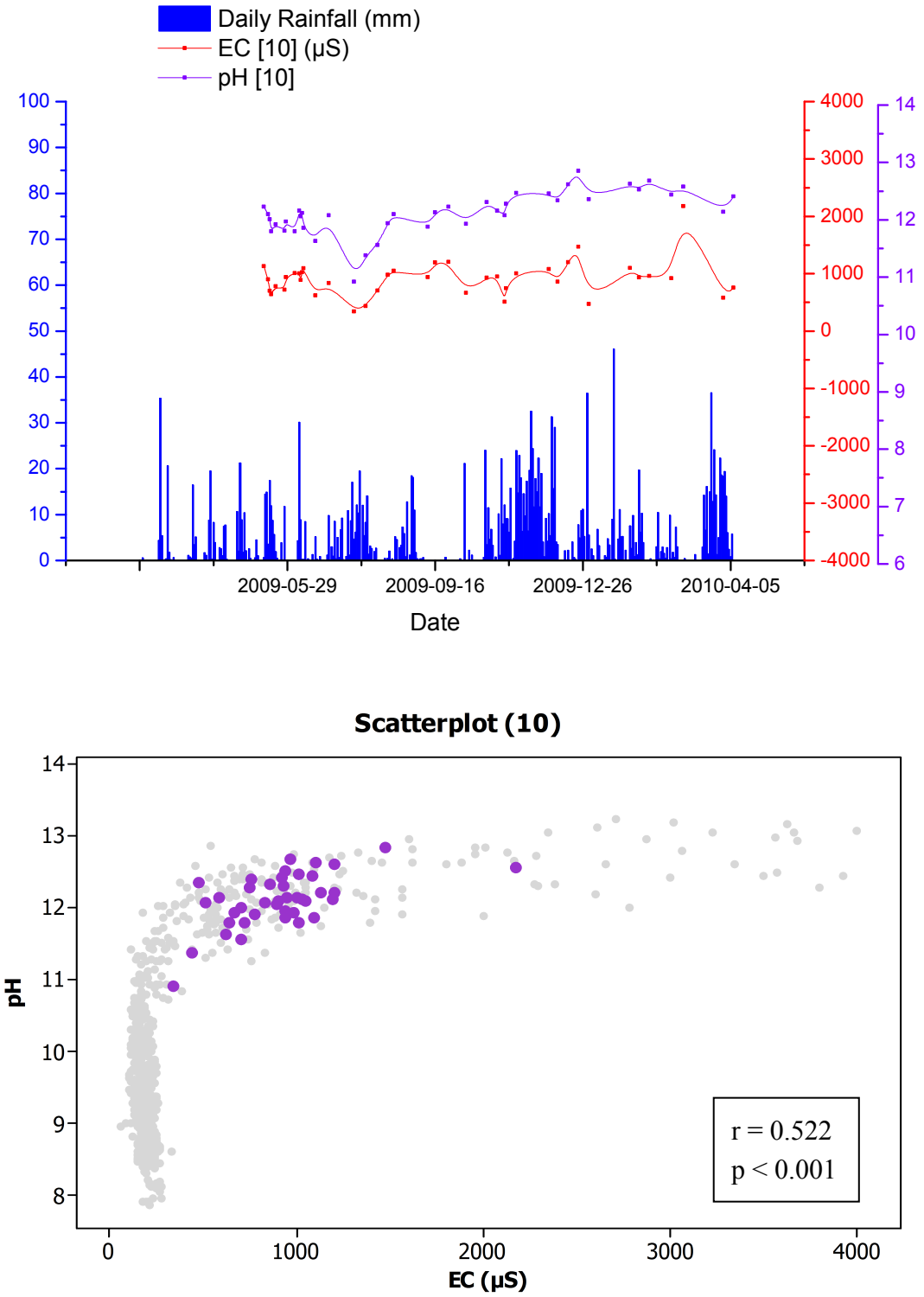

Figure 3.4.2j. [Above] Annual variability in rainfall, pH and electrical conductivity (EC) for geochemical site 10. [Below] Scatterplot of pH and EC for site 10 (purple) and the whole site (light grey). Spearman's rank correlation values (r) and confidence level (p) for site 10 are inset.

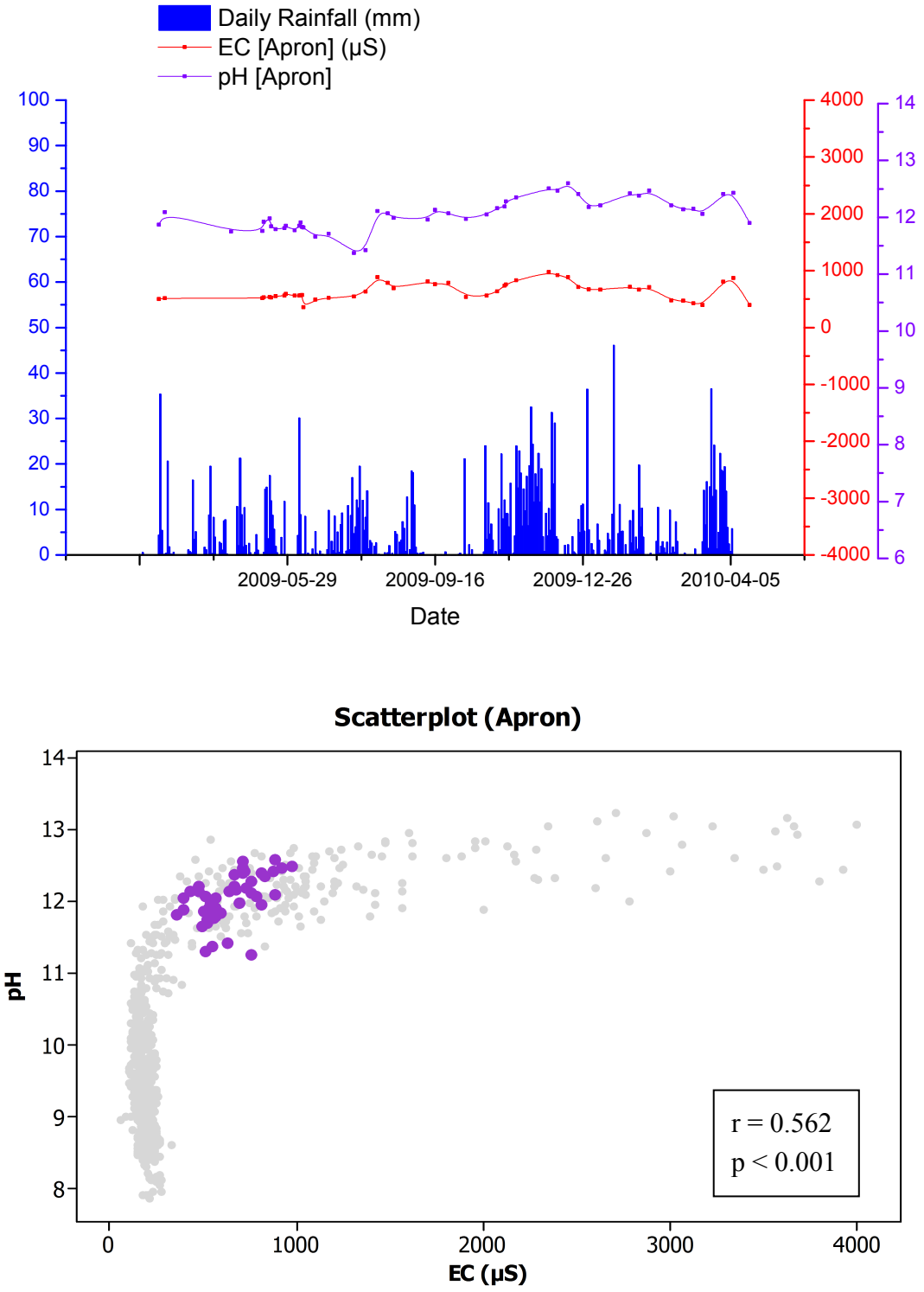

Figure 3.4.2k. [Above] Annual variability in rainfall, pH and electrical conductivity (EC) for geochemical site 'Apron'. [Below] Scatterplot of pH and EC for site 'Apron' (purple) and the whole site (light grey). Spearman's rank correlation values (r) and confidence level (p) for site 'Apron' are inset.

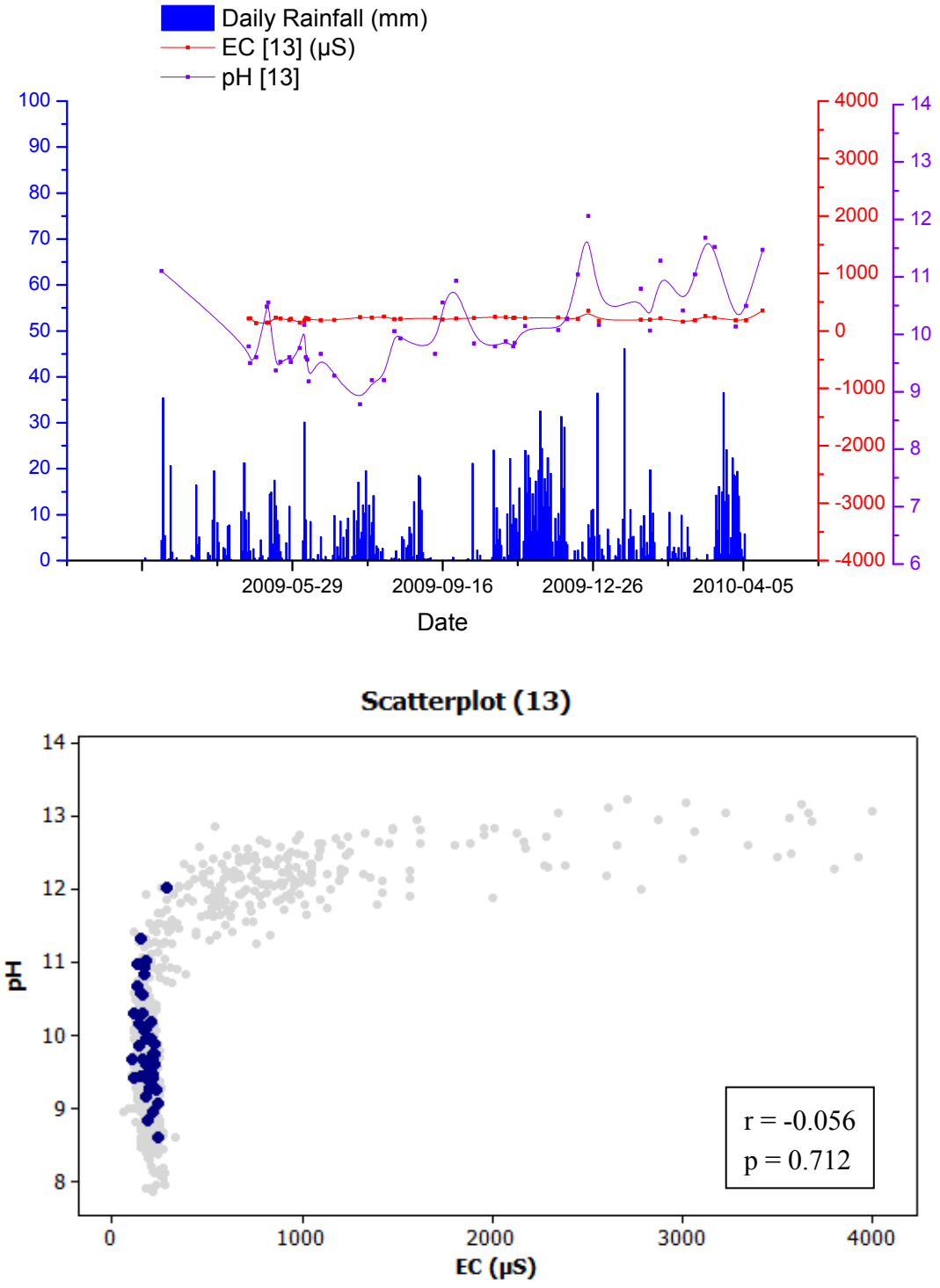

Figure 3.4.2l. [Above] Annual variability in rainfall, pH and electrical conductivity (EC) for geochemical site 13. [Below] Scatterplot of pH and EC for site 13 (purple) and the whole site (light grey). Spearman's rank correlation values (r) and confidence level (p) for site 13 are inset.

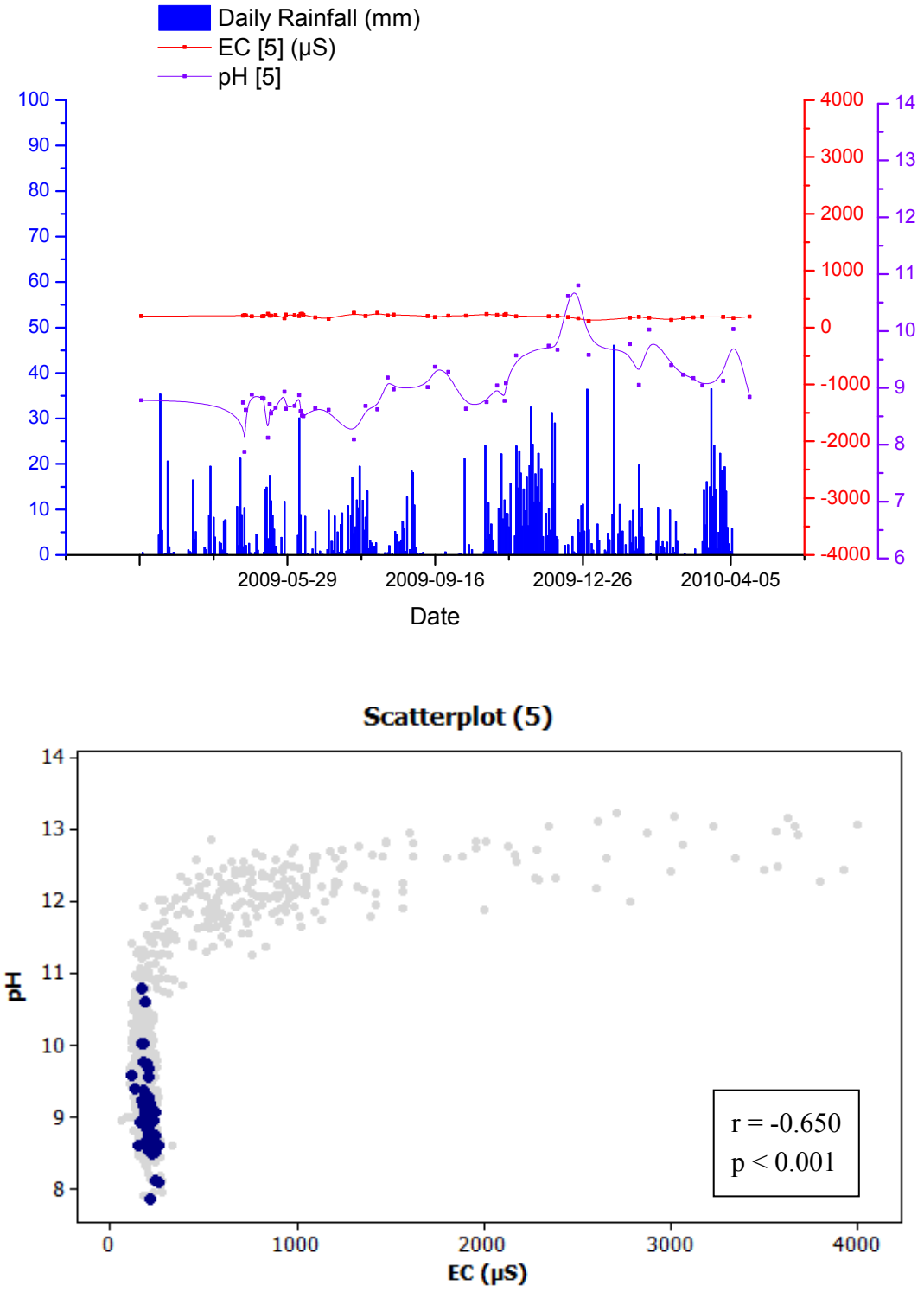

Figure 3.4.2m. [Above] Annual variability in rainfall, pH and electrical conductivity (EC) for geochemical site 5. [Below] Scatterplot of pH and EC for site 5 (purple) and the whole site (light grey). Spearman's rank correlation values (r) and confidence level (p) for site 5 are inset.

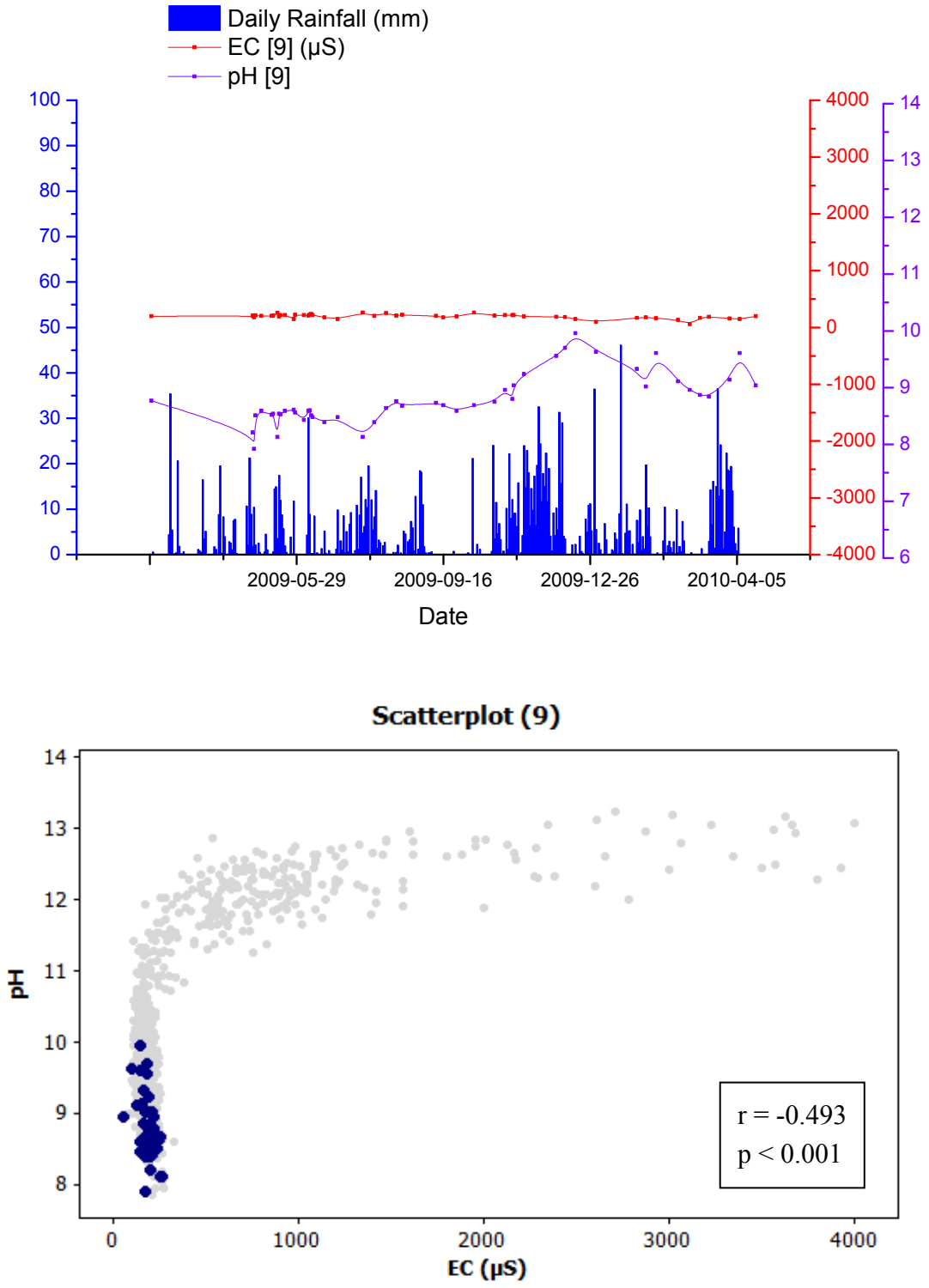

Figure 3.4.2n. [Above] Annual variability in rainfall, pH and electrical conductivity (EC) for geochemical site 9. [Below] Scatterplot of pH and EC for site 9 (purple) and the whole site (light grey). Spearman's rank correlation values (r) and confidence level (p) for site 9 are inset.

3.4.3. Storm event hydrochemistry

Discharge lag time is very short (<12 hrs) and antecedent discharge is quickly restored following a storm event (figure 3.4.3a).

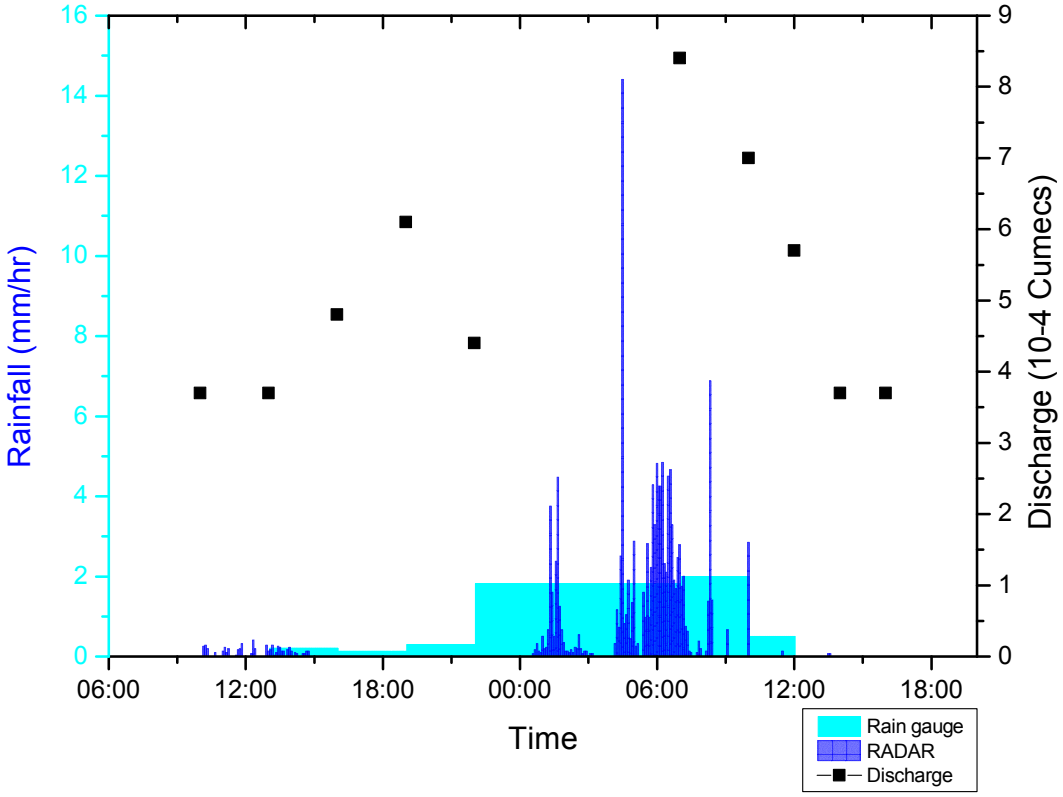

Figure 3.4.3a. Discharge variability with respect to rainfall on Foel Fawr.

Hydrochemistry, unlike discharge (figure 3.4.3a), does not return to its antecedent state. Preceding a storm event, proximal (apron) hydrochemistry is dominated by OH^- and CO_3^{2-}, and this pervades downstream (carbonate mud pool) (figure 3.4.3b).

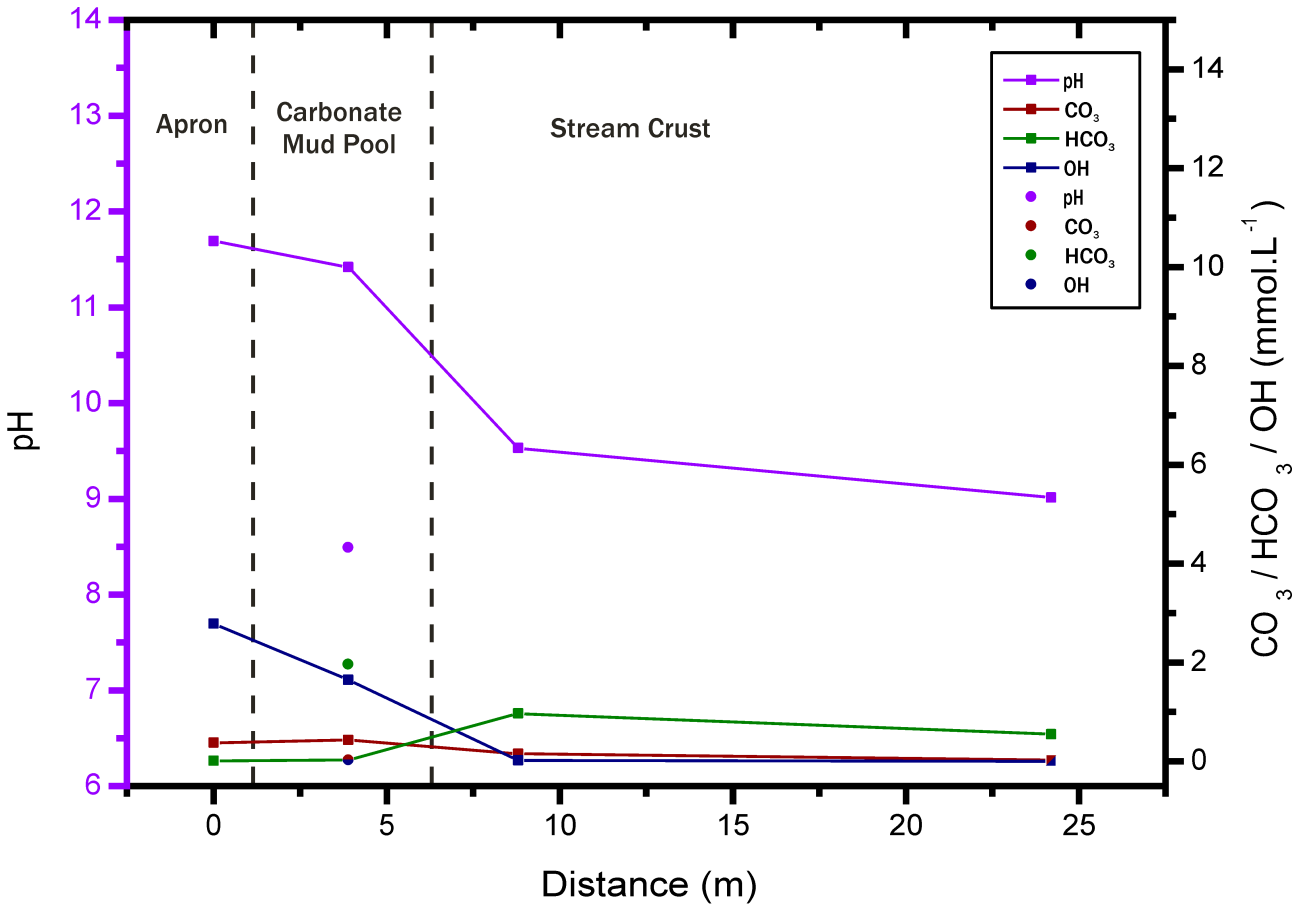

Figure 3.4.3b. Pre-stormflow hydrochemistry. Square symbols and lines represent downstream traverse through tufa facies (site 10, 11, 13, 14, figures 3.4.2c and 3.4.2d). Circular dots represent tributary/runoff input (site 12, figures 3.4.2c and 3.4.2d) into carbonate mud pool facies (where values intersect with downstream traverse, square symbols have been omitted for clarity).

During stormflow proximal (apron) pH remains high, although there is a slight shift towards CO_3^{2-} dominated buffering. Downstream, increased input from runoff causes a dramatic shift to bicarbonate buffering and an associated drop in pH (figure 3.4.3c).

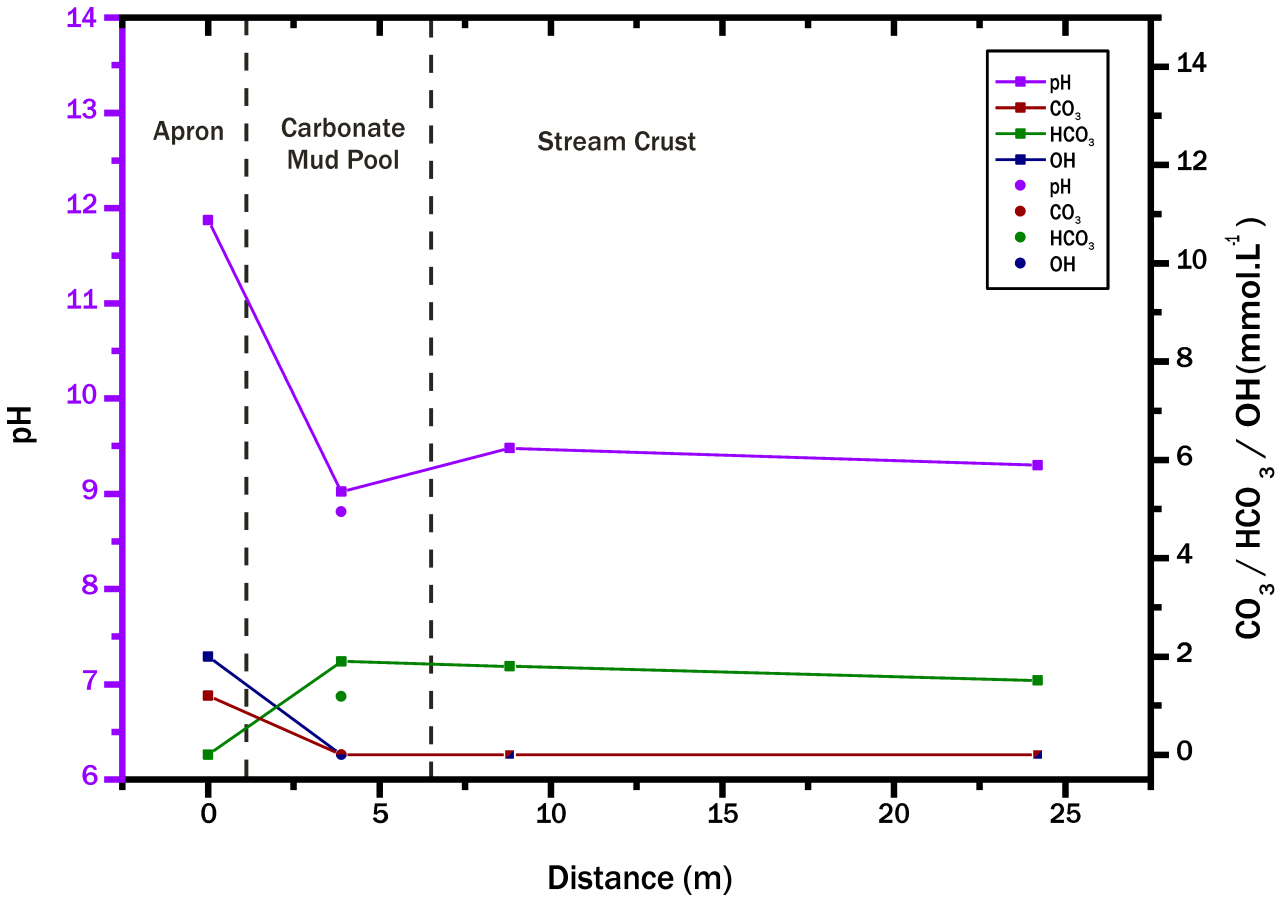

Figure 3.4.3c. Stormflow hydrochemistry. Square symbols and lines represent downstream traverse through tufa facies (site 10, 11, 13, 14, figures 3.4.2c and 3.4.2d). Circular dots represent tributary/runoff input (site 12, figures 3.4.2c and 3.4.2d) into carbonate mud pool facies (where values intersect with downstream traverse, square symbols have been omitted for clarity).

Following a storm event, proximal (apron) hydrochemistry is enriched with OH^- and pH is slightly higher. Downstream, input from runoff continues to consume OH^- and create a HCO_3^- dominated system; however, HCO_3^- concentrations are elevated with respect to antecedent levels (figure 3.4.3d).

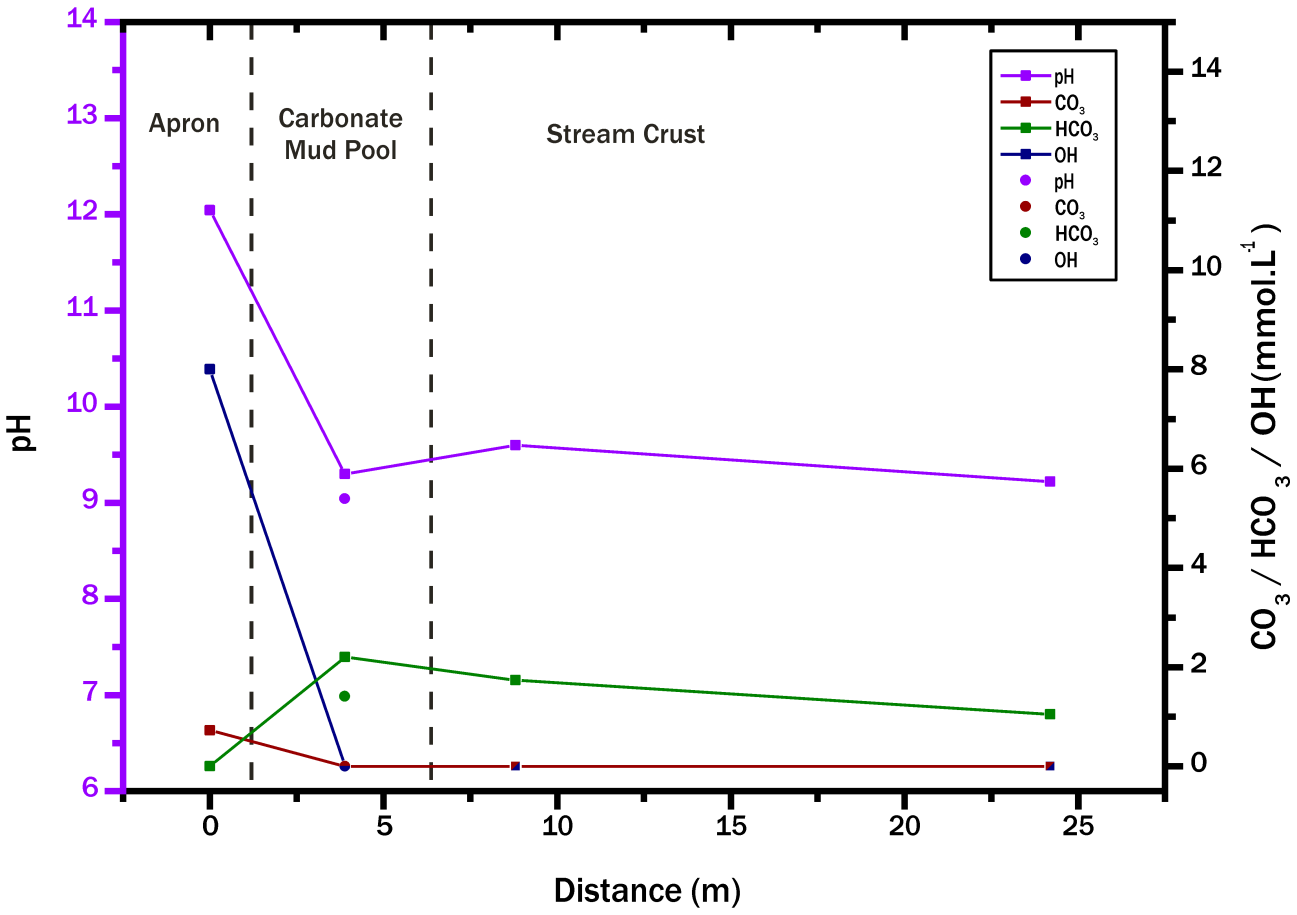

Figure 3.4.3d. Post-stormflow hydrochemistry. Square symbols and lines represent downstream traverse through tufa facies (site 10, 11, 13, 14, figures 3.4.2c and 3.4.2d). Circular dots represent tributary/runoff input (site 12, figures 3.4.2c and 3.4.2d) into carbonate mud pool facies (where values intersect with downstream traverse, square symbols have been omitted for clarity).

3.4.4. Deposit geochemistry

X-Ray diffraction analysis reveals that deposits are almost exclusively composed of calcite (table 3.4.4a). Other minerals of lesser significance may occur where there is a clastic component (i.e. pools, outwashes, pisoid cores). Quartz is the most significant, likely due to its resistance to both chemical and physical weathering.

Sample	Dominant mineral	Other minerals
Pisoid Core	Calcite	Illite
Pisoid Cortex	Calcite	
Carbonate Mud Pool (geochemical site 1)	Calcite	Quartz
Carbonate Mud Pool (margins)	Calcite	Quartz, Dolomite
Carbonate Mud (geochemical site 4)	Calcite	Quartz, Kaolinite
Carbonate Mud	Calcite	Quartz

Table 3.4.4a. Summary of geochemistry of tufa deposits.

3.5. Biology

Biological analyses were undertaken in order to provide additional perspective to apparent biological influence of facies described in section 3.2. Higher plants and bryophytes were sampled and recorded from across the site. In proximal environments, eukaryotes are precluded; however, prokaryotes may be able to survive. Results of cell counts and other microbial observations are recorded in section 3.5.2. Several species of animal are apparent within the system - these are noted in section 3.5.3.

3.5.1. Plant communities

Higher plants living within the system are also present in the surrounding peat-bog system. Species observed within the distal reaches of the tufa system are listed in table 3.5.1a. Although the plants are from an acidic peat-bog community, there is an apparent prevalence for species with an affinity for neutral and alkaline environments in the sub-community present within the tufa system.

	Species
Acid wetland	*Carex nigra*
	Carex panicea
	Eriophorum angustifolium
	Juncus effusus
	Juncus squarrosus
Neutral & alkaline wetland	*Agrostis stolonifera*
	Carex flava
	Carex hostiana
	Eleocharis quinqueflora
	Equisetum fluviatile
	Equisetum palustre
	Juncus articulatus
	Pinguicula vulgaris
	Sagina procumbens
	Triglochin palustre
Others	*Thymus serpyllum*

Table 3.5.1a. Higher plants on Foel Fawr, grouped by typical environment.

There are a great variety of bryophytes living on Foel Fawr. The most abundant species are identified in table 3.5.1b, and are grouped by their observed environment.

	Species
Acid wetland	*Calliergonella cuspidata*
	Polytrichum commune
	Polytrichum juniperinum
	Sphagnum auriculatum
	Sphagnum recurvum
	Sphagnum palustre
Lime tips	*Calliergonella cuspidata*
	Amblystegium serpens
	Homalothecium sericeum

Table 3.5.1b. Most abundant bryophytes on Foel Fawr grouped according to environment.

3.5.2. Microbial communities

Both eukaryotes and prokaryotes are represented within the microbial communities on Foel Fawr. Diatoms are ubiquitous, except in the most alkaline environments. Alongside diatoms, other algae are also present (figures 3.5.2a and 3.5.2b)

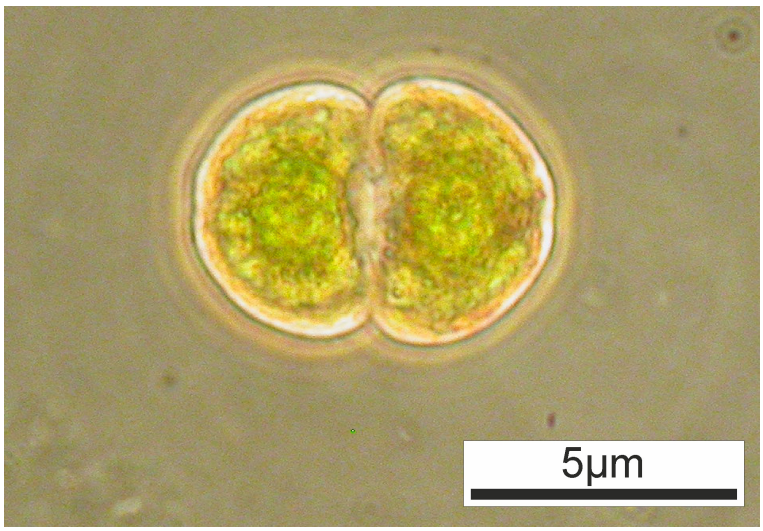

Figure 3.5.2a. Algal cell from marginal waters on Foel Fawr

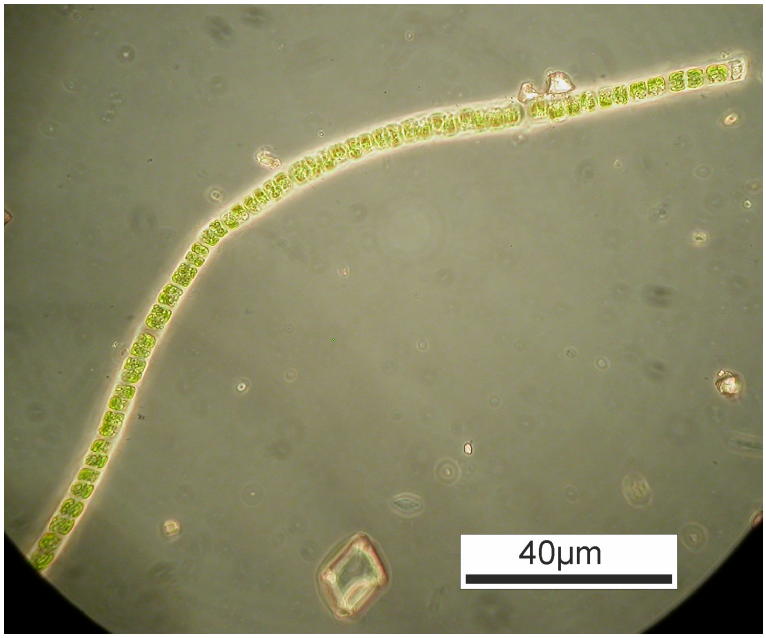

Figure 3.5.2b. Filamentous algae from marginal waters on Foel Fawr

Cell counts from a proximal carbonate mud pool (see figure 3.4.2b) reveal active microbial communities within the sediment. Sediment cores from the centre of a carbonate mud pool (hydrochemical site 1) reveal a decrease in the number of cells and their activity near the surface (figure 3.5.2c). This is likely due to the hydrochemistry of the overlying water (see figure 3.4.2i).

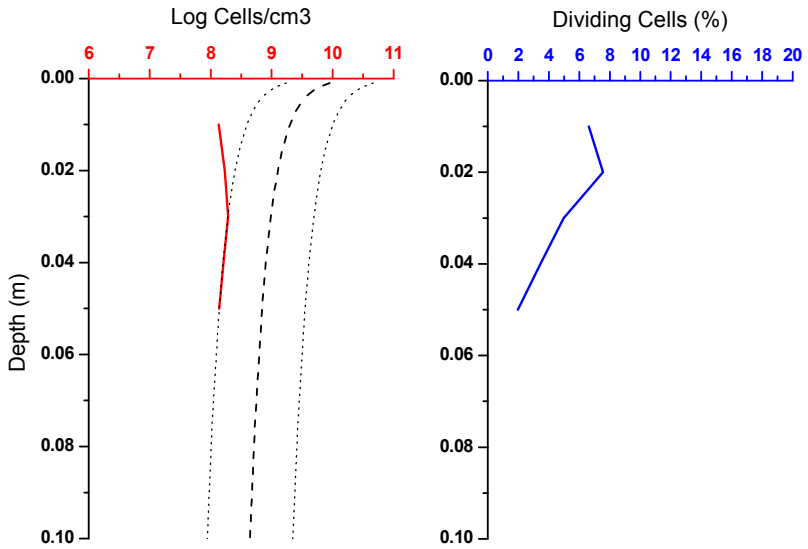

Figure 3.5.2c. Total cell count and activity from middle of carbonate mud pool (hydrochemical site 1). Dashed line represents mean expected cells, dotted lines represent 95% confidence intervals for this mean.

On pool margins, where pH is more neutral (mean pH 9.83, hydrochemical sample site 1d), cell counts are higher and communities are significantly more active (figure 3.5.2d).

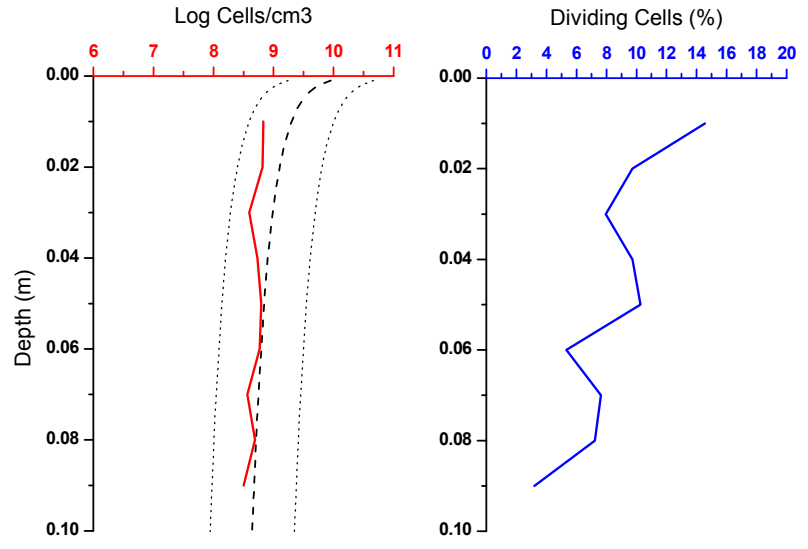

Figure 3.5.2d. Total cell count and activity from margin of carbonate mud pool (hydrochemical site 1d). Dashed line represents mean expected cells, dotted lines represent 95% confidence intervals for this mean.

3.5.3. Animals

Amphibians are the most conspicuous aquatic animals on Foel Fawr (figure 3.5.3a). Spawn is laid by the common frog (*Rana temporaria*) in February – March, with tadpoles developing by April - June.

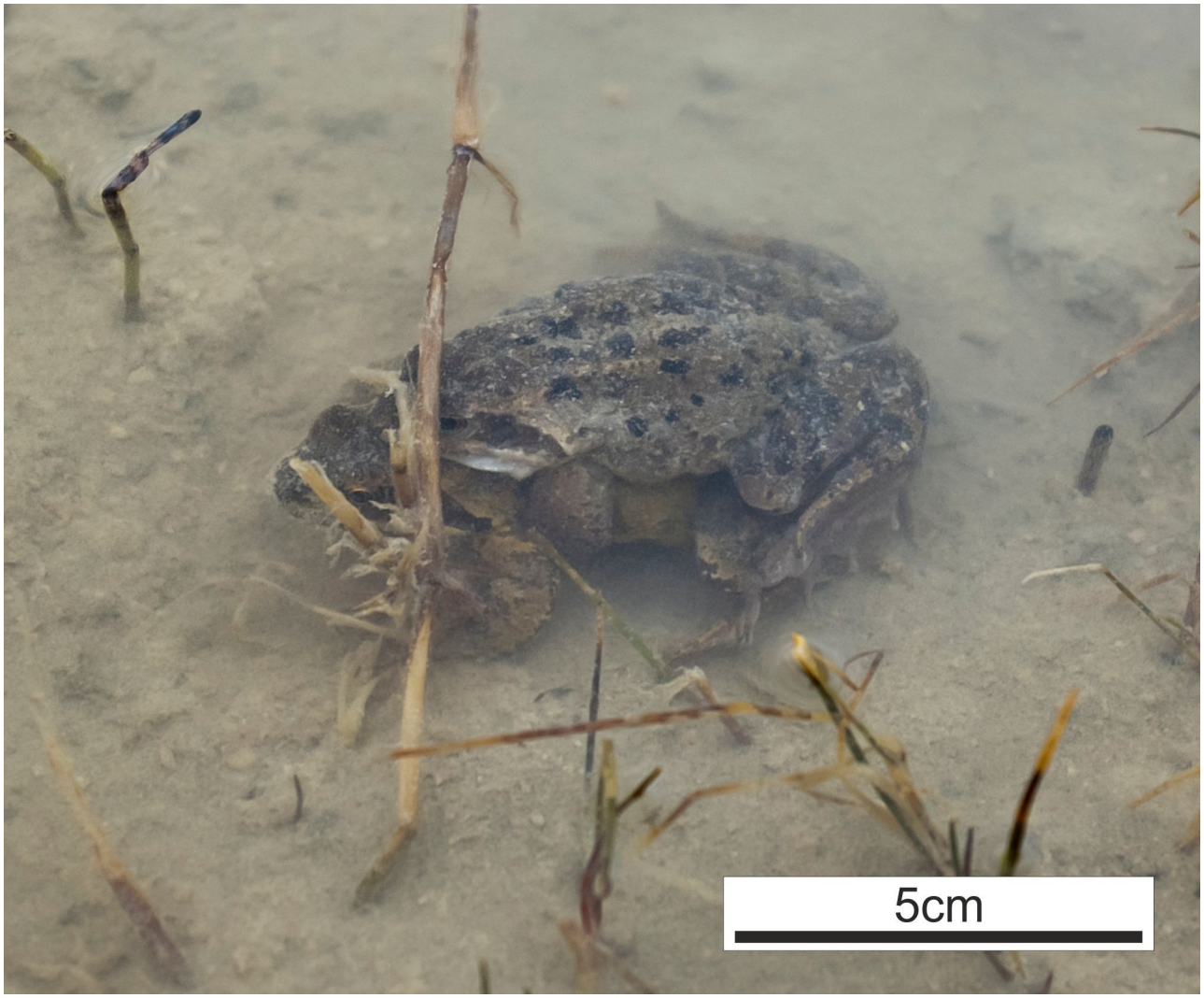

Figure 3.5.3a. Two frogs mating on the margins of a carbonate mud pool [17/03/10]. MACB.

Frogspawn may be found in proximal pools; however, it is always restricted to the margins where pH is more neutral (circa. pH 8). Where spawn drifts into higher pH waters (circa. pH 10-11), mortality rates are high. The coalescence of frogspawn offers some protection at the centre of the clump (figure 3.5.3b).

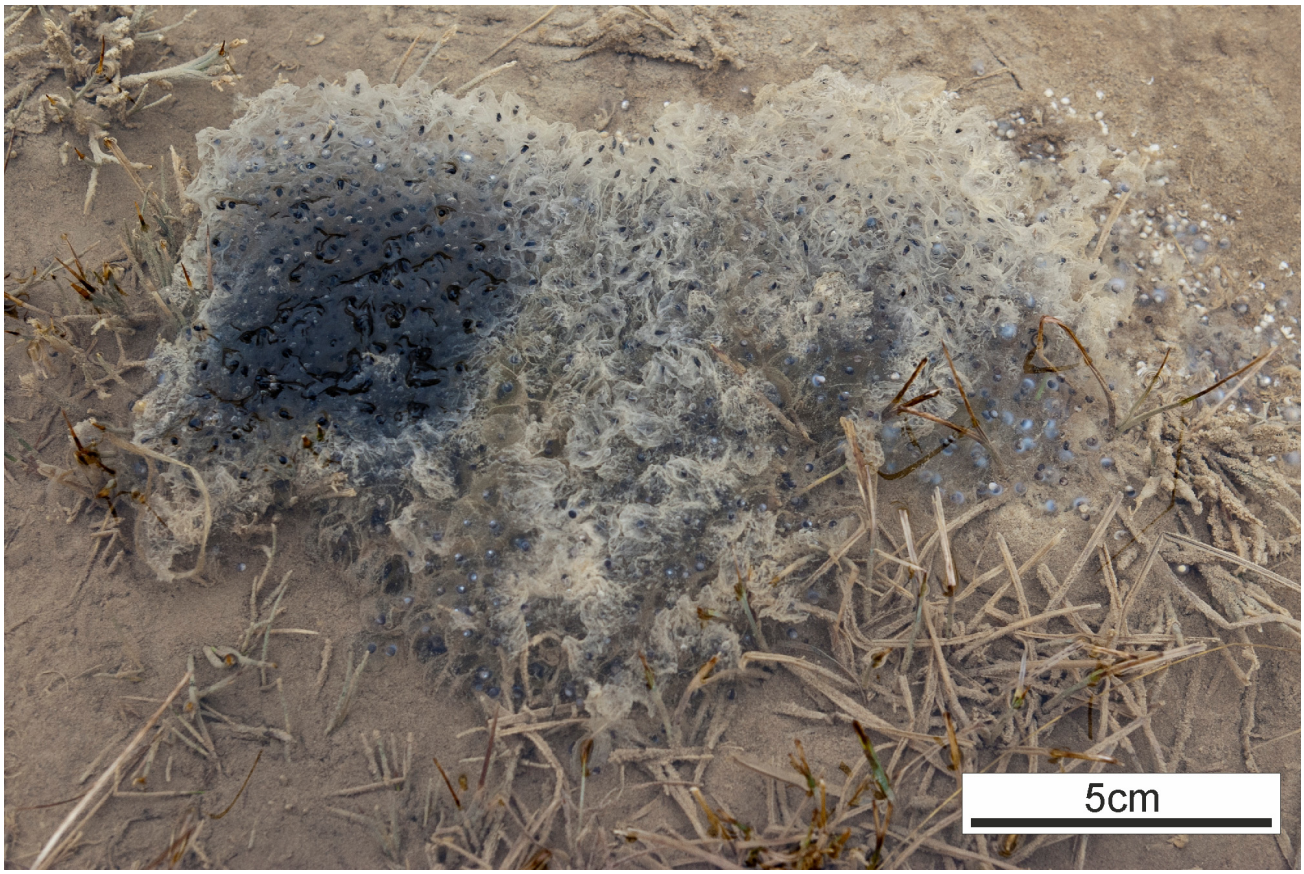

Figure 3.5.3b. Frogspawn clump on edge of carbonate mud pool. Elevated pH has led to mortality of spawn, but spawn contained within the clump and closer to the (more neutral) edge of the pool are still alive (image left). MACB.

Palmate newts (*Lisotriton helveticus*) are also found in pools on Foel Fawr (figure 3.5.3c), although they are notably absent from proximal pools. Spawn is not observed, although this is likely due to its inconspicuousness.

Figure 3.5.3c. Palmate newt on the margins of a carbonate mud pool [03/06/10].

Herds of semi-feral Welsh Mountain Ponies (*Equus ferus caballus*) (figure 3.5.3d) and domestic sheep (*Ovis aries*) are common. Faeces of both species are found on tufa deposits, sometimes calcified. These ungulates trample the tufa deposits and likely contribute to fracturing and decay.

Figure 3.5.3d. Welsh Mountain Ponies standing in front of carbonate gravel facies on Foel Fawr. MACB.

Humans also have a significant effect on the breakdown of the system. The area is used extensively by walkers, as well as for off-road motorbiking and quad biking (often by shepherds), which may result in damage to the deposits (figure 3.5.3e)

Figure 3.5.3e. Quad bike tracks through a carbonate mud pool.

3.6. Accretion experiments

3.6.1. Time-lapse photography

Time lapse imagery of stream crust demonstrates active growth is still occurring at this site. The series shown in figure 3.6.1a was taken following the pipe being cleared (it was previously blocked); rubble remaining from the clearing can be seen in image 1. Progressively, the development of stream crust/apron facies surface can be seen downstream of the pipe.

3.6.1a. Time-lapse imagery of apron forming through pipe under road at approximately monthly intervals between August 2009 and March 2010. 1: 12th August, 2: 11th September, 3: 14th October, 4: 3rd November, 5: 16th December, 6: 21st January, 7: 10th February, 8: 11th March. Pipe diameter circa. 40 cm. MACB.

3.6.2. Accretion rate

Accretion rates of proximal stream crust terrace (see section 3.1.3) vary through the year. Between 12th August 2009 and 11th March 2010, an equivalent annual accretion rate of 2.4 mm/a was measured. The rate of accretion was not consistent over this period, varying from around 0 to over 4 mm/a equivalent (figure 3.6.2a). Accretion is highest during frequent rainfall events; however, it is slowest following prolonged periods of rainfall.

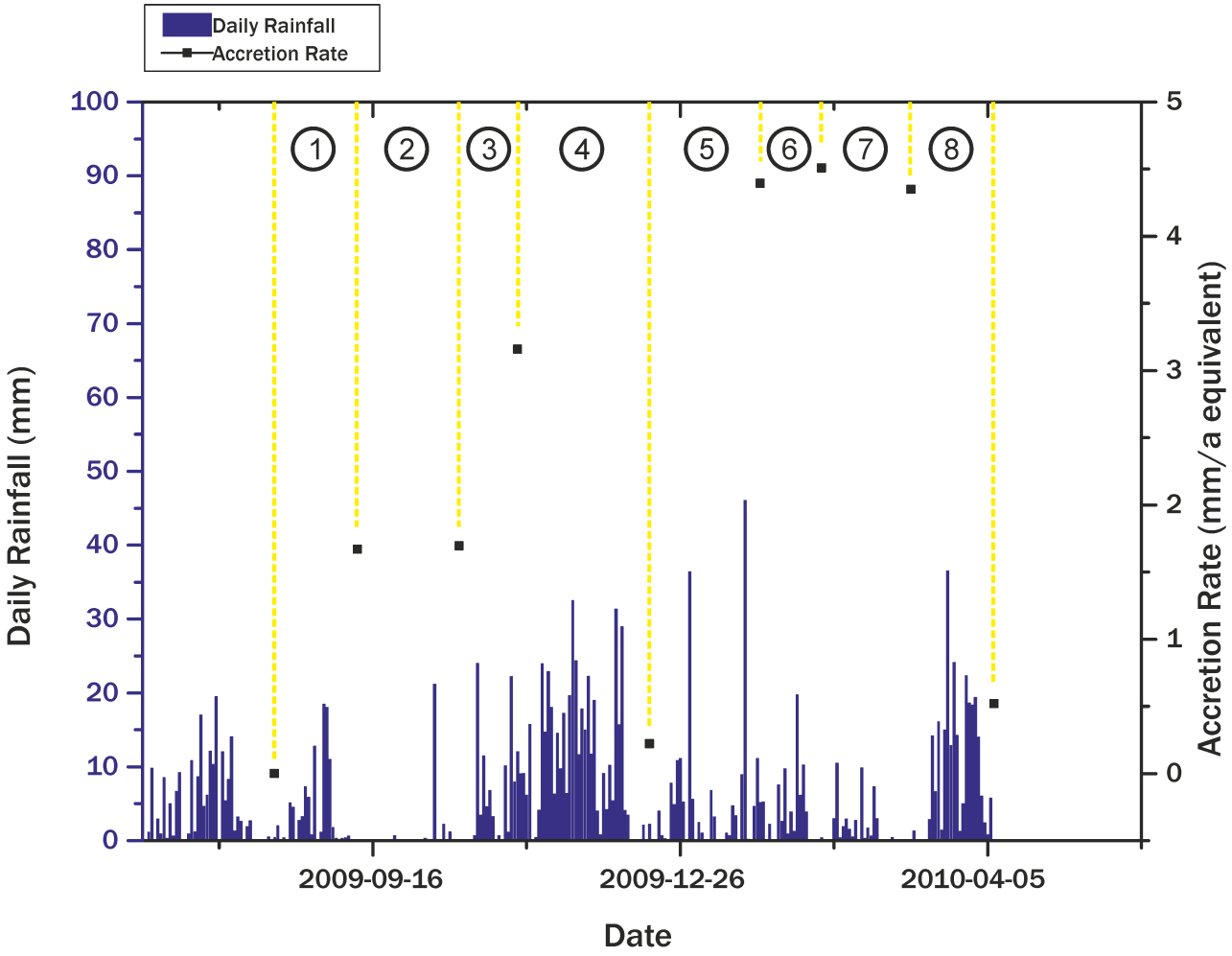

Figure 3.6.2a. Accretion rate compared with rainfall on Foel Fawr. Numbered intervals correspond to the succeeding growth rate. 1: Several rainfall events, moderate growth rate. 2: One rainfall event, moderate growth rate. 3: Several extended rainfall events, high growth rate. 4: Prolonged, heavy rainfall, low growth rate. 5: Several severe rainfall events, very high growth rate. 6: Several rainfall events, very high growth rate. 7: Several low intensity rainfall events, very high growth rate. 8: Prolonged, heavy rainfall, low growth rate.

Long-term experiments on older stream crust (see section 3.1.3) using nails affixed to the stream crust showed no measurable growth (precision = +/-0.5 mm) between 05/03/2009 and 12/01/2012 (figure 3.6.2b).

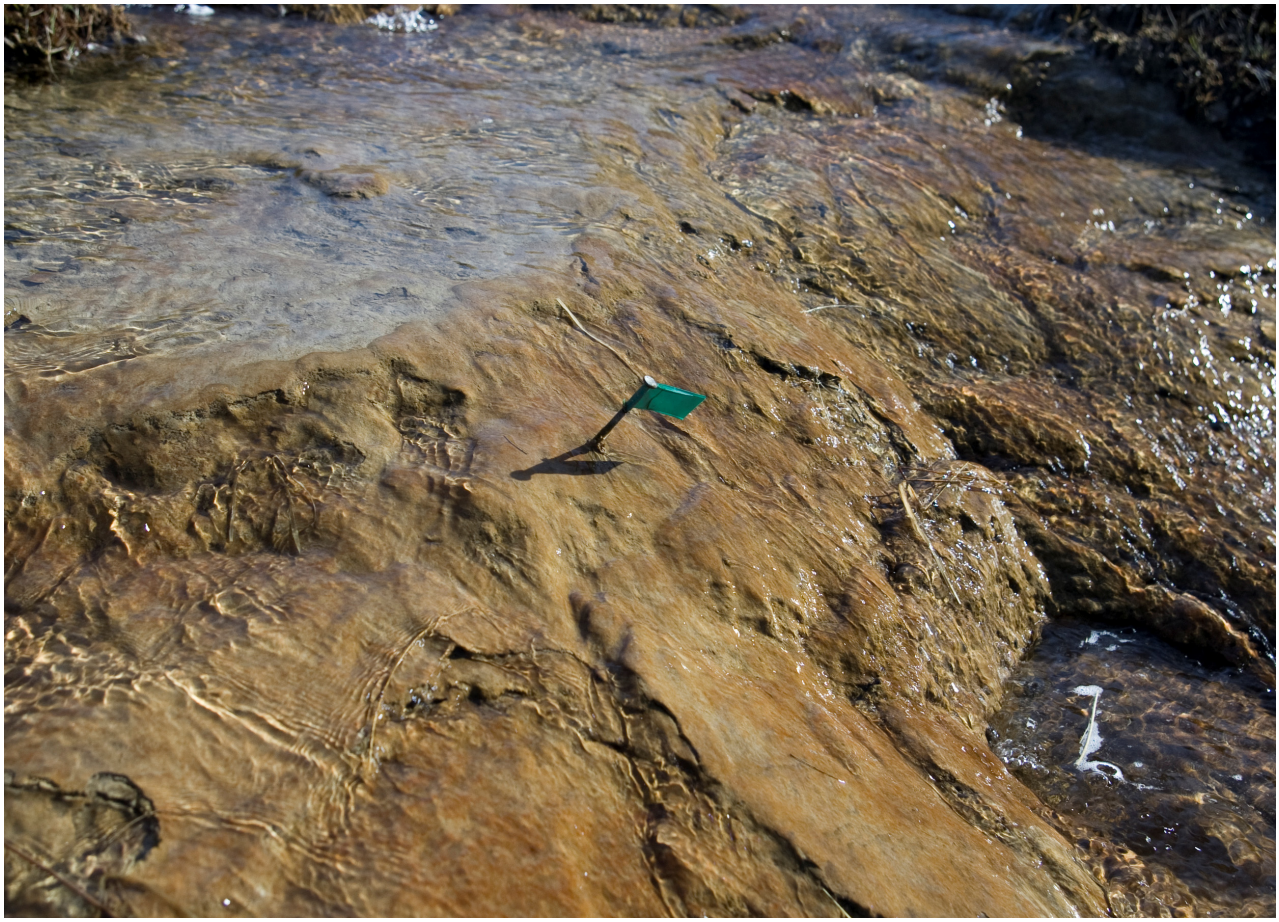

Figure 3.6.2b. Nail affixed to stream crust on Foel Fawr showed no accretion. Exposed nail length: 50 mm.

3.7. Comparative sites

3.7.1. Harpur Hill, Derbyshire, UK.

A similar tufa system forming from lime kiln waste is found at Harpur Hill, Derbyshire (405632 370879 OSGB). The site was active between 1872 and 1944 (Anon, 2008), the extent of the deposits is smaller than Foel Fawr and the range of facies is less varied. The bulk of the deposits consists of friable terraces and fine-grained carbonate mud forming a single deposit up to 50 m wide (figure 3.7.1a).

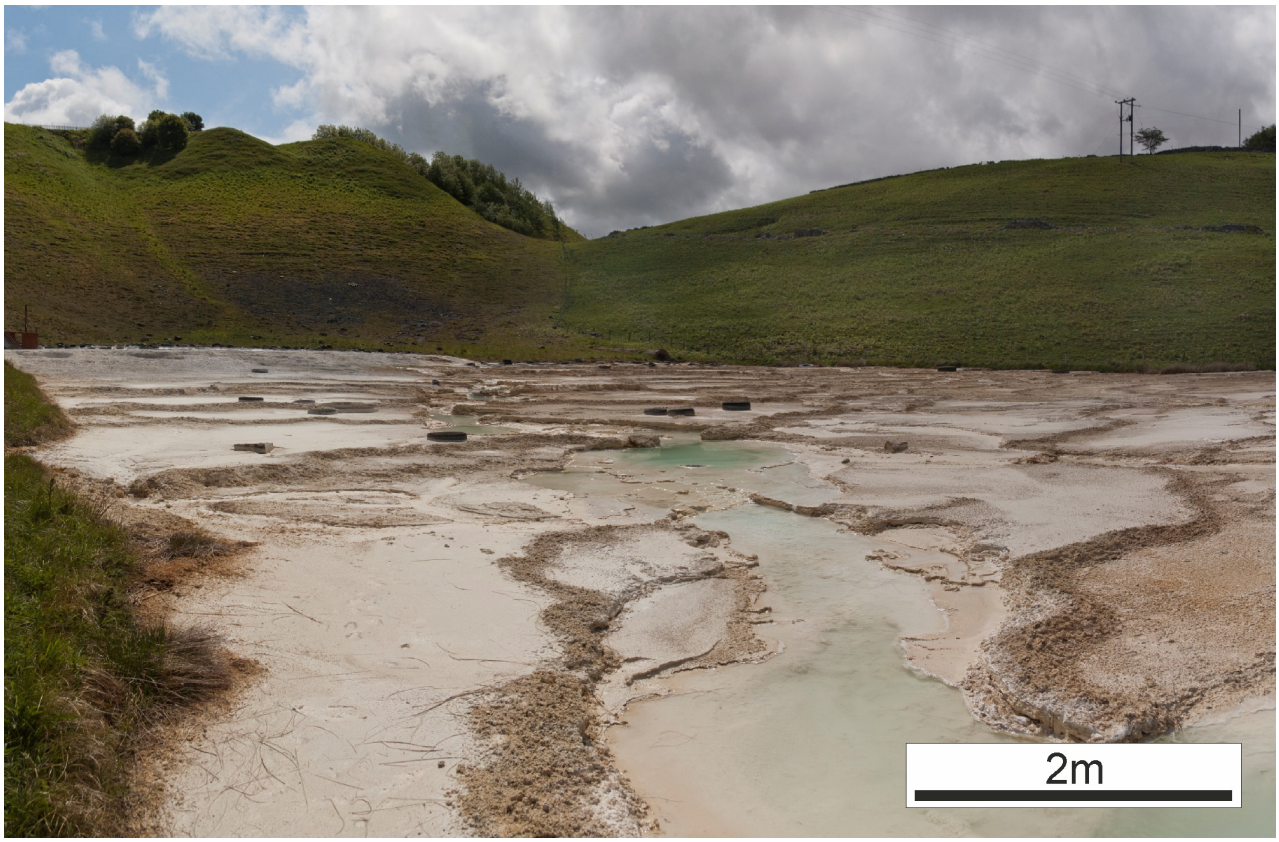

Figure 3.7.1a. Tufa forming from lime kiln waste at Harpur Hill. MACB.

Discharge apparently comes from two sources: a point source issuing from a small tunnel (figure 3.7.1b) and a seep. The tunnel contains friable terracettes and outflows into a small carbonate mud pool. The precipitation of terraces within the tunnel is comparable to those seen on Foel Fawr (see figure 3.1.3d and 3.1.3e) and demonstrates that precipitation of these features is not light dependant.

Figure 3.7.1b. Outflow tunnel at Harpur Hill. Note microterracettes forming inside tunnel. MACB.

The seep is at the base of a large spoil tip and forms a large carbonate mud pool, which contains numerous discarded tyres (figure 3.7.1c). Water depth is of the order of several cm and precipitates fine grained carbonate mud. Water flow is very slow (i.e. not discernable by eye), forming on approximately flat ground. Carbonate rafts were not observed, although these are only an ephemeral feature of carbonate mud pools on Foel Fawr.

Figure 3.7.1c. Outflow seep forming carbonate mud pool at Harpur Hill. MACB.

Below this pool, there are extensive outwashes of fine grained carbonate mud. These outwashes are deposited on low slopes (comparable to carbonate mud outwashes on Foel Fawr), often forming friable terraces across their surface. The outwashes are waterlogged and typically have a shallow covering of water on their surface with a slow, but readily discernable flow rate (i.e. faster than in carbonate mud pool forming at the seep). Incision and erosion of terraces is observed where flow is highest (figure 3.7.1d). The absence of incision downstream of this (figure 3.7.1e) suggests that this is a result of increased local discharge, rather than symptomatic of declining precipitation and highlights the transient nature of terraces formed from such friable material.

Figure 3.7.1d. Erosion of friable terraces where flow rates are highest. MACB

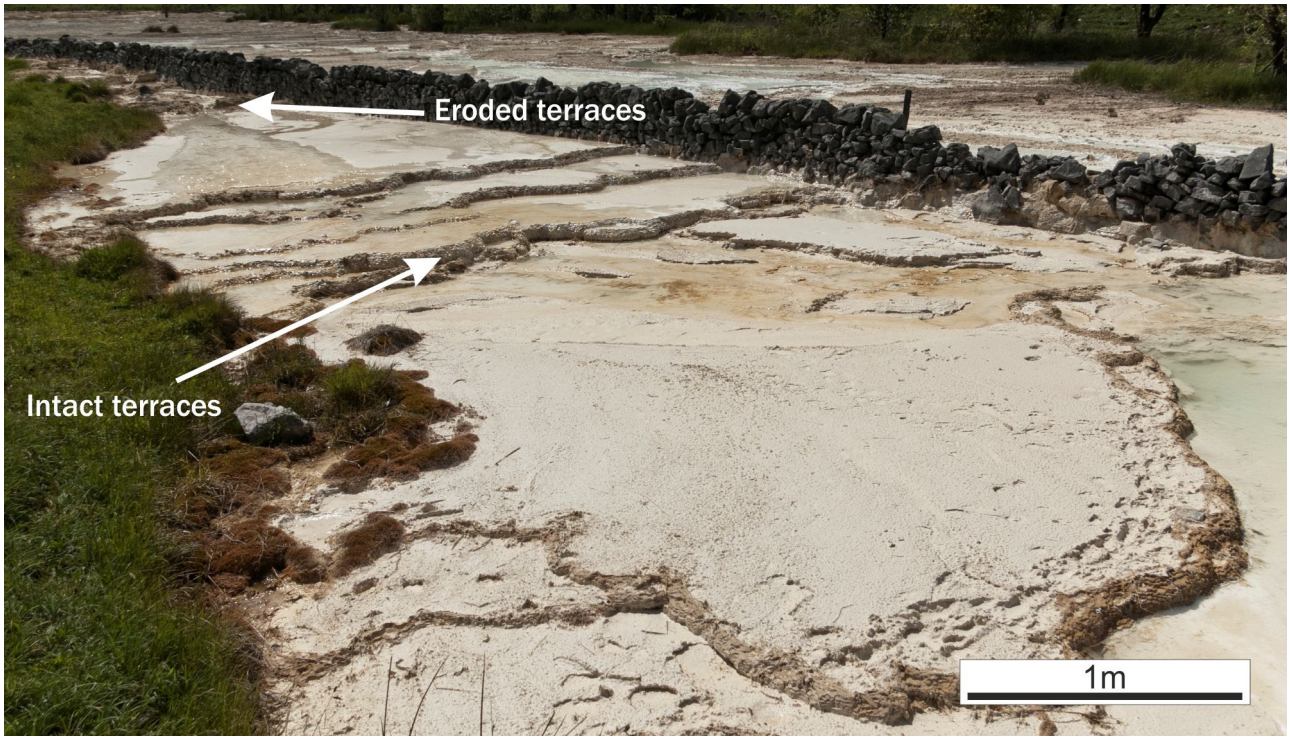

Figure 3.7.1e. Terraces downstream of channelised high flow areas (figure 3.7.1d) are still intact. MACB.

Further downstream (c.200 m), water flows through constrained channels and harder precipitates form. Terraces are common, forming pools filled with carbonate mud behind them (figure 3.7.1f). These deposits are similar to the stream crusts deposited on Foel Fawr, however, the presence of fine grained carbonate mud is a notable difference. This may be the result of transported fine-grained material from the expansive carbonate mud deposits upstream (see figure 3.7.1a), which are not present on Foel Fawr.

Figure 3.7.1f. Terrace forming across streamway at Harpur Hill. MACB.

Marginal areas and areas subject to periodic inundation may feature encrustation of plants (figure 3.7.1g). These encrustations appear to be predominantly external moulds, similar to those observed on Foel Fawr.

Figure 3.7.1g. Encrusted plants at Harpur Hill, formed as a result of the inundation of plants growing in and adjacent to streams. MACB.

There are several notable differences between this site and Foel Fawr. Many of the facies observed on Foel Fawr are absent here; pisoids, oncoids, carbonate gravel, aprons and vertical aprons are all missing. The reason for this is likely due to the different setting and hydrological regime of the site. Harpur Hill is a valley fill deposit, where precipitation is concentrated into a valley bottom site. This setting creates a single hydrological system (whereas on Foel Fawr, there are many independent sources, each with its own hydrology) and reduces the variability of depositional environments at the site. There are no pisoids or oncoids formed, because there are no shallow pools for them to form; there are no point sources with low flow to precipitate aprons; no vertical faces to form vertical aprons; and no flat areas for spoil to wash out and form carbonate gravel.

The hydrological regime may also explain the broad scale differences between the sites. The deposits are generally more friable than those on Foel Fawr, and appear to be universally subaerial. The concentration of the resurgence within a single valley likely reduces the impact of storm events on the discharge at the site and means that deposits are more continually subaqueous than those on Foel Fawr. This results in more continual precipitation, and the continual input and precipitation of fine grained carbonate mud to the site, preventing the growth of large laminated prismatic calcite, which generates the hard crystalline fabrics observed on Foel Fawr.

3.7.2. Other limekilns in South Wales

There are many other limekilns in South Wales; none of the kiln sites, though, are on the same scale as those on Foel Fawr. Table 3.7.2a contains a list of the kiln sites visited, of which only one site has evidence of tufa precipitation. The site (at Aberthaw, Vale of Glamorgan) is far smaller in scale than that at Foel Fawr, and tufa precipitation is autochthonous, with tufa precipitating within or on the surface of tips.

The tufa forming at Aberthaw differs from that at Foel Fawr and Harpur Hill. Tufa is formed internally within the tips and has subsequently been exposed at the surface. The scale of the site is also greatly reduced. Figure 3.7.2a shows the extent of tufa formation at Aberthaw.

Figure 3.7.2a. Aberthaw limeworks and spoil tips. MACB.

Site Name	Location (OSGB)	Description
Llandybie, Carmarthenshire	2615 2167	Extensive site with at least ten kilns, but no tufa precipitation. Site developed around 1856 and expanded around 1900 (Kitching, 2012).
Henllys Vale, Carmarthenshire	2762 2137	Four well-preserved kilns, but with no tufa precipitation. Active between mid 19th century and 1880s (Brecon Beacons National Park, undated).
Llangattock, Monmouthshire	3206 2171	Two kilns, no tufa precipitation. Developed in 1814 (Kitching, 2005).
Llangattock, Monmouthshire	3206 2172	Four kilns, no tufa precipitation. Thought to be active until mid-1920's (Kitching, 2012).
Blackrock Limeworks, Monmouthshire	3217 2127	Three kilns, no tufa precipitation. Kilns thought to date from the 19th century, and still active in 1915 (Kitching, 2012).
Llanelli Quarry, Monmouthshire	3222 2124	Two kilns. No tufa precipitation.
Clydach Limeworks, Monmouthshire	3233 2126	Four kilns, no tufa precipitation. Kilns thought to be discontinuously active from before 1862 until 1955 (Kitching, 2012).
Clydach Limeworks, Monmouthshire	3234 2125	Single kiln. Thought to predate the other kilns at Clydach Limeworks (Kitching, 2012). There are notable amounts of lime spoil remaining, however no evidence of tufa formation from leachate or exposure of tips.
Gilwern, Monmouthshire	3242 2147	Four kilns, no tufa precipitation.
Pen-Sarn, Newport	3284 1885	Single kiln, no tufa precipitation. Constructed around 1795-1796 (Kitching, 2012).
Llandewi, Swansea	2462 1887	Single kiln, no tufa precipitation.
Great Tor, Swansea	2531 1879	Single kiln, no tufa precipitation.
Lunnon, Swansea	2545 1900	Single kiln, no tufa precipitation.
Vennaway, Swansea	2565 1896	Single kiln, no tufa precipitation.
Aberthaw, Vale of Glamorgan	3038 1661	Two kilns, active between 1888 and 1926 (Brown, 2005).

Table 3.7.2a. List of kilns in South Wales including 8 figure OSGB grid reference and brief description of kilns, spoil and any tufa forming.

Precipitation is restricted to the spoil tips, forming predominantly friable white calcite precipitates (figure 3.7.2b). While much of the tips has been colonised by plants, small areas where the surface soil and vegetation have slipped and exposed the underlying tips are common, highlighting the poorly developed soil layer covering the tips. Precipitates are comprised mainly of micrite and often

contains fibrous material from the kilns (figure 3.7.2c). Larger crystals and evidence of biological activity are notably absent.

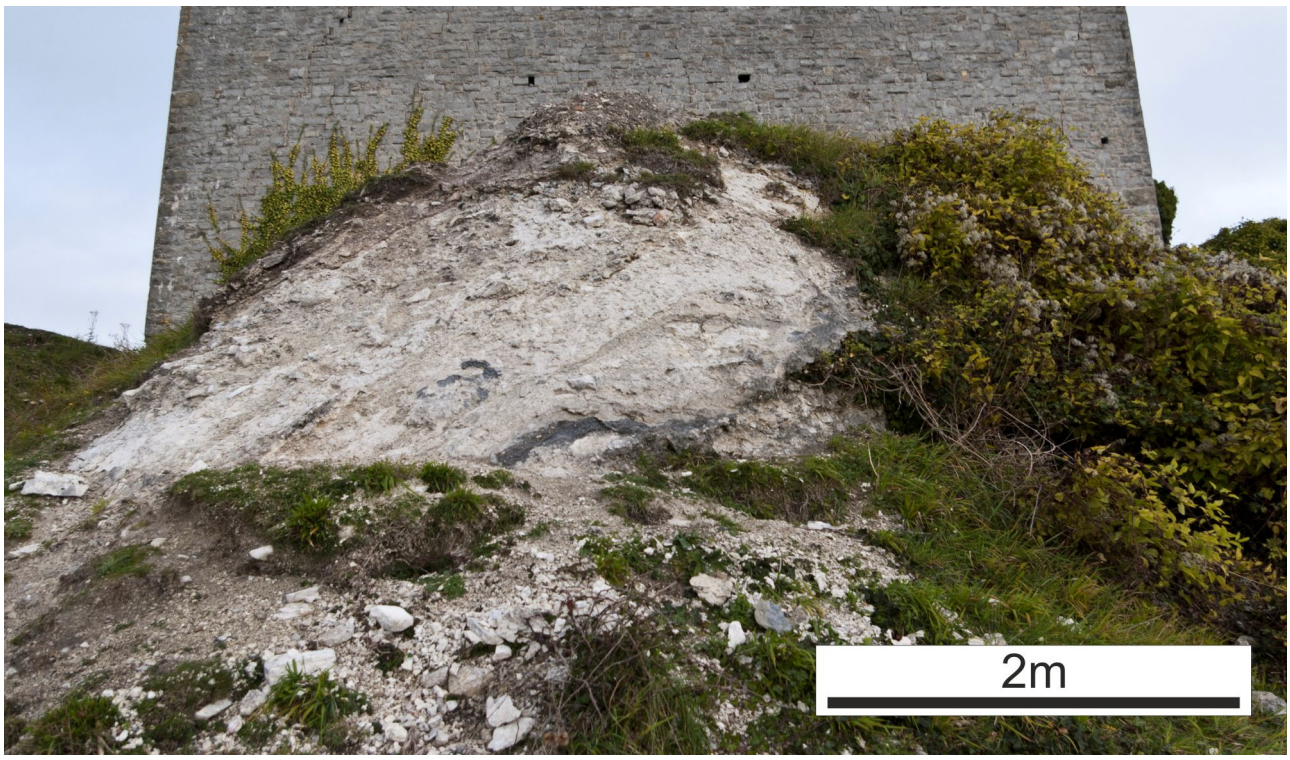

Figure 3.7.2b. Tufa deposition within a tip at Aberthaw, South Wales. MACB.

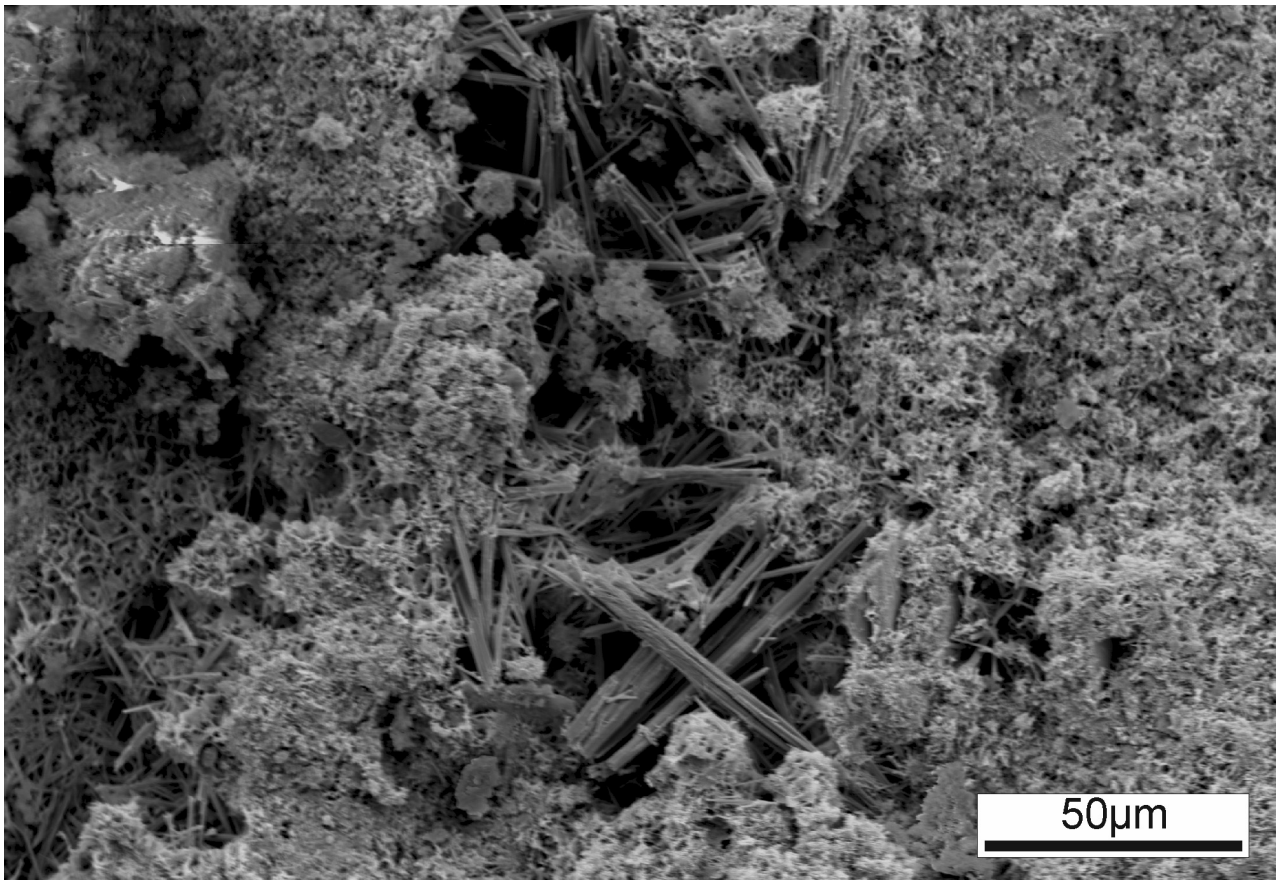

Figure 3.7.2c. Micrite and fibrous minerals from tufa/lime spoil at Aberthaw.

3.7.3. Hot-spring travertine systems

Several hot spring systems have been observed and briefly analysed in order to be compared to the system on Foel Fawr. Superficially, there are morphological similarities between the travertine systems observed and that on Foel Fawr. Systems at Pamukkale, Turkey; Bagni San Fillipo, Italy and San Giovanni, Tuscany all feature crystalline precipitates, notable for their absence of plants. The predominance of crystalline precipitates can be observed by the bright white colour of active precipitates.

Figure 3.7.3a. Travertine deposits at Pamukkale, Turkey. Note the white colour of deposits resulting from the predominance of crystalline precipitates and absence of biological/detrital input. Note people for scale. MACB.

Figure 3.7.3b. Vent pool at Il Bollore, Bagni San Filippo, Italy. Fine grained carbonate precipitates are deposited here, forming in proximal pools.

Proximally, hot springs may form deposits which share many of the characteristics of proximal deposits on Foel Fawr. Where pools are formed, fine grained carbonate mud is precipitated (figure 3.7.3b), forming an environment analogous to proximal pools on Foel Fawr. Where pools are not formed and water is able to flow more readily, laminated crystalline precipitates are common (figure 3.7.3c), analogous to the aprons and vertical aprons formed on Foel Fawr.

Figure 3.7.3c. Laminated crystalline crusts at Terme San Giovanni, Italy. Note microterracettes forming on the surface, similar to those forming on vertical aprons on Foel Fawr.

Similar microterracettes are also observed on actively precipitating crusts (figure 3.7.3d) and where deeper pools are formed behind terraces, carbonate mud is precipitated (figure 3.7.3e). As on Foel Fawr, carbonate rafts may be precipitated at the air-water interface in such pools (figure 3.7.3f).

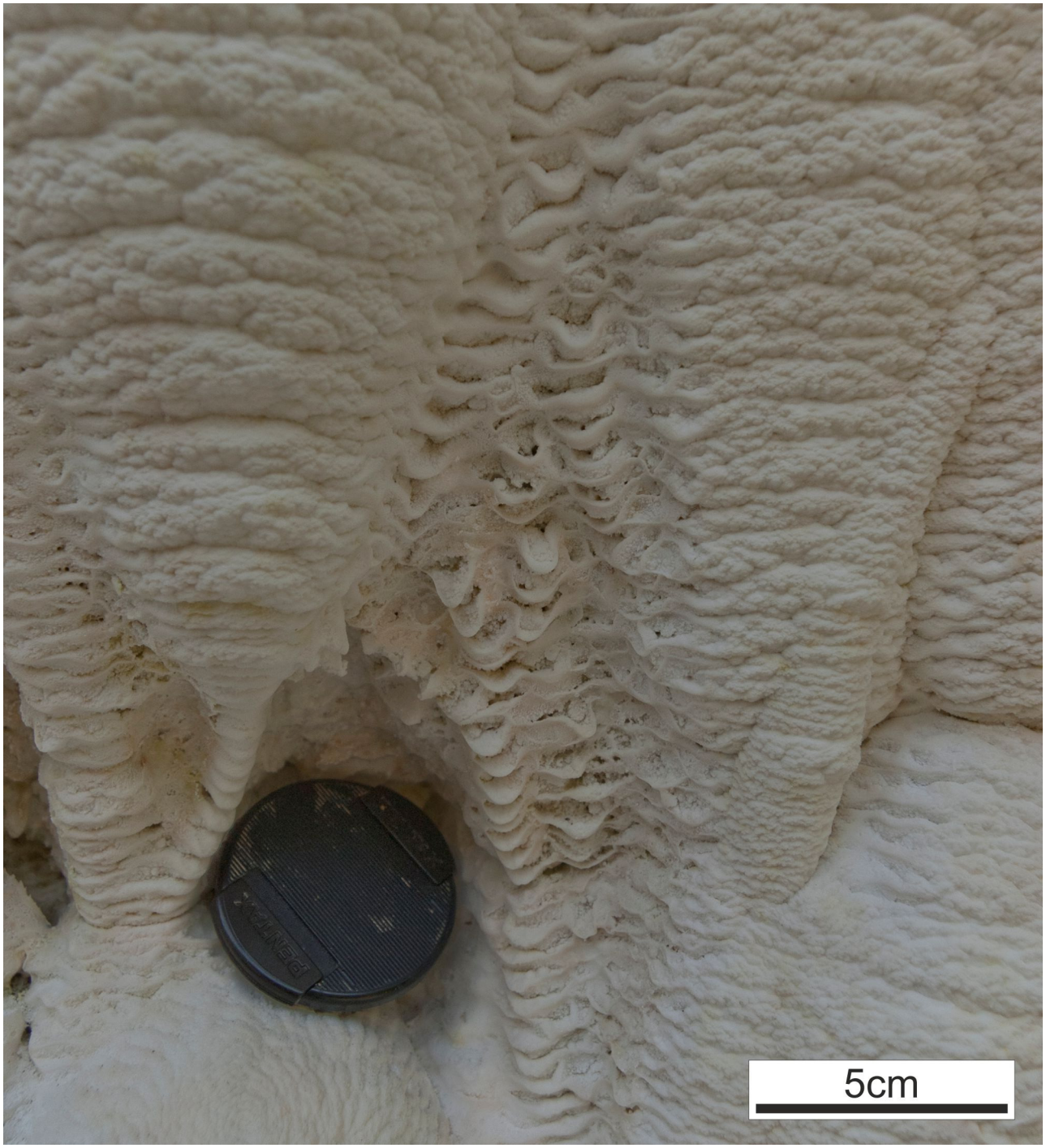

Figure 3.7.3d. Microterracettes forming on the surface of travertine at Bagni San Filippo, Italy. MACB.

Figure 3.7.3e. Carbonate mud forming in an artificially constructed terrace pool at Pamukkale, Turkey. MACB.

Figure 3.7.3f. Carbonate rafts forming at the air-water interface of a travertine pool. © Bruce Fouke, University of Illinois at Urbana-Champaign.

Despite the striking similarities in morphology, the deposits are not necessarily formed from identical crystal fabrics (figure 3.7.3g). However, the fabrics are similar in the predominance of phyisco-chemical precipitates and are often devoid of an apparent biological component.

Away from proximal locations, there is often a transition to facies more typical of tufa systems. At Bagni San Filippo, Italy, many large scale tufa barrages are formed downstream of active travertine deposits (figure 3.7.3h). The formation of these barrages is likely the result of the mixing of highly saturated waters from the travertine and 'natural' waters flowing in the valley bottom. This is analogous to the mixing that occurs on the margins of deposits on Foel Fawr, where tufaceous facies form (marginal biological encrustations).

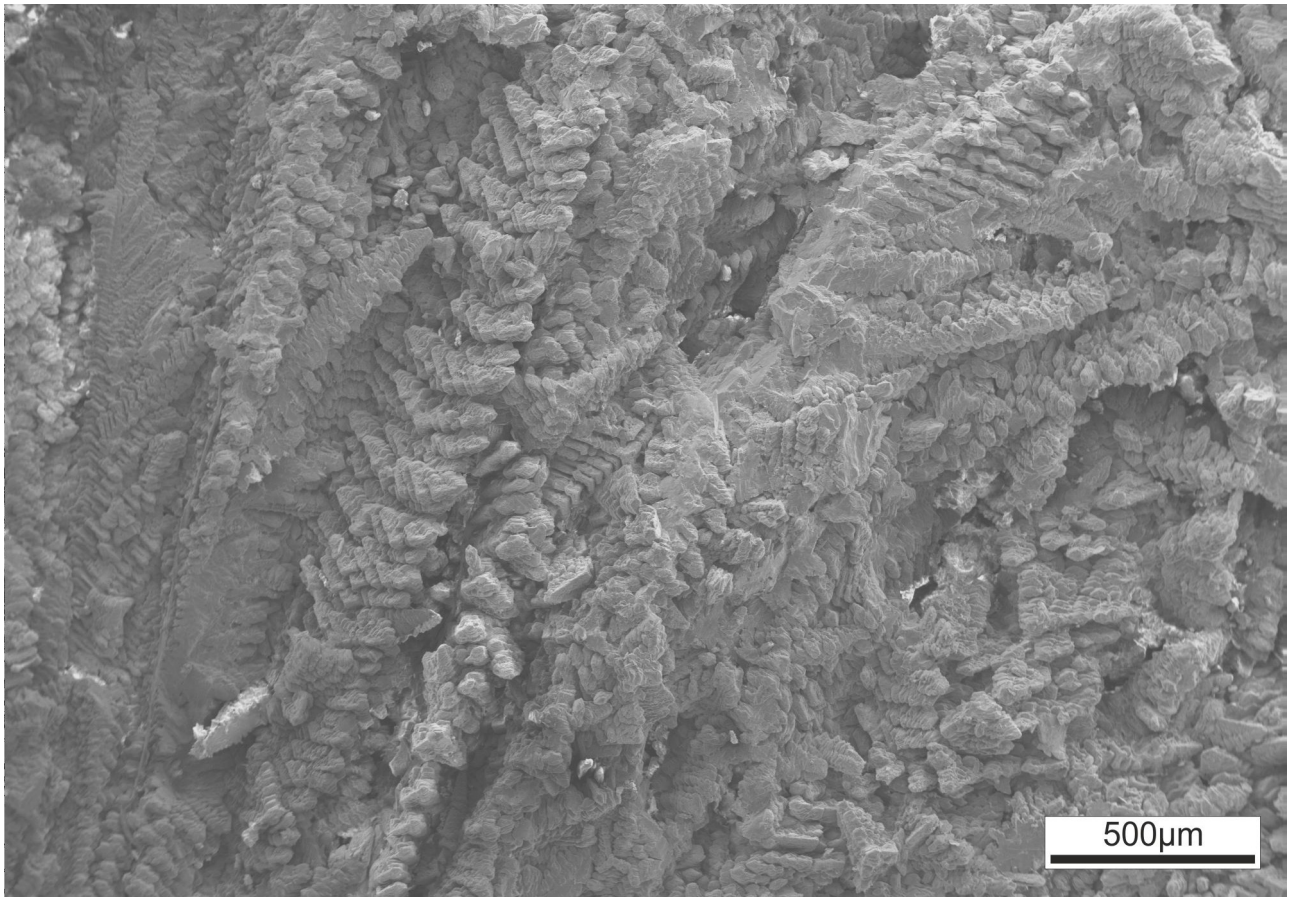

Figure 3.7.3g. Laminated crystalline crusts at Terme San Giovanni, Italy.

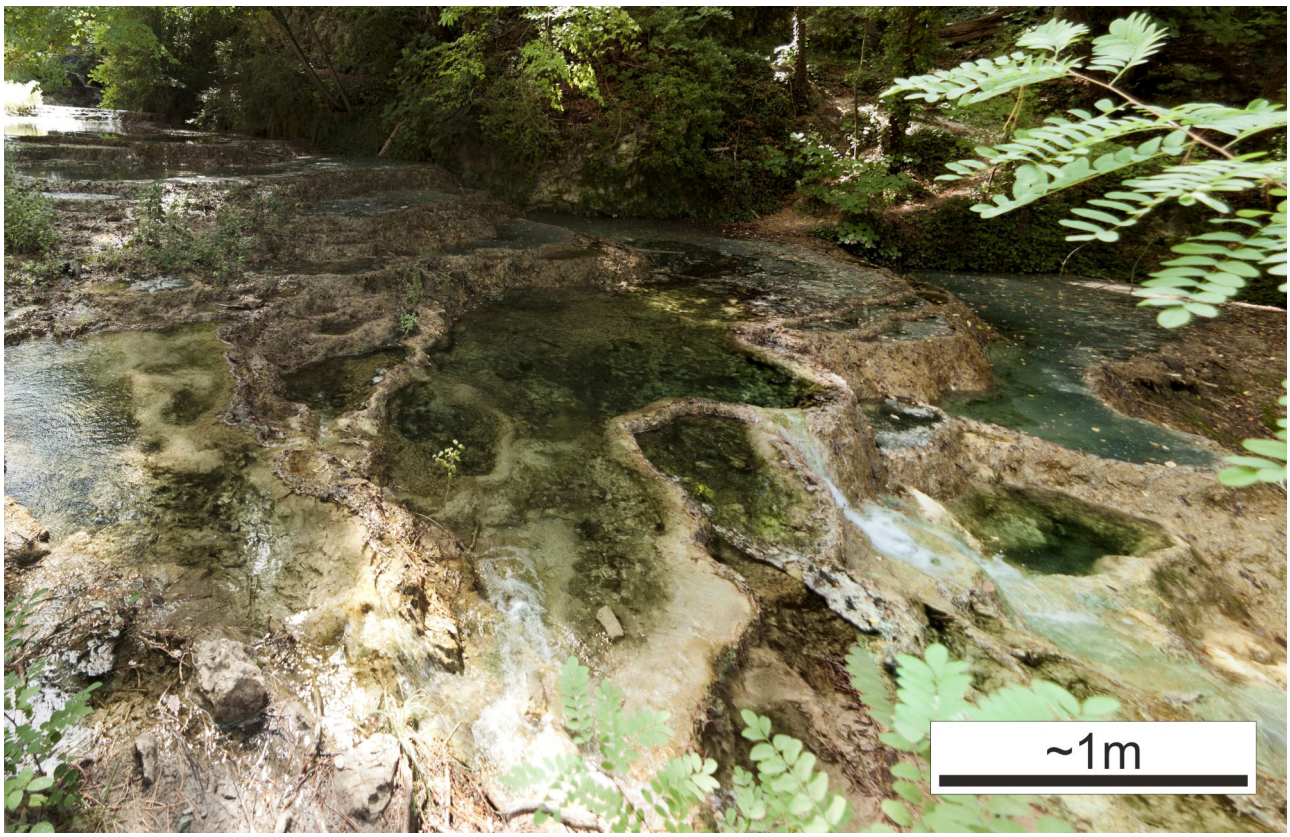

Figure 3.7.3h. Tufa barrages forming downstream of travertine deposits at Bagni San Filippo, Italy. MACB.

Chapter 4: Discussion

4.1. Introduction

The facies and associated environments observed on Foel Fawr represent an unusual and previously poorly described tufa environment. The variation of hydrochemistry and morphology, both spatially and temporally, generate a system with many parallels to hot-spring environments. The extreme pH of the environment creates pressures on organisms, restricting their growth and development. This, in turn, controls the partitioning of facies within the system.

The hydrology of the system is a crucial control on the hydrochemistry of the system. Low residence times within the porous lime spoil tips allow rapid shifts in hydrochemistry during storm events, and the alkaline baseflow limits the dissolution of the tufa deposits. Hydrology is also a crucial control on many facies' development; some associated with stormflow outwashes (carbonate mud, carbonate gravel) and others reliant upon the variable flow associated with low residence times (aprons).

The following discussion considers each aspect of the site separately, comparing and contrasting the deposits with existing deposits. The final section considers these discussions at the system scale. This synthesis of the different aspects of the site seeks to identify how the deposits on Foel Fawr (and other invasive tufas) relate to other terrestrial carbonates and suggests how they may fit into the existing classification systems.

4.2. Morphologies and fabrics

4.2.1. Factors controlling morphology

Pedley and Rogerson (2010a) suggest that the deposition and morphology of tufas, travertines and speleothems are the result of interplay between physico-chemical and biological factors. They propose a model of deposition, whereby different forcing factors (i.e. darkness, temperature, chemistry) restrict the importance of biology and increase the importance of physico-chemical controls on deposition. The deposits on Foel Fawr represent an unusual and poorly described environment, where the forcing factor (chemistry) is anthropogenic in origin.

Morphology can be influenced by biology in several ways. Both macrobiology and microbiology can create a framework for deposition; each affects fabrics and morphology on a different scale. While the effect of macrobiology on morphology is often self evident (e.g. plant moulds), the role of microbial life is more contentious. Microbes have been linked to calcite precipitation by many authors (Chafetz and Folk, 1984; Chafetz and Buczynski, 1992; Freytet and Verrecchia, 1999; Riding, 2000; Jones, 2009; Pedley et al., 2009; Rainey and Jones, 2009; Di Benedetto et al., 2011; Manzo et al., 2012). However, the question of whether their role is active or passive is still a matter of debate (Aloisi et al., 2006; Shiraishi et al., 2008a; Sanchez-Moral et al., 2012). A similar problem exists in siliceous systems, where microbes are also commonly observed in association with sinter deposits (e.g. Childs et al., 2008; Tobler et al., 2008; Tobler and Benning, 2011).

Physico-chemical factors also influence morphology, by controlling precipitation rates (see section 4.2.2) and by excluding biology. Such factors are never absolute, and vary within a system. Pentecost (2003b) highlights the complexities involved in differentiating hot springs, thermal springs, warm springs and cold springs; in reality, such classifications only apply to emergence temperatures, and complete systems occupy a region of a continuum of physico-chemical parameters. This continuum is responsible for the variability in morphology described in Pedley and Rogerson (2010a). Interestingly, morphology often transcends crystallography, forming similar morphologies in siliceous systems and also from water ice (see sections 4.2.4 and 4.2.5).

4.2.2. Growth rates

Deposition on Foel Fawr has apparently stopped in most areas (see section 3.6.2), so active growth rates are unobtainable for the majority of the system. Estimates can be made by assessing fractured areas of stream crust. Assuming that deposition began and ended with active lime burning and that no erosion has occurred, an average growth rate of around 2 mm per annum is possible. It was likely significantly higher than this when the system was at its most active. Where deposition is still actively occurring, a growth rate of around 2.3 mm per annum is measured. This measured growth rate is only a local growth rate, and does not imply anything about the growth rate elsewhere in the deposits.

High deposition rates are one distinguishing feature of travertines, which typically grow between 1 mm and 10 cm per annum (Pentecost, 2005). Some travertines may even exceed this rate; Narrow Gauge, Mammoth Hot Springs was found to grow by 30 cm in 10 months (Houseal et al., 2010). Pentecost and Coletta (2007) demonstrated that no diurnal variation in deposition occurred at La Zitelle, Italy, despite the microbial community being almost entirely phototrophic. This may suggest that all precipitation is abiotic, controlled principally by flow rate. These observations agree with modelling by Hammer et al. (2007), who found flow rate and growth rate to be positively correlated in travertine terraces. Even in sites where biotic influence is considered important for deposition, flow rate is generally accepted to be an important factor (Fouke, 2011). Flow rate within a travertine system is controlled by the discharge at the source. As a result of this, some travertines are thought to be influenced by (and, consequently, records of) hydrological and climatic factors (Dilsiz et al., 2004; Faccenna et al., 2008).

Absolute measurements of growth rates in tufa systems are difficult to relate to Foel Fawr, owing to their high porosity (and therefore low density). Despite this, the factors affecting their growth rate are still of relevance. Pedley and Rogerson (2010b) used flumes to assess the effect of flow rate on tufa precipitation and found that higher flow rates generate faster deposition. This observation is also common in natural systems (Kano et al., 2003; Chen et al, 2004; Liu et al., 2010; Vásquez-Urbez et al., 2010), although biological controls are sometimes thought to be more important (Kawai et al., 2009).

Speleothems typically have slower growth rates than travertines and tufas, normally growing around 0.002-0.9 mm per annum (Pentecost, 2005; Perrette and Jaillet, 2010). This does not

preclude faster growth rates in unusual circumstances, and rates as high as 2 cm per annum have been recorded (Hill and Forti, 1997b). As in travertine and tufa systems, drip (flow) rate is strongly linked to precipitation rate, although other factors (e.g. cave-air pCO_2 and drip water hydrochemistry) have an important influence on seasonal variations in growth rate (Banner et al., 2007).

Growth rates in siliceous sinter systems are affected by hydrology (Jones et al., 2011), although they can also be correlated with silica saturation (Mountain et al., 2003). Extrapolated growth rates of 8.4 mm per annum made by Mountain et al. (2003) are comparable to travertine growth rates. Other authors have found rates ranging from 0.2 mm/a to5 cm/a (Jones et al., 1999; Jones et al, 2001; Berelson et al., 2011), suggesting the variation in growth rates is comparable to travertine systems.

On Foel Fawr, flow rate is highly variable (see section 3.4.3). The low residence time of water in the tips results in flashy streams dominated by stormflow. As a result, precipitation is linked to storm events (see section 4.4.2).

While some systems are either entirely or primarily abiotic, there are many systems which are affected by both biotic and abiotic factors (Rainey and Jones, 2009; Fouke, 2011). Pentecost et al. (1997) actually demonstrated that microbial community distribution on active travertines is linked to flow rate, making it difficult to separate the importance of each factor to deposition. In travertines where temperature is excluding organisms, flow rate is also important as it controls the temperature distribution and thus the partitioning of facies.

It is also important to note that microbial communities vary greatly, and changes in community may be important to variation in precipitation. Bissett et al. (2008) demonstrated that biofilm communities in tufa systems are able to create a stable geochemical microenvironment. This may be crucial for promoting and regulating precipitation. Furthermore, Rogerson et al. (2010) suggest that lamination is likely the result of strong variability in either physico-chemical conditions or microbial communities.

4.2.3. Carbonate mud pools

Carbonate mud pools are characterised by their close proximity to the lime spoil, often forming around seeps. Carbonate mud lines the base of the pools, carbonate rafts are commonly seen on the surface of the pools and fragments of sunken rafts rest on the bottom.

Carbonate mud is precipitated in a variety of different low energy environments and can form in tufa, travertine and cave systems. It is typically associated with ponds and shallow lake environments in both tufas (Pedley et al., 2003; Arenas-Abad et al., 2010) and travertines (Pentecost, 2005; Jones and Renaut, 2010).

Carbonate rafts, also known as floe calcite, carbonate ice, paper-thin rafts and other similar terms, form in pools in tufas, travertines (Fouke et al., 2000; Taylor et al., 2004; Jones and Renaut, 2009) and caves (Jones, 1989; Hill and Forti, 1997a; Taylor and Chafetz, 2004). They form where gaseous exchange occurs at the air-water interface. In travertine systems, this process is often the result of degassing at the vent; in caves, it is likely the result of very stable conditions allowing growth to occur without the rafts being disturbed (Hill and Forti, 1997a).

Taylor and Chafetz (2004) found that the rafts can form in cave pools with saturation states close to equilibrium, but under these circumstances they form small equant crystals as opposed to the large prismatic crystals which form in supersaturated pools. On Foel Fawr, rafts grow radially from a central point (see figure 3.1.5d), and continue to grow until they become too large or are disturbed and sink. These observations are mirrored in cave environments (Pomar et al., 1976; Hill and Forti, 1997a). Carbonate rafts are associated with coated bubbles in travertines (Guo and Riding, 1999; Fouke et al., 2000). Bubbles are not associated with carbonate rafts on Foel Fawr, likely due to the absence of degassing in proximal pools where carbonate rafts are formed.

Plants (typically reeds and sedges) can grow in hot spring pools where temperatures are cool enough (Guo, 1993; Guo and Riding, 1998). In travertines, they are preserved as moulds of finely crystalline carbonate, and often form in clumps (Guo, 1993). *Juncus effusus* is not tolerant of extreme pH or highly calcareous soils (United States Department of Agriculture Nature Resources Conservation Service, undated), yet it is often associated with proximal carbonate mud pools on Foel Fawr. Since the hydrochemistry of the pool is relatively constant, it is likely surviving by

drawing on water from beneath the sediment, which is influenced by the surrounding acidic wetland.

4.2.4. Aprons and stream crust

Although mapped as distinct facies, aprons and stream crust facies are discussed together. They are part of a continuum of laminated crystalline fabrics, but are distinguished by differences in hydrology and geochemistry.

Aprons and stream crust facies both feature terracing at different scales (see figures 3.1.2b and 3.1.3b). Terraces are common on travertine aprons (Goldenfeld et al., 2006; Hammer et al., 2010; figure 4.2.4a). They are also found in caves, where they are known as gours, gourpools or microgours (Hill and Forti, 1997a; Hammer et al., 2005; Pentecost, 2005; Genty et al., 2011). The naming convention (i.e. terraces, teracettes and microterracettes) set out in Fouke et al. (2000) and Hammer et al. (2010) is used throughout; additionally, terrace is used as a general term for all sizes of terrace where appropriate.

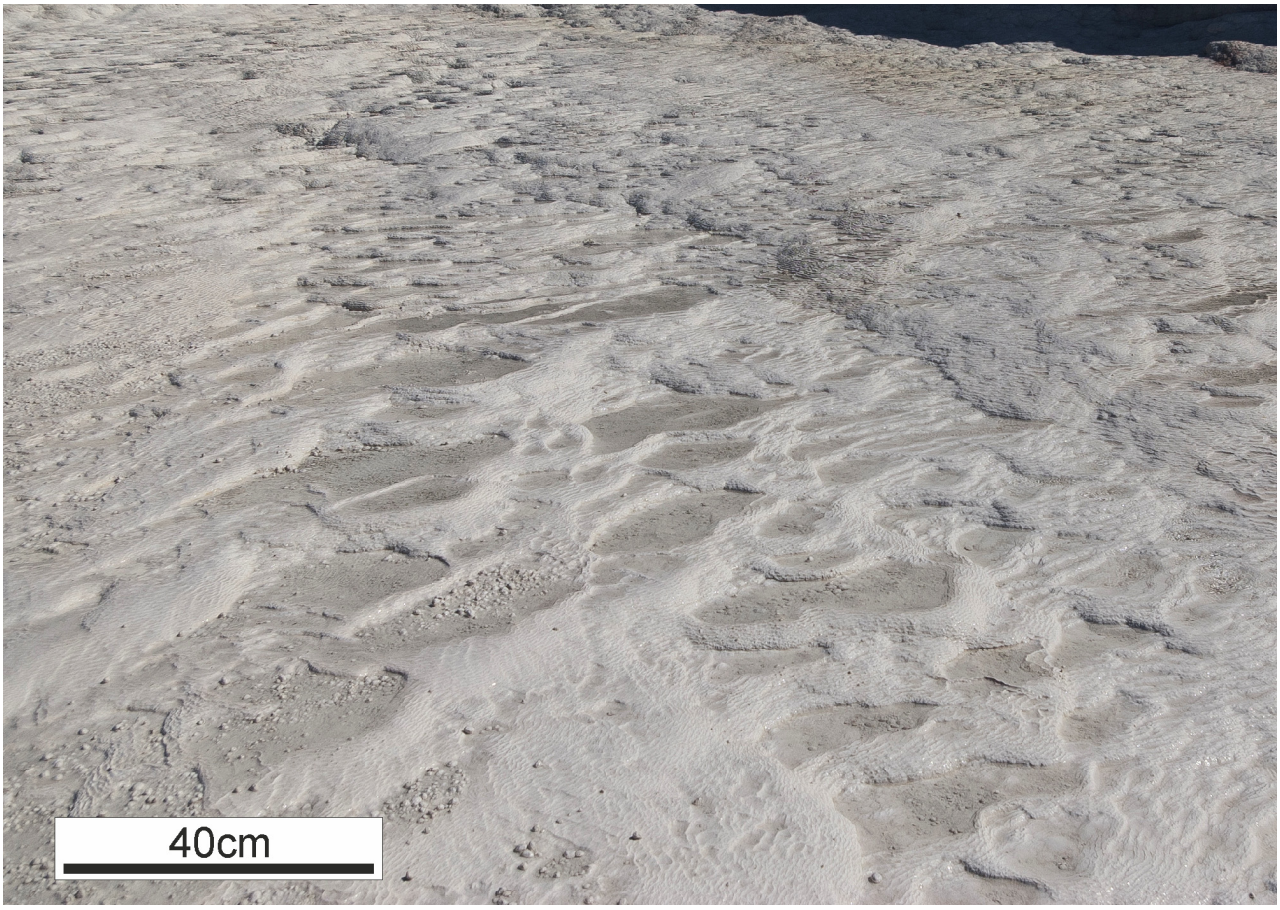

Figure 4.2.4a. Microterracettes forming on an apron surface at Pamukkale, Turkey. MACB.

Terrace patterns are scale invariant, and can be modelled without including biotic influence (Goldenfeld et al., 2006; Jettestuen et al., 2006; Hammer et al., 2007; Veysey and Goldenfeld, 2008). Fouke (2011) suggests that this means terracing may be abiotically controlled. On Foel Fawr, an inverse relationship between slope and terrace size is observed (see figure 3.1.2d). Microterracettes are restricted to proximal areas, suggesting that both chemistry and flow dynamics may also be important. Similar observations of the relationship between terrace formation and slope have been made at Pamukkale (Ekmekci et al., 1995). They also observed that the formation of microterracettes is reliant upon a discontinuous flow regime.

Stream crust forms on the base of channels carrying deeper water. These crusts typically feature bulbous botryoidal surfaces, which may form large terraces. Small microterracettes are almost entirely absent. Ekmekci et al. (1995) found that flow regime strongly affected the morphology of crystalline crusts, with continuous flow resulting in laminated stream crusts instead of terraced aprons. In caves, crystalline crusts (known as flowstone) formed in channels typically exhibit similar morphology, commonly forming at cascades (Hill and Forti, 1997a). Pedley (2000) and Gradsinski (2010) suggest that microbial colonisation is impeded in high energy environments, preventing microbial fabrics from forming. This suggests that physico-chemical precipitation may be more important at cascades in tufa and travertine systems.

Where temperatures are below 0°C in cave systems, crystalline crusts (flowstone) can form from water ice (Hill and Forti, 1997a; Ford and Williams, 2007). They are formed from freezing of infiltration water, can be perennial and can form deep in cave systems (Luetscher and Jeannin, 2004). Morphologically, the water ice crusts are similar to carbonate crusts, featuring bulbous botryoidal surfaces (personal observation, Tiergarten Höhle, Austria). Similar crusts can also form in iron crust systems, forming crystalline crusts (flowstone) where flow rates are high (figure 4.2.4b).

The branching crystal structures forming laminations in Foel Fawr aprons (see figure 3.1.2i) have previously been described as feather crystals in travertines (Folk et al. 1985; Guo and Riding, 1992; Guo and Riding, 1998; Rainey and Jones, 2009). They are generally found in extreme environments (i.e. high precipitation rates, high temperatures) and are uncommon elsewhere (Pentecost, 2005). Feather crystals are formed on sloping aprons and are friable when fresh, but form compact, hard laminae in older deposits (Guo and Riding, 1999). Chafetz and Guidry (1999) suggest that there is a

relationship between bacterial shrubs and feather crystals, with bacterial mediation more important in the former and physico-chemical precipitation more important in the latter.

Figure 4.2.4b. Iron crust formation in the Tawe Valley, South Wales (281512 212489 OSGB). MACB.

Stream crust features different fabrics (see figure 3.1.3k); however, they are still associated with travertine crystalline crusts. Guo and Riding (1998) describe thick crusts of elongated crystals growing perpendicular to the crust surface in older crystalline crusts. These large crystals are generally considered to be physico-chemically precipitated; however, both Love and Chafetz (1988) and Freytet and Verrecchia (1999) suggest that they may be formed from microbially associated recrystallized spar and micritic laminae. On Foel Fawr, equant rhombs forming transient microterracettes (see figure 3.1.3m) are not observed in older crust. It seems likely that the biofilms which colonise between these physico-chemical precipitation events may be biodegrading this surface. Hence, it appears that this combination of physico-chemical precipitation followed by biologically mediated recrystallization may be responsible for the precipitation of stream crust here.

4.2.5. Vertical aprons

On vertical faces, laminated crusts can form very different morphologies to aprons on flatter ground. Many of the morphologies are common cave formations (Hill and Forti, 1997a), but also feature on the downstream side of overhanging tufa and travertine terraces (figure 4.2.5a).

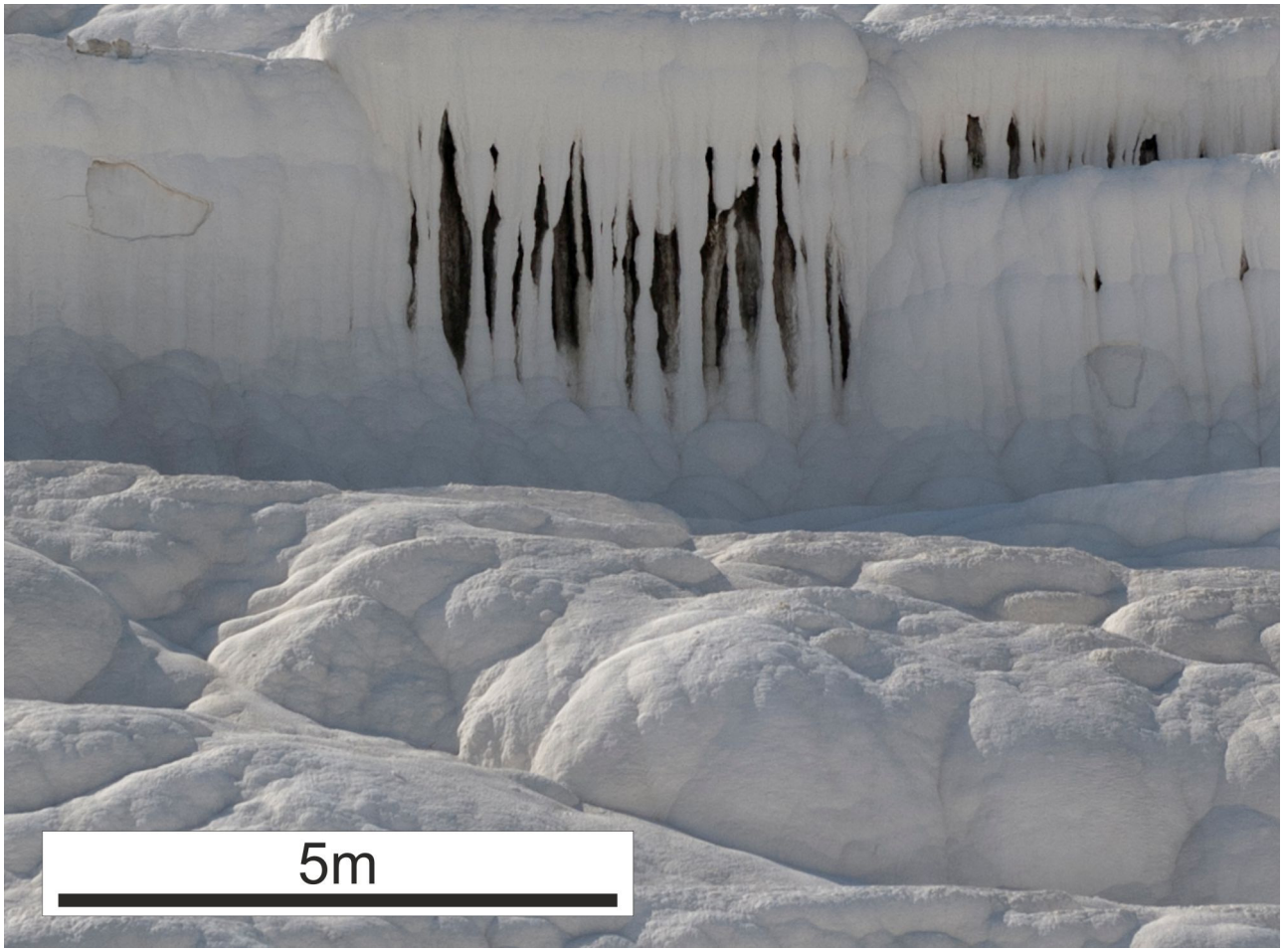

Figure 4.2.5a. Stalactitic morphologies (columns) at Pamukkale, Turkey.

At Foel Fawr, the absence (or very low relief) of microterracettes on vertical slopes is characteristic of vertical aprons. Where they do form (see figure 3.1.4c), their size is limited to a few cm. Overhanging microterracettes are observed in many other deposits (Pentecost, 2005); however, they are not present at Foel Fawr. Growth of terraces results in a steepening of the (downstream) drop wall, and on vertical faces this causes growth to be constrained by the adhesion of water to the drop wall. This is borne out by field studies, which find that slope and dam size are inversely linked (Eckmecki et al., 1995; Pentecost, 2005). This adhesion of water to the face also allows draperies to form from laminated crystalline crusts (see figure 3.1.4e). These morphologies are also observed in travertine systems (see figure 4.2.5b).

Figure 4.2.5b. Draperies forming on the underside of an overhang at Bagni San Fillipo, Tuscany, Italy.

Stalactitic morphologies (see figure 4.3.4c) are well documented in cave systems, forming where water drips from a roof (Hill and Forti, 1997a). Similar morphologies are also found on the underside of travertine terraces (Jones and Renaut, 2010) and tufa barrages (Carthew et al., 2006). Lamination resulting from alternation of fabrics is commonly observed in speleothems (Pentecost, 2005), especially where there is a strong seasonal variability in the overlying climate (Baker et al., 2008).

Where temperatures are below 0°C in cave systems, speleothems can form from water ice (Hill and Forti, 1997a). Water ice speleothems form at a much faster rate than carbonate speleothems,

growing as much as 15 cm in a week (Benedict, 1979). Despite the disparity in growth rate, morphology is often remarkably similar, forming stalactites, stalagmites and draperies (Hill and Forti, 1997a). Siliceous stalactites and draperies are also described on the underside of overhanging sinter terraces (Jones et al., 2001). This suggests that these morphologies are independent of mineralogy.

4.2.6. Pisoidal pools

Pisoids are well documented in travertine systems (Jones and Wilkinson, 1978; Folk and Chafetz, 1983; Slocek and Urbanek, 1995; Guo and Riding, 1998; Tekin et al., 2000; Tekin and Ayyildiz, 2001; Tazaki et al., 2006). In caves, they are known as cave pearls (Hill and Forti, 1997a), but are morphologically analogous (Flügel, 2004). Flügel (2004) distinguishes pisoids from other coated grains by the presence of concentric laminations, which may be physico-chemically or biochemically precipitated; they are distinct from oncoids (see section 4.2.3.), which are characterised by irregular, frequently overlapping algal or microbial laminations.

It is worth noting that problems can arise from the focus on marine environments in classification systems. Tucker and Wright (1990) suggest distinquishing pisoids from oncoids by the presence of discontinuous laminae in the cortex (with an implied biogenic origin). This is problematic where pisoids are forming in shallow pools and precipitation may not be possible on all sides, giving rise to discontinuous laminae.

Pisoid morphology can vary from spheroidal to flat disc shaped (see figures 3.1.6e and 3.1.6f). The sphericity is influenced by both the shape of the core and the rate of movement (Pentecost, 2005). Pisoids forming in pools can form shelfstone (also known as lilypads) around their edges, developing a ‘biscuit morphology’. Shelfstone is found in travertine and cave pools (Hill and Forti, 1997; Renaut et al. 1999), as well as in siliceous hot springs (Braunstein and Lowe, 2001). The formation of shelfstone is closely linked to carbonate rafts, and they are commonly associated with one another (Hill and Forti, 1997a).

On Foel Fawr pisoids have a core of granular carbonate, likely from the spoil tips or fragments of earlier formed pisoids. Flügel (2004) observes that bioclasts occasionally form the core of a pisoid; on Foel Fawr, fragments of plant encrustations form the core of some pisoids (figure 3.1.6d). These encrustations are allochthonous, either from plant fragments blown into the pools or fragments of

encrustations from elsewhere, though the mechanism for transporting these fragments to the pools is unclear.

The cortex of the pisoids varies in type and thickness (see section 3.1.6). Most laminae are of prismatic calcite, growing perpendicular to the lamina surface (figure 3.1.6g). Micritic laminae sometimes intersperse the prismatic laminae, forming a structure comparable to the alternating laminae seen in stream crust, but on a smaller scale. Similar structures are found in the cortices of pisoids in travertine deposits (Pentecost, 2005).

Spicular textures (see section 4.5.6) form on the (ephemerally) submerged portions of pisoids and on the bases of associated pools. Similar textures have been observed on pisoids forming in travertines (Chafetz and Meredith, 1983). 'Shrubs' have also been noted in siliceous hot springs (Guidry and Chafetz, 2003b), forming similar morphologies in corresponding environments.

Carbonate rafts (figure 3.1.5b) are commonly observed forming on the surface of the pools; their formation is discussed in section 4.2.3.

4.2.7. Carbonate gravel

Carbonate gravel is an unusual facies formed from clastic material (lime spoil) rather than fluvial precipitates. Similar grains have been described in travertines (Richter and Besenecker, 1983; Pentecost, 2005); however, these grains are typically formed in pools. Coated grains forming above the water level, as a result of evaporation, have been termed caliche pisoids by Flügel (2004).

The carbonate gravel on Foel Fawr is formed from coated fragments of kiln waste (figure 3.1.8d) and consequently represents a facies not present in normal tufas or travertines. Concentric precipitation around the grains is likely driven by evaporation at the grain surface. Evaporation driven by heat at hot springs has been suggested to promote precipitation (Benedetto et al., 2011; Smith et al., 2011); drying has also been shown experimentally to induce precipitation (Wedin and Berström, 2005).

4.2.8. Oncoids

Oncoids are associated with static pools of water, or may be subaerially exposed (figure 3.1.7a). This exposure is likely the result of hydrological changes and not a distinct depositional

environment. In tufa systems, oncoids are typically formed in lakes and streams with moderate flow rates (Pedley, 1990; Flügel, 2004; Pentecost, 2005).

Oncoid morphology is distinct from pisoid morphology primarily due to the irregularity of the grains. This distinction is often attributed to the presence of algae or cyanobacteria on the surface of the oncoids (Fritsch and Pantin, 1946; Flügel, 2004; Pentecost, 2005). Pentecost (2005) argues that sphericity is maintained by periodic flipping of grains, by currents in streams or by wave action in lakes. Flügel (2004), however, suggests that repetitive turning is not necessary to form oncoids. On Foel Fawr, oncoids form in small pools with no currents/waves. They are generally sub-spherical, however, their range of morphology includes more spherical grains. The absence of any clear mechanism for regular agitation, suggests the assertion by Flügel (2004) that this is unnecessary may be correct.

While oncoids represent one of the most biogenic facies on Foel Fawr, they appear to have a significant abiotic element to their precipitation (see figure 3.1.7c). In spite of differing hydrochemistry, they share many morphological and environmental similarities with oncoids in other environments. Oncoids are typically formed around a nucleus, which may be allochthonous or autochthonous in origin and may be lithological or biological (Pentecost, 2005). The shape of the nucleus can influence the shape of the oncoid (Flügel, 2004); however, nuclei can also be sufficiently small as to be insignificant. The cortex is typically formed from asymmetric discontinuous laminae, although many oncoids feature concentric lamination (Flügel, 2004). It has been suggested that the cortex of oncoids is closely related to the formation of biofilms on the oncoid surface (Davaud and Girardclos, 2001).

Oncoids have previously been described forming in a lake contaminated with waste rich in calcium chloride from soda ash production (Dean and Eggleston, 1984). While the contaminated lake has considerably elevated salinity with respect to freshwater, its pH remains circumneutral or moderately alkaline. On Foel Fawr, oncoids do not form adjacent to the tips where pH and salinity are highest, suggesting they are constrained by hydrochemistry.

4.2.9. Fossil tufa channels

Fossil Tufa Channels are an unusual facies, rarely described in tufa and travertine systems. On Foel Fawr, they form discontinuous linear features with elevated relief (see figure 3.1.11a), which appear

to have previously been drainage channels. Similar features have been described at Pammukale (figure 4.2.9a), where they have formed both at natural drainage channels and around man-made irrigation channels (Özkul et al., 2002), likely related to the Greco-Roman spa at Hierapolis. Marginal accretion of the channels leads to growth in a manner comparable to levee development on river banks. Channels can also grow upwards, forming walls up to 10 m high (Altunel and Hancock, 1993). The channels on Foel Fawr are far smaller than this, but the length of time for which they were precipitating was likely to have been very short. Decay of these laminated crusts is far more advanced than in adjacent features, suggesting that their precipitation was not contemporaneous and related to surface drainage early in the history of the site rather than leachate from deeper within the tips.

Figure 4.2.9a. Raised channel forming at Hierapolis, Turkey. MACB.

4.3. Facies distribution and environmental requirements

Facies distribution is controlled by the interplay of chemical, hydrological and physical factors. Obviously these parameters can vary spatially, making classification difficult. In travertine systems, proximity to the vent/fissure is often of principal importance, although hydrological controls (e.g. flow regime, flow rate, extraneous hydrological input) and physical controls other than temperature (e.g. underlying slope) also influence facies. In fluvial tufa systems, underlying relief and biological factors may be more important.

When considered in context, the distribution of facies can provide a useful tool for understanding the parameters controlling precipitation and facies development within a system. Figure 4.3a demonstrates a simplified model of deposition for Foel Fawr and the relationships between facies. The underlying lithology is responsible for creating both the hydrological regime and the relief, which are crucial to the control of facies on Foel Fawr.

Proximally, waters emerge as both point source springs and diffuse seeps. The location and discharge of these resurgences dictates the facies association. Where waters resurge on slopes or quarry faces, aprons are precipitated (see figures 3.3.4d, e, f, h, 3.3.5a, c, e and 3.3.6a, c, f, h), often lasting for several tens of metres. Where waters emerge on level ground, carbonate mud pools and pisoidal pools are formed (see figures 3.3.4b, d and 3.3.6d, h). The former is associated with high resurgence rates, the later with small, discontinuous resurgences. Where resurgences are not evident, carbonate gravel is often found accumulated on flat ground and gentle slopes (see figures 3.3.4a, b, c, f, g, h, 3.3.5a, b, c, d and 3.3.6a, b, c, d, e, g, h, i, k). Whilst not associated with a fluvial channel, these clastic deposits are likely transported fluvially by overland flow during storm events.

Further from tips, where waters are dispersed across flat areas, carbonate mud is precipitated (see figures 3.3.4d, and 3.3.5c, d, e). Where pools form, oncoids may develop, growing submerged within the water (see figures 3.3.4b and 3.3.6d). Hydrology may later shift, leaving the pools dry. Channelization of several streams containing lime-affected waters occurs as waters travel away from the tips and onto steeper slopes. Here, stream crust is precipitated (see figure 3.3.7). The downstream extent of the deposits is often abrupt, owing to the higher flow rates easily entraining and transporting any loose precipitates.

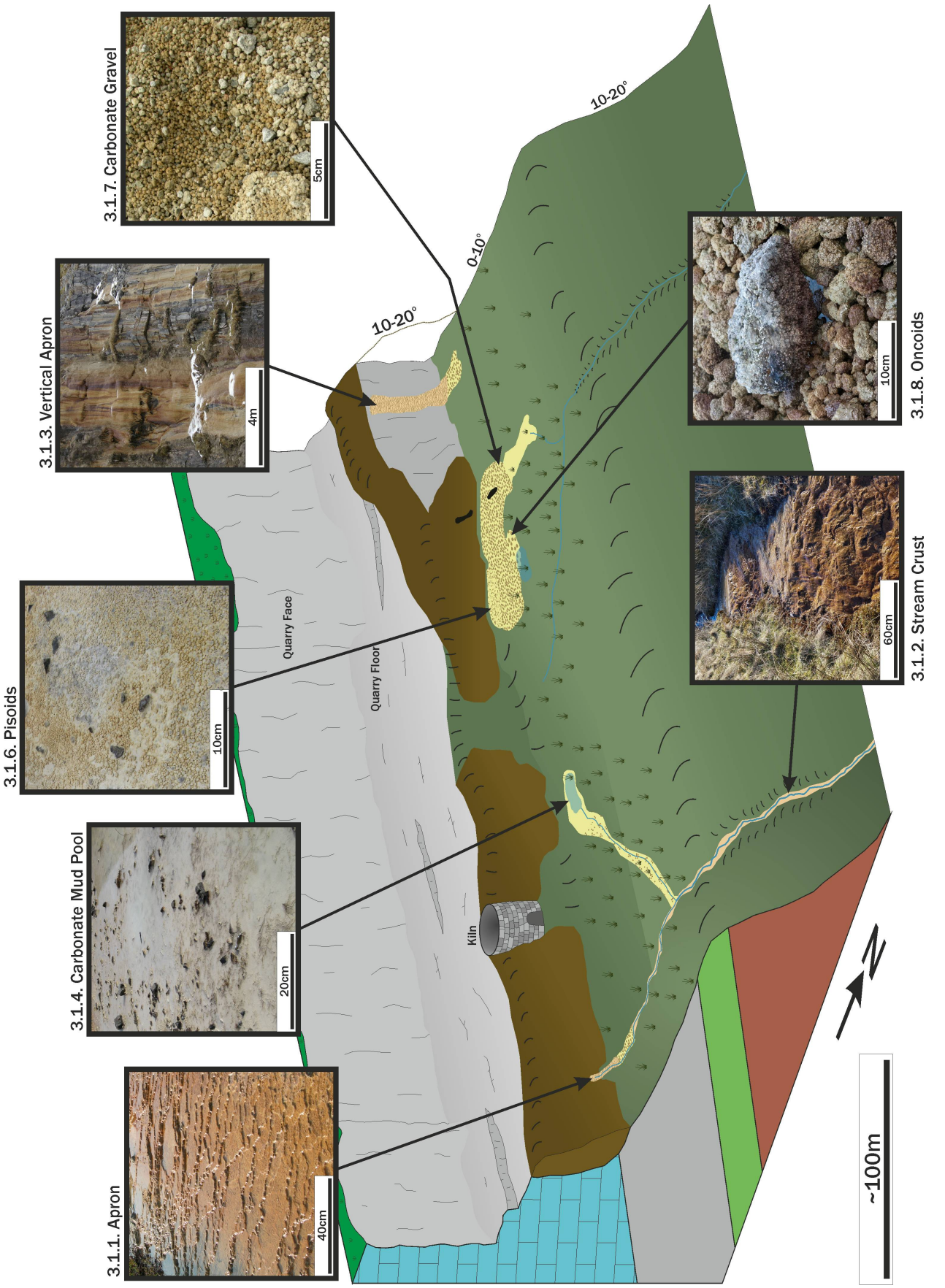

Figure 4.3a. Depositional Model for Foel Fawr. Key to symbols is provided in section 3.3.2. Lithology of cross section is, in ascending order: Red - sandstone, Green – quartz conglomerate, Grey – interbedded mudstones and limestones, Blue – limestone.

Proximal facies (aprons, vertical aprons, carbonate mud pools and pisoidal pools) are considered separately from distal facies (oncoids, stream crust and carbonate mud) and unusual facies (carbonate gravel, fossil tufa channels).

4.3.1. Proximal facies

Foel Fawr features similar proximal facies to those found in proximal hot spring environments. A summary of the interpreted environmental requirements of proximal facies is given in table 4.3.1a at the end of this section.

Aprons with microterracettes form proximally at many hot springs (e.g. Pamukkale, Turkey; see figure 4.2.4a). The 'shrubby' laminae from which they are formed can also be associated with hot-spring environments. Chafetz and Guidry (2003) note that shrubs may form in water from 35^{o}C to 70^{o}C at Mammoth Hot Springs, suggesting temperature is not an important control. The crystal fabrics which form these fabrics vary, and have been attributed to microbial processes (Chafetz and Folk, 1984; Guo and Riding, 1994). Chafetz and Guidry (1999) recognise a continuum of shrub textures, dependant on the importance of microbially-mediated and inorganically-mediated precipitation.

Bargar (1978) provides an overview of the facies found at Mammoth Hot Springs. Small springs at Bath Lake, Painted Pool, Sulfur Spring, Soda Spring and Poison Spring form carbonate precipitating pools, and there are many other smaller pools in the Highland Terrace area. Cones are noted at many point sources; this morphology is not found on Foel Fawr, although the porous peat bogs surrounding such point sources would preclude the build up of sufficient artesian pressure for such morphologies to form.

Carbonate mud pools forming on Foel Fawr are comparable with pools forming at point source vents on the top of fissure ridge travertines. Guo and Riding (1999) describe ephemeral pools forming at San Giovanni, which feature carbonate rafts forming at the surface and coated bubbles. Coated bubbles have been described in both tufa and travertine (Schreiber et al., 1981; Chafetz and Folk, 1984; Guo and Riding, 1998), and may be formed either by microbial activity or (at hot springs) rapid degassing (Jones and Renaut, 2009). Coated bubbles are not found in proximal pools forming on Foel Fawr, likely because there is no degassing occurring and microbial activity is too low. The other features of such pools (carbonate rafts and carbonate mud) are present, however, and

their proximal situation is analogous to travertine pools. In siliceous hot-spring systems, sediment filled pools also form around vents. In Yellowstone National Park, pools of 8-10m in diameter may form; however, precipitation rates are generally low (Guidry and Chafetz, 2003a).

Some limited precipitation of hard crystalline crusts occurs in carbonate mud pools, restricted to vertical plant moulds and precipitation onto lithoclasts at the air-water interface. The absence of hard precipitates elsewhere in the pools, given that they are able to precipitate in this environment, is likely due to a continual degree of flocculation that persists in the pools. Nevertheless, it is clear that there is not a hydrochemical difference responsible for the different form of precipitation.

Smaller, ephemeral pools form laminated shelfstone edges and contain pisoids. These pools are typically smaller than carbonate mud pools and have lower resurgence rates. In travertine systems, pisoids are found in proximal pools, often associated with terrace systems around vents (Guo and Riding, 1998; Özkul et al., 2002). Small pisoids (<5 cm diameter) have been described from the vent pool of Arima Hot Springs, Japan; they have a higher sphericity than typical pisoids, likely due to repeated agitation by eruptions (Tazaki et al., 2006).

On Foel Fawr, slope (and consequently flow rate) plays an important role in controlling facies. At springs forming on slopes, aprons develop. Obviously, fine grained precipitates (i.e. carbonate mud) cannot accumulate where flow rate is high, meaning precipitation is limited to crystalline crusts.

	Water depth		Discharge		Flow rate		Slope	
Facies	<2cm	>2cm	Low	High	Low	High	<5°	>5°
Carbonate Mud Pool		×	×	×	×		×	
Pisoidal Pool	×		×		×		×	
Apron/Vertical Apron	×		×	×		×		×

Table 4.3.1a. Proximal facies inferred environmental parameters. Comparative categories are only relevant to facies contained within this table and are not comparable with distal facies (Table 4.3.2a.)

4.3.2. Distal facies

Distal facies share similarities with both tufa and travertine facies. Each facies is associated with self-evidently different environments: stream crust forms in channels, where water is deeper and flows year-round; carbonate mud is precipitated in stormflow channels and oncoids form in pools.

Stream crust forms where channelling occurs and resembles crystalline crusts in travertines. At San Giovanni, Italy, such crusts have formed in a distal channel due to the increased slope (and consequently higher flow rate) inducing precipitation (Guo and Riding, 1999). Stream crust is sometimes associated with an increase in slope on Foel Fawr; however, this is not exclusively true. It is also associated with an artificial drainage channel (where rapid precipitation of stream crust regularly blocks the channel) and with natural channelization on relatively gentle slopes.

In artificial channels in Pontecagnano, southern Italy, laminated tufa crusts have been described; however, the crusts differ from those on Foel Fawr, forming from stromatolitic laminae (Anazlone et al., 2007). In cave systems, flowstone forming underwater is termed subaqueous flowstone and does not feature the microterracettes which are found on subaerial flowstone (Hill and Forti, 1997a; personal observation). These crusts form from laminated (equant to prismatic) crystals and may be associated with cascades (Hill and Forti, 1997a), similar to the crusts found on Foel Fawr.

On Foel Fawr, channelization does not occur proximally due to the gentle relief and diffuse nature of resurgences. Stream crust, however, does appear to be inextricably tied to channelized areas, rather than distance from source. This fits with observations of proximal crystalline crusts in some travertine systems, which are often associated with channelization (Fouke et al., 2000).

Laminated stream crust has been described in siliceous systems, associated with shrubby laminae and occasionally detrital material (Guidry and Chafetz, 2003a). Although these laminated crusts are formed from different minerals and feature different microfabrics, they are morphologically similar and are also found proximally to vent pools.

The formation of laminated crusts from a variety of laminated fabrics suggests that macro-morphology is independent from the process of precipitation and likely controlled primarily by hydrological factors. Both channelization and increase in slope may generate stream crust on Foel

Fawr. Consequently, there is a distinction between aprons with microterracettes precipitating from very shallow films of water and channelized, deeper flow creating stream crust.

Oncoids are more typically associated with tufas than with travertines (Pentecost, 2005). On Foel Fawr, they are limited to small distal pools with no appreciable flow. Subaerial oncoids are not likely to be actively accreting, but rather the result of post-depositional exposure, caused by hydrological change. Lacustrine tufas commonly feature oncoids (Davaud and Girardclos, 2001; Flügel, 2004; Pentecost, 2005); however, oncoids are also associated with pools in streams (Fritsch and Pantin, 1946; Carthew et al., 2006). In both cases, they form in low energy environments. This is also true on Foel Fawr, where oncoids are only observed in stagnant pools.

Oncoids have been described in travertine systems. Chafetz and Guidry (2003) describe a fossil lacustrine system featuring oncoids, associated with ostracod fossils and likely precipitating from waters far cooler than those associated with proximal vents. Similar observations may be made in active systems, where pisoids are the more typical coated grain found proximally (Jones and Renaut, 1994; Tazaki et al., 2006), while oncoids form distally where waters are cooler (Rainey and Jones, 2009).

Barite oncoids have been described by Bonny and Jones (2008), who suggest they formed in weakly supersaturated ephemeral pools. The slower precipitation rate in these pools may allow biofilms to form on the surface of the oncoids (Pentecost, 2005; Bonny and Jones, 2008).

Carbonate mud on Foel Fawr forms in distal stormflow channels flowing away from the main site. These environments are relatively high energy during stormflow (when water may be flowing over the surface), but require low energy in order for deposition to occur. In travertine systems, carbonate mud precipitates on distal slopes, where flow is diffuse and consequently slow. At Terme San Giovanni, lateral flats forming next to the fissure ridge are associated with organic-rich fine-grained travertine deposition (Guo and Riding, 1999). It is suggested that organic colonisation of these facies is possible due to dilution by rainwater (Guo and Riding, 1999), and consequently cooler temperatures. Similarly, on Foel Fawr the colonisation of these environments by plants might be reliant on rainwater input and mixing with water from the surrounding peat bog. In tufa systems, fine grained carbonates are also associated with low energy, slow-flow conditions (Vasquez-Urbez et al., 2010).

	Water depth		Flow rate		Slope		Sub-mersion	
Facies	<2cm	>2cm	Low	High	Low	High	Continuous	Discontinuous
Stream Crust	×	×		×		×	×	×
Oncoids		×	×		×		×	
Carbonate Mud	×			×	×	×		×

Table 4.3.2a. Distal facies inferred environmental parameters. Comparative categories are only relevant to facies contained within this table and are not comparable with proximal facies (Table 4.3.1a).

4.3.3. Carbonate gravel and fossil tufa channels

Carbonate gravel is a proximal facies on Foel Fawr; however, it is not found in travertine or tufa systems. Distribution is controlled by hydrology and the associated washout beneath kiln waste. Carbonate gravel is never associated with pools or streamways, and it is suggested that stormflow washout from the tips is responsible. The resulting accumulations are preserved only where slope gradients are sufficiently low.

Fossil tufa channels are another unusual facies, restricted to proximal areas but not commonly found in travertine or tufa systems. At Pamukkale, channels are often associated with channelling of water (Özkul et al., 2002); conversely, on Foel Fawr comparable channels appear to delineate natural drainage routes from the spoil tips. They are constrained laterally, forming only narrow linear features, likely due to the self-channelling effect observed at Pamukkale (Altunel and Hancock, 1993). They are now almost entirely decayed, with only small patches remaining. The increased frequency of such fragments at the eastern end of the deposits suggests that they represent rapidly decaying deposits formed during active lime production.

4.3.4. Facies partitioning

The partitioning of facies, both on Foel Fawr and in travertine systems, is inextricably linked to the nature of the water source. The extreme hydrochemistry on Foel Fawr precludes the colonisation of plants in a manner analogous to the extreme temperature and/or chemistry in hot spring systems (see table 4.3.4a).

At Angel Terrace, Mammoth Hot Springs facies vary with temperature. Aprons and terrace pools are found close to the vent, where temperatures are up to 60°C; further away from the vent, where temperatures are lower, laminated stream crusts containing encrusted plants form (Fouke et al., 2000). Veysey et al. (2008) go further, demonstrating a facies partitioning against temperature and pH. An analogous partitioning is seen on Foel Fawr, and a comparison of similar facies is given in table 4.3.4a.

	Facies Temperature (°C) / pH	
Facies	Foel Fawr[1]	Angel Terrace[2]
Vent/Carbonate Mud Pool	Ambient/10.68-12.33	69.6/6.29
Apron Channel/Apron	Ambient/12.06-12.12	64.1/6.62
Distal Slope/Stream Crust	Ambient/8.79-9.02	34.1/8.14

[1]Average: April 29th 2009-April 19th 2010. [2] Values from 2005, Veysey et al. (2008).

Table 4.3.4a. Comparison of facies environmental parameters for Foel Fawr and Angel Terrace.

Andrews and Riding (2001) contest the assertion in Fouke et al. (2000) that only distal facies have an active biological element to their precipitation. Fouke (2001), however, argues that the extreme temperatures (~70°C), combined with a good correlation with Rayleigh-type fractionation modelled from Usdowski et al. (1979) and Michaelis et al. (1985), suggest that microbial activity is not important for precipitation near the vent. Fouke et al. (2000) conclude that rapid degassing (and the resulting carbonate deposition) prevents microbial influence on precipitation. Given that this is the case, it seems likely that rapid ingassing (and the resulting deposition) on Foel Fawr would also preclude microbial influence on precipitation.

Microbial ecology and distribution may also be strongly affected by the physico-chemical properties of a hot spring system (Fouke et al., 2003; Tobler and Benning, 2011). On Foel Fawr, there are microbial communities in carbonate mud pools (figure 3.5.2c and d) and biofilms are observed elsewhere (figure 3.1.3c). The assertion that the presence of these communities must therefore be the cause of precipitation risks the possibility of a third cause fallacy (figure 4.3.4b). It has been demonstrated that abiotic precipitation is possible in hydroxide systems (Pedley et al., 2009), though clearly this does not preclude biology having any influence on morphology and facies development.

The uniform darkness in cave systems results in a uniform exclusion of biota, yet partitioning of facies still occurs. Variable hydrology is the likely facies control; however, microbial or

geochemical variation cannot be ruled out. Microbial communities have been documented in caves and on speleothems (Groth et al., 2001; Jones, 2001; Cuezva et al., 2009; Legatzki et al., 2011), although their presence does not necessarily indicate an active role in precipitation.

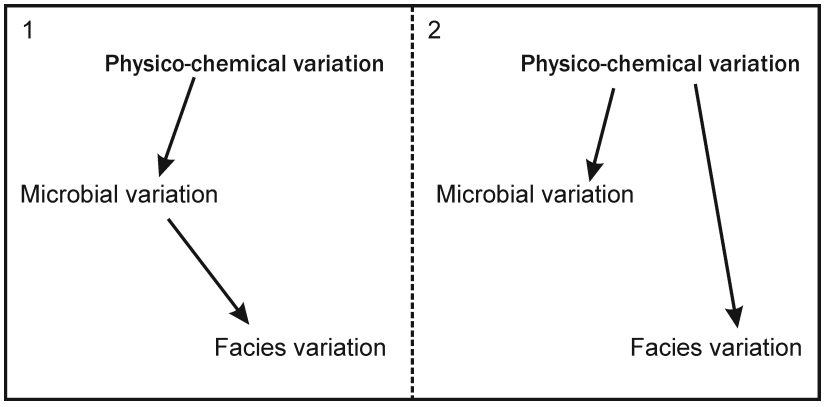

Figure 4.3.4b. The observation of covariance of microbial communities and facies allows the possibility of a third cause fallacy being made, whereby facies variation is mistakenly identified as being caused by microbial variation (1), while the reality may in fact be that both observed variables are controlled by physico-chemical variation (2).

Hydrology is thought to play an important role in controlling the morphology of many speleothems. Variation in crystalline crust morphology (see section 4.3.2) has clear links to travertine systems; however, there are other speleothems which offer insight into the influence of hydrology on morphology. Helictites (see figure 4.3.4c) are an irregular counterpart to 'soda straw' stalactites, and have been linked to seeping water as opposed to the dripping or flowing water associated with stalactites (Hill and Forti, 1997). The term helictite is used to refer to a variety of speleothems; Self and Hill (2003) observe that in one common form of helictite there is competition for precipitation at the growth tip, generating irregular growth and, consequently, sudden changes in growth direction. This process is surely analogous to the slow, discontinuous flow required to form microterracettes on aprons (see section 4.2.4), resulting in irregular precipitation.

The distinction between hot spring travertines and ambient temperature tufa systems is ill-defined (discussed in section 4.2.1). As hot spring travertine source waters cool, commonly an intergrading of morphologies is observed (Pentecost and Zhang, 2001). This change obviously occurs downstream, although it may also be seen in marginal areas (Guo and Riding, 1999). Downstream and marginal morphological change is observed on Foel Fawr, with plant moulds and other biotically influenced fabrics becoming more common. On aprons, a variation occurs across the surface, with endolithic colonisation restricted to areas of slow, diffuse flow (figure 3.1.2h).

Figure 4.3.4c. The Courtesan, Agen Allwedd, South Wales. A helictite forming from the roof with a stalagmite forming beneath. Note the absence of helictitic morphology on the stalagmite, resulting from the high energy environment where water lands. MACB. ©John Stevens, Chelsea Spelaeological Society, 2006.

4.3.5. Invasive tufa systems

While it has been demonstrated that there is a strong link between biology (specifically biofilms) and precipitation in 'normal' tufas, the extreme physico-chemical environment on Foel Fawr is able to generate rapid physico-chemical precipitation, preventing the need for biology. Pedley et al. (2009) observed that precipitation in hydroxide systems can easily occur, regardless of the presence of a biofilm. In spite of this, the facies controls in hydroxide systems may be considered comparable to those in travertine (and tufa) systems. The exclusion of macrophytes precludes their influence on morphology; consequently, morphological variability is predominantly the result of physico-chemical factors.

Source waters comparable in chemistry to Foel Fawr are described from several invasive tufas associated with serpentinized rocks in California (e.g. Adobe Canyon, Cazadero [Barnes and O'Neil, 1971]). These include travertine aprons and vertical aprons as high as 12 m. Whilst shallow (<1 cm), flowing $Ca(OH)_2$ springs form hard, laminated aprons, deeper quiescent pools are associated with carbonate sludge. As at Foel Fawr, this variability of macro-morphology is predominantly dependent on physico-chemical variability, and is also analogous to variation in hot spring systems and caves. While this variability is apparently independent of biology, the impact of biological factors on microfabrics is poorly described in hydroxide systems.

Blank et al. (2009) describe some biologically influenced deposits forming in creeks near Adobe Springs, CA. Microbial mats were found associated with laminated cements, massive cements and dentate calcite crystals. The pH in this system (~9) is lower than either Foel Fawr (~11) or the systems described by Barnes and O'Neill (1971). On Foel Fawr, pH drops through the length of the system; however, the isotopic signature of calcite precipitated remains indicative of precipitation from hydroxide waters (Andrews et al., 2007). This may be either the result of stormflow related precipitation (see section 4.4.2) or the result of precipitation when the system was younger. This uncertainty makes it difficult to link facies to environmental conditions on Foel Fawr.

4.4. Hydrochemical impacts on precipitation and biology

4.4.1. Alkaline buffering systems

Carbonate-bicarbonate (CO_3^{2-}-HCO_3^-) buffering systems are the predominant natural buffering systems in karstic waters. The baseflow at Foel Fawr is predominantly flowing from limestone aquifers, and as such shares many of the geochemical characteristics of natural karstic springs.

A cave, Ogof Pasg, allows access to the aquifer. Emery (2008) analysed the water inside Ogof Pasg, and calculated 0.7 millimolars CO_3^{2-} and 1.3 millimolars HCO_3^-. This is slightly higher than the value of 1.17 millimolars HCO_3^- (0.00 millimolars CO_3^{2-}) measured in the nearest natural waterway to Foel Fawr, the Afon Clydach (see figure 3.3.2). This is typical of the relationship between surface and groundwater chemistry (Langmuir, 1997). Both of these values are low compared with typical concentrations of HCO_3^- in tufa and travertine systems (3-5 $mmol.L^{-1}$ [tufa] and 10-20 $mmol.L^{-1}$ [travertine]) summarised by Pentecost (2005, pp.88). Other buffers are low in concentration and are of minor importance (Emery, 2008).

In the area surrounding Foel Fawr, there is no tufa precipitating in streams unaffected by lime burning; however, there are speleothems (stalactites, stalagmites and flowstone) precipitated in Ogof Pasg (personal observation). Natural precipitation may be constrained by climatic factors; the altitude of the site keeps temperatures relatively low, which may prevent precipitation due to reduced degassing and biological activity (Ford, 1989).

Although no precipitation occurs in 'natural streams' near Foel Fawr, the groundwater geochemistry still plays an important role in the hydrochemistry in the other streams. Outgassing of CO_2 is typically attributed as the cause of precipitation in natural tufa systems (Usdowski et al., 1979; Herman and Lorah, 1987; Dreybrodt et al., 1992; Merz-Preiß and Riding, 1999; Lu et al., 2000; Che et al., 2004). Some authors favour a (partially or exclusively) biological removal of CO_2 by photosynthesis (Arenas et al., 2007; Rogerson et al., 2008; Vásquez-Urbez et al., 2009); however, the end result is the same (i.e. removal of CO_2). This process does not occur on Foel Fawr (Andrews et al., 1997), meaning the mechanism for any precipitation of CO_3^{2-}-HCO_3^- must be different. Any dissolved CO_2 (and CO_3^{2-}-HCO_3^-) in groundwater passing through tips is inevitably precipitated by the same mechanism as emergent waters (see equations 7 and 8 below).

The pH of natural CO_3^{2-}-HCO_3^- buffered tufa systems is generally circumneutral or moderately alkaline (Pentecost, 2005). CO_3^{2-}-HCO_3^- concentrations and pH are inextricably linked by the balance of equation 6:

$$CO_2 + H_2O \longleftrightarrow H_2CO_3 \longleftrightarrow H^+ + HCO_3^- \longleftrightarrow 2H^+ + CO_3^{2-}$$

[Equation 6]

HCO_3^- is the dominant buffer between pH 6.35 and pH 10.33 (Langmuir, 1997), and is therefore dominant in most tufa and travertine systems. $CO_{2(aq)}$ tends to equilibrate with the $CO_{2(g)}$ in the surrounding environment, resulting in an increase in $[H^+]$ of the solution. Consequently, pH is reduced when atmospheric pCO_2 is high.

OH^- buffered systems are typically formed by anthropogenic influence (Langmuir, 1997); however, natural waters issuing from serpentinized and ultramafic rocks can also produce similar systems (Barnes et al., 1967; Neal and Stanger, 1983; Flinn and Pentecost, 1995; Marques et al., 2008; Blank et al., 2009).

The CO_3^{2-}-HCO_3^- created through this process then reacts with dissolved $Ca(OH)_2$, causing precipitation of $CaCO_3$:

$$Ca(OH)_2 + 2H^+ + CO_3^{2-} \longrightarrow CaCO_3 + 2H_2O$$

[Equation 7]

$$Ca(OH)_2 + H^+ + HCO_3^- \longrightarrow CaCO_3 + 2H_2O$$

[Equation 8]

Lime spoil tips are a quasi-sealed system, inside which pH remains high. Internal precipitation of $CaCO_3$ (by the mechanism set out in equations 7 and 8) neutralises the natural acidity of infiltrated rain, which comes predominantly from carbonic acid (Langmuir, 1997). $CO_{2(g)}$ within the tips is also consumed, and atmospheric recharge is likely impeded by internal cementation of the tips. $Ca(OH)_2$ does not become stable until pCO_2 is less than $\sim 10^{-13}$ bar at 25°C (Langmuir, 1997); however, even in less depleted environments transition to the stable phase (calcite) will be retarded. The resulting leachate therefore contains no CO_3^{2-}-HCO_3^-, and as such streams unaffected by other water bodies contain an entirely atmospheric CO_3^{2-} origin.

A comparison between the principal alkalinities (of emergent waters) from invasive tufa systems, natural tufas and speleothems is shown in figure 4.4.1a. Some invasive waters develop CO_3^{2-}-HCO_3^- alkalinity before all OH^- is consumed. This must be due either to incomplete precipitation within the aquifer, or the rate of ingassing exceeding the rate of precipitation. Most waters, however, do not, and precipitation is therefore likely limited by the rate of CO_2 ingassing for most waters.

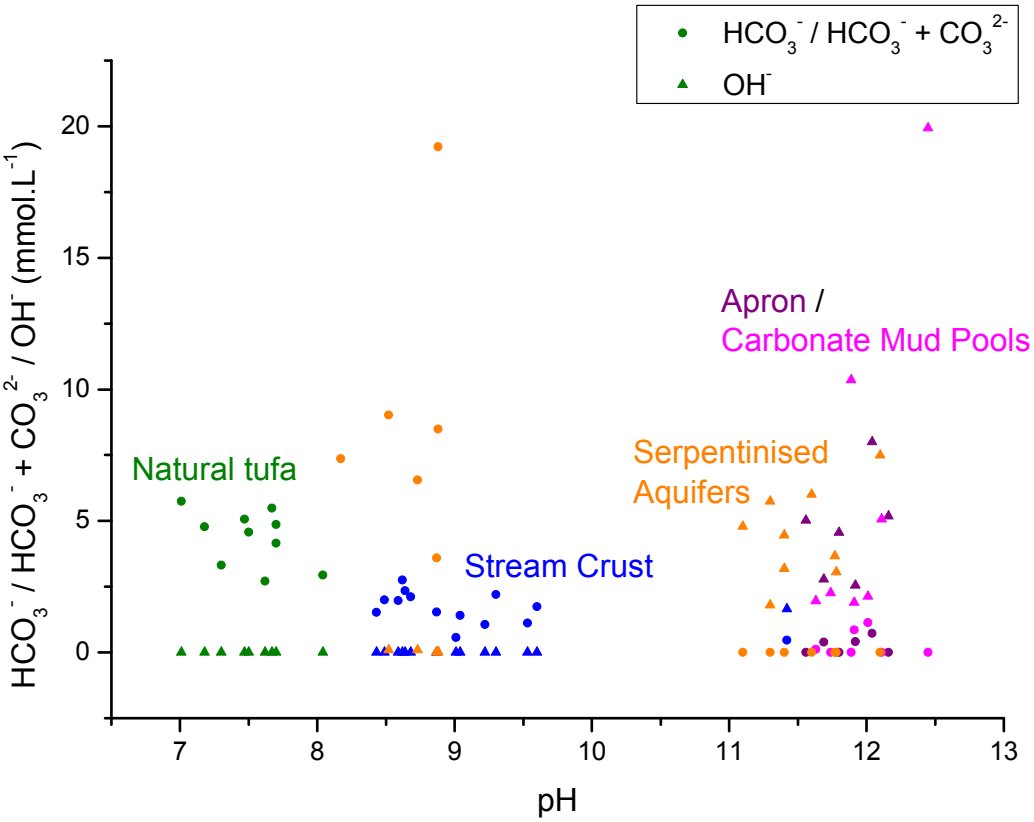

Figure 4.4.1a. Graph showing the hydrochemistry of proximal (apron and carbonate mud pool) facies on Foel Fawr, compared with distal (stream crust) facies, invasive tufa systems as reported by Barnes and O'Neil (1971) and Blank et al. (2009) and natural tufa systems as summarised by Pentecost (2005). Note the transition from emergent waters (very high pH, OH-rich waters) to distal waters (high pH, OH-poor, CO_3^{2-}-HCO_3^- containing waters). Also note the lower levels of CO_3^{2-}-HCO_3^- on Foel Fawr compared to serpentinized systems.

In much smaller lime-tip systems (e.g. Aberthaw Lime Kilns, South Wales; Clydach Limeworkings, South Wales), $Ca(OH)_2$ dissolved in pore water is consumed by CO_3^{2-}-HCO_3^- dissolved in infiltration water and therefore leachate does not contain OH^- and does not generate precipitation outside of the tips (see section 3.7.2). The volume of lime spoil on Foel Fawr is essential to producing leachate of correct composition and sufficient volume to generate precipitates. The karstic origin of baseflow on Foel Fawr may also important, although quantifying its effect on chemistry is difficult. Irrespective of this, actively precipitating waters contain no CO_3^{2-} or HCO_3^- on emergence, therefore any input of CO_3^{2-} from baseflow must be precipitated within the tips. In these environments, it is therefore assumed that all CO_3^{2-} comes from ingassing of $CO_{2(atm)}$.

Away from proximal environments on Foel Fawr, convergence of streams containing CO_3^{2-}-HCO_3^- occurs. In these environments, precipitation is not limited by CO_2 diffusion, and any remaining OH^- within the water is rapidly consumed. This is borne out by observations that precipitation ceases downstream of such confluences (section 3.3.3).

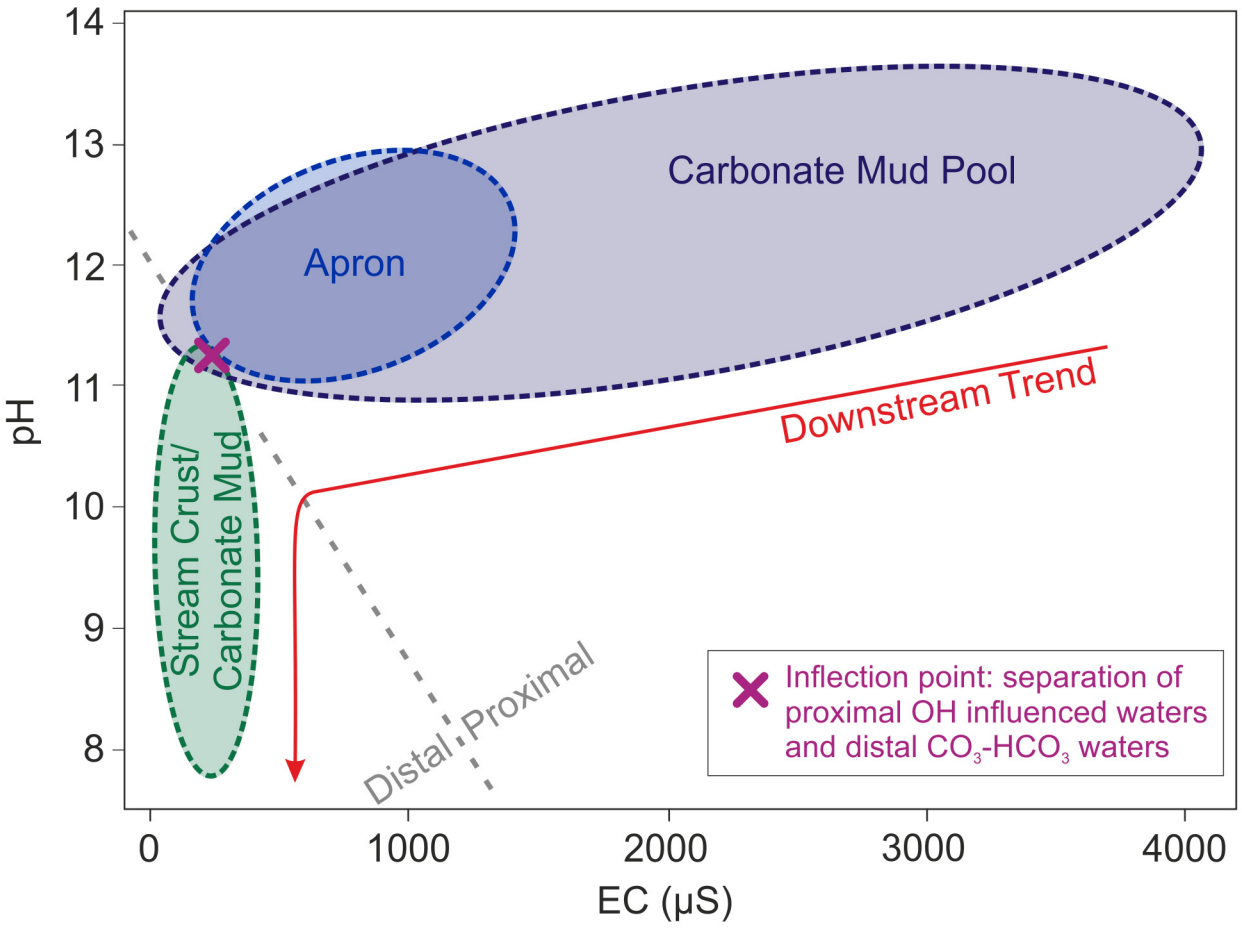

Figure 4.4.1b Overview of downstream changes in hydrochemistry on Foel Fawr.

Figure 4.4.1b represents a summary of the hydrochemical data presented in section 3.4.1. The general downstream trend observed in the hydrochemistry on Foel Fawr represents a transition from proximal OH influenced waters to distal CO_3-HCO_3 influenced waters.

The relationship between EC and electrolyte concentration is complex and changes result not just from removal and addition of electrolytes (i.e. OH^-, CO_3^{2-}, HCO_3^-), but also as a result of change of electrolyte. Since precipitation on Foel Fawr is the result of a change in buffers, it is difficult to separate these two causes of changing EC. The relative effect of NaOH compared to $NaHCO_3$ on EC is reported by McCleskey (2011) as being approximately double. It is assumed that the

relationship for the Ca-equivalents is comparable. Given this, it is clear that any reduction in EC as a result of change in electrolytes is minimal.

The broad trend is for a decrease in both pH and EC downstream, until all OH^- is consumed (largely by precipitation) (see section 3.4.2). At this point, EC stabilises at a few hundred $\mu S.cm^{-1}$, marking the end of precipitation. In spite of this, pH continues to drop, likely as a result of both natural stabilisation of the buffering resulting from ingassing of CO_2 and mixing with other waters.

It is important to note that the areas represented in figure 4.4.1b are derived from a time series and the values at a particular site vary temporally (as well as downstream) within the parameters of those areas. Considering the variability recorded at individual sites (see section 3.4.1), there is clearly a significant difference in the temporal variability of EC and pH in different environments. Of particular note is the differences between aprons (see figures 3.4.2j and k) and carbonate mud pools (see figures 3.4.2g, h and i); there is far greater variability in carbonate mud pools. The reason for this is likely related to the differing water depths between these two environments (see section 3.2). Since precipitation is limited by CO_2 ingassing, the elevated EC are likely the result of diffusion limited ingassing rates in this environment (a consequence of the decreased surface-to-volume ratio of the water body from which this facies is precipitated).

This apparent input of $Ca(OH)_2$ to the system at a rate in excess of the precipitation regulated by CO_2 ingassing does not, however, result in a concordant spatial expansion of precipitation. This is likely due to a sudden reduction in surface-to-volume ratio downstream ensuring any remaining $Ca(OH)_2$ is rapidly consumed by precipitation.

4.4.2. Hydrological effects on hydrochemistry

For clarity, the term rainfall is used throughout this section to refer to all kinds of atmospheric precipitation, while the term precipitation is reserved for mineral precipitation (i.e. tufa).

At the broadest scale, the geological setting of Foel Fawr is crucial for its development as a tufa depositing site. There is a great abundance of abandoned kilns in South Wales (table 3.7.2a), and yet only Foel Fawr is associated with precipitation of tufa (outside the spoil tips). An essential part of the site is doubtless the presence of a springline, which coincides with the line of tips running

along the hill (see figure 1.2.1b). This setting generates the volume of flowing water required to form the deposits, a feature that is also observed at Harpur Hill (see section 3.7.1).

Stormflow events play an important role in the dynamics of the hydrochemical system on Foel Fawr (section 3.4.3). The porosity of the spoil tips creates a very short lag time, and consequently discharge is variable. Variability of flow in tufa and travertine systems is poorly reported; however, increased discharge may generate an increase in tufa precipitation (Malusa et al., 2003; Pentecost, 2005). On Foel Fawr the relationship appears to be more complex (see figure 3.4.3b, c and d).

Discharge on Foel Fawr is inextricably linked to rainfall (see figure 3.4.3a). In tufa systems (and other karstic springs) discharge is also typically linked to rainfall (Liu et al., 2011); however, lag times are usually larger (Labat et al., 2011; Coustau et al., 2012). Lag (and more generally hydrology) of karstic aquifers is controlled principally by the lithology and can vary significantly between systems (Fetter, 1994). Aquifer residence time has an effect on the stormflow of the resurging waters, as does the antecedent water table level (Fiorillo, 2009).

Hydrothermal systems may be affected by meteoric input of water (Kharaka et al., 2000; Lowenstern et al., 2012); however, the time required for meteoric waters to circulate through the hydrothermal system is far greater than residence times in karst systems (Dilsiz et al., 2004; Pasvanoğlu and Chandrasekharam, 2011). Therefore, only long-term meteorological variations (i.e. annual or longer) are important to spring flow. Discharge variability has been noted in travertine systems (Ekmekci et al., 1995; Carr et al., 2010; Takashima et al., 2011) and may demonstrate geyser-like behaviour (Pearce et al., 2011).

At Foel Fawr there is a regional seasonal variability in rainfall (see figure 4.4.2a). This seasonal trend is from mean rainfall, however, and precipitation variability on Foel Fawr is actually related more closely to the frequency of storm events, rather than their magnitude. Consequently there is little variation in the baseflow chemistry throughout the year, any seasonal variability is the result of increased frequency of stormflow events.

There are extensive periods of groundfrost during the winter (figure 4.4.2b), which can result in freezing of surface waters on Foel Fawr (see figure 3.1.1c). These periods likely reduce

throughflow of the tips, as soil frost (and analogously frozen pore water within the tips) reduces infiltration rates (Orradottir et al., 2008).

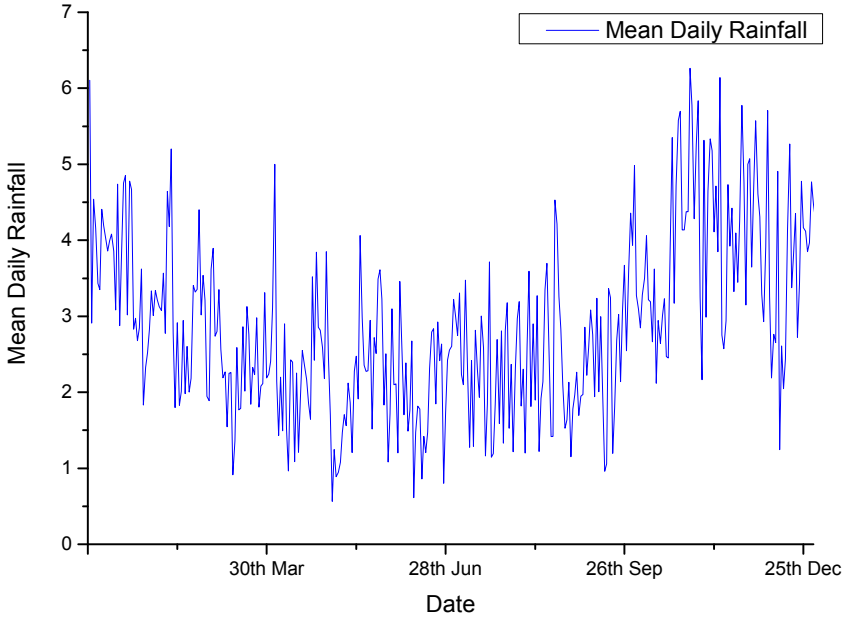

Figure 4.4.2a. Average daily rainfall for the south west United Kingdom 1990-2010. © Met Office, 2012.

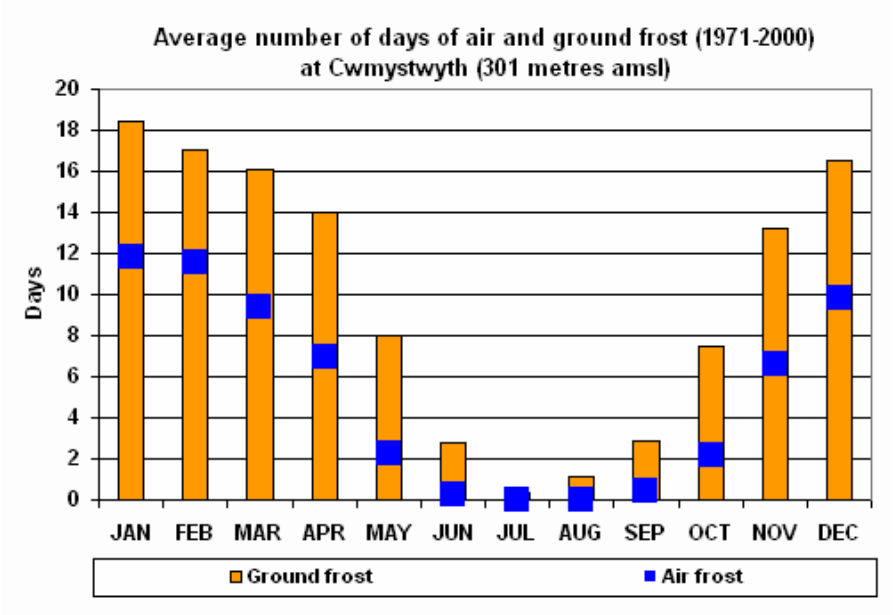

Figure 4.4.2b. Days of frost at Cwmystwyth meteorological station, Wales. This station is the closest station for which records are available however; it is around 100m below Foel Fawr, meaning the amount of frost is likely underestimated. © Met Office, 2012.

While some of the hydrochemical variability in carbonate mud pools discussed in section 4.4.1 is the result of spatial variability, much of the variability is in fact the result of temporal changes (see figures 3.4.2g, 3.4.2h and 3.4.2i). These large, rapid changes in hydrochemistry are a product of the hydrology of the system.

The surge in discharge following storm events results in variation in hydrochemistry. While proximal hydroxide alkalinity is increased, mixing with larger volume streams and runoff rich in dissolved inorganic carbon (DIC) occurs downstream. Although the DIC concentration of rainwater (0.6 - 5.5 $mg.l^{-1}$; Lee and Krothe, 2001; Górka et al., 2011) is an order of magnitude lower than the OH^- concentration on Foel Fawr following storm events (34 – 136 $mg.l^{-1}$), the disparity in volume counteracts this, allowing all OH^- to be consumed rapidly.

The relationship between rainfall and tufa precipitation is complex. While the geochemical conditions for precipitation are created by stormflow events, during long-lasting periods of stormflow tufa precipitation is low. This may be the result of preferential flow paths within the spoil tips. During repeated storm events, infiltrated water quickly flows along these paths; consequently, ion exchange with interstitial water does not occur, $Ca(OH)_2$ concentrations are reduced and precipitation is constrained to proximal localities.

It must also be considered that during the early stages of precipitation, these preferential flow paths would likely not have been as well developed. Additionally, they would not have been so depleted of $Ca(OH)_2$. Consequently, it seems likely that longer duration storm events may have been responsible for the long-reaching intermittent precipitation responsible for the generation of stream crust, extending downstream for several hundred metres (see figure 3.3.7).

4.4.3. Environmental pressures on organisms on Foel Fawr

The extreme pH in hydroxide buffered environments such as Foel Fawr causes a number of problems for organisms, and restricts or precludes the growth of some organisms. Although the current biological communities are almost certainly different from when the site was active (see section 4.7), the impact of chemistry on biological partitioning today can still help inform the facies partitioning. The stressed environment on Foel Fawr partitions biology, with an increase in the diversity of communities further from the spring/seep. This general principle of exclusion informs the distribution of facies observed on Foel Fawr (see section 4.3.)

Despite the stresses placed upon them, there are many organisms able to tolerate high pH, and all eukaryotic kingdoms are represented at pH values as high as 11 (Rothschild and Mancinelli, 2001). This does not, however, mean that all species are able to survive at such extreme pH.

Plants are affected simply by the inundation associated with aquatic and semi-aquatic habitats. Inundation can both increase and decrease plant growth rates (Lowe et al., 2010; Miao and Zou, 2012); furthermore, high sedimentation rates can either compound or reduce these effects (Lowe et al., 2010; Zhan et al., 2010; Pan et al., 2012).

The high precipitation rates can cause rapid encrustation, smothering plants. The reduction in their ability to photosynthesise (by both the blocking of light and the blocking of stomata) makes survival difficult, even in advantageous biochemical conditions. In many environments, a relationship between plant communities and sedimentation rate has been noted (Ellis et al., 2004; Holm et al., 2008; Jolley et al., 2010), likely due to the pressures placed on the plants in such conditions (Lowe et al., 2010).

On Foel Fawr, sedimentation and encrustation are combined with extreme pH, placing further stress on plants. Proximally, hydroxide consumes dissolved CO_2 (see section 4.4.1), reducing its bioavailability and making photosynthesis difficult. Strictly submerged aquatic plants are able to utilise bicarbonate when pCO_2 is low (Demars and Trémolières, 2009; Cavalli et al., 2012); however, proximal bicarbonate is typically absent, and terrestrial and amphibious plants do not have this ability anyway (Sand-Jensen et al., 1992). Chambers et al. (2001) observed the eradication of submersed aquatic plants when slaked lime was added to two hardwater ponds. They were unable to generate a consistent response when conducting mesocosm experiments; however, they posit that the eradication was the result of removal of CO_2 and bicarbonate.

It is suggested that the limited macrophyte colonisation of proximal pools on Foel Fawr (predominantly *Juncus sp.*) is by rhizomatous growth (see figure 3.1.5b). Rhizomatous (and analogously stoloniferous) plants use this mechanism to colonise inhospitable environments (Xiao et al., 2010; Liu et al., 2012). It has been suggested that rhizomes and stolons may be advantageous for plants stressed by flooding (Mony et al., 2010) and that clonal growth (especially rhizomatous growth) is the dominant form of reproduction in wetlands (Sosnová et al., 2010).

Further from tips, where pH is only moderately alkaline, plant numbers and biomass is still reduced (figure 3.1.9a). The observation that lime can be used to reduce biomass is not uncommon (Zhang and Prepas, 1996; Prepas et al., 2001; Reedyk et al., 2001; Leoni et al., 2007; James, 2008). Long

term, liming can also benefit some species; *Juncus bulbosus,* for instance, has been noted to thrive after the addition of lime (Roelofs et al., 1994; Roelofs et al., 1995; Lucassen et al., 1999). It is suggested by these studies that liming results in a long term increase in CO_2 levels and eutrophic conditions, combined with high levels of ammonia (resulting from the anoxic conditions). Similar anoxic conditions can occur as a result of flooding (Blom and Voesenek, 1996), meaning plants adapted to flooding are likely to survive in lime contaminated wetlands too.

Ellenberg indicator values are used to classify the ecological niche of higher plants (Hill et al., 1999). Many authors have used these values to identify the impact of stresses across a plant community, by assessing the effect of stresses on the Ellenberg values of a plant community (e.g. Diekmann and Dupré, 1997; Mayes et al., 2005; Zvereva and Zozlov, 2011; Lee and Power, 2013; Rahman et al., in press). It is important to note that the values are indicators of a niche, and do not represent ecological requirements. Nonetheless, when considering collective values for plants on Foel Fawr, Ellenberg indicator values can help to demonstrate the origin of those communities. A summary of Ellenberg indicator values for plants growing on and marginally to distal facies is given in table 4.4.3a. Ellenberg indicator values for British flora, based on those initially published by Ellenberg et al. (1991), are taken from Hill et al. (1999).

At Foel Fawr, all species are tolerant of well-lit environments and all species (excluding *Thymus serpyllum*) favour wetter than average soils, with many typical of waterlogged or shallow water sites. pH preferences are almost exclusively for neutral to acidic conditions (*Carex flava* is indicative of moderately alkaline soils). Nitrogen requirements indicate that most species favour infertile soils.

	Species	Indices				
		Light	Moisture	pH	Salinity	Nitrogen
Acid wetland	*Carex hostiana*	8	9	6	0	2
	Carex nigra	7	8	4	0	2
	Carex panicea	8	8	4	0	2
	Eriophorum angustifolium	8	9	4	0	1
	Equisetum fluviatile	8	10	6	0	4
	Equisetum palustre	7	8	6	0	3
	Juncus articulatus	8	9	6	1	3
	Juncus effusus	7	7	4	0	4
	Juncus squarrosus	7	7	2	0	2
	Pinguicula vulgaris	8	8	6	0	2
	Sagina procumbens	7	6	6	1	5
	Triglochin palustre	8	9	6	2	2
Neutral /Alkaline wetland	*Agrostis stolonifera*	7	6	7	1	6
	Carex flava	7	9	8	0	2
	Eleocharis quinqueflora	9	9	7	0	2
Others	*Thymus serpyllum*	8	2	5	0	2

Table 4.4.3a. Wetland plant species from Foel Fawr. Ellenberg indicator values for each index range from 1-9 for light, pH and nitrogen. Salinity values range from 0-9, and moisture values range from 1-12. Higher values indicate an increase in the indexed variable, relevant indicator values from Hill et al. (1999) are summarised in a table overleaf (table 4.4.3b).

Index	Value	Definition
Light	7	Plant generally in well-lit places, but also occurring in partial shade
	8	Light-loving plant rarely found where relative illumination in summer is less than 40%
	9	Plant in full light, found mostly in full sun
Moisture	1	Indicator of extreme dryness, restricted to soils that often dry out for some time
	3	Dry-site indicator, more often found on dry ground than in moist places
	5	Moist-site indicator, mainly on fresh soils of average dampness
	7	Dampness indicator, mainly on constantly moist or damp, but not on wet soils
	9	Wet-site indicator, often on watersaturated, badly aerated soils
	10	Indicator of shallow-water sites that may lack standing water for extensive periods
pH	1	Indicator of extreme acidity, never found on weakly acid or basic soils
	3	Acidity indicator, mainly on acid soils, but exceptionally also on nearly neutral ones
	5	Indicator of moderately acid soils, only occasionally found on very acid or on neutral to basic soils
	7	Indicator of weakly acid to weakly basic conditions; never found on very acid soils
	9	Indicator of basic reaction, always found on calcareous or other high-pH soils
Salinity	0	Absent from saline sites; if in coastal situations, only accidental and nonpersistent if subjected to saline spray or water (85% of the British flora)
	1	Slightly salt-tolerant species, rare to occasional on saline soils but capable of persisting in the presence of salt; includes dune and dune-slack species where the ground water is fresh but where some inputs of salt spray are likely
	2	Species occurring in both saline and nonsaline situations, for which saline habitats are not strongly predominant
Nitrogen	1	Indicator of extremely infertile sites
	3	Indicator of more or less infertile sites
	5	Indicator of sites of intermediate fertility
	7	Plant often found in richly fertile places

Table 4.4.3b. Key to Ellenberg indicator values used in table 4.4.3a. Values beyond the range observed on Foel Fawr and intermediate values are omitted. After Hill et al. (1999).

Plants colonising carbonate mud facies on Foel Fawr are from the peripheral peat-bog community; however, their growth is typically stunted (see figure 3.1.9a). Many of the species native to the peat-bog system (e.g. *Carex nigra*, *Carex panicea*, *Equisetum palustre*, *Eriophorum angustifolium*, *Juncus articulatus*, *Juncus effusus*, *Pinguicula vulgaris*) have previously been described in calcareous environments (Pentecost, 2005; van Bodegom et al., 2008; Ilomets et al., 2010; Hájkova

et al., 2012). The pH of even distal environments on Foel Fawr, however, is high in relation to natural calcareous environments. While serpentine systems share many hydrochemical similarities with Foel Fawr, these environments are typically stressed by low Ca:Mg ratios and high quantities of heavy metals (Brady et al., 2005; Briscoe et al., 2009), resulting in unusual floras (Swale et al., 2010).

Most of the species (e.g. *J. effusus*, *J. squarrosus*, *C. nigra*) are flood tolerant and favour waterlogged soils (Justin and Armstrong, 1987; Visser et al., 2000). However, van Bodegom et al. (2008) found that while submergence had little effect on growth of *Carex nigra*, hypoxia/anoxia caused signs of root oxygen stress. The hypoxia/anoxia reduces the production of adenosine triphosphate (ATP), causing an energy crisis (Colmer and Voesenek, 2009). Plants adapt to this stress either by reducing growth to conserve energy or by increasing growth to obtain oxygen (Bailey-Serres and Voesenek, 2008; Colmer and Voesenek, 2009). On Foel Fawr, the former adaptation results in the stunted growth of species colonising the tufa system.

Bryophytes form an important part of many plant communities, and there are many species on Foel Fawr. Tolerance to pH and extreme geochemistry is poorly understood and, as such, bryophytes are typically classified as simply calcicole (found on $CaCO_3$ rich rocks) or calcifuge (found on acidic substrata devoid of $CaCO_3$) (Bates, 2000). While the two groups seem vaguely defined, it has been observed that a dramatic increase of both pH and Ca^{2+} is lethal to many species of *Sphagnum* (Clymo, 1973), and that conversely, many calcicoles are strongly intolerant of low pH (Bates, 2000).

Colonisation of spoil tips on Foel Fawr is predominantly by bryophytes. The most common species (*Calliergonella cuspidata*, *Amblystegium serpens* and *Homalothecium sericeum*) are all nationally distributed (Atherton et al., 2010). Despite the porous nature of the tips, these species favour moist conditions (Atherton et al., 2010) and *C. cuspidata* has been shown to be drought intolerant (Bates et al., 2005). This is likely due to cementation of pore spaces by $CaCO_3$ in the surface layers of the spoil tips, reducing the permeability of the substrate and allowing sufficient moisture retention for these species to survive.

Bryophytes living on distal portions of the deposits and in marginal areas (see table 3.5.1b) are mostly typical of acid wetland vegetation and are all nationally distributed (Atherton et al., 2010).

Colonisation within leachate influenced alkaline waters is limited, likely due to the predominance of calcifuge bryophytes in the surrounding wetland. Although *C. cuspidata* is not uncommon in acidic wetlands, it is more typically associated with base-rich environments (Atherton et al., 2010). Bergamini and Peintinger (2002) tentatively suggest that it adapts branching density to light levels, which may make it competitive in many communities.

Diatoms are common on Foel Fawr, living in almost all environments despite the high pH and relatively low (c.40 $\mu mol.L^{-1}$) silicon levels (Emery, 2008). The frustules formed by diatoms are made from a combination of amorphous silica and organic matter (Desikachary and Dweltz, 1961; de Vrind-de Jong and de Vrind, 1997; Abramson et al., 2009), and form a remarkably strong protective layer (Hamm et al., 2003).

Monosilicic acid ($Si(OH)_4$) is the predominant form of dissolved silicon in both marine and freshwater environments and is thought to be the form taken up by marine diatoms (Del Amo and Brzezinski, 1999). They are well adapted to silicic acid uptake and typically represent >70% plankton communities even when silicon concentrations are as low as 2 $\mu mol.L^{-1}$ (Sumper and Brunner, 2008). Richthammer et al. (2011) found that proteins associated with silica biomineralization increased during silica starvation, allowing frustules to grow even when silicic acid levels are very low. In the presence of portlandite, silica readily reacts to form calcium silicate hydrates (Leemann et al., 2011). Given that monosilicic acid is required to form frustules, diatoms are likely abated by its removal in proximal environments.

High pH conditions also create a problematic environment. Hubbard and Riley (1984) demonstrated that at pH 8 diatom frustules dissolve more quickly than at pH 6. It has been suggested that no organisms are associated with hyperalkaline industrial pollution, for example cement workings (Grant and Tindall, 1986; Ulukani and Diğrak, 2002). Other authors have found that microorganisms may be associated with such conditions, albeit with reduced numbers and diversity compared with natural systems (Hemida, 2005; Maguire et al., 2006; Olaleye and Oluyemi, 2010).

Photosynthetic microorganisms (such as diatoms), like plants, require CO_2 for photosynthesis. Like many aquatic plants, diatoms are able to utilise bicarbonate (Tortell et al., 1997; Burkhardt et al., 2001). It has been suggested that their siliceous cell walls (frustules) may even be specifically adapted for this purpose (Milligan and Morel, 2002). The absence of diatoms from proximal

environments on Foel Fawr is likely due primarily to the absence of CO_2 and bicarbonate in these environments. Since the transition from hydroxide to carbonate-bicarbonate buffering on Foel Fawr happens rapidly (see section 3.4.2), diatoms are apparent in all other environments.

The most abundant genera (*Achnanthes*, *Achnanthidium*) preserved in tufa on Foel Fawr are periphytic monoraphid diatoms, with *Achnanthidium minutissimum* dominant. *Achnanthes minutissimum* (sensu Kützing, 1833) dominates (91%) the epilithic flora of travertine forming at Bagni Vignoni, Tuscany (Pentecost, 2001). Similar observations have also been made in siliceous environments (Channing and Wujek, 2010). The nomenclatorial history of *Achnanthidium minutissimum* is complex (Potapova and Hamilton, 2007); however, it may be considered synonymous with *Achnanthes minutissimum*.

Although eukaryotes are able to adapt to extreme conditions (Islam and Schulze-Makuch, 2007), the most extreme environments are dominated by prokaryotes (Konnhauser, 2007; Pikuta et al., 2007). Proximal carbonate mud pools on Foel Fawr contain active prokaryote communities (see figures 3.5.2c and d); however, there are also macrophytes associated with this environment (see figure 3.1.5b). The absence of unicellular eukaryotes in the sediment suggests that these macrophytes are able to survive here only because their roots are able to extend below the $Ca(OH)_2$ rich pore water at the top of the sediment.

A distinction is made between alkaliphilia and alkalitolerance in organisms; alkaliphiles grow optimally in alkaline conditions (Grant et al., 1990), whereas alkalitolerant organisms can survive only temporarily in these conditions. Proximal pools feature a surface pH in excess of 11 all year. Microbial cell counts are reduced close to the surface (figure 3.5.2c), suggesting that conditions may change deeper in the sediment. At Harpur Hill (see section 3.7.1), microbial communities were found associated with organic material deep in the lime sediment (Burke et al., 2012). The increase in organic matter is not associated with a decrease in pH, which remains above 12 to a depth of 30 cm. Unsurprisingly, communities are restricted, being dominated by a single species of β-proteobacteria. While the hydrology of Foel Fawr and Harpur Hill differ significantly, it seems likely that these pools are comparable and may offer a good environment for studying true alkaliphiles.

The principal difficulty for prokaryotes living in hyperalkaline environments is the need to maintain a neutral cytoplasmic pH (Konhauser, 2007). This is typically achieved with the use of a Na^+/H^+ (or K^+/H^+) antiporters and adaptations to increase cytoplasmic proton retention (Krulwich et al., 1997; Padan et al., 2005). Antiporters are enzymes which selectively exchange solutes across the cell wall; the precise mechanism for this selective exchange in Na^+/H^+ antiporters is unknown, but it is not thought to be by selective binding of solutes (Alhadeff et al., 2011).

The prokaryote communities may be further partitioned in high pH systems. Cyanobacteria can often play an important role in travertine formation (Takashima and Kano, 2008; Di Benedetto et al., 2011; Okumura et al., 2011; Okumura et al., 2012), likely due to their tolerance to heat, high pCO_2 and desiccation (Castenholz, 2002; Pentecost, 2005). On Foel Fawr, they are excluded from proximal environments by the low pCO_2.

Endolithic colonisation by photosynthetic microbes on inactive and marginal areas of aprons on Foel Fawr is common (see figure 3.1.2h). In travertine systems, endolithic cyanobacteria have been described on both active and fossil deposits (Pentecost et al., 1997; Pentecost, 2005; Norris and Castenholz, 2006; Pentecost and Coletta, 2007). Such communities are often conspicuous when the exposed surface is not colonised by epilithic organisms (Bell, 1993), the endolithic environment likely offering a buffer to environmental stresses at the surface (Friedmann, 1982). On Foel Fawr, perennially submerged active aprons do not have apparent endolithic communities, likely because the continuity of the hydroxide environment precludes photosynthetic organisms (and their conspicuous pigmentation) from colonising this environment.

Common frogs (*Rana temporaria*) are commonly observed on Foel Fawr, living in carbonate mud pools (see figure 3.5.3a). The reproductive strategy of these frogs is apparently beneficial to their survival; by laying spawn in clumps, the outermost areas of spawn act as a sacrificial buffer, protecting the other spawn (see figure 3.5.3b).

On Foel Fawr, there is a clear partitioning of biology in the present environment. While the boundaries of this partitioning have inevitably shifted as the hydrochemistry has decayed (see section 4.7.1), the relationship between biology and hydrochemistry is likely still comparable.

On Foel Fawr today, plants are restricted to the most marginal areas, only able to grow where inundation with waters is sufficiently infrequent. The presence of plant moulds in fossil tufa deposits on Foel Fawr today (see figure 3.1.10c) suggests that this present day partitioning has been representative of the site throughout its formation. More complicated is the relationship between microbial organisms currently on Foel Fawr and their historic presence at the site. It has been observed that present day microbial communities are able to thrive in all but the most extreme environments. Despite this, there is a disparity between this observation and the facies observed on the site. For example, stream crust today can often develop thick biofilm communities relatively close to the tips (see figure 3.1.3c), yet analysis of the fossil deposits reveals an increase in the presence of micritic (biofilm influenced) laminae downstream (see figure 3.1.3j). Since there is no significant change in environment downstream, this change is attributed not to a change in preservation, but rather a recession of the hydrochemistry, allowing an increase in the colonisable surface.

4.5. Fabrics, biofabrics and taphonomy

Biological influence on morphology and precipitation can vary significantly within and between tufa and travertine systems. This variability is inextricably linked to physico-chemical variability and its influence on precipitation. Biological frameworks can function at both the macro and micro scales to affect precipitation and morphology. While Pedley (2000) found no evidence of biofabrics forming at Harpur Hill (see section 3.7.1), there is evidence on Foel Fawr of a partitioning of biology and the associated fabrics (e.g. oncoids, stream crust).

4.5.1. Preservation potential and biomineralization in carbonate systems

Terrestrial carbonate systems such as tufa and travertine systems can offer an environment of rapid deposition which is advantageous for preservation (e.g. Swennen et al., 1999; Rainey and Jones, 2010). Despite this, the degree of preservation seen in comparable siliceous systems (e.g. Channing and Edwards, 2008) is not normally observed in tufas and travertines.

Many organisms use biomineralization to form structural features (Bauer et al., 2011). While silica often completely forms as inclusions in plants, which fill cell lumina preserving morphology, calcium carbonate typically only encrusts cell walls (Dickison, 2000). In some environments, calcium oxalate (CaC_2O_4) is precipitated within plant tissues (Cailleau et al., 2011; Nakata, 2012). Cao et al. (2011) show that calcium oxalate is preferentially precipitated by calcifuge plants, whereas calcicole plants preferentially bioaccumulate calcium as calcium pectate; however, it has been shown that calcium oxalate is not commonly formed in tufas and travertines (Freytet and Verrecchia, 1996).

On Foel Fawr, although biomineralization of plants is of minor importance, diatoms are close to ubiquitous. The processes of silica uptake utilised by diatoms are discussed in section 4.4.3. The preservation of frustules is often very good (see figure 3.1.3o), although the age of those frustules is unknown. In marine settings frustule decomposition is the result of bacterial removal of organic material, followed by chemical dissolution of the frustule (Loucaides et al., 2012).

4.5.2. Biofabrics

Biofabric is an umbrella term for a variety of biologically influenced fabrics. Although biology is obviously fundamental to the formation of a biofabric, they are in fact the culmination of biological, chemical and detrital contributions (Goin and Cady, 2009).

While biology plays a crucial role in the formation of a biofabric, its role in the process of precipitation is less clear. On Foel Fawr precipitation is not reliant on biology (see section 4.4.1). Contrasting this, in natural carbonate systems the association of (microbial) organisms and precipitation has been suggested to be the most important factor for carbonate precipitation (Aloisi et al., 2006). It remains unclear whether precipitation is linked to biological processes or to indirect precipitation onto biological nucleation sites. Some authors highlight the importance of the former (Aloisi et al., 2006; Shiraishi et al., 2008b; Pedley et al., 2009), others the latter (Dupraz et al., 2004), while yet others consider both together (Merz-Preiß and Riding, 1999; Dupraz et al., 2009). Identifying the mechanism may seem superfluous when considering biofabrics; however, the mechanism has profound impacts on both the fabric and where it develops.

Photosynthesis is commonly linked to precipitation. Both marine and terrestrial organisms are well linked to calcium carbonate biomineralization, often using the process to generate morphology (e.g. corals, coccolithophores) (Raven and Giordano, 2008). Cyanobacteria (and other photosynthetic microorganisms) have been associated with biomineralization of calcium carbonate in travertine systems (Pentecost, 2005). The importance of photosynthetic organisms on Foel Fawr may be reduced due to the differing hydrochemical environment to travertine systems (see section 4.4.3).

4.5.3. Phytoherms and oncoids

Phytoherms (freshwater reefs) are formed from the accretion of calcite around a macrobiological framework. While macrophytes are conspicuously preserved as moulds in the phytoherm, microbial communities are also common (Pedley, 1990). Large barrage phytoherms are absent on Foel Fawr; however, small clastic accretions (i.e. oncoids) are not (see figure 3.1.7a). Pedley (1990) distinguishes oncoids from phytoclasts (the clastic equivalent of phytoherms) by the absence of macrophytes, with cyanobacterial associations predominant. The distinction is not made here, however, and grains on Foel Fawr associated with macrophytes are still termed oncoids.

Although oncoids are typically associated with marine settings, they are also well documented in terrestrial settings. Jones (1991) describes oncoids forming in sinkholes on the Cayman Islands, and they are also commonly observed in tufa systems (Pedley, 1987; Riding, 1991; Pedley, 1993; Merz-Preiß and Riding, 1999). They are most prevalent where conditions are favourable for biology (i.e.

circumneutral pH, moderate temperatures), often allowing macrophytes to play an important role in their formation.

Oncoids have been described in siliceous systems. Jones and Renaut (1997) found oncoids forming in flood pools near to a vent. Although they are forming proximal to the vent, the conditions are likely to be milder than other proximal environments as they are only temporarily inundated and these oncoids lack any macrophyte content. In other ephemeral pools fed by hot springs, pisoids form instead of oncoids (Jones and Renaut, 1994). The reason for the difference in grains is unclear, but may be due to the higher salinity in the pisoidal pools.

4.5.4. Lamination

On Foel Fawr, alternating laminated fabrics form stream crust (figure 3.1.3j) and coat pisoids (see section 3.1.6). Typically, prismatic laminae are interspersed with micritic laminae, with micritic laminae becoming more important in the most distal areas. Alternating laminae indicate variability in environment; on Foel Fawr, this alternation of environment appears to be related to stormflow events (see section 4.4.2). In tufas, they are sometimes attributed to seasonal variability (Kano et al., 2003; Kawai et al., 2006; Kawai et al., 2009; Brasier et al., 2010; Liu et al., 2010), and while a similar relationship may be inferred to exist on Foel Fawr, the relationship may be more complex (see section 3.6.2).

In terrestrial settings, microbial activity is thought to play an important role in the formation of laminated carbonates (Wright, 1989). Micritic laminae are commonly found in algal travertines (Pentecost, 2005), and are associated with microbes (Janssen et al., 1999; Riding, 2000). Porous laminae have also been described in speleothems, although these layers are formed from aragonite and are not suggested to be microbially derived (Duan et al., 2012). At Foel Fawr, Extracellular Polymeric Substances (EPS) and diatoms are commonly associated with porous micritic laminae in stream crust (figure 3.1.3l). EPS secreted by microbes can act as nucleation points for calcite precipitation (Pentecost, 1985; Souza-Egipsy et al., 2006). Diatoms are associated with the EPS, and their frustules are preserved in stream crust. Whether diatoms play a role in precipitation is unclear, and they have been accused of both causing (Freytet and Verrecchia, 1998) and inhibiting precipitation (Arp et al., 2001; Arp et al., 2010).

Prismatic calcite laminae on Foel Fawr are probably physico-chemically precipitated. Similar prismatic laminae are common in speleothems (White, 1976), where they are not associated with micritic laminae (Pentecost, 2005). While such formations may seem abiotically generated, Jones (2010) highlights the danger of making that assumption. Indeed, there are many examples bacteria associated with speleothems (e.g. Laiz et al., 2000; Baskar et al., 2006; Legatzki et al., 2011). Conversely, it should not be assumed that the presence of microbes implies they play an active role in precipitation.

The alternating physico-chemical (prismatic) and biogenic (micritic) laminae forming on Foel Fawr are likely linked to the ephemeral submersion in this environment. The alternation of hydrochemical and hydrological parameters (see section 4.4.2) allows the colonisation of the tufa surface between physico-chemical precipitation events. Micritic laminae within proximally forming pisoids are sparse and less regular than those within stream crust, likely due to the higher pH of this environment precluding microbial colonisation for longer periods of time.

4.5.5. Microbial shrubs and feather crystals

Microbial shrubs have been described in many travertines (Chafetz and Folk, 1984; Pentecost, 1990; Guo and Riding, 1994; Chafetz and Guidry, 1999). Chafetz and Guidry (1999) recognise a continuum of morphology between three shrub types (with decreasing microbial importance respectively): bacterial shrubs, crystal shrubs and ray-crystal shrubs.

On Foel Fawr, branching shrub-like layers are found on proximal aprons (figure 3.1.2i). These shrubs differ from the Chafetz and Guidry (1999) model due to their notable absence of micrite. Chafetz and Guidry (1999) suggest that such clumps are indicative of microbial influence, though the question of whether the role of bacteria in the formation of shrubs is active or passive is contentious (Pentecost, 2005). Guo et al. (1996) measured $\delta^{13}C$ isotopic fractionation associated with shrubs, which is indicative of photosynthetic activity. However, this metric is problematic on Foel Fawr, due to the unusual isotopic effects.

On Foel Fawr, shrubs are associated with equant rhombic crystals, which precede the growth of the elongate, branched crystals (figure 3.1.2j). It seems likely that these equant crystals may be responsible for disrupting the growth of the elongate crystals in an analogous manner to the way (microbially derived) micritic areas do so in other environments. The absence of evidence of

microbial influence on these shrubs corresponds with evidence of impeded microbial communities in proximal locations (figure 3.5.2c). The regular desiccation on proximal aprons means that colonisation is likely impeded further. Additionally, the decaying geochemistry of the system (see section 4.7.1) means the presence of microbial organisms during the early history of the site is perhaps even less likely.

4.5.6. Spicular surfaces

The spicular surfaces associated with pisoidal pools on Foel Fawr (see figure 3.1.6c) form on submerged areas of ephemeral pools. Siliceous spicules have been suggested to be associated with thin films of silica rich water coating the surface of ephemeral pools when water levels are low (Jones et al., 2000). Similar (but more overtly crystalline) fabrics are also found on the roofs of caves, apparently associated with evaporation (figure 4.5.6a).

Figure 4.5.6a. Crystals from the roof of 'The Nunnery', Ogof Draenen, South Wales. This section of the cave often contains a significant flow of air, which may enhance evaporation on the surface of the crystals.

4.5.7. Unconsolidated fine grained carbonates

Fine grained carbonate mud forms subaqueously on Foel Fawr and also subaerially, though typically combined with coarser grains and widespread macrophyte colonisation. In proximal pools, active prokaryote communities living within the mud may be related to its formation, though this is uncertain.

Moonmilk, formed either subaerially or subaqueously in caves, is composed of microcrystalline minerals (typically calcite). Although subaerial moonmilk is morphologically different to carbonate mud forming on Foel Fawr, the two sediments are texturally very similar. The processes leading to precipitation of moonmilk are disputed; some authors prefer an abiogenic origin (Hill and Forti, 1997a), whilst others favour a microbial origin (White, 1976; Curry et al., 2009; Baskar et al., 2011). Sanchez-Moral et al. (2012) suggest that bacteria may be responsible for initiating precipitation; however, chemical processes then gain importance for precipitation.

4.5.8. Summary

Many of the fabrics on Foel Fawr are associated with hot-springs and speleothems. While many of these environments are now recognised as having a biogenicity to the fabrics forming at them, the facies on Foel Fawr appear to be less influenced by biology than their analogues. Biologically influenced fabrics on Foel Fawr become more important in distal and marginal parts of the deposit (e.g. figure 3.1.3j), however, physico-chemical processes are likely still responsible for precipitation.

4.6. Relevance to astrobiology

4.6.1. Early environments on Earth (and Mars)

The system on Foel Fawr (and similar systems) offers an exciting site for astrobiological research and opportunities to study the potential origin of life on Earth. Since water is the only essential requirement for all known life (Gómez et al., 2012), aquatic environments understandably dominate the search for life's origin, both on Earth and its potential origin on other planets (Davis and McKay, 1996; Shock, 1996; Zubay, 2000; Knoll and Grotzinger, 2006; Schultz-Makuch et al., 2008; Gómez et al., 2012). Agreement on the existence of water on the early Earth is good (Kramers, 2003; Lunine, 2006), although its existence on Mars is less certain (Carr, 2012; Hand, 2012; Kula and Baldwin, 2012).

Although the composition of water bodies on early Earth and Mars are unknown (Schulte et al., 2006), it is likely that they were influenced by their interaction with the underlying geology, which was likely comparable to ultramafic ophiolites (Sleep et al., 2004). Serpentinization commonly occurs today at subduction zones, mid ocean ridges and elsewhere on the ocean floor (Hyndman and Peacock, 2003; Kodolányi et al., 2012), generating comparable hydrochemical systems to those on Foel Fawr.

There are several problematic differences between Foel Fawr and comparable early Earth environments. Waters issuing from serpentinized aquifers may be enriched with $Mg(OH)_2$ as well as $Ca(OH)_2$. It has been suggested that inorganic reactions involving Mg^{2+} may have been an important precursor to the development of life (Holm, 2012). Serpentinized systems (unlike Foel Fawr) are also a potential source of H_2, which provides a potential energy source for microbial communities (Oze and Sharma, 2006; Okland et al., 2012). Finally, the presence of life in modern environments and the existence of these environments on the early Earth and other planets does not demonstrate that life originated there (Cleaves II and Chalmers, 2004). Despite these potential problems, Foel Fawr is a useful place to study the adaptations required by organisms to survive in hydroxide based systems.

4.6.2. Origins of life on Earth (and Mars)

The use of analogues to study early (or extraterrestrial) life is widespread (Léveillé, 2010). Serpentinized systems offer a potential analogue for early life ecosystems, and several authors have

proposed or used them as analogues for the origin of life (Holm and Baltscheffsky, 2011; Fryer, 2012). While there are notable differences in the hydrochemical environment on Foel Fawr (see section 4.6.1), organisms face similar pressures due to the hydroxide buffering system.

The high pH environment on Foel Fawr necessitates adaptations by organisms that survive there. These adaptations may be either evolutionary modification of function (e.g. development of specific antiporters/uniporters; see section 4.4.3), modification of lifestyle or development of a symbiotic relationship. The study of organisms on Earth is essential to developing criteria for assessing any evidence of similar organisms on Mars (or other planets and moons).

Despite the predominantly abiotic precipitation on Foel Fawr, microorganisms are often present (see section 3.5.2). The site provides a convenient location for studying microorganisms in high pH environments, and specifically to use remote sensing equipment to identify microbial environments. The PanCam, which is planned to be part of the instrument suite mounted on the (European Space Agency's) ExoMars Rover (European Space Agency, 2012), has been tested at Foel Fawr. The PanCam uses two cameras to produce a three-dimensional image of the surface, with the aim of identifying suitable sample sites on Mars. The apparently abiotically driven precipitation on Foel Fawr, however, suggests that it would be possible to generate similar morphologies in a sterile system.

While this highlights a key problem for astrobiological research - identifying biology from lithological environments - it also presents an opportunity to identify mechanisms to differentiate between biotic and abiotic systems. For example, while the morphology of stream crust facies on Foel Fawr (see section 3.1.3) may be reproducible in an abiotic system, the alternating micritic and prismatic laminae are reliant upon repeated colonisation (see section 4.5.4). Without the colonisation of the surface, any alternation of fabric would likely be limited to clastic material. Identifying stream crust on Mars and resolving these (or the absence of these) laminated fabrics (which are resolvable with a camera) would provide crucial evidence to the debate.

The endolithic communities on Foel Fawr may have relevance to both astrobiological and panspermial research. Endolithic photosynthetic communities are near ubiquitous (see figure 3.1.2h), despite being periodically inundated by high pH, low CO_2 waters. The endolithic environment has been identified as a good environment for organisms wishing to buffer their

exposure to stresses at the surface (Friedmann, 1982). It has also been suggested as a suitable vehicle for microbes to be transported between planets (Walker and Pace, 2007).

While there are internationally better sites for conducting astrobiological research, there is a paucity of such environments (hot springs, salt lakes etc.) in Britain. Consequently, Foel Fawr represents a useful resource to scientists in the UK wishing to test equipment and methods for astrobiological research.

4.7. Decay and its associated morphological changes

4.7.1. Hydrochemical evolution of the system

Although lime burning ceased several decades ago, the geochemistry of the present day system makes it self-evident that there is still portlandite remaining within the tips. Dabo et al. (2009) found that leachate from ash containing portlandite used as road aggregates has dropped from pH 12.4 to pH 7.6 in around 3 years. They observe a continual decline in leachate pH over the three year period - an observation not repeated on Foel Fawr, which suggests that the system is not rapidly declining.

Despite the persistence of high pH levels proximally, pH drops through the system as the hydroxide system is transformed into a carbonate-bicarbonate system. This change occurs before the downstream limit of tufa precipitation, which indicates that a recession of the hydroxide system has occurred.

The complex history of lime burning at the site complicates the hydrochemical evolution of the system. There are a variety of different kilns on the site, from 18th century field kilns and 19th century masonry kilns through to more modern concrete kilns (Jones, undated). The lower eastern kilns are likely early 19th century (Duncan Schlee, Dyfed Archaeological Trust, personal communication 2012), and there are a few younger kilns higher up the hill. In this area, some kilns were active as late as the 1950s (Percival, 1986). The western kilns all predate these modern concrete kilns, and the quarries are notably older in appearance. Despite this, there is no significant change in hydrochemistry between comparable settings within the system on the east and west of the site. This suggests that the hydrochemistry of the two sites is relatively stable and that the change in hydrochemistry happened relatively quickly after the cessation of lime burning.

4.7.2. Precipitation changes through time

The limit of active precipitation is currently around 40 m downstream of the closest spring, yet stream crust extends as much as 400 m downstream of the closest spring. The recession of active precipitation is due to the geochemical evolution of the system as the tips become ever more depleted of portlandite.

Proximal fossil tufa channels are remnants of very early precipitation of laminated crusts. They are now typically associated with carbonate gravel, which was likely accreted both contemporaneously and following the formation of the fossil tufa channels. These channels may represent the inevitable fate of the later deposits (see section 4.7.3).

4.7.3. Decay of the deposits

In many places, decay of the system is visible. Fracturing of stream crust is the most obvious decay, with large (cm-m scale) blocks of tufa detached from the main stream crust.

Physical decay of tufa and travertine can come from a number of physical factors. Crystalline crust travertine is relatively strong under compression (Yagiz, 2010); however, its strength is dependent upon orientation and is weaker when loaded perpendicularly to the laminations (Çobanoğlu and Çelik, 2012). The rapid fracturing at the downstream limits of stream crust on Foel Fawr is likely accelerated due to undercutting by the stream.

Upstream, physical decay is limited to exfoliation of laminae. The reduced rate of decay of stream crust closer to the tip may be due to decreased dissolution and reduced frost action as a result of its lower porosity. Frost action and evaporation can both cause crystals to form within travertine laminae, leading to delamination and degradation of the travertine strength (Akin, 2010; Pinińska et al., 2010). Strength may also be reduced when travertine is saturated by water (Török and Vásárhelyi, 2010).

Animals place additional pressures on the deposits at Foel Fawr. Horses and sheep roam freely on Foel Fawr, inevitably damaging deposits by trampling. The activities of humans may also be of relevance. Pentecost (2010) highlights the vulnerability of (young, active) deposits to trampling. While the visitor numbers to international tourist destinations is significantly higher than at Foel Fawr, the addition of motorised vehicles to the trampling on Foel Fawr (see figure 3.5.3e) means their effect may still be significant.

Chemical dissolution of the deposits may play an important role in their decay. Although groundwater on Foel Fawr is of carbonate-bicarbonate type, the peripheral acidic peat-bog environment and direct rainfall onto the deposits could potentially lead to dissolution. Chemical weathering has been noted on buildings constructed from travertine (Dubelaar et al., 1997; Török,

2006). Webb et al. (1992) measured the dissolution rate of Portland Limestone by rain and found low (10s $g.m^{-2}.a^{-1}$) dissolution rates. Furthermore, a weathered surface on limestone offers significant protection from dissolution (Thornbush and Viles, 2007), suggesting that chemical dissolution is of minor importance on Foel Fawr.

Inactive and decaying areas often feature epilithic colonisation leading to discolouration. Discolouration by either epilithic or endolithic colonisation has been shown to both increase thermal gradients between the surface and interior of limestone and increase the rate of temperature change at the surface (Carter and Viles, 2004). High thermal gradients may lead to fracturing (Hall and Hall, 1991), likely as the result of differential expansion within the rock (Gómez-Heras et al., 2006). Discolouration (invariably darkening) of the surface of tufa on Foel Fawr leads to increased absorption of solar radiation; rapid temperature changes of a rock surface may be associated with fracturing due to thermal stress (Jenkins and Smith, 1990; Hœrlé, 2006).

Proximally, epilithic colonisation is precluded; however, endolithic colonisation is still common. Unlike epilithic colonisation, endolithic colonisation is typically associated with a stabilising of the substrate (Pohl and Schneider, 2002; Concha-Lozano et al., 2012). It seems likely that breakdown of proximal environments (including inactive sites) will likely be abated until the hydrochemistry of such environments permits epilithic colonisation.

4.8. Geoconservation and geoheritage issues

The site on Foel Fawr represents both an unusual tufa environment and an important piece of geoarchaeological history. Quarrying and lime burning on Foel Fawr are extensive, both spatially and historically. A geoconservation project, CALCH, is currently being run by Dyfed Archaeological Trust (in association with Brecon Beacon's Trust, Black Mountain Centre, Brecon Beacons National Park, Welsh Government and National Museum Wales). The project aims to describe the historical development and evolution of lime burning at the site. The presence of such a site history creates a unique possibility for contextualising the development of the tufa deposits.

Although technically pollution, the deposits are part of the legacy of lime production in Britain. There is a paucity of heritage sites concerning lime burning in South Wales, and much information is limited to museums. The CALCH project represents a chance to incorporate geological education into a publicly available resource.

The deposits themselves represent the largest of a very limited number of invasive tufa deposits described in the UK. They are important not only because of their rarity, but also because of their potential for future research. Using Rhondda Cynon Taff's criteria for assessing geoconservation and management, the site scored 405 for geoconservation and 45 for management (figure 4.8a & 4.8b). This suggests the site has potential SSSI or GCR status and good potential for successful management.

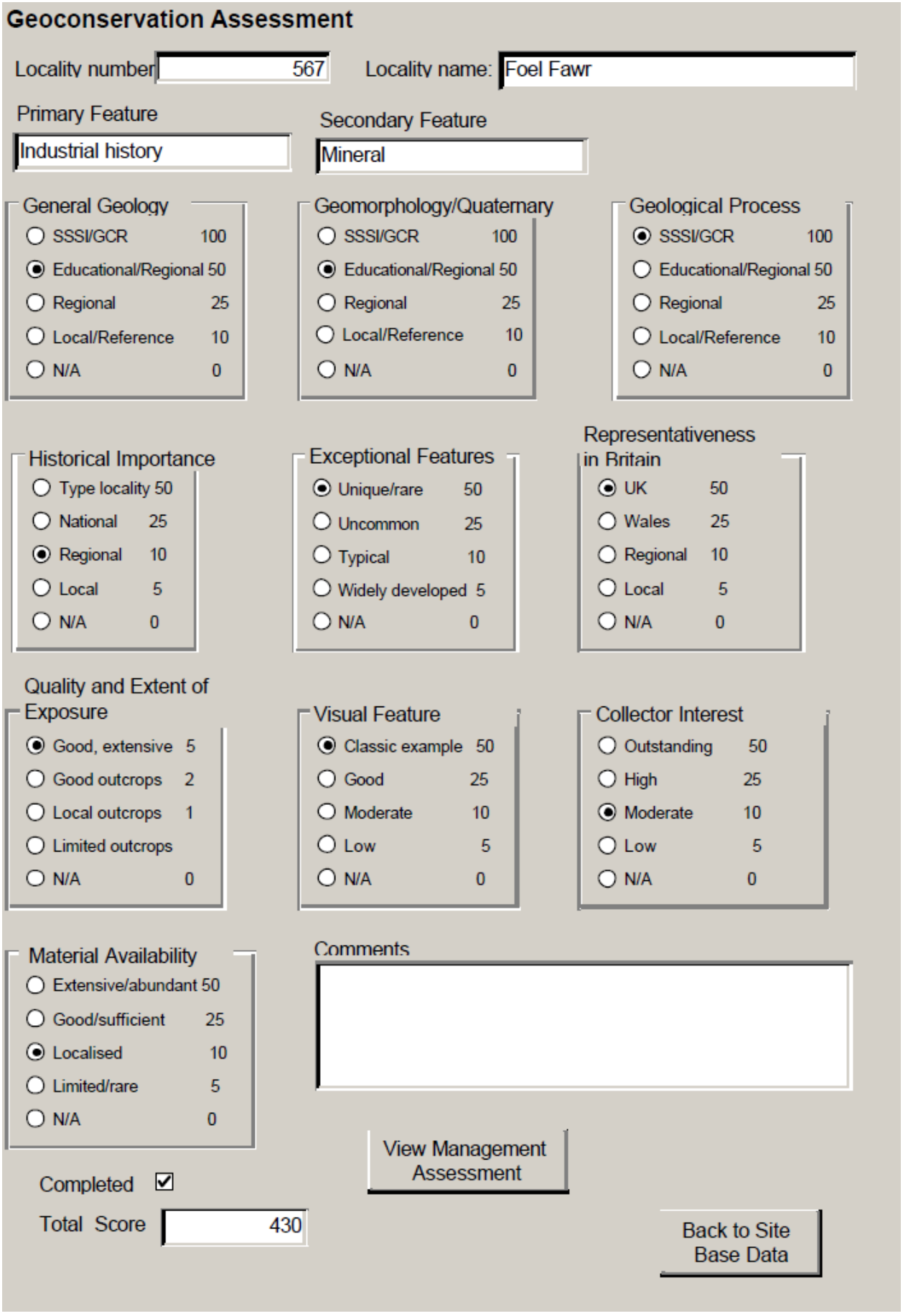

Figure 4.8a. Geoconservation assessment for Foel Fawr

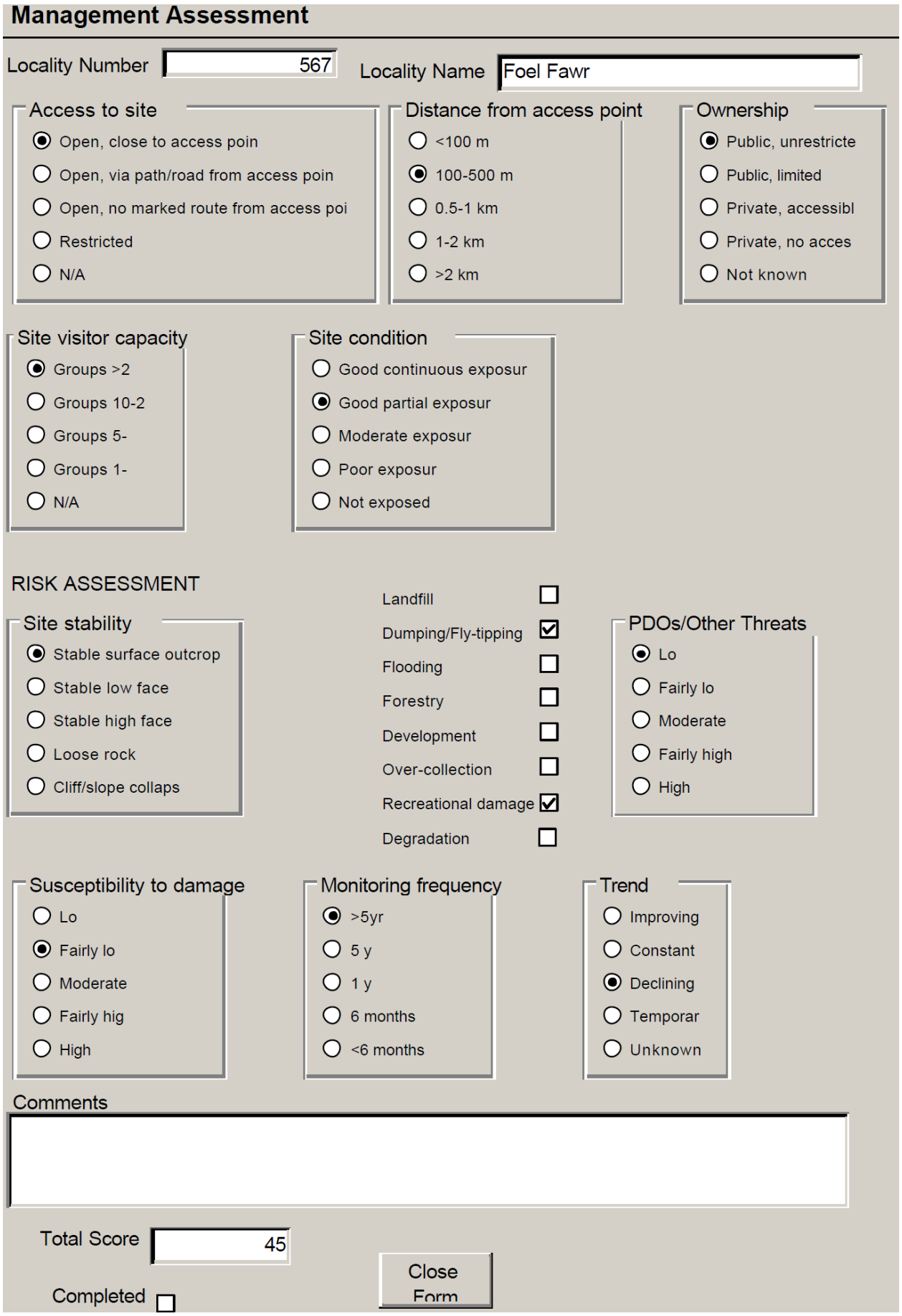

Figure 4.8b. Management assessment for Foel Fawr.

4.9. Summary discussion and classification of Foel Fawr deposits

The preceding sections discuss each aspect of the tufa deposits on Foel Fawr separately. In order to consider the relationship between them and other terrestrial carbonate systems, they must be considered at a broader, system level.

Sections 4.2 and 4.3 discuss the similarities between the facies on Foel Fawr and the facies observed in both hot-spring travertine and cave systems. As well as the obvious, superficial similarities between these systems (lack of vegetation, carbonate precipitates), there are similarities at the facies level. Crystalline precipitates are common in all of these environments, often with associated finer grained sediments.In both travertine and cave systems, these precipitates form facies which are analogous to those observed on Foel Fawr. The distribution of these facies on Foel Fawr mirrors that observed in many travertines (comparison with distributions in cave systems is difficult owing to the differing geometry of the depositional environments).

This similarity of morphology at a facies level comes despite a wholly different set of physico-chemical parameters between these three systems. In section 4.4, it is established that the unusual hydrochemistry on Foel Fawr is responsible for the exclusion of biota from the deposits on Foel Fawr. While the physico-chemical pressures generating exclusion are different in cave and travertine systems, the effects of exclusion are the same; physico-chemical processes dominate these environments.

Despite the processes of deposition varying significantly between these environments, there are apparent similarities in their morphological variability. On Foel Fawr, hydrology is the primary control of hydrochemical variation and is also linked to facies distribution (section 4.3). This control also appears to be crucial to travertine and speleothem formation, although its importance has perhaps been underemphasised with recent research interest in geomicrobiology.

At a fabric scale, there are some differences between the deposits on Foel Fawr and travertines and speleothems (section 4.5). While these differences demonstrate that the comparable facies in each environment are not tied to a particular fabric, there is a broader link between fabrics and facies. A continuum of physico-chemically dominated and biologically dominated fabrics exists within all of these different systems and plays an important role in the control of facies. This relationship is a

direct result of the physico-chemical pressures within these systems, excluding biota and allowing physico-chemical processes (especially hydrology) to dominate. The extreme pH and rapid precipitation rates on Foel Fawr generate proximal precipitates that are apparently entirely physico-chemical. When placed in the context of other terrestrial carbonate deposits (figure 4.9a), invasive tufas, such as those on Foel Fawr, represent another physico-chemically dominated system. Where these systems are not in decay (see section 4.4 and 4.7), they likely represent a purely physico-chemical end member to this continuum.

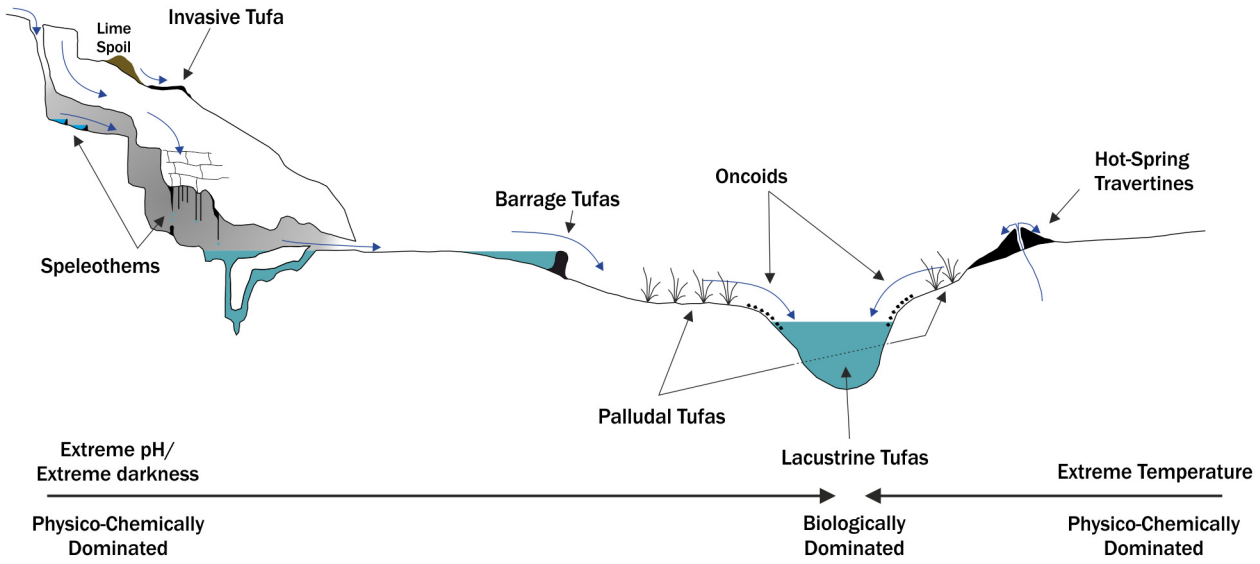

Figure 4.9a. Schematic diagram of terrestrial carbonate deposition showing the relationship between physico-chemically and biologically dominated systems and morphology. Modified from Pedley & Rogerson (2010a).

Foel Fawr and other invasive tufa systems are of great value to terrestrial carbonate research due to their relationship to other systems. The use of analogue systems allows testing of concepts, by isolation of variables, and a wholly physico-chemical system presents opportunities for clarifying the role of biofabrics in terrestrial carbonates. Specifically, Foel Fawr is an extremely valuable site, owing to its size and the range of facies present.

Foel Fawr is also valuable for a multitude of other reasons. The extreme hydrochemistry provides an excellent system for studying alkaliphilia and alkalitolerance in organisms. The periodic shifts in hydrochemistry owing from the hydrology of the system (section 4.4) allow the effects of periodic inundation possible, as well as organism continually inundated by hydroxide-rich waters. The present state of decay (section 4.7) presents a snapshot of the site, with decay more prevalent in distal parts. As the hydrochemistry of the system decays (section 4.4), the associated incursion of biota will allow the processes of biological decay (section 4.7) to be studied at a single locality. The

importance of Foel Fawr to geoarchaeology (section 4.8) is inextricably linked to its geological importance. The history of lime burning has generated and is recorded in the tufa deposits, and the understanding of each of these aspects is mutually beneficial for the other.

Chapter 5: Conclusions

The tufa deposits on Foel Fawr, Black Mountain represent an uncommon and poorly described type of tufa system. The extent of the system is unparalleled in the United Kingdom and is contingent upon a specific combination of geology, hydrology and anthropogenic factors.

The deposits are highly unusual for ambient temperature carbonate precipitating springs. Morphologically, the deposits are analogous to other stressed carbonate precipitating environments (hot springs, speleothems), owing to the extreme chemistry of the site. Many of the facies are directly comparable to their analogues: aprons with microterracettes forming at springs are morphologically identical to their hot spring counterparts; carbonate mud pools are analogous to vent pools; vertical facies generate stalactitic morphologies. The direct comparability of facies on Foel Fawr, both morphologically and spatially, with hot spring environments surely indicates parallel controls on their formation.

Exclusion of biology on Foel Fawr is the result of extreme chemistry rather than temperature (in hot springs) or darkness (in caves). The partitioning of biology observed in the present demonstrates that the processes of exclusion are still occurring. In fossil deposits, this exclusion has resulted in partitioning of facies; proximal environments are dominated by physico-chemical precipitation, while distal and marginal environments are influenced more by biology.

The hydroxide system creates a low-CO_2, low [H^+] environment. While this environment is extremely inhospitable for life, the tenacity of some organisms allows them to colonise these environments; from endolithic cyanobacteria growing on aprons, to frogspawn in proximal carbonate mud pools, biological colonisation is incredibly prevalent, in spite of the highly stressed environment. The hydrological regime may play an important role in allowing such a wide range of organisms to survive here. The present day conditions create a variable hydrochemistry, producing more favourable conditions for organisms during extended periods of both low and high flow, either by reduced leaching or by dilution.

Despite the presence of microbial communities at the site, present day biology does not appear to correspond with the fabrics associated with each facies. Abiotic fabrics dominate proximal facies, likely due to a historical hydrochemistry that was even more hostile to biological colonisation than today. The ability of these physico-chemically dominated environments to precipitate morphologies

analogous to those formed by biomediated fabrics in hot-spring environments is significant. It suggests that, although a practical impossibility on Earth, a sterile system may be able to generate many of the morphologies observed in hot spring systems.

Given the natural analogues to Foel Fawr in serpentinised systems, and the potential for similar environments on extra terrestrial planets, there are serious implications for astrobiological research. When attempting to use morphological features to identify potential habitats for extra terrestrial life, caution is essential to avoid falsely identifying biofabrics which are in fact abiotic.

The site also represents an important piece of geoarchaeological history. The archaeological history of the site is significant enough to merit study, and the tufa deposits form an inseparable part of this archaeological history. Furthermore, the decay of the system makes it important that any future studies are conducted promptly.

5.1. Future research

There are many future avenues for research to be undertaken at the site (some of which have already begun progressing at the Department of Earth Sciences, University College London). The utilisation of biosignatures to inform the origin of past precipitates would provide further evidence regarding the balance of physico-chemical and biologically influenced precipitation at the site. Comparison studies with other sites, especially with active serpentinised systems, would prove very useful in further demonstrating the relative roles of physico-chemical and biomediated precipitation in invasive tufa systems.

Foel Fawr also represents a potential site for studying alkaliphiles, providing a variety of extreme pH environments from which microbes may be sampled. Additionally, the site hosts a wide range of environments where both microbes and macrophytes are periodically exposed to extreme pH conditions. There is clearly good potential here for studying stress tolerances in these organisms.

Glossary

Alkaliphile	Organisms with a high optimum growth pH (>9).
Alkalitolerant	Organisms able to tolerate high pH (>9), however their optimum growth pH is more neutral
Antiporter	A protein within the cell wall that exchanges molecules or ions across the cell wall
ATP	Adenosine triphosphate. Produced by cells as means for storing energy
Calcicole	Calcareous loving plant
Calcifuge	Plant that does not tolerate calcareous soils
Carbonate Ice	Calcium carbonate crystal precipitated at the air-water interface due to degassing
Cusped Terrace	Overhanging morphology observed on **terraces** forming on steep slopes
Drapery	**Speleothem** forming beneath overhangs, forming curtain-like structures.
Flowstone	**Speleothem** precipitated from thin films of water flowing over a surface
Frustule	Hard silica shell precipitated by diatoms
Helictite	Irregular **speleothem** characterized by branching and twisting shapes
Invasive Tufa	**Tufa** formed by the ingassing of CO_2 into hydroxide rich waters
Micrite	Micro-crystalline calcite <4μm
Microspar	Micro-crystalline calcite 5-30μm
Microterrace	Small **terrace** (forming m^2 scale pools)
Microterracette	Very small **terrace** (forming cm^2 scale pools)
Moonmilk	Soft **speleothem** forming

Oncoid	mm-cm sized irregular grains formed largely of micritic laminae. On Foel Fawr, prismatic laminae are also common
Pisoid	mm-cm sized subspherical grains formed around a core with densely laminated cortex
Pollution	"Physical impurity or contamination; (now) esp. the presence in or introduction into the environment (esp. as a result of human activity) of harmful or poisonous substances, or excessive levels of light, noise, organic waste, etc." OED
Rhizome	cf. **stolon**. A subterranean stem which grows laterally and sends out roots and shoots. Plants growing using this method are known as rhizomatous.
Speleothem	Mineral precipitate within a cave, calcite is by far the most common mineral in most caves.
Stalactite	A **speleothem** forming beneath an overhang. Commonly formed from dripping water.
Stalagmite	A **speleothem** growing vertically upwards. Commonly associated with **stalactites**, forming where drip waters land.
Stolon	cf. **Rhizome**. A stem which grows along the soil surface putting down roots and new plants. Plants growing using this method are known as stoloniferous.
Symporter	A protein within the cell wall that moves two (or more) different molecules or ions across the cell wall
Terrace	A build up of tufa or travertine perpendicular to the water flow, creating a dam and pool. Can form on a range of scales (see **terracette**, **microterracette**)
Travertine	Calcium carbonate precipitated subaerially from geothermally heated waters
Tufa	Calcium carbonate precipitated subaerially from ambient temperature waters
Uniporter	A protein or channel that allows specific molecules or ions to travel in one direction across the cell wall

Acknowledgements

I thank Dr. Alan Channing and Dr. Lesley Cherns, who have provided invaluable assistance and advice on all aspects of the project. I also thank Prof. John Parkes and Dr. Henrik Sass for their assistance, both in the field and in the laboratory.

I thank Dr. Barry Cragg, Mr. Pete Fisher, Mr. Tony Oldroyd and Mrs. Xiaohong Tang for their assistance in analytical work. Thanks to Mr. William Lee for invaluable assistance with *Python.* Additional thanks to Mr. Rhys Davies, Dr. Giovanna Della Porta, Mr. Jason Gotel, Dr. Alan Hemsley, Dr. Heather Price and Dr. Tony Ramsey for their assistance in the field and to Dr. Tracy Aze, Mr. Luke Dixon and Mr. Giles Langston for proof-reading.

Final thanks to Ms. Menna Bell, Dr. Claire Cousins, Ms. Jennifer Harris, Dr. Lottie Hobday, Mr. Shaun Lewis and Mr. Duncan Schlee for providing providing insights into other aspects of the site.

Funded by the Natural Environment Research Council.

Reference List

Abramson, L. Wirick, S. Lee, C. Jacobsen, C. and Brandes, J.A. 2009. The use of soft X-ray spectromicroscopy to investigate the distribution and composition of organic matter in a diatom frustule and a biomimetic analog. *Deep-Sea Research Part II* ***56***, pp. 1369-1380.

Akin, M. 2010. Salt crystallization deterioration in yellow travertines. Rock Engineering in Difficult Ground Conditions - Soft Rocks and Karst - Proceedings of the Regional Symposium of the International Society for Rock Mechanics, EUROCK 2009. Dubrovnik, Croatia. pp. 175-179.

Alhadeff, R. Ganoth, A. Krugliak, M. and Arkin, I.T. 2011. Promiscuous binding in a selective protein: the bacterial Na^{+}/H^{+} antiporter. *PLoS ONE* ***6***, e25182.

Allwood, A.C. Walter, M.R. Burch, I.W. and Kamber, B.S. 2007. 3.43 billion-year-old stromatolites reef from the Pilbara Craton of Western Australia: ecosystem-scale insights to early life on Earth. *Precambrian Research* ***158***, pp. 198-227.

Allwood, A.C. Walter, M.R. Kamber, B.S. Marshall, C.P. and Burch, I.W. 2006. Stromatolite reef from the Early Archaean era of Australia. *Nature* ***441***, pp. 714-718.

Aloisi, G. Gloter, A. Krüger, M. Wallmann, K. Guyot, F. and Zuddas, P. 2006. Nucleation of calcium carbonate on bacterial nanoglobules. *Geology* ***34***, pp. 1017-1020.

Altunel, E. and Hancock, P.L. 1993. Morphology and structural setting of Quaternary travertines at Pamukkale, Turkey. *Geological Journal* ***28***, pp. 335-346.

Andrews, J.E and Riding, R. 2001. Depositional facies and aqueous-solid geochemistry of travertine-depositing hot springs (Angel Terrace, Mammoth Hot Springs, Yellowstone National Park, U.S.A.)-discussion. *Journal of Sedimentary Research* ***71***, pp 496-497.

Andrews, J.E. Gare, S.G. and Dennis, P.F. 1997. Unusual isotopic phenomena in Welsh quarry water and carbonate crusts. *Terra Nova* ***9***, pp. 67-70.

Anon. 2008. Flame which burned in Harpur for decades. *Buxton Advertiser*. Buxton, UK: Johnston Press Digital Publishing. < http://www.buxtonadvertiser.co.uk/community/nostalgia/flame-which-burned-in-harpur-for-decades-1-653039> [accessed 03/09/2012].

Anzalone, E. Ferreri, V. Sprovieri, M. and D'Argenio, B. 2007. Travertines as hydrologic archives: the case of the Pontecagnano deposits (southern Italy). *Advances in Water Resources* ***30***, pp. 2159-2175.

Arenas, C. Cabrera, L. and Ramos, E. 2007. Sedimentology of tufa facies and continental microbialites from the Palaeogene of Mallorca Island (Spain). *Sedimentary Geology* ***197***, pp. 1-27.

Arp, G. Wedermeyer, N. and Reitner, J. 2001. Fluvival tufa formation in a hard-water creek (Deinschwanger Bach, Franconian Alb, Germany). *Facies **44***, pp. 1-22.

Arp, G. Bissett, A. Brinkmann, N. Cousin, S. De Beer, D. Friedl, T. Mohr, K.I. Neu, T.R. Reimer, A. Shiraishi, F. Stackebrandt, E. and Zippel, B. 2010. Tufa-forming biofilms of German karstwater streams: microorganisms, exopolymers, hydrochemistry and calcification. In: Pedley, H.M. and Rogerson, M. eds. *Tufas and Speleothems: Unravelling the Microbial and Physical Controls*. London, UK: The Geological Society. pp. 83-118.

Appelo, C.A.J. and Postma, D. 2005. *Geochemistry, groundwater and pollution (2nd edition)*. CRC Press.

Arenas-Abad, C. Vásquez-Urbez, M. Pardo-Tirapu, G. and Sancho-Marcén, C. 2010. Fluvial and associated carbonate deposits. In: Alonso-Zarza, A.M. and Tanner, L.H. eds. 2010. *Carbonates In Continental Settings*. Amsterdam, The Netherlands: Elsevier. pp. 133-175.

Atherton, I. Bosanquet, S. and Lawley, M. 2010. *Mosses and Liverworts of Britain and Ireland a field guide*. UK: Britsh Bryological Society.

Bailey-Serres, J. and Voesenek, L.A.C.J. 2008. Flooding stress: acclimations and genetic diversity. *Annual Reviews In Plant Biology **59***, pp. 313-339.

Baker, A. Smith, C.L. Jex, C. Fairchild, I.J. Genty, D. and Fuller, L. 2008. Annually laminated speleothems: a review. *International Journal of Speleology **37***, pp. 193-206.

Baldini, J.U.L. 2010. Cave Atmospheres and Stalagmites. In: Pedley, H.M. and Rogerson, M. eds. *Tufas and Speleothems: Unravelling the Microbial and Physical Controls*. London, UK: The Geological Society. pp. 283-294.

Ball, P. 2004. Astrobiology: water, water, everywhere? *Nature **427***, pp. 19-20.

Banks, E.D. Taylor, N.M. Gulley, J. Lubbers, B.R. Giarrizzo, J.G. Bullen, H.A. Hoehler, T.M. and Brown, H.A. 2010. Bacterial calcium carbonate precipitation in cave envinroments: a function of calcium homeostasis. *Geomicrobiology Journal **27***, pp. 444-454.

Banner, J.L. Guilfoyle, A. James, E.W. Stern, L.A. and Musgrove, M. 2007. Seasonal variations in modern speleothem calcite growth in Central Texas, U.S.A. *Journal of Sedimentary Research **77***, pp. 615-622.

Banowetz, G.M. Azevedo, M.D. and Stout, R. 2008. Morphological adaptations of hot springs panic grass (Dichanthelium lanigunosum var sericeum (Schmoll)) to thermal stress. *Journal of Thermal Biology **33***, pp. 106-116.

Bargar, K.E. 1978. Geology and thermal history of Mammoth Hot Springs, Yellowstone National Park, Wyoming. *Geological Survey Bulletin **1444***, pp. 1-55.

Barnes, I. LaMarche, V.C. Jr. and Himmelberg, G. 1967. Geochemical evidence of present-day serpentinization. *Science* ***156***, pp. 830-832.

Barnes, I. and O'Neil, J.R. 1971. Calcium – Magnesium carbonate solid solutions from Holocene conglomerate cements and travertines in the Coast Range of California. *Geochimica et Cosmochimica Acta* ***35***, pp. 699-718.

Barton, H.A. Spear, J.R. and Pace N.R. 2001. Microbial life in the underworld: biogenicity in secondary mineral formations. *Geomicrobiology Journal* ***18***, pp. 359-368.

Baskar, S. Baskar, R. Mauclaire, L. and McKenzie, J.A. 2006. Microbially induced calcite precipitation in culture experiments: possible origin for stalactites in Sahastradhara caves, Dehradun, India. *Current Science* ***90***, pp. 58-64.

Baskar, S. Baskar, R. and Routh, J. 2011. Biogenic evidences of moonmilk deposition in the Mawmluh Cave, Meghalaya, India. *Geomicrobiology Journal* ***28***, pp. 252-265.

Bates, J.W. 2000. Mineral nutrition, substratum ecology, and pollution. In: Shaw, A.J. and Goffinet, B. eds. *Bryophyte Biology*. Cambridge, UK: Cambridge University Press. pp. 248-311.

Bates, J.W. Thompson, K. and Grime, J.P. 2005. Effects of simulated long-term climatic change on the bryophytes of a limestone grassland community. *Global Change Biology* ***11***, pp. 757-769.

Bauer, P. Elbaum, R. and Weiss, I.M. 2011. Calcium and silicon mineralization in land plants: transport, structure and function. *Plant Science* ***180***, pp. 746-756.

Bell, R.A. 1993. Cryptoendolithic algae of hot semiarid lands and deserts. *Journal of Phycology* ***29***, pp. 133-139.

Benedict, E.M. 1979. Ice candles of Malheur. *National Speleological Society News* ***37***, pp. 65-66.

Benedetto, F.D. Montegrossi, G. Minisalle, A. Pardi, L.A. Romanelli, M. Tassi, F. Delgado Huertas, A. Pampin, E.M. Vaselli, O. and Borrini, D. 2011. Biotic and inorganic control on travertine deposition at *Bullicame 3* spring (Viterbo, Italy): A multidisciplinary approach. *Geochimica et Cosmochimica Acta* ***75***, pp. 4441-4455.

Berelson, W.M. Corsetti, F.A. Pepe-Ranney, C. Hammond, D.E. Beaumont, W. and Spear, J.R. 2011. Hot spring siliceous stromatolites from Yellowstone National Park: assessing growth rate and laminae formation. *Geobiology* ***9***, pp. 411-424.

Bergamini, A. and Peintinger, M. 2002. Effects of light and nitrogen on morphological plasticity of the moss *Calliergonella cuspidata*. *OIKOS* ***96***, pp. 355-363.

Bersenev, J.I. 1989. Karst of the Russian Far East. Moscow, Russia: Nauka.

Bissett, A. Reimer, A. de Beer, D. Shiraishi, F. and Arp, G. 2008. Metabolic microenvironmental control by photosynthetic biofilms under changing macroenvironmental temperature and pH conditions. *Applied and Environmental Microbiology **74***, pp. 6306-6312.

Blank, J.G. Green, S.J. Blake, D. Valley, J.W. Kita, N.T. Treiman, A. and Dobson, P.F. 2009. An alkaline spring system within the Del Puerto Ophiolite (California, USA): A Mars analog site. *Planetary and Space Science **57***, pp. 533-540.

Blom, C.W.P.M. and Voesenek, L.A.C.J. 1996. Flooding: the survival strategies of plants. *Trends in Evolution and Ecology **11***, pp. 290-295.

Bonny, S.M. and Jones, B. 2008. Petrography and textural development of inorganic and biogenic lithotypes in a relict barite tufa deposit at Flybye Springs, NT, Canada. *Sedimentology **55***, pp. 275-303.

Boyer, B.W. 1994. Alkaline leachate and calcareous tufa originating from slag in a highway embankment near Baltimore, Maryland. *Transportation Research Record **1434***, pp. 3-7.

Brady, K.U. Kruckeberg, A.R. and Bradshaw Jr., H.D. 2005. Evolutionary ecology of plant adaptation to serpentine soils. *Annual Review of Ecology **36***, pp. 243-266.

Braithwaite, C.J.R. 1979. Crystal textures of recent fluvial pisolites and laminated crystalline crusts in Dyfed, South Wales. *Journal of Sedimentary Petrology **49***, pp. 181-194.

Brasier, M. McLoughlin, N. Green, O. and Wacey, D. 2006. A fresh look at the fossil evidence for early Archaean cellular life. *Philosophical Transactions of the Royal Society B: Biological Sciences **361***, pp. 887-902.

Brasier, A.T. Andrews, J.E. Marca-Bell, A.D. and Dennis, P.F. 2010. Depostional continuity of seasonally laminated tufas: Implications for δ18O based palaeotemperatures. *Global and Planetary Change **71***, pp. 160-167.

Braunstein, D. and Lowe, D.R. 2001. Relationship between spring and geyser activity and the deposition and morphology of high temperature (>73^{o}C) siliceous sinter, Yellowstone National Park, Wyoming, U.S.A. *Journal of Sedimentary Research **71***, pp. 747-763.

Brecon Beacons National Park. 2007. *Quarrying of Limestone*. <http://www.breconbeacons.org/content/geopark/understanding/archaeology-industrial-heritage/quarrying-of-limestone> [accessed 28/03/2008].

Briscoe, L.R.E. Harris, T.B. Broussard, W. Dannenberg, E. Oldlay, F.C. and Rajakaruna, N. 2009. Brophytes of adjacent serpentine and granite outcrops on the Deer Isles, Maine, U.S.A. *Rhodora **111***, pp. 1-20.

Brown, M. 2005. The Aberthaw pebble limekilns. *Archive **46***, pp. 19-24.

Burke, I.T. Mortimer, R.J.G Palaniyajndi, S. Whittleston, R.A. Lockwood, C.L. Ashley, D.J. and Stewart, D.I. 2012. Biogeochemical reduction processes in a hyper-alkaline leachate affected soil profile. *Geomicrobiology Journal **29***, pp. 769-779.

Burkhardt, S. Amoroso, G. Riebesell, U. and Sültmeyer, D. 2001. CO_2 and HCO_3^- uptake in marine diatoms acclimated to different CO_2 concentrations. *Limnology and Oceanography **46***, pp. 1378-1391.

Cacchio, P. Contento, R. Ercole, C. Cappuccio, G. Martinez, M.P. and Lepidi, A. 2004. Involvement of microorganisms in the formation of carbonate speleothems in the Cervo Cave (L'Aquila-Italy). *Geomicrobiology Journal **21***, pp. 497-509.

Cailleau, G. Braissant, O. and Verrecchia, E.P. 2011. Turning sunlight into stone: the oxalate-carbonate pathway in a tropical tree ecosystem. *Biogeosciences **8***, pp. 1755-1767.

Canet, C. Prol-Ledesma, R.M. Torres-Alvarado, I. Gilg, H.A. Villanueva, R.E. and Cruz, R.L-S. 2005. Silica-carbonate stromatolites related to coastal hydrothermal venting in Bahía Concepción, Baja California Sur, Mexico. *Sedimentary Geology **174***, pp. 97-113.

Cao, J-H. Zhu, M-J. Huanf, F. and Lu, Q. 2011. Comparison study on calcium forms in plant leaves under different geological backgrounds-a case study in maoian, Guizhou province. *Bullentin of Mineralogy Petrology and Geochemistry **30***, pp. 251-260.

Carr, B.B. Jaworowski, C. and Heasler, H.P. 2010. It's not drying up, just changing. *Yellowstone Science **18***, pp. 15-22.

Carr, M.H. 2012. The fluvial history of Mars. *Philosophical Transactions of the Royal Society A: Mathematical, Physical and Engineering Sciences **370***, pp. 2193-2215.

Carter, N.E.A. and Viles, H.A. 2004. Lichen hotspots: raised rock temperatures beneath *Verrucaria nigrescens* on limestone. *Geomorphology **62***, pp. 1-16.

Carthew, K.D. Taylor, M.P. and Drysdale, R.N. 2006. An environmental model of fluvial tufas in the monsoonal tropics, Barkly karst, northern Australia. *Geomorphology **73***, pp. 78-100.

Castenholz, R.W. 2002. Cyanobacteria. In: Boone, D. and Castenholz, R.W. eds. *Bergey's Manual of Systematic Bacteriology, Vol.1*. Baltimore, Maryland, USA: Williams and Wilkins. pp. 473-599.

Cavalli, G. Riis, T. and Baattrup-Pedersen, A. 2012. Bicarbonate use in three aquatic plants. *Aquatic Botany **98***, pp. 57-60.

Chafetz, H.S. and Buczynski, C. 1992. Bacterially induced lithification of microbial mats. *Palaios 7*, pp. 277-293.

Chafetz, H.S. and Folk, R.L. 1984. Travertines: depositional morphology and the bacterially constructed constituents. *Journal of Sedimentary Research* ***54***, pp. 289-316.

Chafetz, H.S. and Guidry, S.A. 2003. Bacterial shrubs, crystal shrubs, and ray-crystal shrubs: bacterial vs. abiotic precipitation. *Sedimentary Geology* ***126***, pp. 57-74.

Chafetz, H.S. and Guidry, S.A. 2003. Deposition and diagenesis of Mammoth Hot Springs travertine, Yellowstone National Park, Wyoming, U.S.A. *Canadian Journal of Earth Sciences* ***40***, pp. 1515-1529.

Chafetz, H.S. and Meredith, J.C. 1983. Recent travertine pisolites (pisoids) from southeastern Idaho, U.S.A. In: Peryt, T.M. ed. *Coated Grains.* Berlin, Germany: Springer-Verlag. pp. 450-455.

Chambers, P.A. Perpas, E.E. Ferguson, M.E Serediak, M. Guy, M. and Holst, M. 2001. The effects of lime addition on aquatic macrophytes in hard water: *in situ* and microcosm experiments. *Freshwater Biology* ***46***, pp. 1121-1138.

Channing, A. and Edwards, D. 2004. Experimental taphonomy: silicification of plants in Yellowstone hot-spring environments. *Transactions of the Royal Society of Edinburgh: Earth Sciences* ***94***, pp. 503-521.

Channing, A. and Edwards, D. 2008. Silicification of higher plants in geothermally influenced wetlands: Yellowstone as a Lower Devonian Rhynie analog. *Palaios* ***24***, pp. 505-521.

Channing, A. Schweitzer, M.H. Horner, J.R. and McEneaney, T. 2005. A silicified bird from Quaternary hot spring deposits. *Proceedings of the Royal Society B: Biological Sciences* ***272***, pp. 905-911.

Channing, A. and Wujek D.E. 2010. Preservation of protists within decaying plants from geothermally influenced wetlands of Yellowstone National Park, Wyoming, United States. *Palaios* ***25***, pp. 347-355.

Chen, J. Zhang, D.D. Wang, S. Xiao, T. and Huang, R. 2004. Factors controlling tufa deposition in natural waters at waterfall sites. *Sedimentary Geology* ***166***, pp. 353-366.

Childs, A.M. Mountain, B.W. O'Toole, R. and Stott, M.B. 2008. Relating microbial community and physiochemical parameters of a hot spring: Champagne pool, wai-o-tapu, New Zealand. *Geomicrobiology Journal* ***25***, pp. 441-453.

Clark, I.D. Fontes, J.-C. and Fritz, P. 1992. Stable isotope disequilibria in travertine from high pH waters: laboratory investigations and field observations from Oman. *Geochimica et Cosmochimica Acta* ***56***, pp. 2041-2050.

Cleaves II, H.J. and Chalmers, J.H. 2004. Extremophiles may be irrelevant to the origin of life. *Extremophiles* ***4***, pp. 1-9.

Clymo, R.S. 1973. The growth of *Sphagnum*: some effects of environment. *Journal of Ecology* ***61***, pp. 849-869.

Çobanoğlu, İ. and Çelik, S.B. 2012. Determination of strength parameters and quality assessment of Denizli travertines (SW Turkey). *Engineering Geology* ***129-130***, pp. 38-47.

Colmer, T.D. and Voesenek, L.A.C.J. 2009. Flooding tolerance: suites of plant traits in variable environments. *Functional Plant Biology* ***36***, pp. 665-681.

Concha-Lozano, N. Gaudon, P. Pages, J. de Billerbeck, G. Lafon, D. and Eterradossi, O. 2012. Protective effect of endolithic fungal hyphae on oolitic limestone buildings. *Journal of Cultural Heritage* ***13***, pp. 120-127.

Coustau, M. Bouvier, C. Borrell-Estupina, V. and Jourde, H. 2012. Flood modelling with a distributed event-based parsimonious rainfall-runoff model: case of the karstic Lez river catchment. *Natural Hazards and Earth System Science* ***12***, pp. 1119-1133.

Cragg, B.A. Law, K.M. Cramp, A. and Parkes, R.J. 1998. The response of bacterial populations to sapropels in deep sediments of the eastern Mediterranean (site 969). *Proceedings of the Ocean Drilling Program, Scientific Resultsn* ***160***, pp. 303-307.

Cuezva, S. Sanchez-Moral, S. Saiz-Jimenez, C. and Cañaveras, J.C. 2009. Microbial communities and associated mineral fabrics in Altamira Cave, Spain. *International Journal of Speleology* ***38***, pp. 83-92.

Curry, M.D. Boston, P.J. Spilde, M.N. Baichtal, J.F. and Campbell, A.R. 2009. Cottonballs, a unique subaqueous moonmilk, and abundant subaerial moonmilk in Cataract Cave, Tongass National Forest, Alaska. *International Journal of Speleology* ***38***, pp. 111-128.

Dabo, D. Badreddine, R. De Windt, L. and Drouadaine, I. 2009. Ten-year chemical evolution of leachate and municipal solid waste incineration bottom ash used in a test road. *Journal of Hazardous Materials* ***172***, pp. 904-913.

Dandurand, J.L. Gout, R. Hoefs, J. Menschel, G. Schott, J. and Usdowski, E. 1982. Kinetically controlled variations of major components and Carbon and Oxygen isotopes in a calcite-precipitating spring. *Chemical Geology* ***36***, pp. 299-315.

Das, S. and Mohanti, M. 2005. Sedimentology of Holocene tufa carbonates in Orissa State, India. *Carbonates and Evaporites* ***20 (1)***, pp. 8-33.

Davaud, E. and Girardclos, S. 2001. Recent freshwater ooids and oncoids from western Lake Geneva (Switzerland): indications of a common organically mediated origin. *Journal of Sedimentary Research **71***, pp. 423-429.

Davis, W.L. and McKay, C.P. 1996. Origins of life: a comparison of theories and application to Mars. *Origins of Life and Evolution of the Biosphere **26***, pp. 61-73.

Dean, W.E. and Eggleston, J.R. 1984. Freshwater oncolites created by industrial pollution, Onondaga Lake, New York. *Sedimentary Geology **40***, pp. 217-232.

Decho, A.W. and Kawaguchi, T.K. 2003. Extracellular polymers (EPS) and calcification within modern marine stromatolites. In: Krumbein, W.E. Paterson, D.M. and Zavarzin, G.A. eds. *Fossil and Recent Biofilms*. Dordrecht, The Netherlands: Kluwer Academic Publishers. pp. 227-240.

Del Amo, Y. and Brzezinski, M.A. 1999. The chemical form of dissolved Si taken up by marine diatoms. *Journal of Phycology **35***, pp. 1162-1170.

Demars, B.O.L. and Trémolières, M. 2009. Aquatic macrophytes as bioindicators of carbon dioxide in groundwater fed rivers. *Science of The Total Environment **407***, pp. 4752-4763.

Desikachary, T.V. and Dweltz, N.E. 1961. The chemical composition of the diatom frustule. *Proceedings of the Indian Academy of Sciences (Section B) **53***, pp. 157-165.

De Silva, P. Bucea, L. Sirivivatnanon, V. and Moorehead, D.R. 2007. Carbonate binders by “cold sintering” of calcium carbonate. *Journal of Materials Science **42***, pp. 6792-6797.

De Vrind-de Jong, E.W. and De Vrind, J.P.M. 1997. Algal deposition of carbonates and silicates. In: Banfield, J.F. and Nealson, K.H. eds. *Geomicrobiology: Interactions Between Microbes and Minerals*. Washington, DC, USA: Mineralogical Society of America. pp. 267-307.

Di Benedetto, F. Montegrossi, G. Minissale, A. Pardi, L.A. Romanelli, M. Tassi, F. Delgado Huertas, A. Pampin, E.M. Vaselli, O. and Borrini, D. 2011. Biotic and inorganic control on travertine deposition at *Bullicame 3* spring (Viterbo, Italy): a multidisciplinary approach. *Geochimica et Cosmochimica Acta **75***, pp. 4441-4455.

Dickison, W.C. 2000. *Integrative Plant Anatomy*. San Diego, California, USA: Harcourt/Academic Press.

Diekmann, M. and Dupré, C. Acidification and eutrophication of deciduous forests in northwestern Germany demonstrated by indicator species analysis. *Journal of Vegetation Science **8***, pp. 855-864.

Dilsiz, C. Marques, J.M and Carreira, P.M.M. 2004. The impact of hydrological changes on travertine deposits related to thermal springs in the Pammukkale area (SW Turkey). *Environmental Geology **45***, pp. 808-817.

Dorofeev, E.P. 1970. Ice crystals in an underground lake. *Priroda **4***, pp.105.

Dreybrodt, W. Buhmann, D. Michaelis, J. and Usdowski, E. 1992. Geochemically controlled calcite precipitation by CO_2 outgassing: field measurements of precipitation rates in comparison to theoretical predictions. *Chemical Geology **97***, pp. 285-294.

Duan, W. Kotlia, B.S. and Tan, M. 2012. Mineral composition and structure of the stalagmite laminae from Chulerasim cave, Indian Himalaya, and the significance for palaeoclimatic reconstruction. *Quaternary International*, pp. 1-5.

Dubelaar, C.W. Koch, R. Lorenz, H. 1997. Weathering of travertine in a temperate humid climate National Monument, Amsterdam, Netherlands. *Engineering geology and the environment: Proceedings: International Symposium on Engineering Geology and the Environment vol. 3*. Athens, Greece. 23-27 June 2007. pp. 3135-3141.

Dupraz, C. Visscher, P.T. Baumgartner, L.K. and Reid, R.P. 2004. Microbe-mineral interactions: early carbonate precipitation in a hypersaline lake (Eleuthera Island, Bahamas). *Sedimentology **51***, pp. 745-765.

Dupraz, C. Reid, R.P. Braissant, O. Decho, A.W. Norman, R.S. Visscher, P.T. 2009. Processes of carbonate precipitation in modern microbial mats. *Earth Science Reviews **96***, pp. 141-162.

Ekmekci, M. Gunay, G. and Simsek, S. 1995. Morphology of rimstone pools Pamukkale, western Turkey. *Cave and Karst Science **22***, pp. 103-106.

Ellenberg, H. Weber, H.E. Düll, R. Wirth, V. Werner, W. and Paulissen, D. 1991. Zeigerwerte von Pflanzen in Mitteleuropa. *Scripta Geobotanica **18***, pp. 1-248.

Ellis, J. Nicholls, P. Craggs, R. Hofstra, D. and Hewitt, J. 2004. Effects of terrigenous sedimentation on mangrove physiology and associated macrobenthic communities. *Marine Ecology Progress Series **270***, pp. 71-82.

Emery, L.F. 2008. *Life in extreme environments: the morphology, geochemistry and taphonomy of industrially formed cold seep tufa deposits on Black Mountain, South Wales*. Unpublished MESci Thesis. Cardiff University, UK.

Emery, L. Cherns, L. Channing, A. Parkes, J. and Sass, H. 2011. Life on the edge: an industrially created tufa system. *Rendiconti Online Societa Geologica Italiana **16***, pp. 17.

European Space Agency. 2012. The *ExoMars Rover Instrument Suite*. < http://exploration.esa.int/science-e/www/object/index.cfm?fobjectid=45103&fbodylongid=2127> [accessed 18/09/12].

Faccenna, C. Soligo, M. Billi, A. Filippis, L.D. Funiciello, R. 2008. Late Pleistocene depositional cycles of the Lapis Tiburtinus travertine (Tivoli, Central Italy): Possible influence of climate and fault activity. *Global and Planetary Change* ***63***, pp. 299-308.

Fetter, C.W. 1994. *Applied Hydrogeology*. Englewood Cliffs, New Jersey, USA: Prentice-Hall, Inc.

Finsinger, K. Scholz, I. Serrano, A. Morales, S. Uribe-Lorio, L. Mora, M. Sittenfeld, A. Weckesser, J. and Hess, W.R. 2008. Characterization of true-branching cyanobacteria from geothermal sites and hot springs of Costa Rica. *Environmental Microbiology* ***10***, pp. 460-473.

Fiorillo, F. 2009. Spring hydrographs as indicators of droughts in a karst environments. *Journal of Hydrology* ***373***, pp. 290-301.

Flinn, D. and Pentecost, A. 1995. Travertine-cemented screes on the serpentine seacliffs of Unst and Fetlar, Shetland. *Mineralogical Magazine* ***59***, pp. 259-265.

Flügel, E. 2004. *Microfacies of carbonate rocks*. Berlin, Germany: Springer-Verlag.

Folk, R.L. and Chafetz, H.S. 1983. Pisoliths (pisoids) in Quaternary travertines of Tivoli, Italy. In: Peryt, T.M. ed. *Coated Grains.* Berlin, Germany: Springer-Verlag. pp. 474-487.

Folk, R.L. Chafetz, H.S. and Tiezzi, P.A. 1985. Bizarre forms of depositional and diagenetic calcite in hot springs, central Italy. In: Schneidermann, N. and Harris, P. eds. *Carbonate Cements***.** Tulsa, Oklahoma, USA: Society of Economic Palaeontologists and Mineralogists. pp. 349-369.

Ford, T.D. 1989. Tufa – the whole dam story. *Cave and Karst Science* ***16***, pp. 39-49.

Ford, T.D. and Pedley, H.M. 1996. A review of tufa and travertine deposits of the world. *Earth-Science Reviews* ***41***, pp. 117-175.

Ford, D. and Williams, P. 2007. *Karst Hydrogeology and Geomorphology*. Chichester, UK: John Wiley & Sons.

Fouke, B.W. 2001. Depositional facies and aqueous-solid geochemistry of travertine-depositing hot springs (Angel Terrace, Mammoth Hot Springs, Yellowstone National Park, U.S.A.)-reply. *Journal of Sedimentary Petrology* ***71***, pp. 497-500.

Fouke, B.W. 2011. Hot-spring systems geobiology: abiotic and biotic influences on travertine formation at Mammoth Hot Springs, Yellowstone National Park, USA. *Sedimentology* ***58***, pp. 170-219.

Fouke, B.W. Bonheyo, G.T. Sanzenbacher, B. and Frias-Lopez, J. 2003. Partitioning of bacterial communities between travertine depositional facies at Mammoth Hot Springs, Yellowstone National Park, U.S.A. 2003. *Canadian Journal of Earth Sciences* ***40***, pp. 1531-1548.

Fouke, B.W. Farmer, J.D. Des Marais, D.J. Pratt, L. Sturchio, N.C. Burns, P.C. and Discipulo, M.K. 2000. Depositional facies and aqueous-solid geochemistry of travertine-depositing hot springs (Angel Terrace, Mammoth Hot Springs, Yellowstone National Park, U.S.A.). *Journal of Sedimentary Research* ***70***, pp. 565-585.

Freytet, P. and Verrecchia, E.P. 1996. Discovery of Ca oxalate crystals associated with fungi in moss travertines (bryoherms, freshwater heterogeneous stromatolites). *Geomicrobiology Journal* ***13***, pp. 117-127.

Freytet, P. and Verrecchia, E.P. 1998. Freshwater organisms that build stromatolites: a synopsis of biocrystallization by prokaryotic and eukaryotic algae. *Sedimentology* ***45***, pp. 535-563.

Freytet, P. and Verrecchia, E.P. 1999. Calcitic radial palisadic fabric in freshwater stromatolites: diagenetic and recrystallized feature or physicochemical sinter crust? *Sedimentary Geology* ***126***, pp. 97-102.

Friedman, G.M. 1965. Terminology of crystallization textures and fabrics in sedimentary rocks. *Journal of Sedimentary Research* ***35***, pp. 643-655.

Friedmann, E.I. 1982. Endolithic microorganisms in the Antarctic cold desert. *Science* ***215***, pp. 1045-1053.

Fritsch, F.E. and Pantin, C.F.A. 1946. Calcareous concretions in a Cambridgeshire stream. *Nature* ***157***, pp. 397-399.

Fryer, P. 2012. Serpentinite mud volcanism: observations, processes, and implications. *Annual Review of Marine Science* ***4***, pp. 345-373.

Genty, D. Konik, S. Valladas, H. Blamart, D. Hellstrom, J. Touma, M. Moreau, C. Dumoulin, J-P. Nouet, J. Dauphin, Y. and Weil, R. 2011. Dating the Lascaux cave gour formation. *Radiocarbon* ***53***, pp. 479-500.

Goh, F. Allen, M.A. Leuko, S. Kawaguchi, T. Decho, A.W. Burns, B.P. and Neilan B.A. 2008. Determining the specific microbial populations and their spatial distribution within the stromatolite ecosystem of Shark Bay. *The ISME Journal* ***3***, pp. 383-396.

Goin, J.C. and Cady, S.L. 2009. Biosedimentological processes that produce hot spring sinter biofabrics: examples from the Uzon Caldera, Kamchatka Russia. In: Seckbach, J. and Walsh, M. eds. *From Fossils to Astrobiology*. Berlin, Germany: Springer Science + Business Media B.V. pp. 159-179.

Goldenfeld, N. Chan, P.Y. and Veysey, J. 2006. Dynamics of presipitation pattern formation at geothermal hot springs. *Physical Review Letters* ***96***, pp. 1-4.

Gómez, F. Rodríguez-Manfredi, J.A. Rodríguez, N. Fernández-Sampedro, F.J. Caballero-Castrejón, F.J. and Amils, R. in press. Habitability: where to look for life? Halophilic habitats: Earth analogs to study Mars habitability. *Planetary and Space Science*

Gómez-Heras, M. Smith, B.J. and Fort, R. 2006. Surface temperature differences between minerals in crystalline rocks: implications for granular disaggregation of granites through thermal fatigue. *Geomorphology **78***, pp. 236-249.

Górka, M. Sauer, P.E. Lewicka-Szczebak, D. and Jędrysek, M-O. 2011. Carbon isotope signature of dissolved inorganic carbon (DIC) in precipitation and atmospheric CO_2. *Environmental Pollution **159***, pp. 294-301.

Gradziński, M. 2010. Factors controlling growth of modern tufa: results of a field experiment. In: Pedley, H.M. and Rogerson, M. eds. *Tufas and Speleothems: Unravelling the Microbial and Physical Controls*. London, UK: The Geological Society. pp. 143-191.

Grant, W.D. and Tindall, B.J. 1986. The alkaline saline environment. In: Herbert, R.A. and Codd, G.A. (eds.) *Microbes in Extreme Environments*. Orlando, Florida, USA: Society for General Microbiology. pp. 25-54.

Grant, W.D. Mwatha, W.E. and Jones, B.E. 1990. Alkaliphiles: ecology, diversity and applications. *FEMS Microbiology Reviews **75***, pp. 255-270.

Groth, I. Schumann, P. Laiz, L. Sanchez-Moral, S. Cañaveras, J.C. and Saiz-Jimenez, C. 2001. Geomicrobiological study of the Grotta dei Cervi, Porto Badisco, Italy. *Geomicrobiology Journal **18***, pp. 241-258.

Guidry, S.A. and Chafetz, H.S. 2003a. Anatomy of siliceous hot springs: examples from Yellowstone National Park, Wyoming, USA. *Sedimentary Geology **157***, pp. 71-106.

Guidry, S.A. and Chafetz, H.S. 2003b. Siliceous shrubs in hot springs from Yellowstone National Park, Wyoming, U.S.A. *Canadian Journal of Earth Sciences **40***, pp. 1571-1583.

Guo, L. 1993. *Fabrics and facies of Quaternary travertines, Rapolano Terme, central Italy*. Unpublished PhD Thesis. University of Wales, Cardiff.

Guo, L. Andrews, J. Riding, R. Dennis, P. and Dresser, Q. 1996. Possible microbial effects on stable carbon isotopes in hot-spring travertines. *Journal of Sedimentary Research **66***, pp. 468-473.

Guo, L. and Riding, R. 1992. Micritic aragonite laminae in hot water travertine crusts, Rapolano Terme, Italy. *Sedimentology **39***, 1067-1079.

Guo, L. and Riding, R. 1994. Origin and diagenesis of Quaternary travertine shrub fabrics, Rapolano Terme, central Italy. *Sedimentology **41***, pp. 499-520.

Guo, L. and Riding, R. 1998. Hot-spring travertine facies and sequences, Late Pleistocene, Rapolano Terme, Italy. *Sedimentology **45***, pp. 163-180.

Guo, L. and Riding, R. 1999. Rapid facies change in Holocene fissure ridge hot spring travertines, Rapolano Terme, Italy. *Sedimentology **46***, pp. 1145-1158.

Hájkova, P. Grootjans, A. Lamentowicz, M. Rybníčková, E. Madaras, M. Opravilová, V. Michaelis, D. Hájek, M. Joosten, H. and Wolejko, L. 2012. How a *Sphagnum fuscum*-dominated bog changed into a calcareous fen: the unique Holocene history of a Slovak spring-fed mire. *Journal of Quaternary Science **27***, pp. 233-243.

Hall, K. and Hall, A. 1991. Thermal gradients and rock weathering at low temperatures: some simulation data. *Permafrost & Periglacial Processes **2***, pp. 103-112.

Hamm, C.E. Merkel, R. Springer, O. Jurkojc, P. Maier, C. Prechtel, K. and Smetacek, V. 2003. Architecture and material properties of diatom shells provide effective mechanical protection. *Nature **421***, pp. 841-843.

Hammer, Ø. Dysthe, D.K. and Jamtveit, B. 2007. The dynamics of travertine dams. *Earth and Planetary Science Letters **256***, pp. 258-263.

Hammer, Ø. Dysthe, D.K. and Jamtveit, B. 2010. Travertine terracing: patterns and mechanisms. In: Pedley, H.M. and Rogerson, M. eds. *Tufas and Speleothems: Unravelling the Microbial and Physical Controls*. London, UK: The Geological Society. pp. 283-294.

Hammer, Ø. Jamtveit, B. Benning L.G. and Dysthe, D.K. 2005. Evolution of fluid chemistry during travertine formation in the Troll thermal springs, Svalbard, Norway. *Geofluids **5***, pp. 140-150.

Hand, E. 2012. Dreams of water on Mars evaporate. *Nature **484***, pp. 153.

Handley, K.M. Turner, S.J. Campbell, K.A. and Mountain B.W. 2008. Silicifying biofilm exopolymers on a hot-spring microstromatolite: templating nanometer-thick laminae. *Astrobiology **8***, pp. 747-770.

Harris, P.M. Kendall, C.G.St.C. and Lerche, I. 1985. Carbonate cementation – a brief review. In: Schneidermann, N. and Harris, P.M. eds. *Carbonate Cements*. Tulsa, Oklahoma, USA: Society of Economic Palaeontologist and Mineralogists, pp. 79-95.

Hemida, S.K. 2005. Fungal and bacterial populations in cement-incorporated soil. *International Journal of Agriculture & Biology **7***, pp. 158-161.

Herman, J.S. and Lorah, M.M 1987. CO_2 outgassing and calcite precipitation in Falling Spring Creek, Virginia, U.S.A. *Chemical Geology **62***, pp. 251-262.

Hill, C. and Forti, P. 1997a. *Cave Minerals of the World*. Huntsville, Alabama, USA: National Speleological Society.

Hill, C. and Forti, P. 1997b. Speleothem growth rates. In: Hill, C. and Forti, P. eds. *Cave Minerals of The World*. Huntsville, Alabama, USA: National Speleological Society, pp. 285-287.

Hill, M.O. Mountford, J.O. Roy, D.B. and Bunce, R.G.H. 1999. *ECOFACT 2a Technical Annex – Ellenberg's indicator values for British Plants*. ISBN: 1 870393 48 1. (http://www.ceh.ac.uk/products/publications/untitled.html) [accessed 25/06/12]

Hœrlé, S. 2006. Rock temperatures as an indicator of weathering processes affecting rock art. *Earth Surface Processes and Landforms* ***31***, pp. 383-389.

Holm, Jr., G.O. Bevington, A.E. Twilley, R.R. and Sasser, C.E. 2008. *Sediment elevation and plant community change during rapid delta growth*. [Poster] Louisiana State University (http://www.clear.lsu.edu/pdfs/clear_poster_20081010150821.pdf) [accessed 09/06/12]

Holm, N.G. 2012. The significance of Mg in prebiotic history. *Geobiology* ***10***, pp. 269-279.

Holm, N.G. and Baltscheffsky, H. 2011. Links between hydrothermal environments, pyrophosphate, Na^{+}, and early evolution. *Origins of Life and Evolution of the Biosphere* ***41***, pp. 483-493.

Houseal, A.K. Fouke, B.W. Sanford, R. Fuhrmann, R. and Petrick, E. 2010. Mammoth Hot Springs where change is constant. *Yellowstone Science* ***18***, pp.7-14.

Hubbard, L.M.L. and Hubbard, J.P. 1984. Kinetic studies of the rate of dissolution of silica and diatom tests in sea water. *Journal of the Oceanographic Society of Japan* ***40***, pp. 148-154.

Hyndman, R.D. and Peacock, S.M. 2003. Serpentinization of the forearc mantle. *Earth and Planetary Science Letters* ***212***, pp. 417-432.

Ikner, L.A. Toomey, R.S. Nolan, G. Neilson, J.W. Pryor, B.M. and Maier, R.M. 2007. Culturable microbial diversity and the impact of tourism in Kartchner Caverns, Arizona. *Microbial Ecology* ***53***, pp. 30-42.

Ilomets, M. Truus, L. Pajula, R. and Sepp, K. 2010. Species composition and structure of vascular plants and bryophytes on the water level gradient within a calcareous fen in North Estonia. *Estonian Journal of Ecology* ***61***, pp. 19-38.

Islam, M.R. and Schulze-Makuch, D. 2007. Adaptations to environmental extremes by multicellular organisms. *International Journal of Astrobiology* ***6***, pp. 199-215.

James, W.F. 2008. Effects of lime-induced inorganic carbon reduction on the growth of three aquatic macrophyte species. *Aquatic Botany* ***88***, pp. 99-104.

Janssen, A. Swennen, R. Podoor, N. and Keppens, E. 1999. Biological and diagenetic influence in recent and fossil tufa deposits from Belgium. *Sedimentary Geology* ***126***, pp. 75-95.

Jenkins, K.A. and Smith, B.J. 1990. Daytime rock surface temperature variability and its implications for mechanical rock weathering: Tenerife, Canary Islands. *Catena* ***17***, pp. 449-459.

Jettestuen, E. Jamtveit, B. Podladchikov, Y.Y. deVilliers, S. Amundsen, H.E.F. and Meakin, P. 2006. Growth and characterization of complex mineral surfaces. *Earth and Planetary Science Letters* ***249***, pp. 108-118.

Jolley, R.L. Lockaby, B.G. Cavalcanti, G.G. 2010. Changes in riparian forest composition along a sedimentation rate gradient. *Plant Ecology* ***210***, pp. 213-224.

Jones, B. 1989. Calcite rafts, peloids, and micrite in cave deposits from Cayman Brac, British West Indies. *Canadian Journal of Earth Sciences* ***26***, pp. 654-664.

Jones, B. 1991. Genesis of terrestrial oncoids, Cayman Islands, British West Indies. *Canadian Journal of Earth Sciences* ***28***, pp. 382-397.

Jones, B. 2001. Microbial activity in caves – a geological perspective. *Geomicrobiology Journal* ***18***, pp. 345-357.

Jones, B. 2009. Cave pearls – the integrated product of abiogenic and biogenic processes. *Journal of Sedimentary Research* ***79***, pp. 689-710.

Jones, B. 2010. Microbes in caves: agents of calcite corrosion and precipitation. In: Pedley, H.M and Rogerson, M. eds. *Tufas and Speleothems: Unravelling the Microbial and Physical Controls*. London, UK: The Geological Society. pp. 7-30.

Jones, B. and Peng, X. 2012. Amorphous calcium carbonate associated with biofilms in hot spring deposits. *Sedimentary Geology* ***269-270***, pp. 58-68.

Jones, B. and Renaut, R.W. 1994. Crystal fabrics and microbiota in large pisoliths from Laguna Pastos Grandes, Bolivia. *Sedimentology* ***41***, pp. 1171-1202.

Jones, B. and Renaut, R.W. 1995. Noncrystallographic calcite dendrites from hot-spring deposits at Lake Bogoria, Kenya. *Journal of Sedimentary Research A* ***65***, pp. 154-169.

Jones, B. and Renaut, R.W. 1997. Formation of silica oncoids around geysers and hot springs at El Tatio, northern Chile. *Sedimentology* ***44***, pp. 287-304.

Jones, B. and Renaut, R.W. 2009. Calcareous spring deposits in continental settings. *Developments in Sedimentology* ***61***, pp. 177-224.

Jones, B. and Renaut, R.W. 2010. Calcareous Spring Deposits in Continental Settings. In: Alonso-Zarza, A.M. and Tanner, L.H. eds. 2010. *Carbonates In Continental Settings*. Amsterdam, The Netherlands: Elsevier. pp. 177-224.

Jones, B. Renaut, R.W. and Konhauser, K.O. 2005. Genesis of large siliceous stromatolites at Frying Pan Lake, Waimangu geothermal field, North Island, New Zealand. *Sedimentology **52***, pp. 1229-1252.

Jones, B. Renaut, R.W. and Owen, R.B. 2011. Life cycle of a geyser discharge apron: evidence from Waikite Geyser, Whakarewarewa geothermal area, North Island, New Zealand. *Sedimentary Geology **236***, pp. 77-94.

Jones, B. Renaut, R.W. and Rosen, M.R. 1999. Actively growing siliceous oncoids in the Waiotapu geothermal area, North Island, New Zealand. *Journal of the Geological Society **156***, pp. 89-103.

Jones, B. Renaut, R.W. and Rosen, M.R. 2000. Trigonal dendritic calcite crystals forming from hot spring waters at Waikite, North Island, New Zealand. *Journal of Sedimentary Research **70***, pp. 586-603.

Jones, B. Renaut, R.W. and Rosen, M.R. 2001. Microbial construction of siliceous stalactites at geysers and hot springs: examples from the Whakarewarewa Geothermal Area, North Island, New Zealand. *Palaios **16***, pp. 73-94.

Jones, F.G. and Wilkinson, B.H. 1978. Structure and growth of lacustrine pisoliths from recent Michigan Marl lakes. *Journal of Sedimentary Petrology **48***, pp. 1103-1110.

Justin, S.H.F.W. and Armstrong, W. 1987. The anatomical characteristics of roots and plant response to soil flooding. *New Phytologist **106***, pp. 465-495.

Kano, A. Matsuoka, J. Kojo, T. and Fujii, H. 2003. Origin of annual laminations in tufa deposits, southwest Japan. *Palaeogeography, Palaeoclimatology, Palaeoecology **191***, pp. 243-262.

Kawai, T. Kano, A. Matsuoka, J. and Ihara, T. 2006. Seasonal variation in water chemistry and depositional processes in a tufa-bearing stream in SW-Japan, based on 5 years of monthly observations. *Chemical Geology **232***, pp. 33-53.

Kawai, T. Kano, A. and Hori, M. 2009. Geochemical and hydrological controls on biannual lamination of tufa deposits. *Sedimentary Geology **213***, pp. 41-50.

Kendall, A.C. and Tucker, M.E. 1973. Radaxial fibrous calcite: a replacement after acicular carbonate. *Sedimentology **12***, pp. 365-389.

Kendall, A.C. 1985. Radiaxial fibrous calcite: a reappraisal. In: Schneidermann, N. and Harris, P.M. eds. *Carbonate Cements*. Tulsa, Oklahoma, USA: Society of Economic Palaeontologist and Mineralogists, pp. 59-77.

Kharaka, Y.K. Sorey, M.L. and Thorsden, J.J. 2000. Large-scale hydrothermal fluid discharges in the Norris-Mammoth corridor, Yellowstone National Park, USA. *Journal of Geochemical Exploration* ***69-70***, pp. 201-205.

Kitching, D. 2012. *Limekiln Database: Wales*. < http://www.brocross.com/industrial%20history/database/limekiln%20data%20wales.htm> [accessed 13/04/2012]

Knoll, A.H. and Grotzinger, J. 2006. Water on Mars and the prostect of martian life. *Elements* ***2***, pp. 169-173.

Koban, C.G. and Schweigert, G. 1993. Microbial origin of travertine fabrics - two examples from Southern Germany (Pleistocene Stuttgart travertines and Miocene riedöschingen Travertine). *Facies* ***29***, pp. 251-263.

Kodolányi, J. Pettke, T. Spandler, C. Kamber, B.S. and Ling, K.G. 2012. Geochemistry of ocean floor and fore-arc serpentinites: constraints on the ultramafic input to subduction zones. *Journal of Petrology* ***53***, pp. 235-270.

Konhauser, K.O. Jones, B. Reysenbach, A.-L. and Renaut, R.W. 2003. Hot spring sinters: keys to understanding Earth's earliest life forms. *Canadian Journal of Earth Sciences* ***40***, pp. 1713-1724.

Konings, W.N. Tolner, B. Speelmans, G. Elferink, M.G.L. de Wit, J.G. and Driessen, A.J.M. 1992. Energy transduction and transport processes in thermophilic bacteria. *Journal of Bioenergetics and Biomembranes* ***24***, 601–609.

Kula, J. and Baldwin, S.L. 2012. On hematite as a target for dating aqueous conditions on Mars. *Planetary and Space Science* ***67***, pp. 101-108.

Kullberg, R.G. 1982. Algal succession in a hot spring community. *American Midland Naturalist* ***108***, pp. 224-244.

Kramers, J.D. 2003. Volatile element abundance patterns and an early liquid water ocean on Earth. *Precambrian Research* ***126***, pp. 379-394.

Krulwich, T.A. and Guffanti, A.A. 1992. Proton-coupled bioenergetic processes in extremely alkaliphilic bacteria. *Journal of Bioenergetics and Biomembranes* ***24***, pp. 587-599.

Krulwich, T.A. Ito, M. Gilmour, R. Hicks, D.B. and Guffanti, A.A. 1997. Mechanisms of cytoplasmic pH regulation in alkaliphilic strains of *Bacillus*. *Extremophiles* ***1***, pp. 163-170.

Krulwich, T.A. Ito, M. and Guffanti, A.A. 2001. The Na^+ - dependence of alkaliphily in *Bacillus*. *Biochimica et Biophysica Acta: Bioenergetics* ***1505***, pp. 158-168.

Krulwich, T.A. Ito, M. Hicks, D.B. Gilmour, R. and Guffanti, A.A. 1998. pH homeostasis and ATP synthesis: studies of two processes that necessitate inward proton translocation in extremely alkaliphilic *Bacillus* species. *Extremophiles* ***2***, pp. 217-222.

Kützing, F.T. 1833. Synopsis diatomearum oder Versuch einer systematischen zussamenstellung der diatomeen. *Linnaea* ***8***, pp. 529-620.

Labat, D. Masbou, J. Beaulieu, E. and Mangin, A. 2011. Scaling behaviour of the fluctuations in stream flow at the outlet of karstic watersheds, France. *Journal of Hydrology* ***410***, pp. 162-168.

Laiz, L. Groth, I. Schumann, P. Zezza, F. Felske, A. Hermosin, B. and Saiz-Jimenez, C. 2000. Microbiology of the stalactites from Grotta Dei Cervi, Porto Badisco, Italy. *International Microbiology* ***3***, pp. 25-30.

Langmuir, D. 1997. *Aqueous Environmental Geochemistry*. New Jersey, U.S.A.: Prentice Hall.

Lauritzen, S-E. and Lundberg, J. 1999. Speleothems and climate: a special issue of The Holocene. *The Holocene* ***9***, pp. 643-647.

Lee, E.S. and Krothe, N.C. 2001. A four-component mixing model for water in a karst terrain in south-central Indiana, USA. Using solute concentration and stable isotopes as tracers. *Chemical Geology* ***179***, pp. 129-143.

Lee, M.A. and Power, S.A. 2013. Direct and indirect effects of roads and road vehicles on the plant community composition of calcareous grasslands. *Environmental Pollution* ***176***, pp. 106-113.

Leemann, A. Le Saout, G. Winnefeld, F. Rentsch, D. and Lothenbach, B. 2011. Alkali-silica reaction: the influence of calcium on silica dissolution and the formation of reaction products. *Journal of the American Ceramic Society* ***94***, pp. 1243-1249.

Legatzki, A. Ortiz, M. Neilson, J.W. Dominguez, S. Andersen, G.L. Toomey, R.S. Pryor, B.M. Pierson III, L.S. and Maier, R.M. 2011. Bacterial and archaeal community structure of two adjacent calcite speleothems in Kartchner Caverns, Arizona, USA. *Geomicrobiology Journal* ***28***, pp. 99-117.

Leoni, B. Morabito, G. Rogora, M. Pollastro, D. Mosello, R. Arisci, S. Forasacco, E. and Garibaldi, L. 2007. Response of planktonic communities to calcium hydroxide addition in a hardwater eutrophic lake: results from a mesocosm experiment. *Limnology* ***8***, pp. 121-130.

Léveillé, R. 2010. A half-century of terrestrial analog studies: from craters on the Moon to searching for life on Mars. *Planetary and Space Science* ***58***, pp. 631-638.

Liu, L. Chen, X. Xu, G. and Shu, L. 2011. Use of hydrologic time-series data for identification of hydrodynamic function and behaviour in a karstic water system in China. *Hydrogeology Journal* ***19***, pp. 1577-1585.

Liu, B. Liu, Z. and Wang, L. 2012. The colonisation of active sand dunes by rhizomatous plants through vegetative propagation and its role in vegetation restoration. *Ecological Engineering* ***44***, pp. 344-347.

Liu, Z. Sun, H. Baoying, L. Xianling, L. Wenbing, Y. and Cheng, Z. 2010. Wet-dry season variations of hydrochemistry and carbonate precipitation rates in a travertine-depositing canal at Baishuitai, Yunnan, SW China: Implications for the formation of biannual laminae in travertine and for climatic reconstruction. *Chemical Geology* ***273***, pp. 258-266.

Liu, Z. Svensson, U. Dreybrodt, W. Daoxian, Y. and Buhmann, D. 1995. Hydrodynamic control of inorganic calcite precipitation in Hunaglong Ravine, China: field measurements and theoretical prediction of deposition rates. *Geochimica et Cosmochimica Acta* ***59***, pp. 3087-3097.

López-Archilla, A.I. Moreira, D. López-Archilla, P. and Guerrero, C. 2004. Phytoplankton diversity and cyanobacterial dominance in a hypereutrophic shallow lake with biologically produced alkaline pH. *Extremophiles* ***8***, pp. 109-115.

Love, K.M. and Chafetz, H.S. 1988. Diagenesis of laminated travertine crusts, Arbuckle Mountains, Oklahoma. *Journal of Sedimentary Petrology* ***58***, pp. 441-445.

Lowe, B.J. Watts, R.J. Roberts, J. and Robertson, A. 2010. The effect of experimental inundation and sediment deposition on the survival and growth of two herbaceous riverbank plant species. *Plant Ecology* ***209***, pp. 57-69.

Lowenstern, J.B. Bergfeld, D. Evans, W.C. and Hurwitz, S. 2012. Generation and evolution of hydrothermal fluids at Yellowstone: insights from the Heart Lake Geyser Basin. *Geochemistry, Geophysics, Geosystems* ***13***, art. no. Q01017

Loucaides, S. van Cappellen, P. Roubeix, V. Moriceau, B. and Ragueneau, O. 2012. Controls on the recycling and preservation of biogenic silica from biomineralization to burial. *Silicon* ***4***, pp. 7-22.

Lu, G. Zheng, C. Donahoe, R.J. and Berry Lyons, W. 2000. Controlling processes in a CaCO3 precipitating stream in Huanglong Natural Scenic District, Sichuan, China. *Journal of Hydrology* ***230***, pp. 34-54.

Lucassen, E.C.H.E.T. Bobbink, R. Oonk, M.M.A. Brandrud, T-E. and Roelofs, J.G.M. 1999. The effect of liming and reacidification on the growth of *Juncus bulbossus*: a mesocosm experiment. *Aquatic Botany* ***64***, pp. 95-103.

Luetscher, M. and Jeannin, P-Y. 2004. A process-based classification of alpine ice caves. *Theoretical and Applied Karstology* ***17***, pp. 5-10.

Lunine, J.I. 2006. Physical conditions on the early Earth. *Philosophical Transactions of the Royal Society B: Biological Sciences* ***361***, pp. 1721-1731.

Maguire, R.O. Hesterberg, D. Gernat, A. Anderson, K. Wineland, M. and Grimes, J. 2006. Liming poultry manures to decrease soluble phosphorus and suppress the bacteria population. *Journal of Environmental Quality* ***35***, pp. 849-857.

Malusa, J. Overby, S.T. and Parnell, R.A. 2003. Potential for travertine formation: Fossil Creek, Arizona. *Applied Geochemistry* ***18***, pp. 1081-1093.

Manzo, E. Perri, E. and Tucker, M.E. 2012. Carbonate deposition in a fluvial tufa system: processes and products (Corvino Valley – southern Italy). *Sedimentology* ***59***, pp. 553-577.

Marques, J.M. Carreira, P.M. Carvalho, M.R. Matias, M.J. Goff, F.E. Basto, M.J. Graça, R.C. Aires-Barros, L. and Rocha, L. 2008. Origins of high pH mineral waters from ultramafic rocks, Central Portugal. *Applied Geochemistry* ***23***, pp. 3278-3289.

Mattock, G. 1961. *pH Measurement and Titration*. London, UK: Spottiswoode, Ballantyne and Co. Ltd.

McDonald, I. and Viljoen, K.S. 2006. Platinum-group element geochemistry of mantle eclogites: a reconnaissance study of xenoliths from the Orapa kimberlite, Botswana. *Transactions of the Institutions of Mining and Metallurgy, Section B: Applied Earth Science* ***115***, pp. 81-93.

McCleskey, R.B. 2011. Electrical conductivity of electrolytes found in natural waters from (5 to 90) °C. *Journal of Chemical & Engineering Data* ***56***, pp. 317-327.

McLoughlin, N. Wilson L.A. and Brasier, M.D. 2008. Growth of synthetic stromatolites and wrinkle structures in the absence of microbes – Implications for the early fossil record. *Geobiology* ***6***, pp. 95-105.

Merz-Preiß, M. and Riding, R. 1999. Cyanobacterial tufa calcification in two freshwater streams: ambient environment, chemical thresholds and biological processes. *Sedimentary Geology* ***126***, pp. 103-124.

Miao, S.L. and Zou, C.B. 2012. Effects of inundation on growth and nutrient allocation of six major macrophytes in the Florida Everglades. *Ecological Engineering* ***42***, pp. 10-18.

Michaelis, J. Usdowski, E. and Menschel, G. 1985. Partitioning of ^{13}C and ^{12}C on the degassing of CO_2 and the precipitation of calcite: Rayleigh-type fractionation and a kinetic model. *American Journal of Science* ***285***, pp. 318-327.

Milligan, A.J. and Morel, F.M.M. 2002. A proton buffering role for silica in diatoms. *Science* ***297***, pp. 1848-1850.

Mony, C. Mercier, E. Bonis, A. and Bouzillé, J.B. 2010. Reproductive strategies may explain plant tolerance to inundation: a mesocosm experiment using six marsh species. *Aquatic Botany* ***92***, pp. 99-104.

Mountain, B.W. Benning, L.G. and Boerema, J.A. 2003. Experimental studies on New Zealand hot spring sinters: rates of growth and textural development. *Canadian Journal of Earth Sciences* ***40***, pp. 1643-1667.

Nakata, P.A. 2012. Plant calcium oxalate crystal formation, function, and its impact on human health. *Frontiers in Biology* ***7***, pp. 254-266.

Neal, C. and Stanger, G. 1983. Hydrogen generation from mantle source rocks in Oman. *Earth and Planetary Science Letters* ***66***, pp. 315-320.

Norris, T.B. and Castenholz, R.W. 2006. Endolithic photosynthetic communities within ancient and recent travertine deposits in Yellowstone National Park. *FEMS Microbiology Ecology* ***57***, pp. 470-483.

Northup, D.E. Reysenbach, A-L. and Pace, N.R. 1997. Microorganisms and speleothems. In: Hill, C. and Forti, P. eds. *Cave Minerals of The World*. Huntsville, Alabama, USA: National Speleological Society.

Okland, I. Huang, S. Dahle, H. Thorseth, I.H. and Pedersen, R.B. 2012. Low temperature alteration of serpentinized ultramafic rock and implications for microbial life. *Chemical Geology* ***318-319***, pp. 75-87.

Okumura, T. Takashima, C. Shiraishi, F. Akmaluddin and Kano, A. 2012. Textural transition in an aragonite travertine formed under various flow conditions at Pancuran Pitu, Central Java, Indonesia. *Sedimentary Geology* ***265-266***, pp. 195-209.

Okumura, T. Takashima, C. Shiraishi, F. Nishida, S. Yukimura, K. Naganuma, T. Koike, H. Arp, G. and Kano, A. 2011. Microbial processes forming daily lamination in an aragonite travertine, Nagano-yu Hot Spring, Southwest Japan. *Geomicrobiology Journal* ***28***, pp. 135-148.

Olaleye, V.F. and Oluyemi, E.A. 2010. Effects of cement flue dusts from a Nigerian cement plant on air, water and planktonic quality. *Environmental Monitoring and Assessment* ***162***, pp. 153-162.

O'Neil, J.R. and Barnes, I. 1971. C^{13} and O^{18} compositions in some fresh-water carbonates associated with ultramafic rocks and serpentinites: western United States. *Geochimica et Cosmochimica Acta* ***35***, pp. 687-697.

Orradottir, B. Archer, S.R. Arnalds, O. Wilding, L.P. and Thurow, T.L. 2008. Infiltration in Icelandic andisols: the role of vegetation and soil frost. *Arctic, Antarctic, and Alpine Research* ***40***, pp. 412-421.

Oze, C. and Sharma, M. 2006. Serpentinization and the inorganic synthesis of H2 in planetary surfaces. *Icarus* ***186***, pp. 557-561.

Özkul, M. Varol, B. and Alçiçek, C. 2002. Depositional environments and petrography of Denizli travertines. *Mineral Research and Exploration Bulletin* ***125***, pp. 13-29.

Padan, E. Bibi, E. Ito, M. and Krulwich, T.A. 2005. Alkaline pH homeostasis in bacteria: new insights. *Biochimica et Biophysica Acta – Biomembranes* ***1717***, pp. 67-88.

Pan, Y. Xie, Y. Chen, X. and Li, F. 2012. Effects of flooding and sedimentation on the growth and physiology of two emergent macrophytes from Dongting Lake wetlands. *Aquatic Botany* ***100***, pp. 35-40.

Pasvanoğlu, S. and Chandrasekharam, D. 2011. Hydrogeochemical and isotopic study of thermal and mineralized waters from the Nevşehir (Kozakli) area, Central Turkey. *Journal of Volcanology and Geothermal Research* ***202***, pp. 241-250.

Pawar, N.J. and Kale, V.S. 2006. Waterfall tufa deposits from the Deccan Basalt Province, India: Implications for weathering of basalts in the semi-arid Tropics. *Zeitschrift fur Geomorphologie, Supplementband* ***145***, pp. 17-36.

Pearce, J.M. Kirby, G.A. Lacinska, A. Bateson, L. Wagner, D. Rochelle, C.A. and Cassidy, M. 2011. Reservoir-scale CO2-fluid rock interactions: preliminary results from field investigations in the Pardox Basin, Southeast Utah. *Energy Procedia* ***4***, pp. 5058-5065.

Pedley, H.M. 1987. The Flandrian (Quaternary) Caerwys Tufa, North Wales: an ancient barrage tufa deposit. *Proceedings of the Yorkshire Geological Society* ***46***, pp. 141-152.

Pedley, H.M. 1990. Classification and environmental models of cool freshwater tufas. *Sedimentary Geology* ***68***, pp. 143-154.

Pedley, H.M. 1993. Sedimentology of the late Quaternary barrage tufas in the Wye and Lathkill valleys, north Derbyshire. *Proceedings of the Yorkshire Geological Society* ***49***, pp. 197-206.

Pedley, H.M. 2000. Ambient temperature freshwater microbial tufas. In: Riding, R.E. and Awramik, S.M. eds. *Microbial Sediments*. Berlin, Germany: Springer. pp. 179-186.

Pedley, H.M. 2009. Tufas and travertines of the Mediterranean region: a testing ground for freshwater carbonate concepts and developments. *Sedimentology* ***56***, pp. 221-246.

Pedley, H.M. 2011. Form and function of the freshwater (tufa) microbial biofilm. *Rendiconti Online Societa Geologica Italiana* ***16***, pp. 27.

Pedley, H.M. González Martín, J.A. Ordónez Delgado, S. García Del Cura, M.Á. 2003. Sedimentology of quaternary perched springline and paludal tufas: criteria for recognition, with examples from Guadalajara Province, Spain. *Sedimentology **50***, pp. 23-44.

Pedley, H.M. and Rogerson, M. 2010a. Introduction to tufas and speleothems. In: Pedley, H.M. and Rogerson, M. eds. *Tufas and Speleothems: Unravelling the Microbial and Physical Controls*, London, UK: Geological Society Special Publications. pp. 1-5.

Pedley, H.M. and Rogerson, M. 2010b. *In vitro* investigations of the impact of different temperature and flow velocity conditions on tufa microfabric. In: Pedley, H.M. and Rogerson, M. eds. *Tufas and Speleothems: Unravelling the Microbial and Physical Controls*, London, UK: Geological Society Special Publications. pp. 193-210.

Pedley, H.M. Rogerson, M. and Middleton, R. 2009. Freshwater calcite precipitates from in vitro mesocosm flume experiments: a case for biomediation of tufas. *Sedimentology **56***, pp. 511-527.

Pentecost, A. 1985. Association of cyanobacteria with tufa deposits: identity, enumeration, and nature of the sheath material revealed by histochemistry. *Geomicrobiology Journal **4***, pp. 285-298.

Pentecost, A. 1990. The formation of travertine shrubs: Mammoth Hot Springs, Wyoming. *Geological Magazine **127***, pp. 159-168.

Pentecost, A. 1993. British travertines: a review. *Proceedings of the Geologists' Association **104***, pp. 23-39.

Pentecost, A. 1995. The quaternary travertine deposits of Europe and Asia Minor. *Quaternary Science Reviews **14**,* pp. 1005-1028.

Pentecost, A. 1996. Moss growth and travertine deposition: The significance of photosynthesis, evaporation and degassing of carbon dioxide. *Journal of Bryology **19***, pp. 229-234.

Pentecost, A. 2001. Microdistribution of algae in an Italian thermogene travertine. *Archiv für Hydrobiologie **152***, pp. 439-449.

Pentecost, A. 2003a. Cyanobacteria associated with hot springs. *Canadian Journal of Earth Sciences **40***, pp. 1447–1457.

Pentecost, A. 2003b. What is a hot spring? *Canadian Journal of Earth Sciences **40***, pp. 1443-1446.

Pentecost, A. 2005. *Travertine*. Amsterdam, Netherlands: Elsevier.

Pentecost, A. Bayari, S. and Yesertener, C. 1997. Phototrophic microorganisms of the Pamukkale travertine, Turkey: their distribution and influence on travertine deposition. *Geomicrobiology Journal **14***, pp. 269-283.

Pentecost, A. and Coletta, P. 2007. The role of photosynthesis and CO2 evasion in travertine formation: a quantitative investigation at an important travertine-depositing hot spring, Le Zitelle, Lazio, Italy. *Journal of the Geological Society, London* ***164***, pp. 843-853.

Pentecost, A. and Viles, H. 1994. A review and reassessment of travertine classification. *Géographie physique et Quaternaire* ***48***, pp. 305-314.

Pentecost, A. and Zhang, Z. 2001. A review of Chinese travertines. *Cave and Karst Science* ***28***, pp. 15-28.

Pentecost, A. and Zhang Z. 2002. Bryophytes from some travertine depositing sites in France and the U.K.: relationships with climate and water chemistry. *Journal of Bryology* ***24***, pp. 233–241.

Pentecost, A. and Zhang, Z. 2006. Response of bryophytes to exposure and water availability on some European travertines. *Journal of Bryology* ***28***, pp. 21-26.

Percival, D. 1986. *Rhiw Wen, Modern Limekiln.* < http://www.coflein.gov.uk/en/site/84849/details/RHIW+WEN%2C+MODERN+LIMEKILN/> [accessed 12/09/12]

Perrette, Y. and Jaillet, S. 2010. Spatial distribution of soda straw growth rates at the Coufin Cave (Vercors, France). *International Journal of Speleology* ***39***, pp. 61-70.

Perri, E. Manzo, E. and Tucker, M.E. 2012. Multi-scale study of the role of the biofilm in the formation of minerals and fabrics in calcareous tufa. *Sedimentary Geology* ***263-264***, pp. 16-29.

Petti, C.A. Polage, C.R. and Schreckenberger, P. 2005. The role of 16S rRNA gene sequencing in identification of microorganisms misidentified by conventional methods. *Journal of Clinical Microbiology* ***43***, pp. 6123-6125.

Pikuta, E.V. Hoover, R.B. and Tang, J. 2007. Microbial extremophiles at the limits of life. *Critical Reviews in Microbiology* ***33***, pp. 183-209.

Pinińska, J. Bobrowska, A. and Pamukcu, C. 2010. Laboartoryjne badania procesu deterioracji trawertynowych elementów konstrukcyjnych. *Przegląd Geologiczny* ***58***, pp. 879-885.

Pohl, W. and Schneider, J. 2002. Impact of endolithic biofilms on carbonate rock surfaces. In: Siegesmund, S. Weiss, T. and Vollbrecht, A. eds. *Natural Stone, Weathering Phenomena, Conservation Strategies and Case Studies*. London, UK: The Geological Society. pp. 177-194.

Pomar, L. Ginés, À. and Fontarnau, R. 1976. Las cristalizaciones freaticas. *Endins* ***3***, pp. 3-25.

Potapova, M. and Hamilton, P.B. 2007. Morphological and ecological variation within the *Achnanthidium minutissimum* (Bacillariophyceae) species complex. *Journal of Phycology* ***43***, pp. 561-575.

Prepas, E.E. Pinel-Alloul, B. Chambers, P.A. Murphy, T.P. Reedyk, S. Sandland, G. and Serediak, M. 2001. Lime treatment and its effects on the chemistry and biota of hardwater eutrophic lakes. *Freshwater Biology* ***46***, pp. 1049-1060.

Rahman, M.L. Tarrant, S. McCollin, D. and Ollerton, J. in press. Plant community composition and attributes reveal conservation implications for newly created grassland on capped landfill sites. *Journal for Nature Conservation*

Rainey, D.K. and Jones, B. 2009. Abiotic versus biotic controls on the development of the Fairmont Hot Springs carbonate deposit, British Columbia, Canada. *Sedimentology* ***56***, pp. 1832-1857.

Raven, J.A. and Giordano, M. 2009. Biomineralization by photosynthetic organisms: evidence of coevolution of the organisms and their environment? *Geobiology* ***7***, pp. 140-154.

Reedyk, S. Prepas, E.E. and Chambers, P.A. 2001. Effects of single $Ca(OH)_2$ doses on phosphorous concentration and macrophyte biomass of two boreal eutrophic lakes over 2 years. *Freshwater Biology* ***46***, pp. 1075-1087.

Reid, R.P. Visscher, P.T. Decho, A.W. Stolz, J.F. Bebout, B.M. Dupraz, C. Macintyre, I.G. Paerl, H.W. Pinckney, J.L. Prufert-Bebout, L. Steppe, T.F. and DesMarais, D.J. 2000. The role of microbes in accretion, lamination and early lithification of modern marine stromatolites. *Nature* ***406***, pp. 989-992.

Renaut, R.W. Jones, B. and Turdu, C.L. 1999. Calcite lilypads and ledges at Lorusio Hot Springs, Kenya Rift Valley: Travertine precipitation at the air-water interface. *Canadian Journal of Earth Sciences* ***36***, pp. 649-666.

Richter, D.K. and Besenecker, H. 1983. Subrecent high-Sr aragonitic ooids from hot-springs near Tekke Ilica, Turkey. In: Peryt, T.M. (ed.) *Coated Grains*. Berlin, Germany: Springer-Verlag. pp. 154-162.

Richthammer, P. Börmel, M. Brunner, E and van Pée, K-H. 2011. Biomineralization in diatoms: the role of silacidins. *Chembiochem* ***12***, pp. 1362-1366.

Riding, R. 1991. Classification of microbial carbonates. In: Riding, R. (ed.) *Calcareous Algae and Stromatolites*, Berlin, Germany: Springer-Verlag. pp. 21-51.

Riding, R. 2000. Microbial carbonates: the geological record of calcified bacterial-algal mats and biofilms. *Sedimentology* ***47***, pp. 179-214.

Rodwell, J.S. 1998. *British Plant Communities Volume 2*. Cambridge, UK: Cambridge University Press.

Roelofs, J.G.M Brandrud, T.E. and Smolders, A.J.P. 1994. Massive expansion of *Juncus bulbosus L.*after liming of acidified SW Norwegian lakes. *Aquatic Botany* ***48***, pp. 187-202.

Roelofs, J.G.M. Smolders, A.J.P. Brandrud, T-E. and Bobbink, R. 1995. The effect of acidification, liming and reacidification on macrophyte development, water quality and sediment characteristics of soft-water lakes. *Water, Air and Soil Pollution* ***85***, pp. 967-972.

Rogerson, M. Pedley, H.M. Wadahawan, J.D. and Middleton, R. 2008. New insights into biological influence on freshwater carbonate deposits. *Geochimica et Cosmochimica Acta* ***72***, pp. 4976-4987.

Rothschild, L.J. and Mancinelli, R.L. 2001. Life in extreme environments. *Nature* ***409***, pp. 1092-1101.

Sanchez-Moral, S. Portillo, M.C. Janices, I. Cuezva, S. Fernandez-Cortes, A. Canaveras, J.C. and Gonzalez, J.M. 2012. The role of microorganisms in the formation of calcitic moonmilk deposits and speleothems in Altamira Cave. *Geomorphology* ***139-140***, pp. 285-292.

Sand-Jensen, K. Pedersen, M.F. and Nielsen, S.L. 1992. Photosynthesis use of inorganic carbon among primary and secondary water plants in streams. *Freshwater Biology* ***27***, pp. 283-293.

Schopf, J.W. Kudryavtsev, A.B. Czaja, A.D. and Tripathi, A.B. 2007. Evidence of Archean life: stromatolites and microfossils. *Precambrian Research* ***158***, pp. 141-155.

Schreiber, B.C. Smith, D. and Schreiber, E. 1981. Spring peas from New York State: nucleaction and growth of fresh water hollow ooliths and pisoliths. *Journal of Sedimentary Petrology* ***51***, pp. 1341-1346.

Schulte, M. Blake, D. Hoehler, T. and McCollom, T. 2006. Serpentinization and its implications for life on the early Earth and Mars. *Astrobiology* ***6***, pp. 364-376.

Schulze-Makuch, D. Fairén, A.G. and Davila, A.F. 2008. The case for life on Mars. *International Journal of Astrobiology* ***7***, pp. 117-141.

Self, C.A. and Hill, C.A. 2003. How speleothems grow: an introduction to the ontogeny of cave minerals. *Journal of Cave and Karst Studies* ***65***, pp. 130-151.

Shiraishi, F. Bissett, A. de Beer, D. Reimer, A. and Arp, G. 2008a. Photosynthesis, respiration and exopolymer calcium-binding in biofilm calcification (Westerhofer and Deinschwanger creek, Germany). *Geomicrobiology Journal* ***25***, pp. 83-94.

Shiraishi, F. Reimer, A. Bissett, A. de Beer, D. and Arp, G. 2008b. Microbial effects on biofilm calcification, ambient water chemistry and stable isotope records in a highly supersaturated setting (Westerhöfer Bach, Germany). *Palaeogeography, Palaeoclimatology, Palaeoecology* ***262***, pp. 91-106.

Shock, E.L. 1996. Hydrothermal systems as environments for the emergence of life. In: Bock, G.R. and Goode, J.A. eds. *Evolution of Hydrothermal Ecosystems on Earth (and Mars?)*. Chichester, UK: John Wiley & Sons Ltd. pp. 40-60.

Sleep, N.H. Meibom, A. Fridriksson, Th. Coleman, R.G. and Bird, D.K. 2004. H2-rich fluids from serpentinization: geochemical and biotic implications. *Proceedings of the National Academy of Sciences of the United States of America* ***101***, pp. 12818-12823.

Slocek, V. and Urbanek, J. 1995. Travertine cascades with giant pisoids in the Kladno area. *Vestnik Ceskeho Geologickeho Ustavu* ***70***, pp. 39-45.

Smith, D.J. Jenkin, G.R.T. Petterson, M.G. Naden, J. Fielder, S. Toba, T. and Chenery, S.R.N. 2011. Unusual mixed silica-carbonate deposits from magmatic-hydrothermal hot springs, Savo, Solomon Islands. *Journal of the Geological Society* ***168***, pp. 1297-1310.

Sosnová, M. van Diggelen, R. and Klimešová, J. 2010. Distribution of clonal growth forms in wetlands. *Aquatic Botany* ***92***, pp. 33-39.

Souza-Egipsy, V. Garcia Del Cura, M. Ascaso, C. De Los Rios, A. Wierzchos, J. and Gonzalez-Martin, J.A. 2006. Interaction between Calcite and Phosphorous in Biomineralization Processes in Tufa Carbonates. *International Review of Hydrobiology* ***91***, pp. 222-241.

Spear, J.R. Barton, H.A. Robertson, C.E. Francis, C.A. and Pace, N.R. 2007. Microbial community biofabrics in a geothermal mine adit. *Applied and Environmental Microbiology* ***73***, pp. 6172-6180.

Spötl, C. Unterwurzacher, M. Mangini, A. and Longstaffe, F.J. 2002. Carbonate speleothems in the dry, inneralpine Vinschgau Valley, northernmost Italy: witnesses of changes in climate and hydrology since the Last Glacial Maximum. *Journal of Sedimentary Research* ***72***, pp. 793-808.

Stratford, T. 1995. *Caves of South Wales*. Leicester, UK: Cordee.

Suarez, M.B. Suarez, C.A. Kirkland, J.I. González, L.A. Grandstaff, D.E. and Terry Jr., D.O. 2007. Sedimentology, stratigraphy, and depositional environment of the Crystal Geyser Dinosaur Quarry, east-central Utah. *Palaios* ***22***, pp. 513-527.

Sumper, M. and Brunner, E. 2008. Silica biomerineralisation in diatoms: the model organism *Thalassiosira pseudonana*. *Chembiochem* ***9***, pp.1187-1194.

Swale, J. Luurtsema, S. Philip, E. and Uttley, J. 2010. *The Reserve Plan for Keen of Hamar National Nature Reserve*. Lerwick, Scotland: Scotish Natural Heritage.

Swennen, R. Podoor, N. and Keppens, E. 1999. Biological and diagenetic influence in recent and fossil tufa deposits from Belgium. *Sedimentary Geology* ***126***, pp. 75-95.

Takashima, C. and Kano, A. 2008. Microbial processes forming daily lamination in a stromatolitic travertine. *Sedimentary Geology* ***208***, pp. 114-119.

Takashima, C. Okumura, T. Nishida S. Shimamoto, T. Koike, H. and Kano, A. 2011. Microbial control on lamina formation in a travertine of Crystal Geyser, Utah. *Lecture Notes in Earth Sciences* ***131***, pp. 123-133.

Taylor, P.M. and Chafetz, H.S. 2004. Floating rafts of calcite crystals in cave pools, central Texas, U.S.A.: Crystal habit vs. saturation state. *Journal of Sedimentary Research* ***74***, pp. 328-341.

Taylor, M.P. Drysdale, R.N. and Carthew, K.D. 2004. The formation and environmental significance of calcite rafts in tropical tufa-depositing rivers of northern Australia. *Sedimentology* ***51***, pp. 1089-1101.

Tazaki, K. Okuno, M. Furumoto, M. and Watanabe, H. 2006. Biomineralization of pisoliths in hot springs. *Materials Science and Engineering: C* ***26***, pp. 617-623.

Tekin, E. Kayabali, K. Ayyidiz, T. and Ileri, O. 2000. Evidence of microbiologic activity in modern travertines: Sicakcermik geothermal field, central Turkey. *Carbonates and Evaporites* ***15***, pp. 18-27.

Tekin, E. and Ayyildiz, T. 2001. Petrographic Properties of the recent travertines in the Sicakçermik Geothermal Field (NW Sivas, Turkey). *Geological Bulletin of Turkey* ***44***, pp. 1-13.

Thornbush, M.J. and Viles, H.A. 2007. Simulation of the dissolution of weathered versus unweathered limestone in carbonic acid solutions of varying strength. *Earth Surface Processes and Landforms* ***32***, pp. 841-852.

Tiago, I. Chung, A.P. and Veríssimo, A. 2004. Bacterial diversity in a nonsaline alkaline environment: heterotrophic aerobic populations. *Applied and Environmental Microbiology* ***70***, pp. 7378-7387.

Tiago, I. Mendes, V. Pires, C. Morais, P.V. and Veríssimo, A. 2006. *Chimaereicella alkaliphila* gen. nov., sp. nov., a Gram-negative alkaliphilic bacterium isolated from a nonsaline alkaline groundwater. *Systematic and Applied Microbiology* ***29***, pp. 100-108.

Tice, M.M. and Lowe, D.R. 2004. Photosynthetic microbial mats in the 3,416-Myr-old ocean. *Nature* ***431***, pp. 549-552.

Tobler, D.J. Stefánsson, A . and Benning, L.G. 2008. In-situ grown silica sinters in Iceland geothermal areas. *Geobiology* ***6***, pp. 481-502.

Tobler, D.J. and Benning, L.G. 2011. Bacterial diversity in five Icelandic geothermal waters: temperature and sinter growth rate effects. *Extremophiles* ***15***, pp. 473-485.

Török, Á. 2006. Hungarian travertine: weathering forms and durability. *Proceedings of the International Conference on Heritage, Weathering and Conservation, HWC 2006*. Madrid, Spain. 21-24 June 2006. pp. 199-204.

Török, Á. and Vásárhelyi, B. 2010. The influence of fabric and water content on selected rock mechanical parameters of travertine, examples from Hungary. *Engineering Geology* ***115***, pp. 237-245.

Tortell, P.D. Reinfelder, J.R and Morel, M.M. 1997. Active uptake of bicarbonate by diatoms. *Nature* ***390***, pp. 243-244.

Tucker, M.E. and Wright, V.P. 1990. *Carbonate Sedimentology*. Oxford, U.K.: Blackwell Science.

Ulukani, Z. and Diğrak, M. 2002. Alkaliphilic micro-organisms and habitats. *Turkish Journal of Biology* ***26***, pp. 181-191.

United States Department of Agriculture Nature Resources Conservation Service. Undated. *Juncus effusus characteristics*. < http://plants.usda.gov/java/charProfile?symbol=JUEF> [accessed 07/02/2012]

Usdowski, E. Hoefs, J. and Menschel, G. 1979. Relationship between 13C and 18O fractionation and changes in major element composition in a recent calcite-depositing spring – A model of chemical variations with organic $CaCO_3$ precipitation. *Earth and Planetary Science Letters* ***42***, pp. 267-276.

van Bodegom, P.M. Sorrell, B.K. Oosthoek, A. Bakker, C. and Aerts, R. 2008. Separating the effects of partial submergence and soil oxygen demand on plant physiology. *Ecology* ***89***, pp. 193-204.

Vásquez-Urbez, M. Arenas, C. Sancho, C. Osácar, C. Auqué, L. and Pardo, G. 2010. Factors controlling present-day tufa dynamics in the Monasterio de Piedra Natural Park (Iberian Range, Spain): Depositional environmental settings, sedimentation rates and hydrochemistry. *International Jounral of Earth Sciences* ***99***, pp. 1027-1049.

Veysey, J. and Goldenfeld, N. 2008. Watching rocks grow. *Nature Physics* ***4***, pp. 310-313.

Veysey, J. Fouke, B.W. Kandianis, M.T. Schickel, T.J. Johnson, R.W. and Goldenfeld, N. 2008. Reconstruction of water temperature, pH, and flux of ancient hot springs from travertine depositional facies. *Journal of Sedimentary Research* ***78***, pp. 69-76.

Visser, E.J.W. Bögemann, G.M. van De Steeg, H.M. Pierik, R. and Blom, C.W.P.M. 2000. Flooding tolerance of *Carex* species in relation to field distribution and aerenchyma formation. *New Phycologist* ***148***, pp. 93-103.

Walker, J.J. and Pace, N.R. 2007. Endolithic microbial ecosystems. *Annual Reviews in Microbiology* ***61***, pp. 331-347.

Webb, A.H. Bawden, R.J. Busby, A.K. and Hopkins, J.N. 1992. Studies on the effects of air pollution on limestone degradation in Great Britain. *Atmospheric Environment* ***26B***, pp. 165-181.

White, W.B. 1976. Cave minerals and speleothems. In: Ford, T.D. and Cullingford, C.H.D. eds. *The Science of Speleology*. London, UK: Academic Press. pp. 267-327.

Winsborough, B.M. 2000. Diatoms and benthic microbial carbonates. In: Riding, R. ed. *Microbial Sediments*. Berlin, Germany: Springer-Verlag. pp. 76-83.

Wright, V.P. 1989. Terrestrial stromatolites and laminar calcretes: a review. *Sedimentary Geology* ***65***, pp. 1-13.

Xiao, D. Zhang, L. and Zhu, Z. 2010. The range expansion patterns of *Spartina alterniflora* on salt marshes in the Yangtze Estuary, China. *Estuarine, Coastal and Shelf Science* ***88***, pp. 99-104.

Yagiz, S. 2010. Geomechanical properties of construction stones quarried in south-western Turkey. *Scientific Research and Essays* ***5***, pp. 750-757.

Yim, L.C. Hongmei, J. Aitchison, J.C. and Pointing, S.B. 2006. Highly diverse community structure in a remote central Tibetan geothermal spring does not display monotonic variation to thermal stress. *FEMS Microbiology Ecology* ***57***, pp. 80-91.

Zaihua, L. Svensson, U. Dreybrodt, W. Daoxian, Y. and Buhmann, D. 1995. Hydrodynamic control of inorganic calcite precipitation in Huanglong Ravine, China: Field measurements and theoretical prediction of deposition rates. *Geochimica et Cosmochimica Acta* ***59***, pp. 3087-3097.

Zhan, C-W. Wang, D. Huang, X-F. and Zhou, J. 2010. Effects of burial depth and water depth on sprouting of turions and early growth of *Myriophyllum oguraense* Miki subsp. *Yangtzense* Wang. *Fundamental and Applied Limnology* ***176***, pp. 263-268.

Zhang, D. Zhang, Y. Zhu, A. and Cheng, X. 2001. Physical mechanisms of river waterfall tufa (travertine) formation. *Journal of Sedimentary Research* ***71,*** pp. 205-216.

Zhang, Y. and Prepas, E.E. 1996. Short-term effects of Ca(OH)2 additions on phytoplankton biomass: a comparison of laboratory and in situ experiments. *Water Research* ***30***, pp. 1285-1294.

Zubay, G. 2000. *Origins of Life on the Earth and in the Cosmos*. Burlington, Massachusetts: Harcourt/Academic Press.

Zvereva, E.L. and Kozlov, M.V. 2011. Impacts of industrial polluters on bryophytes: a meta-analysis of observational studies. *Water, Air, and Soil Pollution* ***218***, pp. 573-586.